UNIVERSITY OF OKLAHOMA
GRADUATE COLLEGE

INFLUENCE OF STRESS ON THE PETROPHYSICAL PROPERTIES OF FLOW UNITS IN CLEAN AND SHALY HETEROGENEOUS FORMATIONS

A DISSERTATION
SUBMITTED TO THE GRADUATE FACULTY
IN PARTIAL FULFILLMENT OF THE REQUIREMENTS FOR THE
DEGREE OF
DOCTOR OF PHILOSOPHY

By

SHEDID ALI ELGAGHAH

NORMAN, OKLAHOMA
(1997)

UMI Number: 9808403

INFLUENCE OF STRESS ON THE
PETROPHYSICAL PROPERTIES OF FLOW UNITS
IN CLEAN AND SHALY HETEROGENEOUS FORMATIONS

A DISSERTATION APPROVED FOR
THE SCHOOL OF PETROLEUM AND GEOLOGICAL ENGINEERING

By

ACKNOWLEDGMENTS

The author would like to express his sincerest gratitude to those who, each in his way, contributed to this research. All of these persons offered guidance, encouragement, and much welcomed criticism and suggestions.

The author wishes to express his sincere appreciation and grateful thanks to Dr. Djebbar Tiab and Dr. Samuel Osisanya who served as co-supervisiors of this study for their support, valuable suggestions, interest and helpful guidance.

A special and sincere appreciation to Dr. Donald Menzie for his continued encouragement and very kind advice. Also, the author is very grateful to Dr. Subhash N. Shah and Dr. James Forgotson for serving as supervising committee-members.

The author wishes to express his appreciation to the entire School of Petroleum and Geological Engineering faculty and staff for their help and understanding during the author's entire graduate program. The author appreciates the Egyptian Government for financial support and help.

This work is dedicated to the soul of my mother and to my father, Ali Shedid. Finally, the author will remain forever grateful to his family, his wife, Abeer Elfeky, and his daughters, Nada and Noran, for their patience, encouragement and understanding.

Author

Shedid Ali Elgaghah

LIST OF CONTENTS

LIST OF TABLES

Page

LIST OF FIGURES

ABSTRACT

Reservoir characterization has been considered as a critical component of reservoir development because its main goal is to provide better description and distinguish the essential features of geological/petrophysical parameters affecting fluid flow in the producing formations.

This study is devoted mainly to the reservoir characterization of clean and shaly heterogeneous reservoir rocks under stress effect. This study is divided into five different categories: (1) characterization of clean heterogeneous formations (without stress effect) using core data, (2) characterization of shaly heterogeneous formations (without stress effect), (3) characterization of clean heterogeneous formations under stress effect using well-logging derived data and investigation of the effect of stress on petrophysical properties of flow unit in this type of formation, (4) characterization of shaly heterogeneous formations under stress effect using well-logging derived data and investigation of the effect of stress on petrophysical properties of flow units in shaly heterogeneous reservoirs, and (5) investigation of the effect of stress on the J-function and development of new J-function models in clean and shaly reservoirs using well-logging data.

With respect to the first and the second categories, several practical and theoretical flow unit models were developed for identification and characterization of hydraulic (flow) units in clean and shaly heterogeneous reservoirs. Characterization of clean and shaly heterogeneous formations under stress effect was achieved by developing two new Reservoir Quality Index of formation under stress including Reservoir Quality Index of

clean formation under stress (RQIs) and Shaly Reservoir Quality Index under stress (SRQIs). These newly-developed RQIs and SRQIs were used to study the effect of stress on petrophysical properties of flow units and to derive several new models for characterization and identification of flow units constituting clean and shaly formations under stress effect. Finally, this study has developed new J-function that considers stress effect and presented a new approach by which the utility of well-logging data can be used to estimate the J-function in clean and shaly heterogeneous reservoirs. Validation of these newly-developed J-function models has been proven using actual field data.

The results show that increasing effective stress reduces the value of reservoir quality index under stress (RQIs) for clean formations. In addition increasing effective stress significantly reduces the value of reservoir quality index for shaly formations under stress (SRQIs). Also increasing the change in effective stress leads to change in the fluid flow path patterns and the position of flow units. Therefore, identification of flow units should be updated. The results also show that increasing stress effect leads to a shift of the J-function versus water saturation (S_w) curve in both clean and shaly reservoirs. Therefore. there is a need to correct laboratory acquired J-function values for stress effect.

CHAPTER I

INTRODUCTION, RESEARCH OBJECTIVES AND STRATEGY

I. 1. Introduction

The ultimate goal of petroleum engineering science is to maximize oil recovery at a minimum cost. This goal can be achieved by understanding the heterogeneous nature of the reservoir rock. Reservoir characterization is considered the key to optimum oil exploration and exploitation. Nearly, two-third of initial oil-in-place may remain trapped in the reservoir unless advanced producing techniques are applied and/or better description of the reservoir rock is obtained.

Extensive research has been conducted for homogeneous reservoirs for decades. Heterogeneous reservoirs have long been viewed as a problem. The current thinking is that they should be viewed as an opportunity for recovering more oil. Geological reservoir heterogeneity has been considered as the main reason for poor efficiency of oil recovery. This reservoir heterogeneity causes highly non-uniform patterns of fluid flow and incomplete drainage of oil. A better description of the reservoir rock involves a better understanding of flow and no-flow units constituting this reservoir rock. A hydraulic (flow) unit has been defined as a mappable portion of the reservoir within which geological and petrophysical properties that influence fluid flow are consistent and predictably different from the properties of other reservoir rock volume. In addition, flow unit may also be continuous over a specific reservoir volume which uniquely characterize its dynamic and static states.

Reservoir evaluation and characterization of shaly formations have long been a difficult task, which makes seeking enhanced reservoir description of shaly sand reservoirs more difficult. When reservoir pressure declines due to oil production, reservoir rock will be compacted and the stress on the formation grains increases. In addition, reduction of the reservoir pore-volume causes the overburden to shift which leads to variation in fluid flow paths through the porous rock under the effect of stress.

This study is mainly devoted to characterization of clean/shaly heterogeneous formations and identification of hydraulic (flow) units comprising reservoir rock under stress conditions.

In chapter 2, a brief review of characterization of flow units in clean formations is discussed including definition, importance and required tools for reservoir characterization. In this chapter, five new flow unit models are developed to characterize and identify flow units using core data at initial conditions (without stress effect). The flow unit models are developed using several permeability equations such as: Morris-Biggs, Nuclear Magnetic Resonance (NMR), Wyllie and Rose, Timur, and Jorgensen.

Chapter 3 reviews shale distribution, shale content evaluation, shale models, and determination of well logging parameters for shaly formations. In this chapter, a step-by-step derivation of four new flow unit models for laminated, dispersed, total, and cation exchange capacity (CEC) of shale is developed. Then, a generalized technique is introduced showing how these new models can be used to identify and characterize both the shale type and the flow units comprising the pay zone.

Chapter 4 reviews effects of stress on pore compressibility, porosity, rock density, permeability, and formation resistivity factor. A clean formation under stress requires the development of new reservoir quality index. This is achieved in this study by developing new reservoir quality index for formation under stress (RQIs) and comparing it to conventional reservoir quality index (RQIo). Furthermore, four flow unit models are introduced for characterizing clean reservoirs under stress conditions.

Chapter 5 includes a very brief review of the effect of stress on porosity and water saturation exponents. Stress effect is also extended to porosity and permeability of shaly formations. In addition, a new reservoir quality index for shaly formation under stress effect (SRQIs) is developed and compared with shaly reservoir quality index (SRQIo). Four new flow unit models are developed to characterize flow units considering shale distribution (including: laminated, dispersed, total and cation-exchange capacity (CEC)) in combination with the stress effect on each shale type.

Chapter 6 covers the concept of the J-function and its use for obtaining pore distribution of the reservoir rock. This chapter investigates the effect of stress on the J-function and presents a new approach by which well-logging data can be used to estimate the J-function in clean/shaly reservoirs. Two models are developed to obtain the J-function under stress. Validation of the newly-developed J-function models is proved using actual field data for clean and shaly reservoirs.

Chapter 7 covers summary and conclusions of this study. In addition, the chapter introduces several recommendations as future studies for better reservoir characterization.

1. 2. Research Objectives and Strategy

The main objectives of this study are to identify and characterize hydraulic (flow) units in clean and shaly heterogeneous reservoirs with and without considering stress effect of the formation. These objectives have been achieved by using core data (without stress effect) and/or well-logging data (with stress effect).

Discrimination of rock types has been generally based on geological observation and on empirical correlations between log permeability versus porosity. This classic technique has several limitations such as: (1) permeability may vary by several orders of magnitude, which shows the presence of several flow units, (2) there is no universal permeability equation for shaly formations, (3) correction of porosity for shale will add a new unknown that should be considered during permeability calculation, and (4) available permeability and reservoir quality index (RQI) equations do not consider stress effect which has been shown to be an important factor affecting both the petrophysical properties of reservoir rocks and the distribution of flow units constituting that reservoir rock.

It has been proven that enhanced reservoir description will reduce the amount of oil left in hydrocarbon reservoirs. The central elements of this enhanced reservoir description are determination of pore-body/pore-throat attributes and fluid distribution. Although this has been established for clean formations using conventional reservoir quality index (RQI), ignoring stress effect will lead to serious errors in reservoir description and will hamper reservoir development.

The approach used in this study is based on the development of new characterization relationships for clean and shaly heterogeneous formations under stress conditions. Attainment of these goals creates a real need for new permeability equations for clean and shaly formations under stress effect and also new reservoir quality index (RQI) correlations for shaly formations, clean formations under stress, and shaly formations under stress effect. Several equations are developed in this study to give a new meaning to reservoir quality index (RQI). Equations for shaly reservoir quality index (SRQIo), reservoir quality index of clean formations under stress effect (RQIs), and shaly reservoir quality index under stress effect (SRQIs) are developed.

These newly developed reservoir quality indices have been used effectively to develop several new models capable of characterizing and identifying flow units residing within clean and shaly reservoir rocks under stress effect. In addition, generalized systematic techniques are introduced showing how to use these models for practical and accurate definition of flow units constituting reservoir rock. The use of these newly-developed flow unit and J-function models represents an effective and economic tools to enhance reservoir description and will lead to a more efficient reservoir development.

CHAPTER 2

CHARACTERIZATION OF FLOW UNITS

IN CLEAN FORMATIONS

2. 1. Introduction

The relationship between different petrophysical properties and fluid saturations is well-established for clean sand reservoirs. Several empirical models have been developed to calculate water saturation, and all the required parameters for evaluation of clean reservoirs. There is still a real need however for improving the reservoir description in more detail especially in heterogeneous formations. This can be achieved by subdividing the reservoir into unique flow units.

Characterization of flow units provides a practical mean for reservoir zonation that makes use of both geological and petrophysical data, representing heterogeneity observed at several scales. It also provides an economical technique for reservoir development in the future. The key to improving reservoir description and exploitation is to describe complex variation in pore-geometry with different mappable geological units (facies). This requires establishment of causal relationships among core-derived, microscopic pore-throat parameters and log-derived macroscopic attributes.

2. 2. Reservoir Characterization Methodology

Nearly two-third of initial oil in place (IOIP) may remain trapped in existing reservoirs unless advanced operating practices are used and/or better description of the reservoir rock could be obtained. The principle reason for poor recovery efficiency is the presence of geological heterogeneity, which causes highly non-uniform fluid flow patterns and poor drainage of oil. Better description of the reservoir also requires a better understanding of the distribution and nature of the remaining oil.

Reservoir characterization is a critical component of reservoir development because its main goals are to describe and to distinguish the essential features of geological/petrophysical parameters affecting fluid flow in the producing formations. Successful reservoir characterization program should be a multi-disciplinary endeavor integrating several contributions from petroleum engineering, geology, geophysics, and computer science.

The purpose of reservoir characterization is to outline and specifically integrate several aspects of oil/gas reservoir. These aspects include: reservoir geology, petrophysical properties and diagenesis of reservoir rock, rock-fluid interaction properties, and production features which dictate fluid flow paths and trapping of fluid in reservoirs. The work done by several researchers are now summarized.

The main objective of reservoir characterization is to construct a combined model using geological and engineering data. This data has been classified by Honarpour et al (1990) into two main categories including hard and soft data. Hard data could be dependent upon model construction and interpretation, whereas soft data is based on model construction and interpretation.

2. 2. 1. Reservoir Characterization Definition and Importance

Honarpour et al (1990) indicated that the objective of reservoir characterization is to integrate geological, petrophysical, diagenetic properties of the reservoir rock, in combination with rock-fluid and production features which describe fluid flow paths in the reservoir. Integration can be defined as a coordinated study for constructing a unified picture of the reservoir which is compatible with all sources of information. Improved reservoir characterization is only possible through multi-disciplinary integration and analysis of data concerning depositional process of the formation under investigation.

There are several definitions available for reservoir characterization. Forgotson (1993) defined reservoir characterization as the quantitative description of the physical and chemical properties of a porous medium and its contained fluids. The purpose of such a description is to develop a geological model of a reservoir combined with reservoir fluid properties. In addition, production and pressure data can be used to increase the recovery of oil from the reservoir while maintaining favorable economics. This description should cover a broad range of dimensions from pore throat through reservoir size. Forgotson also added that reservoir characterization must accurately identify flow units within the reservoir including the prediction of the size, shape, internal variation and continuity of these flow units.

The main importance of the reservoir characterization is that it provides a better understanding of the geological depositional environment which can be transformed into a numerical model describing the reservoir. The model then provides a very effective tool for reservoir development during secondary and tertiary oil recovery processes.

Reservoir management usually use several simulation studies based on accurate model derived mainly from reservoir characterization studies. Accurate reservoir characterization models represent a useful tool for extending the life of the reservoir and getting additional oil.

Forgotson also gave the following reasons for the present emphasis on interdisciplinary studies integrating geological, geophysical, and engineering data:

1. The need to recover additional oil from old fields approaching their economic limits,
2. The desire for better economics in the development of management of new fields in areas with high drilling and operating costs, and
3. The development of the computer hardware and software that are cost effective for numerical simulation of reservoir models based on detailed data obtained from comprehensive reservoir characterization.

2. 2. 2. Required Tools For Reservoir Characterization

Measurement of several reservoir rock properties that has to be performed to provide an accurate reservoir characterization studies creates a difficult task. The main reason for this difficult task is the existence of various types of reservoir heterogeneities over a wide range of scale. Honarpour et al primarily grouped geological heterogeneities into four categories:

1. Sedimentological heterogeneity which results from depositional processes and indicates the original framework/architecture of a reservoir,

2. Diagenetic heterogeneity which results from geochemical alterations of reservoir rocks or fluids and improve/deteriorate the quality of the reservoir rock by generating clays, cementing materials, and leaching processes,

3. Structural heterogeneity which mainly results from geologic structures in the reservoir such as faults and fractures. This type of structure is superimposed on the primary framework and may interact with diagenetic processes by acting as channels/barriers for fluid migration, and

4. Formation fluid characteristics including formation water and hydrodynamically induced water and hydrocarbons. These fluids are in an equilibrium state after interacting with the reservoir rock over millions of years. In addition to the new fluids induced to the reservoir during secondary and tertiary recovery processes.

All of these heterogeneties have variable effects on the reservoir performance depending upon the production stage of the reservoir. Honarpour et al (1990) summarized the major heterogeneity based on their geological origins, Table 2. 1. In addition, they also, summarized the critical heterogneities for various stages of production as follows:

1. Primary

    A. net formation thickness,

    B. compartmentalization,

    C. type of drive mechanism,

    D. volumetric fluid distribution, and

    E. fluid properties, relative permeabilities.

2. Secondary

Table 2. 1. Outline of major heterogeneity types based on their geological origins, [Honarpour, 1990]

HETEROGENEITY TYPE manifestations	FUNDAMENTAL CAUSES (PROCESSES)		
	SEDIMENTOLOGIC	GEOCHEMCIAL/DIAGENETIC	TECTONIC
VARIATIONS IN CONTAINER (External Geometry) Pay Thickness Dimensions Continuity Attitude (Dip)	Deposition, Erosion	Leaching, Cementing	Faults, folds, flexure, monocline
BARRIERS/ COMPARTMENTALIZATION	Erosion (Reservoir cut out) Shale Layers	Compacted Zones Tightly Cemented Zones	Sealed Faults Sealed Fractures
BAFFLES e.g. batches of shale	Shale/Siltstone Layers Variations in grain size and sorting Bioturbation	Compacted Zones Partially Cemented Zones	Partially Opened Faults and Fractures
CHANNELS (thief zones)	Coarse Grained, Layers, Well Sorted Layers	Leaches Zones High saturation of gas and water	Open Faults Open Fractures
SPATIAL VARIATIONS OF RESERVOIR ROCK PROPERTIES Vertical Lateral	Environment of Deposition Variations in Grain Size Sorting, Mineralogy, Biogenic Activity	Compaction Cementation/Leaching	
SPATIAL VARIATIONS OF RESERVOIR ROCK-FLUID PROPERTIES	Fluid Origin	Thermal Maturation, Geochemical Environment, Rock Fluid Interaction	

A. compartmentalization/continuity,

B. permeability contrast (channeling),

C. anisotropy, rock fluid interaction (wettability, relative permeability), and

D. clay type (swelling/migration), dip.

3. Tertiary

A. volumetric/fluid distribution,

B. compartmentalization/ continuity,

C. permeability contrast (channeling),

D. anisotropy, rock fluid interaction (wettability, relative permeability), and

E. temperature dip.

It is very important to consider these types of heterogeneity during the process of developing the required reservoir characterization model because the reliability of geological/engineering models will depend mainly upon the quality of the data and the basic assumptions.

All of the previously described types of heterogeneity can be indicated by the following fluid flow characteristics and distributions:

1. formation thickness (pay/non-pay), spatial distribution of pay and non-pay intervals, and reservoir dip (attitude),
2. compartmentalization/ continuity,
3. permeability contrast (channeling),
4. fluid-fluid and rock-fluid interactions,

5. drive mechanisms/gas cap/aquifer size, shape (irregular/tilted connection to other reservoirs with gas cap drive) and its characteristics, and
6. volumetric, fluid distributions.

Consideration of reservoir geology is one of the most important factors for a successfully integrated reservoir characterization. The key attributes of a reservoir that are related to its depositional system include:

1. primary rock type and facies,
2. external geometry and configuration of the reservoir body,
3. internal architecture which controls vertical and lateral variations in both pay and non-pay zones,
4. reservoir facies relationships which may control the sealing and trapping of hydrocarbons,
5. effectiveness of natural water-drive reservoirs, and
6. control of modification of subsequent diagenetic history and the type and abundance of porosity and permeability.

Delineation of facies components provides the basis for establishing the field-wide internal reservoir architecture style. Reservoir heterogeneity may be classified into two scales as follows:

1. Megascopic scale, in which untrapped oil facies occur as either a small number discrete, elongate semi-continuous bodies that are easily missed by the majority of well drilled on a grid or as tabular bodies occurring at deeper, less explored horizons; and

2. Macroscopic scale, in which small scale heterogeneity (in comparison to well spacing) cause local compartmentalization and bypassing of oil during field development (primary and secondary oil recovery).

Another more detailed classification of reservoir heterogeneity was introduced by Forgotson (1993) who classified them into four levels as follows:

1. Microscopic heterogeneity: it results from the variation at the pore-throat scale. This type of scale controls the nature of oil and gas saturation in the reservoir,
2. Mesoscopic heterogeneity: it results from the variation at the lamination to bed scale within distinctive lithofacies deposited during a relatively short period of accumulation. This type of scale can be reflected as flow barriers, laterally and vertically discontinuities in carbonate reservoirs
3. Macroscopic heterogeneity: it results from lateral changes in the lithofacies and lithologic across depositional sequence boundaries. This scale considers the interwell spacing flow properties and can be obtained using well tests and/or well logging data, and
4. Megascopic heterogeneity: it results from lithologic variation across depositional systems and geometry of structural features. It is used to describe the external architecture of reservoirs using the domain of conventional subsurface mapping and the structural and the stratigraphic interpretation of seismic data.

It is important to emphasize that reservoir characterization requires accurate data from all types of these previously described scales with sophisticated averaging and scaling-up methods for estimation of different properties of a flow unit.

Doyle et al (1992) explained that integrated reservoir characterization should gather geological, geophysical, and well test data together. The objective of this study is to verify the descriptive and predictive tools with an equally detailed set of flow measurements. It is very important to develop detailed spatial distribution of reservoir properties (porosity, permeability, and lithology) and to characterize depositional flow units within distinct distributions.

The required sources of data for reservoir characterization are different for each heterogeneity scale and for each scientific discipline. The data can be classified into four main types as follows:

1. Geological and petrophysical data which can be obtained from laboratory measurements using rock cores.
2. Geophysical data which are primarily obtained from acoustic wave methods including surface and cross-well seismic surveys, and
3. Engineering data which can be obtained from cased-hole logs, drill stem tests, bottom-hole pressure tests, tracer studies, injection tests, production history, and reservoir fluid properties.

Data derived from cores can be divided into three categories including:

1. Geological data parameters, including geological core descriptions and petrographic analysis,
2. Data for well completion, and
3. Data for engineering calculations.

Cores can be used specifically for identification of depositional environments, facies, subfacies, erosional events, dip angels and azimuths. In addition, cores can also provide petrographic, petrophysical, mechanical, and geochemical data of reservoir rock and interstitial fluids. Furthermore, cores can also be used to determine rock-fluid interaction parameters which might be used as a reference for log interpretation. More specifically, the following data can be obtained from the cores:

(1) porosity and formation resistivity factor,

(2) relative and absolute permeabilities, compressibility, and rock mechanics properties,

(3) wettability and residual saturations,

(4) dispersivity, diffusivity, adsorption properties. and fractions of dead end pores,

(5) mineralogy, clay type and content, cation exchange capacity,

(6) capillary pressure-saturation relationships, drainage and imbibition properties,

(7) tortuosity, specific surface area, pore-size distribution, grain-size distribution,

(8) water flood and enhanced oil recovery (EOR) type displacement tests, and

(9) sensitivity of rocks and fluids to pressure and temperature conditions.

Well test analysis provides valuable information about major depositional, erosional, diagenetic, tectonic, and rock-fluid interaction, and fluid contacts within the reservoir. Forgotson (1993) summarized the role of different well tests in reservoir characterization as follows: production tests can be used for the determination of thief zones, fractures, coning and limits of producing zones. Interwell tracer tests are used to determine the direction and rate of fluid movement. Single-well tracer tests are used to determine residual oil saturation and dispersion coefficients. Finally, pressure transient tests are used to measure horizontal and vertical permeabilities, porosity, productivity index, reservoir volume, distance to fault or reservoir boundary, vertical zonation, fracture length, length of shale barriers, and average reservoir pressure. For this reason, well-to-well transient and pressure tests data can be used to complete each other.

Well logging provides a wealth of data that could be effectively used in reservoir characterization. With respect to open-hole logs, they are sometimes the only source for gross and net pay thickness, porosity, lithology, position of flow barriers, fluid saturation, and permeability. Open-hole logs are very useful tools for the determination external reservoir geometry, major flow barriers, porosity and fluid saturation.

Seismic surveys provide a map for detecting faults providing traps or segments of the reservoir. Two types of seismic analysis can be performed on 3-D data and some 2-D surveys: (l) mapping of geometric framework to represent detailed attitude of reservoir beds, and (2) interwell interpolations of reservoir properties. Vertical seismic profiling (VSP) provides high resolution for structural and stratigraphic information within a few hundred feet of the well. Tables 2. 2, 2. 3, and 2. 4 list geological significance, benefits of 3-D, and borehole seismic methods, respectively.

Finally, since the primary objective of a reservoir engineer is to obtain the highest possible economic hydrocarbon recovery from oil reservoirs, the following information is necessary:

1. Working description of reservoir including:

   A. model describing fluid flow within the reservoir,

   B. geological control of rock and flow properties including:

- structural,

- stratigraphic, and

- geometric.

C. translate into numerical framework including:

- hard numbers and bounds, and

- preferred flow directions.

D. defined and quantified at simulation grid-block scale.

2. Hydrocarbon distribution including:

A. originally oil in place,

B. where produced and bypassed. and

C. remaining oil in place as a target for further development.

3. Pore-space distribution including:

A. reservoir thickness, and

B. porosity, permeability, and oil saturation.

4. Horizontal and vertical heterogeneity including:

A. horizontal compartmentalization and vertical zonation,

B. simple versus complex geometry's,

C. continuous versus discontinuous layers, and

D. gradual versus sharp changes.

5. Distribution of sweep-controlling reservoir elements including:

A. non reservoir rocks and barriers to fluid flow

- continuous shales and sealing faults, and

Table 2. 2-Geologic significance of seismic reflection parameters used in seismic stratigraphy, [Hoeksema, 1990]

Seismic Facies Parameters	Geologic Interpretation
Reflection configuration	Bedding patterns Depositional processes Erosion and paleotopography Fluid contacts
Reflection continuity	Bedding continuity Depositional processes
Reflection amplitude	Velocity-density contrast Bedding spacing Fluid content
Reflection frequency	Bed thickness Fluid content
Interval velocity	Estimation of lithology Estimation of porosity Fluid content
External form and areal association of seismic facies units	Gross depositional environment Sediment source Geologic setting

Table 2. 3-Benefits of the 3-D seismic methods for reservoir engineering, [Hoeksema, 1990]

Attributes	Geologic Benefits	Engineering Benefits
3-D migration	Accurate geometry	Fewer dry holes
3-D density	Reservoir delineation	More production per well
Data volume	Interpretability	Fewer development wells
Spatial continuity	Heterogeneity	Earlier production Enhanced value of Reserves

Table 2. 4-Benefits of cross-bore holes seismic methods for reservoir engineering, [Hoeksema, 1990]

Attributes	Geologic Benefits	Engineering Benefits
Source and sensors at target depth	Accurate Geometry	Fewer infill wells
Reduced time to depth conversion	Interpretability	Reservoir simulation
Velocity/ attenuation tomography	Reservoir property variations	Monitor hydrocarbon recovery project
Impedance logging	Reservoir characterization	Efficient sweep
Increased resolution	Heterogeneity	More production per well

- non pay versus pay zones

B. high-permeability zones that result in low sweep efficiency and leave by-passed oil including:

- high-permeability layers, and
- fractures and channels.

2. 3. The Concept of Flow Unit

In early studies of reservoir engineering, the reservoirs are assumed to be homogeneous and isotropic, but also non-uniform. In recent studies, however, the porosity -permeability relationship has been used for a better description of the reservoirs having some complex geological continuum. Several authors have recently dealt with the reservoir as heterogeneous and non uniform which may comprise multiple homogeneous and non-uniform, sub-layers that can be referred to as hydraulic (flow) units.

Bear (1972) defined hydraulic (pore geometrical) unit as the representative elementary volume of the total reservoir rock within which the geological and petrophysical properties that affect fluid flow are internally consistent and predictably different from properties of other rock volumes.

The hydraulic unit concept is very useful because it combines several aspects of the reservoir rock and its contained fluids. These aspects include geological (texture and mineralogy) and petrophysical (porosity, permeability and capillary pressure) controls of the reservoir quality for the identification of reservoir rocks of similar fluid flow characteristics.

Ebanks (1983) defined hydraulic (flow) units as a mappable portion of the reservoir within which geological and petrophysical properties that affect the flow of fluids are consistent and predictably different from the properties of other reservoir rock volume. Ebanks also showed that the flow units have the following characteristics:

1. A flow unit is a specific volume of a reservoir, which is composed of one or more reservoir quality lithologies and any non-reservoir quality rock types within that same volume, as well as the fluids they contain,
2. A flow unit is correlative and mappable at the interwell scale,
3. A flow unit zonation is recognizable on wireline logs, and
4. A flow unit may be in communication with other flow units.

Delineation of the flow units requires fundamentally that the reservoir volumes within which properties that affect fluid flow differ are consistently distinguished and should be definable.

Several other definitions are also available for the concept of flow unit. A flow unit is also defined as a continuous body (over a specific reservoir volume) that practically possesses consistent petrophysical and fluid properties. These properties uniquely characterize its static and dynamic state, thus distinguishing it from other rock volumes. Here, a no-flow unit may be defined as reservoir body that does not possess sufficient porosity and permeability to support fluid flow. Flow units are then zones of similar geological facies and of similar pore geometrical attributes.

The description of the reservoir (in terms of flow and no-flow unit) provides a practical tool for enhanced reservoir description, using both geological and engineering information, which will ultimately have a significant effect for economic feasibility of reservoir development and enhanced oil recovery applications. It is well-recognized that improving the reservoir description will increase the oil recovery of that reservoir. Ebanks introduced the concept of flow unit from a geological point of view.

Later, Amaefule et al (1993) showed that it is not possible to get good reservoir description without considering a relationship between pore-throat parameters and log-derived macroscopic attributes. Amaefule et al also introduced the concept of reservoir quality index (RQI) considering the pore-throat, pore and grain distributions and other macroscopic parameters to come up with an equation of the reservoir quality index (RQI) as follows: Geological attributes indicate the existence of distinct rock units with similar pore-throat attributes.

Using the concept of mean hydraulic unit radius (r_{mh}) of Bird et al (1960), for a circular cylindrical tube, the mean hydraulic radius is defined by:

$$r_{mh} = \frac{r}{2} \tag{2-1}$$

where

r = radius of a circular cylindrical tube.

Using the mean-hydraulic radius concept, the Carmen-Kozeny equation (1937) provides this permeability equation:

$$K = \frac{\varphi_e r^2}{8\tau^2} = \frac{\varphi_e r_{mh}^2}{2\tau^2} \tag{2-2}$$

where

τ = tortuosity of the flow path,

The mean hydraulic radius (r_{mh}) can be related to the surface area per unit grain volume (S_{gv}) and effective porosity as follows:

$$S_{gv} = \frac{2}{r}\left(\frac{\varphi_e}{1-\varphi_e}\right) = \frac{1}{r_{mh}}\left(\frac{\varphi_e}{1-\varphi_e}\right) \tag{2-3}$$

Substituting equation (2-3) into the Carmen-Kozeny equation, equation (2-2), results in the following relationship:

$$K = \left(\frac{\varphi_e^3}{(1-\varphi_e)^2}\right)\left[\frac{1}{2\tau^2 S_{gv}^2}\right] \tag{2-4}$$

where

K = permeability, $(\mu \text{ m})^2$

φ_e = effective porosity, (fraction)

The constant 2.0 represents the shape factor in the Carmen-Kozeny equation.

Taking the square root of equation (2-4) and replacing the constant 2.0 by the shape factor (Fs) results in:

$$\sqrt{\frac{K}{\varphi_e}} = \left(\frac{\varphi_e}{1-\varphi_e}\right)\left[\frac{1}{\sqrt{F_s}\tau S_{gv}}\right] \tag{2-5}$$

If the permeability is expressed in milli-darcy (md) in equation (2-5) instead of $(\mu \text{ m})^2$ then the Reservoir Quality Index (RQI) can be expressed by the following equation:

$$RQI(\mu m) = 0.0314\sqrt{\frac{K}{\varphi_e}} \tag{2-6}$$

where

RQI = reservoir quality index, $(\mu \text{ m})$

K = rock permeability, (md)

φ_e = effective porosity of the rock, (fraction).

Amaefule et al (1993) introduced the Flow Zone Indicator (FZI) concept:

$$FZI = \left[\frac{1}{\sqrt{F_s}\tau S_{gv}}\right] = \frac{RQI}{\varphi_z} \qquad (2\text{-}7)$$

where

$$\varphi_z = \frac{Pore - Volume}{Grain - Volume} = \left(\frac{\varphi_e}{1-\varphi_e}\right) \qquad (2\text{-}8)$$

In addition, Amaefule et al (1993) used equation (2-6) to build up a methodology for identification and characterization of hydraulic (flow) units within mappable geological facies by applying logarithm on both sides of equation (2-6) to get the following equation:

$$Log(RQI) = Log\varphi_z + LogFZI \qquad (2\text{-}9)$$

On a log-log plot of equation (2-9), all similar FZI values will lie on a straight line with unit slope. Each straight line will represent samples of similar pore-throat attributes and, thereby, constitute a single flow unit.

Recently, another technique was introduced by Ohen et al (1995) to obtain the reservoir quality index using NMR data. This equation is as follows:

$$RQI(\mu m) = \frac{\rho T_1}{\tau\sqrt{F_s}} \qquad (2\text{-}10)$$

where

ρ = surface relaxtivity (killing strength)from NMR,(μ m /sec)

T_1 = NMR Decay Time (mSec)

F_s = surface area to volume ratio of the pore space (S_p/V_p)

τ = tortuosity of the flow path

Ohen et al used equation (2-10) to obtain more accurate determination for the reservoir quality index (using NMR measurements). Then RQI was plotted versus porosity to obtain a better description of the reservoir rock.

2. 4. Development of New Flow Unit Models for Clean Formations

The purpose of the section is to develop several new models capable of providing a better description of the reservoir, through using the concept of reservoir quality index (RQI), in combination with permeability models appearing in the literature. Five models have been developed for enhancing reservoir description. These models have been validated using both simulated and actual data. Use of these newly-developed models for reservoir descriptions thus represents an economically-feasible tool, because application of these models requires only conventional well-logging derived data, which are available for all old and new oil wells.

2. 4. 1. New Flow Units Model Using Morris-Biggs Permeability Equation

Morris and Biggs (1967) developed the following equation for calculating the permeability of the reservoir rock:

$$K(md) = 250 * \left(\frac{\varphi^6}{S_{wirr}^2} \right) \qquad (2\text{-}11)$$

where

φ = porosity using porosity logs, (fraction)

S_{wirr} = irreducible water saturation, (fraction)

Nuclear Magnetic Resonance (NMR) provides an accurate measurements of several parameters of the reservoir rock. Here, Borgia (1994) introduced the following relation for calculating irreducible water saturation using NMR parameters as follows:

$$(S_{wir})_e = 959 * T_{1g}^{-0.70} * \varphi^{-0.35} \qquad (2\text{-}12)$$

where

T_{1g} = geometric mean longitudinal relaxation time from NMR, (see)

φ = porosity using porosity logs, (fraction)

Substituting equation (2-12) into equation (2-11) results in a new permeability model to calculate the permeability in clean formation as follows:

$$K(md) = 2.72 * T_{1g}^{1.4} * \varphi^{6.7} \qquad (2\text{-}13)$$

Then, this produces a new model for obtaining the permeability in clean formation using porosity and NMR data. Using equation (2-13) in RQI equation, equation (2-6), results in the following equation:

$$RQI(\mu m) = 5.18 * 10^{-4} * T_{1g}^{0.70} * \varphi^{2.85} \qquad (2\text{-}14)$$

where

T_{1g} = geometric mean longitudinal relaxation time from NMR, (sec)

Ohen et al (1995) then proposed a definition for reservoir quality index based on using NMR data as follows:

$$RQI(\mu m) = \frac{\rho T_1}{\tau \sqrt{F_s}} \qquad (2\text{-}15)$$

where

ρ = surface relaxtivity (killing strength)from NMR,(μ m /sec)

T_1 = NMR Decay Time (mSec)

F_s = surface area to volume ratio of the pore space (S_p/V_p)

τ = tortuosity of the flow path.

Equating equations (2-14) and (2-15) and applying logarithm on both sides of the resulting equation leads to:

$$Log(T_l) = 2.85 * Log\varphi + Log\left(\frac{5.18 * 10^{-4}\, \tau T_{1g}^{0.70} \sqrt{F_s}}{\rho}\right) \qquad (2\text{-}16)$$

This is a new flow unit model. It requires only NMR decay time and porosity data. Porosity can also be obtained using NMR. Borgia (1994) showed that porosity from NMR and other sources are almost the same. Fig. 2. 1. Table 2. 5. shows porosity and NMR decay time measurements. obtained by Ohen et al (1995). These measurements are used to validate the newly-developed flow unit model as shown in Fig. 2. 2. A log-log plot of (T_1) versus porosity produces a straight line. with a unique slope equal to 2.85 for each flow unit. with a specific intercept equal to the last term in the developed model. The result indicates that three flow units can be identified by drawing 3 straight lines (each one through a set of data points) of slope equal 2.85 and different intercepts.

The application of this model. equation (2-16). requires porosity and NMR data. However. only NMR data (including NMR porosity and NMR decay time) can be used.

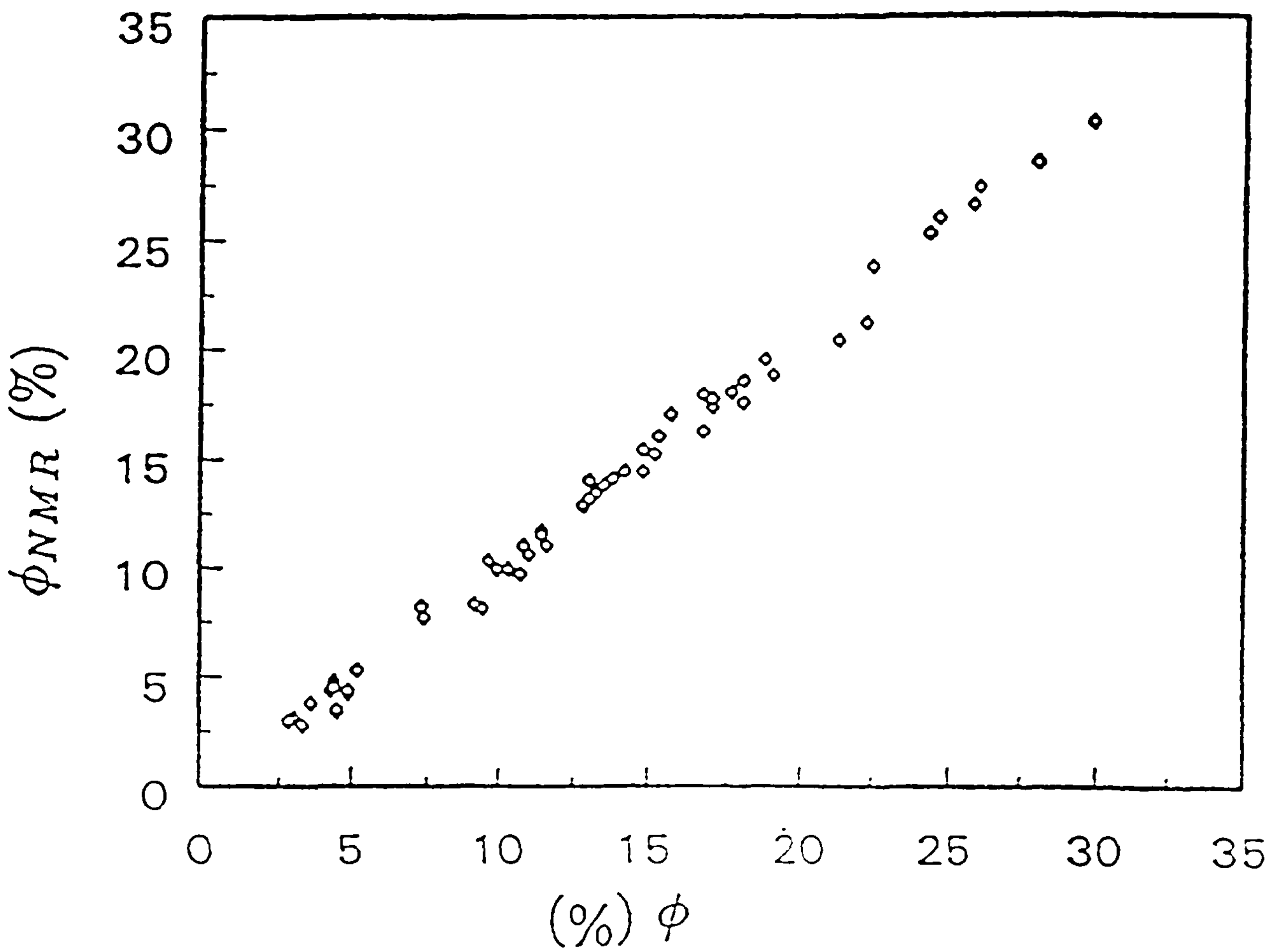

Fig. 2.1- Conventional porosity versus NMR porosity, [Borgia, 1994].

Table 2. 5- Porosity and NMR decay time values, (Ohen, 1995).

Porosity (fraction)	T_1 (see)
0.26	0.12
0.18	0.30
0.23	0.13
0.27	0.11
0.16	0.09
0.25	0.10
0.16	0.07
0.23	0.12
0.25	0.10
0.20	0.06
0.14	0.07
0.22	0.09
0.15	0.06
0.10	0.03
0.05	0.03
0.11	0.03
0.13	0.07

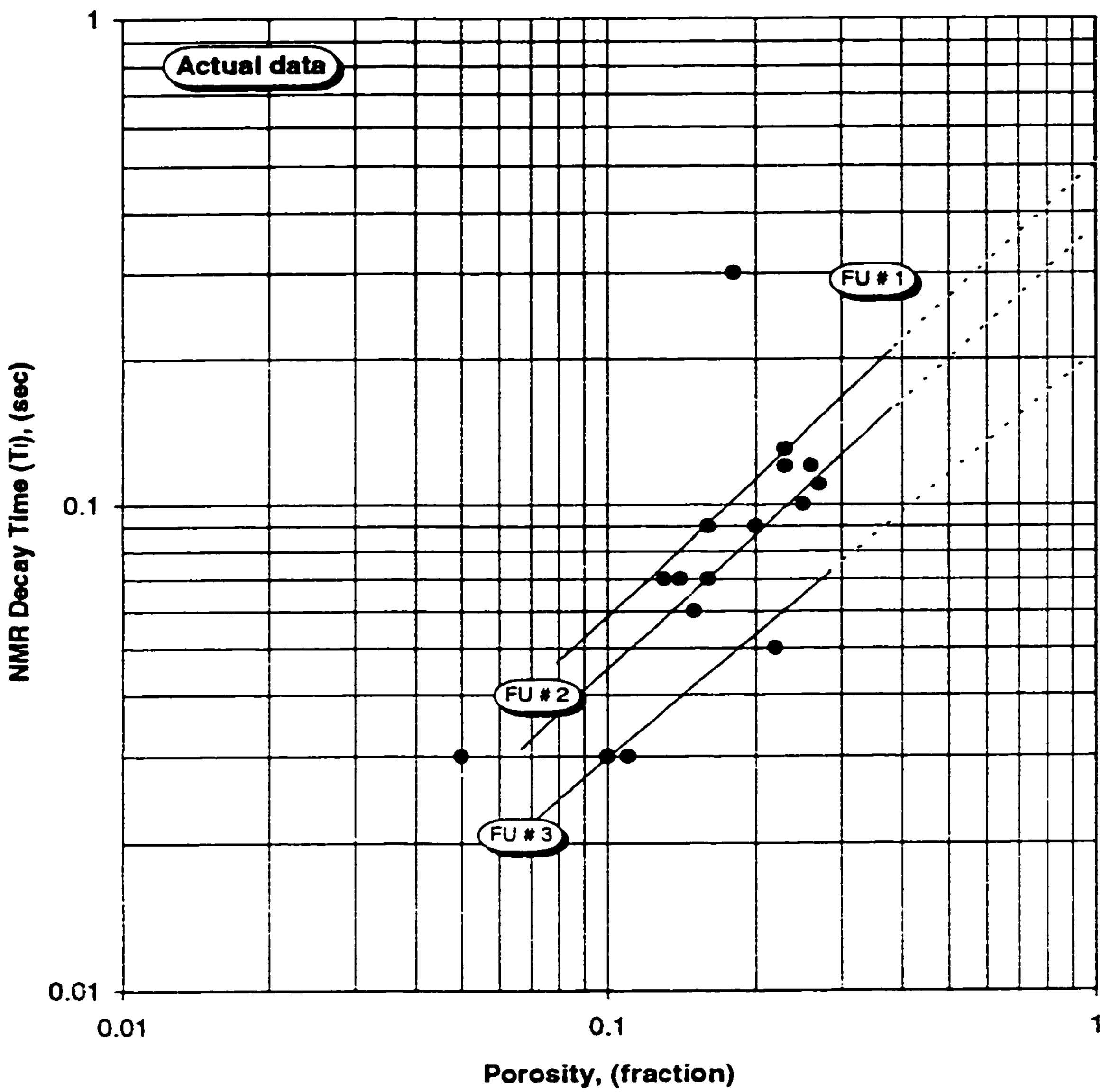

Fig. 2.2-New Flow Unit Model for characterizing clean formations using Morris-Biggs permeability equation (Actual Data, Ohen, 1995)

because calculation of the intercept is not required for the definition of several flow unit (comprising the pay zone of interest) within the reservoir under investigation.

This new model, equation (2-16) and Fig. 2. 2, show a crucial relationship between NMR relaxation time (T_1) and porosity for the purpose of defining flow units. Using Ohen's data (1995), Table 2. 5. of porosity and NMR decay time (T_1), the application of this newly-developed flow unit model defines 3 flow units. Knowing the slope of the straight line defining each flow unit results in an accurate definition for the flow units comprising the reservoir rock even though the number of data points is not sufficient.

Application of this new flow unit model requires only measurements of porosity and relaxation NMR time values for the obtained cores. Then, plot porosity versus relaxation time, with the knowledge that slope of each line equals 2.85, provides a good and effective means for identification flow units residing in the producing zone. This flow unit model has two unique parameters including the slope of straight line defining flow unit (slope = 2.85) and the intercept of that straight line at porosity = 1.0. Each flow unit has its intercept value. For the previously used data in Fig. 2. 2. the intercepts of the 3 flow units have been determined as:

Intercept of flow unit # 1 (I_1) = 0.49

Intercept of flow unit # 2 (I_2) = 0.34

Intercept of flow unit # 3 (I_3) = 0.20

The intercept involves several parameters such as tortousity (τ), NMR relaxation time (T_1), specific surface area (F_s) and surface relaxativity (ρ). Therefore, if only one of these parameters is unknown, then it can be calculated using the corresponding value of that intercept.

2. 4. 2. New Flow Unit Model Using NMR Model

Sen et al (1990) introduced the following equation for the purpose of getting the permeability with the aid of NMR measurements:

$$K(md) = 0.794 * \left(\varphi^{m} T_{l}\right)^{2.15} \qquad (2\text{-}17)$$

where

T_l = NMR Decay Time (sec).

Using the above equation of permeability in the equation of RQI, equation (2-6) results in the following equation:

$$RQI = 0.028 * T_l^{1.075} * \varphi^{(2.15m-1)/2} \qquad (2\text{-}18)$$

Taking the logarithm of equation (2-18) then yields:

$$Log(RQI) = (1.075m - 0.5) Log\varphi + Log\left(0.028 * T_l^{1.075}\right) \qquad (2\text{-}19)$$

Equation (2-19) reveals that, for any hydraulic (flow) unit, a log-log plot of a "Reservoir Quality Index" (RQI) which is defined by equation (2-18) versus porosity (φ), should yield a straight line with a slope equal to {(1.075m) - 0.5} and a unique intercept at porosity (φ) =1.0, equal to the flow zone indicator (FZI)=0.028* $T_l^{1.075}$, Fig. 2. 3.

Application of this new flow unit model requires only the porosity data and the NMR relaxation time. The NMR data in Table 2. 6 is used to calculate the Reservoir

Quality Index (RQI) as follows: porosity reading # 1 = 26 % and NMR time reading # 1= 0.12. Calculation of RQI using equation (2-18) results in RQI # 1 = 0.07.

The calculation is repeated for the rest of the data points to obtain other values of RQI. A plot of the calculated RQI values versus porosity yields Fig. 2. 3 in which two flow units can be drawn. Each flow unit is represented by a single line and reveals consistent values of porosity and RQI.

For the reservoir having several flow units, a group of parallel lines (having the same slope) can then be obtained, where each of these parallel lines represents a single flow unit having similar pore-throat attributes. Each straight line passes through each set of data points having similar values of porosity, permeability, and pore body/pore-throat distribution. Other surface properties of the rock (NMR relaxation time "T_1") defines a single flow unit.

2. 4. 3. New Flow Units Model Using Wyllie and Rose Permeability Equation:

Archie's equation for calculating water saturation is given as

$$S_w^n = \frac{FR_w}{R_t} \tag{2-20}$$

where

n = water saturation exponent (usually n = 2)

S_w = water saturation, (fraction)

F = Formation Resistivity Factor

R_w = Formation Water Resistivity, (ohm-m)

R_t = True Formation Resistivity, (ohm-m)

Table 2. 6- Porosity and NMR Decay Time Values used to calculate Reservoir Quality Index (RQI) for Validating the Flow Unit Model Using NMR Equation.

Porosity (%)	T (see)	RQI (um)
26	0.12	0.07
18	0.30	0.12
23	0.13	0.06
27	0.11	0.06
16	0.09	0 03
25	0.10	0.05
16	0.07	0.02
23	0.12	0.06
25	0.10	0.05
20	0.09	0.04
14	0.07	0.02
22	0.05	0.02
15	0.06	0.02
10	0.03	0.01
5	0.03	0.00
11	0.03	0.01
13	0.07	0.02

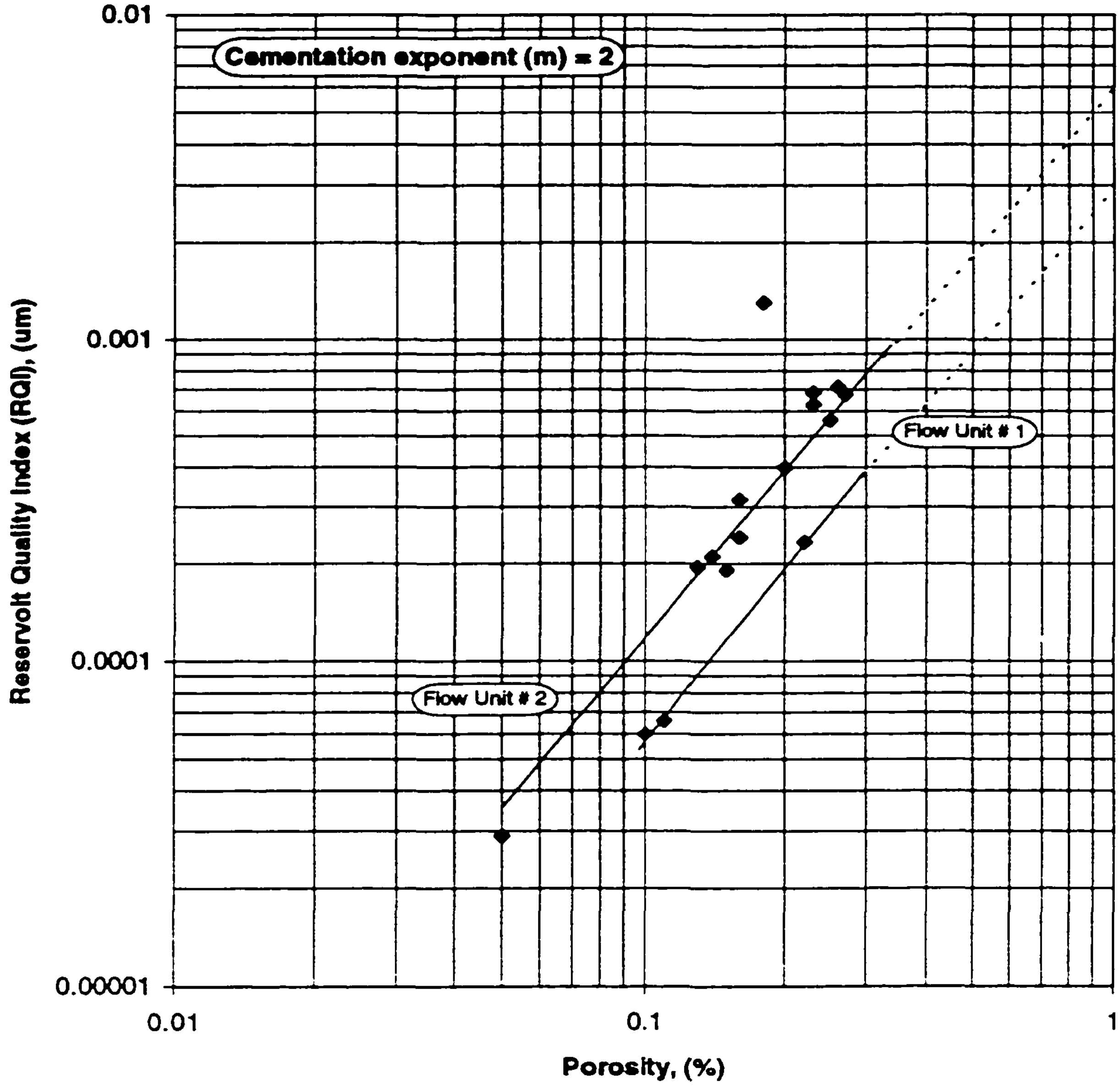

Fig. 2. 3 - Validation of the New Flow Unit Model Using NMR data

Wyllie and Rose (1950) permeability equation is given as follows:

$$K(md) = 62500 * \left(\frac{\varphi^{3m}}{S_{wirr}^{n}} \right) \tag{2-21}$$

where

n = water saturation exponent (usually n = 2)

S_w = water saturation in clean formation, (fraction)

Applying irreducible water saturation condition on equation (2-20) and substituting it into equation (2-21) results in the following equation:

$$K = 62500 * \left(\frac{R_t}{FR_w} \right)_{wirr} * \varphi^{3m} \tag{2-22}$$

Using Archie equation for formation resistivity factor into equation (2-22) yields:

$$K = 62500 * \left(\frac{R_{ti}}{aR_w} \right) * \varphi^{4m} \tag{2-23}$$

where

a = coefficient of Archie's equation

m = porosity exponent (or cementation exponent)

R_w = formation water resistivity, (ohm-m)

K = permeability of the rock, (md)

R_{ti} = true formation resistivity at irreducible water conditions, (ohm-m)

Equation (2-23) represents a new model for getting permeability using the resistivity and porosity data from well logs. The most clear advantage of this derived model is that it correlates the electrical and flow properties of porous medium. In addition, this model is not restricted to calculating irreducible water saturation (as other models do) because it requires only reading the true formation resistivity in oil zone (R_{ti}). Another advantage of this new permeability equation is that it does not require calculation of irreducible water saturation.

Substituting equation (2-23) into RQI equation, equation (2-6), produces an equation for reservoir quality index (RQI) in terms of well-logging data as follows:

$$RQI(\mu m) = 7.85 * \varphi^{\frac{4m-1}{2}} * \left(\sqrt{\frac{R_{ti}}{aR_w}} \right) \qquad (2\text{-}24)$$

Applying logarithm on both sides of equation (2-24) provides:

$$Log(RQI) = \left(\frac{4m-1}{2} \right) Log\varphi + Log\left(7.85 * \left(\sqrt{\frac{R_{ti}}{aR_w}} \right) \right) \qquad (2\text{-}25)$$

Equation (2-25) reveals that in a clean sandstone reservoirs, a log-log plot of Reservoir Quality Index (RQI) versus porosity provides a straight line for each flow unit with a unique slope equal to $\left(\frac{4m-1}{2} \right)$ and a unique intercept equal to ($7.85 * \sqrt{R_{ti} / aR_w}$) at porosity equals unity, when Wyllie and Rose equation is used for calculating the permeability in that specific reservoir.

This newly-developed flow unit model, Equation (2-25), will provide a group of straight lines, with a unique slope, that defines several flow units in clean formation. Each sub-zone of the rock having similar values of rock coefficient (a), formation water resistivity (R_t), true formation resistivity at irreducible water saturation (R_{ti}), porosity (φ), and permeability (K) is expected to produce similar values of Reservoir Quality

Index (RQI). Therefore, it is easy to define a flow unit by drawing a single straight line through each group of similar data points.

Using the simulated data of Table 2. 7, three flow unit are defined as shown in Fig. 2. 4. Data of Table 2. 7 of porosity (for reading #1 = 0.12) and permeability (for reading # 1 = 70 md) is used to calculate the RQI using the following equation:

$$RQI(um) = 0.0314 * \sqrt{K / \varphi_e} = 0.0314 * \sqrt{70 / 0.12} = 0.76.$$

The calculation is repeated for the rest of the data points resulting in several values of Reservoir Quality Index (RQI). A log-log plot of the Reservoir Quality Index (RQI) versus porosity, Fig. 2. 4. shows that three straight lines can be drawn, each one through a group of data points. Each straight line defines a single flow unit and it has a unique slope equals to 1.5 and a specific intercept having the following values for each flow unit.

Intercept of flow unit # 1 (I_1) = 53

Intercept of flow unit # 2 (I_2) = 21

Intercept of flow unit # 3 (I_3) = 14.8

These intercept values represent average values for a group of several parameters including Archie's coefficient (a), formation water resistivity (R_w), true formation resistivity (R_t), and resistivity of 100 % brine-saturated rock (R_o). Each flow unit has its unique average values of all for these parameters.

Table 2. 7 - Simulated data for validating flow unit model based on Wyllie and Rose equation

Reading #	Porosity (fract.)	K (md)	RQI (um)
1	0.12	70	0.758382
2	0.15	130	0.924391
3	0.16	192	1.0877279
4	0.13	48	0.6033629
5	0.18	340	1.3646864
6	0.23	71	0.5516897
7	0.19	476	1.5716518
8	0.25	121	0.6908
9	0.31	482	1.2381473
10	0.34	780	1.5039642
11	0.3	296	0.9863133
12	0.27	310	1.0639681
13	0.26	232	0.9379657
14	0.28	219	0.8781581

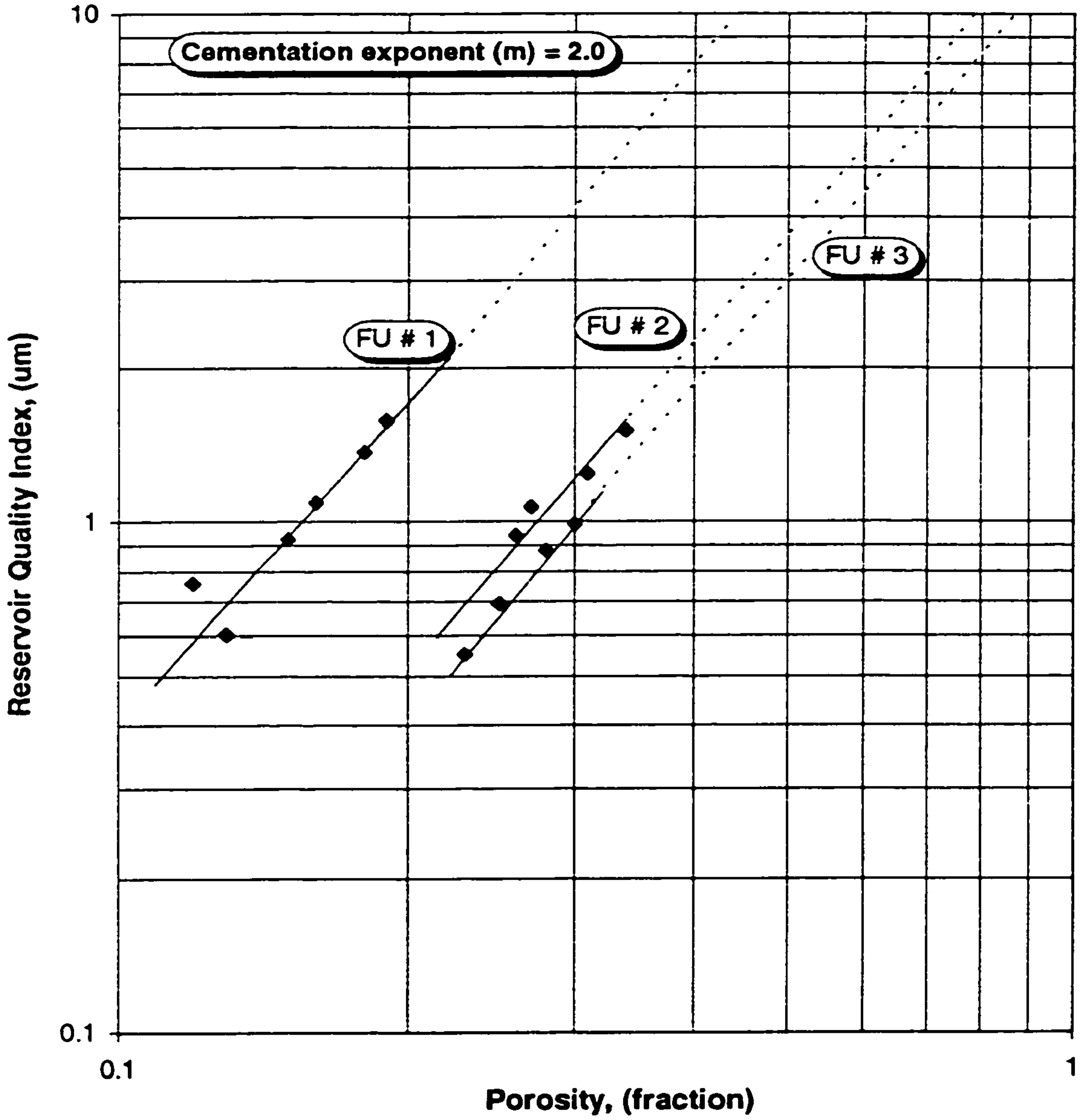

Fig. 2.4-Validation of flow unit model using Wyllie and Rose permeability equation

2. 4. 4. New Flow Unit Model Using Timur Permeability Equation

Timur (1968) used 155 sandstone samples from three different oil fields in North America to establish such a correlation among permeability, porosity and irreducible water saturation. Timur (1968) then proposed the following empirical equation for permeability calculation:

$$K(md) = (93)^2 * \left(\frac{\varphi^{4.4}}{S_{wirr}^2} \right) \tag{2-26}$$

where

n = water saturation exponent of Archie's equation

S_{wirr} = irreducible water saturation, (fraction)

φ = rock porosity, (fraction)

Using Archie's equation for water saturation:

$$S_w^n = \frac{aR_w}{\varphi^m R_t} \tag{2-27}$$

Using irreducible water saruration exponent = n instead of two in equation (2-26) provides more generality for equation (2-26) application. Applying irreducible water saturation (S_{wirr}) condition on equation (2-27), and then using it in equation (2-26) provides the following equation for permeability calculation:

$$K(md) = (93)^2 * \left(\frac{R_{ti}}{aR_w} \right) * \varphi^{(m+4.4)} \tag{2-28}$$

Equation (2-28) is another permeability model for clean formation. Next, using equation (2-28) into the RQI equation, equation (2-6), that was introduced by Amaefule et al (1993) provides the following:

$$RQI(\mu m) = 2.92 * \varphi^{(m/2)+1.7} * \sqrt{\frac{R_{ti}}{aR_w}} \tag{2-29}$$

Applying the logarithm on both sides of equation (2-29) provides

$$Log(RQI) = \left(1.7 + \frac{m}{2}\right) Log\varphi + Log\left(2.92 * \sqrt{\frac{R_{ti}}{aR_w}}\right) \tag{2-30}$$

This equation, (2-30), reveals a new flow-unit model, which has the following two unique features: (1) each flow unit will be represented by a straight line of slope equals [1.7+(m/2)], and (2) a unique intercept equals $\left(2.92 * \sqrt{R_{ti} / aR_w}\right)$ at porosity equals 1.0. The values of rock coefficient (a), formation water resistivity (R_w), true formation resistivity at irreducible water saturation (R_{ti}), porosity (φ), and permeability (K) represent good indication of the similarity of rock pore-throat/pore-body distribution. Therefore, the use of all these parameters can define similar flow units within the rock. This is achieved by drawing straight line though each group of similar data points. Using simulated data of Table 2. 8, each flow unit has a specific intercept which is obtained from Fig. 2. 5 with the following values:

Intercept of flow unit # 1 = 8.5

Intercept of flow unit # 2 = 6.1

Table 2. 8- Simulated data for validating flow unit model using Timur's permeability equation

Interval #	(Phi)o (fract.)	(Ko) (md)	(RQlo) (um)
1.00	0.40	603.31	1.22
2.00	0.38	481.42	1.12
3.00	0.37	1200.40	1.79
4.00	0.36	379.50	1.02
5.00	0.34	670.50	1.39
6.00	0.32	226.02	0.83
7.00	0.29	459.40	1.25
8.00	0.28	125.60	0.67
9.00	0.22	190.00	0.92
10.00	0.24	63.74	0.51
11.00	0.21	200.20	0.97
12.00	0.20	28.58	0.38
13.00	0.18	53.00	0.54
14.00	0.16	10.71	0.26
15.00	0.14	23.00	0.40
16.00	0.12	3.02	0.16
17.00	0.10	7.00	0.26
18.00	0.08	0.51	0.08
19.00	0.06	48.00	0.89
20.00	0.04	0.02	0.02

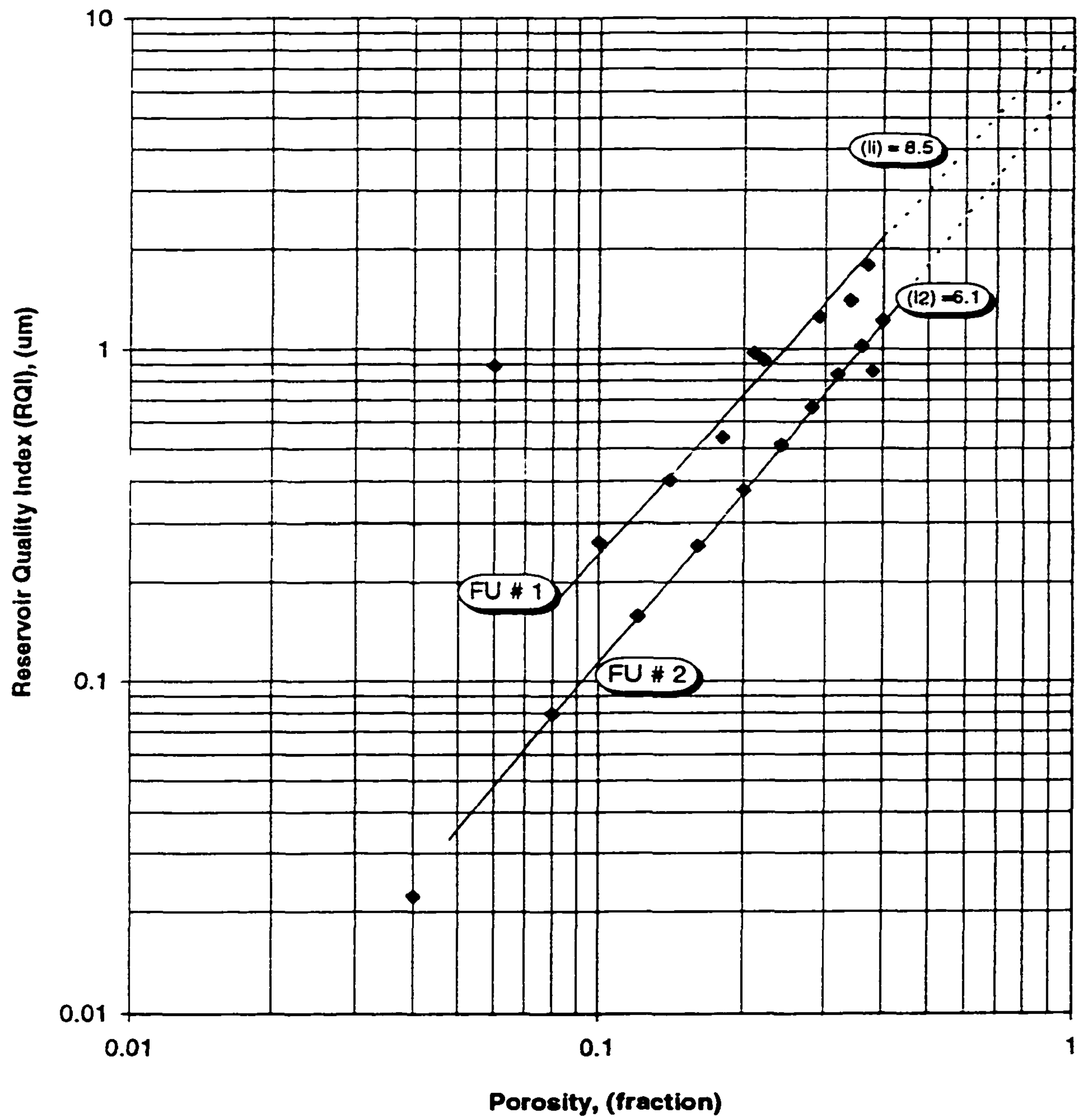

Fig. 2.5-Validation of flow unit model using Timur's permeability equation.

2. 4. 5. New Flow Unit Model Using Jorgensen Permeability Equation

Jorgensen (1986) introduced the following equation to calculate the permeability. The Jorgensen equation is independent of the irreducible water saturation, and also it represents a direct relationship between porosity (fraction) and permeability (md) as follows:

$$K(md) = 84105 * \left[\frac{\varphi^{m+2}}{(1-\varphi)^2} \right] \tag{2-31}$$

By definition of the formation resistivity factor is given by

$$F = \frac{a}{\varphi^m} = \frac{R_o}{R_w} \tag{2-32}$$

Solving equation (2-32) for porosity results in:

$$\varphi^m = \frac{aR_w}{R_o} \tag{2-33}$$

Substituting equation (2-33) into equation (2-31) then results in:

$$K = 84105 * \left(\frac{aR_w}{R_o} \right) * \left(\frac{\varphi}{1-\varphi} \right)^2 \tag{2-34}$$

Substituting the resultant equation of permeability, equation (2-34) into the equation of RQI, that is, equation (2-6), results in:

$$RQI(\mu m) = 9.11 * \left(\frac{\sqrt{\varphi}}{1-\varphi} \right) * \sqrt{\frac{aR_w}{R_o}} \tag{2-35}$$

Applying the logarithm on both sides of equation (2-35) thus provides

$$Log(RQI) = Log\left(\frac{\sqrt{\varphi}}{1-\varphi} \right) + Log\left(9.11 * \sqrt{\frac{aR_w}{R_o}} \right) \tag{2-36}$$

This model, equation (2-36), reveals that for a single flow unit a log-log plot of RQI versus $\left(\sqrt{\varphi}/(1-\varphi)\right)$ provides a straight line (having a slope equal to unity) and a unique intercept equals ($9.11*\sqrt{aR_w / R_o}$). This parameter $\left(\sqrt{\varphi}/(1-\varphi)\right)$, represents the ratio of square root of pore volume to grain volume of the reservoir rock. Use of this parameter $\left(\sqrt{\varphi}/(1-\varphi)\right)$ is better than the conventional ratio of pore to grain volume, because this ratio is more controlled by pore volume than grain volume. In addition, several parameters such as rock coefficient (a), formation water resistivity (R_w), and formation resistivity at 100 % water saturation (R_o) in the model intercept are helpful to secure similarity of rock properties and to define flow units comprising the reservoir rock of interest. Furthermore, Reservoir Quality Index (RQI) includes porosity (φ) and permeability (K) which are proved to be a good reflection for pore-throat/pore-size distribution.

This newly-developed model includes almost all the required measurements for better representation of a single flow unit. Simulated data indicated in Table 2. 9 of porosity and permeability is used to illustrate the application of this new model. A log-log plot of Reservoir Quality Index (RQI) versus the parameter $\left(\sqrt{\varphi}/(1-\varphi)\right)$ shows that two flow units can be identified. In this model it is really difficult to use the intercept at porosity equal to unity because the ratio of $\left(\sqrt{\varphi}/(1-\varphi)\right)$ will be infinity.

Table 2. 9- Simulated Data for Validating Flow Unit Model Based on Jorgensen Permeability Equation.

Porosity (%)	Perm. (K) (md)	RQI (um)	SQRT [Phi/(1-Phi)]
5.00	24.85	0.70	0.24
5.00	342.81	2.60	0.24
7.00	869.71	3.50	0.28
5.00	12.68	0.50	0.24
10.00	101.42	1.00	0.35
15.00	342.31	1.50	0.46
10.00	57.05	0.75	0.35
13.00	1392.68	3.25	0.41
3.00	87.93	1.70	0.18
10.00	171.41	1.30	0.35
15.00	342.31	1.50	0.46
15.00	219.08	1.20	0.46
10.00	1622.78	4.00	0.35
15.00	219.08	1.20	0.46
17.00	3890.24	4.75	0.50
20.00	3245.57	4.00	0.56
25.00	9128.16	6.00	0.67
30.00	1341.84	2.10	0.78
19.00	770.82	2.00	0.54
24.00	1521.36	2.50	0.64
20.00	657.23	1.80	0.56
25.00	649.11	1.60	0.67
33.00	2140.70	2.53	0.86
30.00	4523.60	3.86	0.78
35.00	3726.48	3.24	0.91
40.00	5858.25	3.80	1.05

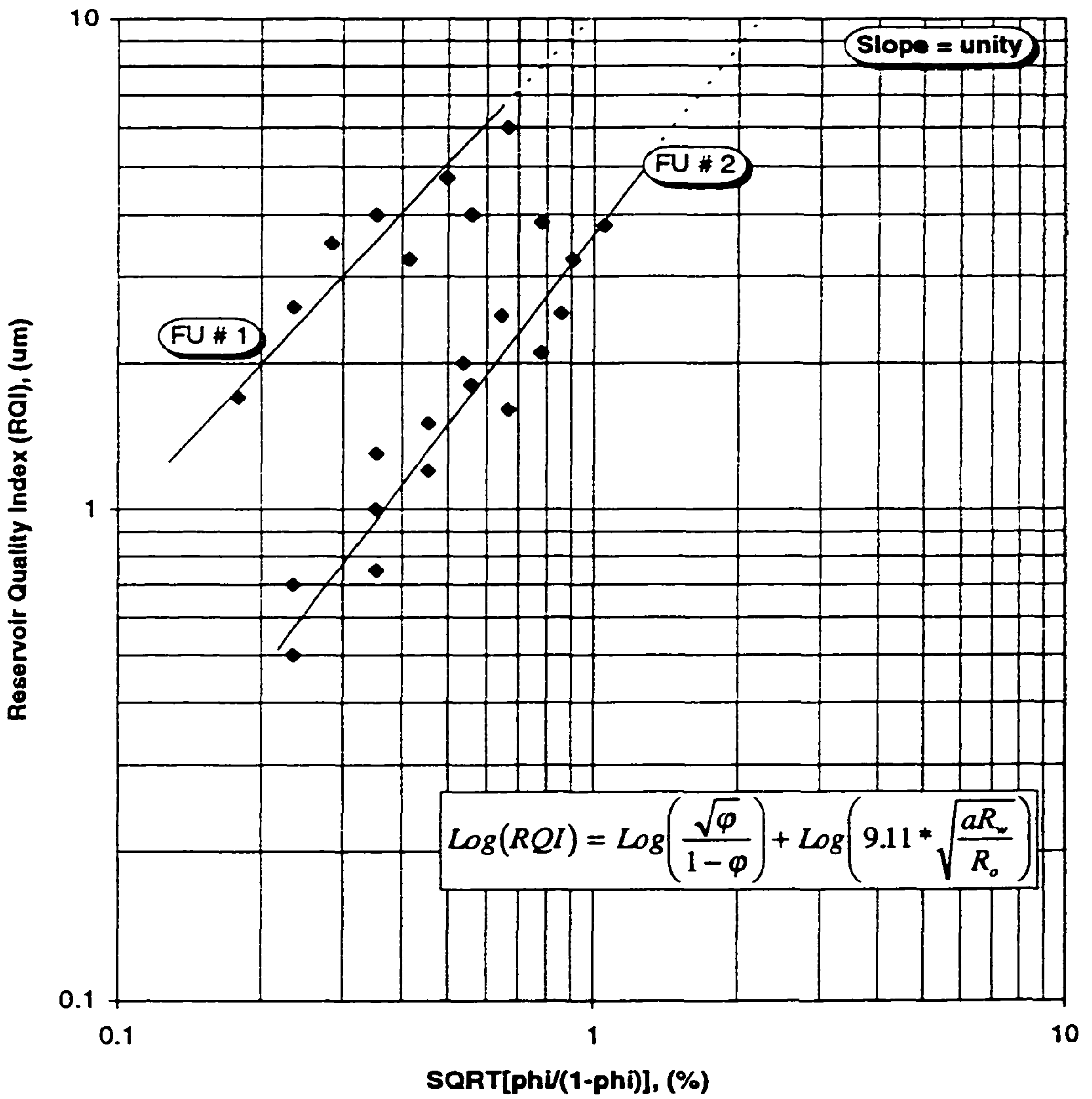

Fig. 2.6-Validation of flow unit model using Jorgensen permeability equation

2. 4. 6. Generalized Model for Reservoir Characterization and Flow Unit Identification in Clean Formations

Several equations are developed to calculate permeability. Ahmed (1991) and Nelson (1994) showed that more than sixty equations are available for obtaining permeability using core, well testing, and well logging data. This big number of permeability models creates a real need for a generalized model capable of identifying flow units and characterizing clean reservoirs. The purpose of this section is to develop a general flow unit model based on any permeability equation which is a function of porosity (φ) and irreducible water saturation (S_{wirr}). A general form of permeability equation (function of φ and S_{wirr}) can be written as follows:

$$K_o = \frac{C_1 * \varphi_o^{C_2 m}}{S_{wirr}^n} \qquad (2\text{-}37)$$

where

K_o = permeability of clean formation at zero stress condition

C_1 = coefficient of permeability equation

C_2 = coefficient of porosity exponent in permeability equation

φ_o = porosity at zero stress condition, (fraction)

S_{wirr} = irreducible water saturation, (fraction)

n = water saturation exponent in Archie's equation

m = porosity exponent

Archie's equation for water saturation, equation (2-27), at irreducible condition can be written as follows:

$$S^{n}_{wirr} = \frac{aR_w}{\varphi^m R_{ti}} \qquad (2\text{-}38)$$

where

a = coefficient of Archie's equation

R_w = formation water resistivity, (ohm-m)

R_{ti} = true formation resistivity at irreducible water condition, (ohm-m)

Substituting equation (2-38) into equation (2-37) yields

$$K_e = \left(\frac{C_1 R_{ti}}{aR_w}\right) * \varphi_e^{(C_2+1)m} \qquad (2\text{-}39)$$

Substituting equation (2-39) into Reservoir Quality Index equation, equation (2-6), results in

$$RQI_e = \left(0.0314 * \sqrt{C_1}\right) * \varphi_e^{\left[\frac{(C_2+1)m-1}{2}\right]} * \sqrt{\left(\frac{R_{ti}}{aR_w}\right)} \qquad (2\text{-}40)$$

Rearranging equation (2-40) and applying logarithm on both sides of the resulting equation yields

$$Log(RQI_e) = \left[\frac{(C_2+1)m-1}{2}\right] Log\varphi_e + Log\left\{\left(0.0314 * \sqrt{C_1}\right) * \sqrt{\left(\frac{R_{ti}}{aR_w}\right)}\right\} \qquad (2\text{-}41)$$

Equation (2-41) is a general model which can be used to identify flow units and characterize clean stress-insensitive formations. This model reveals that a single flow unit can be represented by a straight line having a slope equal to $\{[(C_2 + 1)m-1]/2\}$ and an intercept equal to $\left\{\left(0.0314 * \sqrt{C_1}\right) * \sqrt{\left(\frac{R_{ti}}{aR_w}\right)}\right\}$. This flow unit model is valid for any clean stress-insensitive formation obeying permeability equation (function of porosity (φ) and irreducible water saturation (S_{wirr})).

A comparison of this general flow unit model with the flow unit model using Wyllie and Rose equation, equation (2-25), and the flow unit model using Timur equation, equation (2-30), shows that a pattern of specific slope and intercept can be recognized. The values of permeability coefficients in Wyllie and Rose, and Timur can be listed as follows:

Coefficient	Wyllie and Rose	Timur
C_1	62500	$(93)^2$
C_2	3	2.2

Substituting these coefficients in the general flow unit model, equation (2-41), leads directly to the corresponding flow unit models based on Wyllie and Rose, and Timur permeability equations respectively. For example, using $C_1 = 62500$ and $C_2 = 3$ in equation (2-41) provides the flow unit model based on Wyllie and Rose, equation (2-25). Therefore, if the permeability equation of the reservoir under investigation has not been used by this study. Then, a new flow unit can be obtained by substituting the coefficients of the permeability equation (C_1 and C_2) of permeability equation of that reservoir into equation (2-41).

2. 5. Generalized Systematic Technique For Identifying Flow Units In Clean Formations

The following generalized systematic technique is recommended for using the newly-developed flow unit models or any other appropriate flow unit model for the reservoir of interest.

1. Determine the porosity of the formation at intervals of interest using porosity well-logging data such as the density, sonic, and/or neutron log. Use the porosity with the corresponding resistivity values (R_t and R_w) to calculate irreducible water saturation.
2. Choose a permeability model that was developed for a formation that is very similar to the formation (reservoir) of interest and substitute the previously calculated irreducible water saturation in the chosen permeability equation.
3. Read true formation resistivity (R_t) and the porosity at the same intervals of the well. Then, plot (R_t) versus porosity on a " Pickett Plot". Estimate the slope of the straight line by grouping the data and get the cementation exponent (m). Read the intercept of the same straight line on "Pickett Plot" which equal to (aR_w), then get the value of the coefficient "a", where formation water resistivity (R_w)can be obtained from SP log.
4. Using the previously calculated values of porosity, cementation exponent (m), resistivity of 100 % water saturated formation (R_0), true formation resistivity at irreducible water saturation(R_{ti}), determine the permeability values at chosen intervals of the well, and

5. Calculate values of the Reservoir Quality Index "RQI" using the flow unit model equation that corresponds to the permeability/porosity model. Plot RQI values versus porosity on a log-log graph, and draw straight lines defining several flow units in the formation of interest. Each zone of similar rock and fluid properties (true formation resistivity, water saturation, pore-body/pore-throat distribution) will constitute a single flow unit which can be easily recognized by drawing a straight line through these similar readings of that flow unit.

Table 2. 10 summaries all the flow unit models developed in this chapter to characterize clean heterogeneous formations with their corresponding permeability equation. Table 2.11 shows the assumption(s) and limitation(s) of all of the newly developed flow unit models developed in this chapter for clean formations.

This chapter reviews the concept of Reservoir Quality Index (RQI). Five models are developed for flow unit identification in clean stress-insensitive formations. In addition, a general flow unit model is developed and can be used for reservoir characterization of any formation that obeys a permeability equation (function of porosity and irreducible water saturation).

Table 2. 10- Summary of Newly-Developed Flow Unit Models Characterizing Clean Stress-Insensitive Formations

#	Newly-Developed Flow Unit Model	Used Permeability Equation
1.	$Log(T_l) = 2.85 * Log\varphi + Log\left(\dfrac{5.18 * 10^{-4}\,\tau T_{lg}^{0.70}\sqrt{F_s}}{\rho}\right)$	Morris-Biggs Equation
2.	$Log(RQI) = (1.075m - 0.5)Log\varphi + Log\left(0.028 * T^{1.075}\right)$	NMR (Sen et al) Equation
3.	$Log(RQI) = \left(\dfrac{4m-1}{2}\right)Log\varphi + Log\left(7.85 * \left(\sqrt{\dfrac{R_t}{aR_w}}\right)\right)$	Wyllie and Rose Equation
4.	$Log(RQI) = \left(1.7 + \dfrac{m}{2}\right)Log\varphi + Log\left(2.92 * \sqrt{\dfrac{R_t}{aR_w}}\right)$	Timur Equation
5.	$Log(RQI) = Log\left(\dfrac{\sqrt{\varphi}}{1-\varphi}\right) + Log\left(9.11 * \sqrt{\dfrac{aR_w}{R_o}}\right)$	Jorgensen Equation
6.	$Log(RQI_o) = \left[\dfrac{(C_2+1)m-1}{2}\right]Log\varphi_o + Log\left\{\left(0.0314 * \sqrt{C_1}\right) * \sqrt{\left(\dfrac{R_t}{aR_w}\right)}\right\}$	Generalized

Table 2. 11- List of assumptions and limitations of the newly-developed flow unit models for clean formations

Flow Unit Model Based on	Assumption(s) and Limitation(s)
Morris-Biggs Perm. Equation,	$C_t = (250)^2$ for medium gravity oil - clean formations
Model given by equation (2-16)	Permeability derived from well-log data
NMR Equation,	Permeability and porosity from NMR measurements
Model given by equation (2-19)	Clean formations
Wyllie and Rose Perm Equation.	Clean consolidated sandstones
Model given by equation (2-25)	Assumes P_c is inversely proportional to SQRT(K)
	Permeability derived from well-log data
Timur Perm Equation,	applicable for (a) Gulf Coast field (depth 9,000-12,000 ft)
Model given by equation (2-30)	(b) Colorado field (depth 6,000-7,000 ft), and (c) California field (depth 9,000 ft - 10,000 ft),
	Requires lab. measurements of porosity and permeability,
	Consolidated sandstones
Jorgensen's Equation	Clean sandstone reservoirs
Model given by equation (2-36)	Assumes that perm. is only a function of porosity and (m)
	Requires lab. measurements of porosity and perm.
Generalized Perm. Equation	Perm equation is function of porosity and S_{wirr} .
Model given by equation (2-41)	Clean formations

CHAPTER 3

CHARACTERIZATION OF FLOW UNITS IN SHALY FORMATIONS

The typical clastic reservoir rock consists of a complex and multi-component rock matrix-pore space system. Only very few oil and/or gas bearing sandstone reservoirs are essentially free of shale which contains clay minerals. Reservoir evaluation and characterization of shaly formations has long been a difficult task, which makes seeking enhanced reservoir description of shaly sand reservoirs much more difficult.

Fertl and Chilingarian, (1990) showed that the typical shaly clastic reservoir rocks frequently contain varying amounts of different clay minerals. Most common clay minerals exhibit significant difference in their basic properties including: chemical composition, matrix density, photoelectric cross-sections, hydrogen index (HI), cation exchange capacity (CEC), potassium (%), thorium (%), and uranium (%).

The relationship between different petrophysical properties and fluid saturation is well-known for clean sand reservoirs. The existence of shale in the reservoir rock is however, an extremely-disturbing factor because of the following reasons:

(a) it complicates the determination of oil-in-place,

(b) it considerably reduces the permeability of the reservoir rock for oil production, and

(c) it significantly affects the reservoir characterization of shaly sand producing formations.

In addition, Dewan (1983), showed that the existence of shale in the formation may produce the following effects:

(a) reduce the effective porosity, often significantly,

(b) lower the permeability, sometimes drastically, and

(c) alter the resistivity from that predicted by Archie's equation.

The existence of clay minerals affects all well-logging measurements to different degrees. Hence, shale effect should be considered during the evaluation of reservoir parameters such as porosity and water saturation. Fig. 3. 1 shows the effect of shale on several well logging tools and Fig. 3. 2 shows the fractions and properties of a typical shaly formation constituents.

Well-logging tools have been shown to be influenced by the existence of shale in producing formations. The distribution of shale in the formation affects the response of well logging tools. Well-logging readings in a shaly formation depend mainly on both the shale volume and physical properties of that shale. As a result, the interpretation of shaly formations is expected to be much more difficult and complicated than clean (free-shale) formations.

Shale is mainly composed of clay. The clay itself consists of extremely-fine particles that have very high surface area, and are therefore, capable of capturing a substantial amount of pore volume water to its surfaces. This water is usually called bound water, and contributes to the electrical conductivity of sands. For this reason, a higher amount of shale may kill the permeability and therefore the rate of oil production. Shaly oil-sands show different resistivity behavior than clean oil-sands. This makes interpretation of shaly sands much more complicated than clean formations.

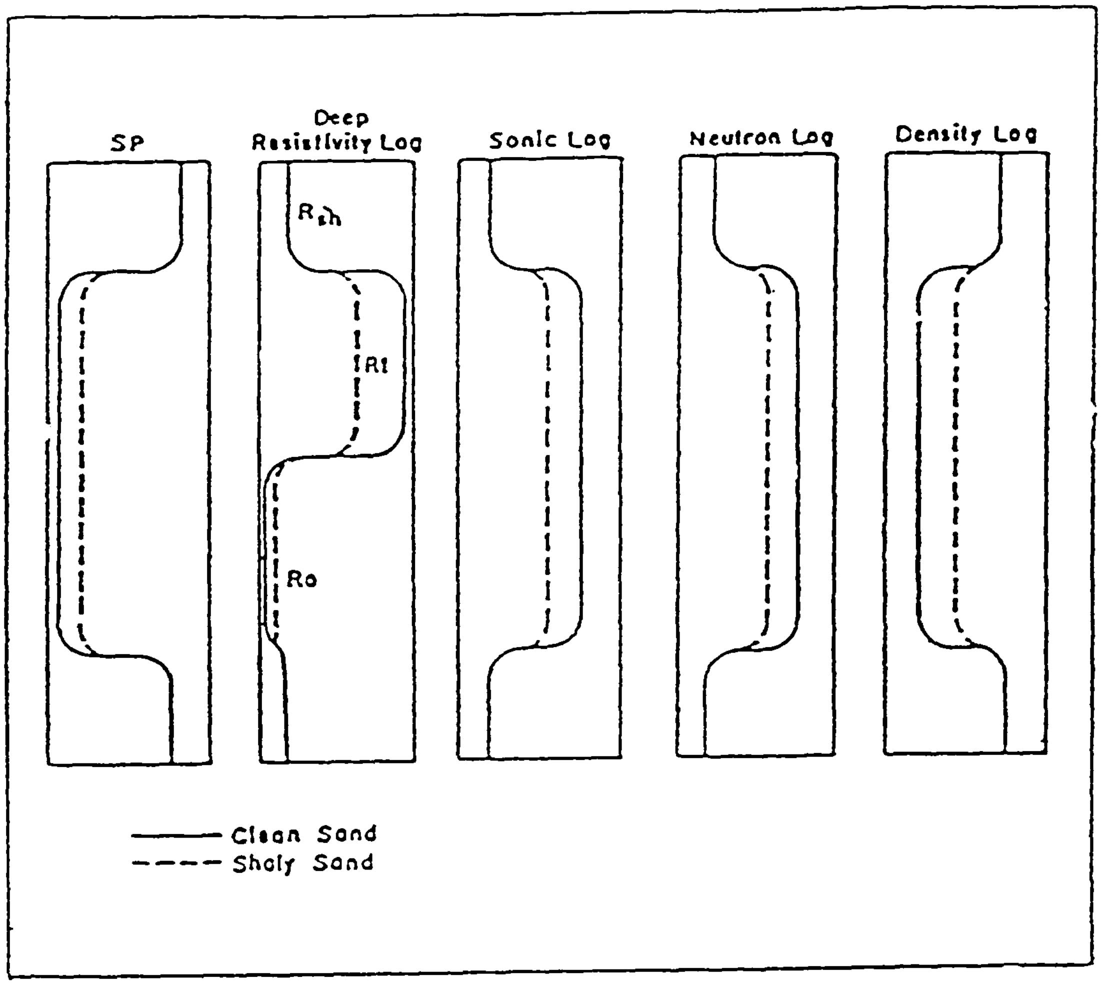

Fig. 3. 1- Idealized response of different tools, [Bassiouni, 1994]

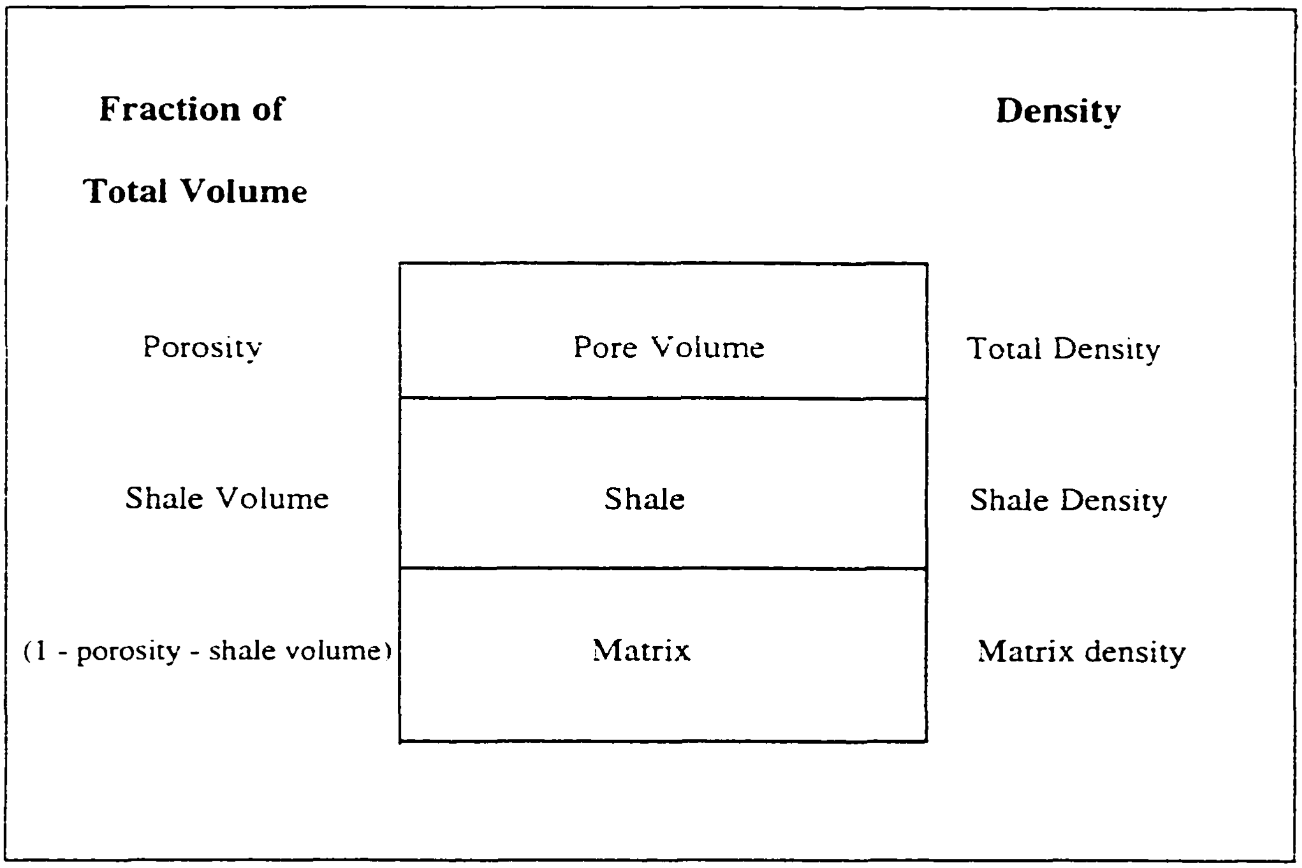

Fig. 3. 2 - Schematic of the fractions and properties of shaly formation constituents, [Bassiouni, 1994].

3. 1. Shale Distribution in Shaly Sands

The existence of shale in shaly-sand reservoirs may be one or more of three types: laminated, structural and dispersed shale. Fig. 3. 3 shows different types of shale. Based on core inspection, Schlumberger (1972) classified the shale distribution within the formation into three main forms:

1. Laminated shale: This shale may exist in the form of laminae between layers of sand. The laminar shale does not affect the porosity and the permeability of the sand streaks themselves. However, with increasing amounts of this type of shale in the porous medium, the porous where decreases leading to decrease in porosity and permeability of the system.
2. Structural shale: This shale may exist as grains or nodules in the formations. The properties of this type of shale are expected to be similar to laminated shale as described above. The effect of this type of shale on both porosity and permeability is expected to be negligible. In this type of shale, the clay grains may accumulate as clay particles (or mudstone clasts) and then take the place of sand grains. The existence of structural shale is minimal.
3. Dispersed shale: This shale material may be dispersed throughout the sand, partially filling the intergranular interstices. Dispersed shale may be in the form of accumulations adhering to the sand grains or may partially fill the smaller pore channels. The dispersed shale in the pores markedly reduces the permeability of the formation.

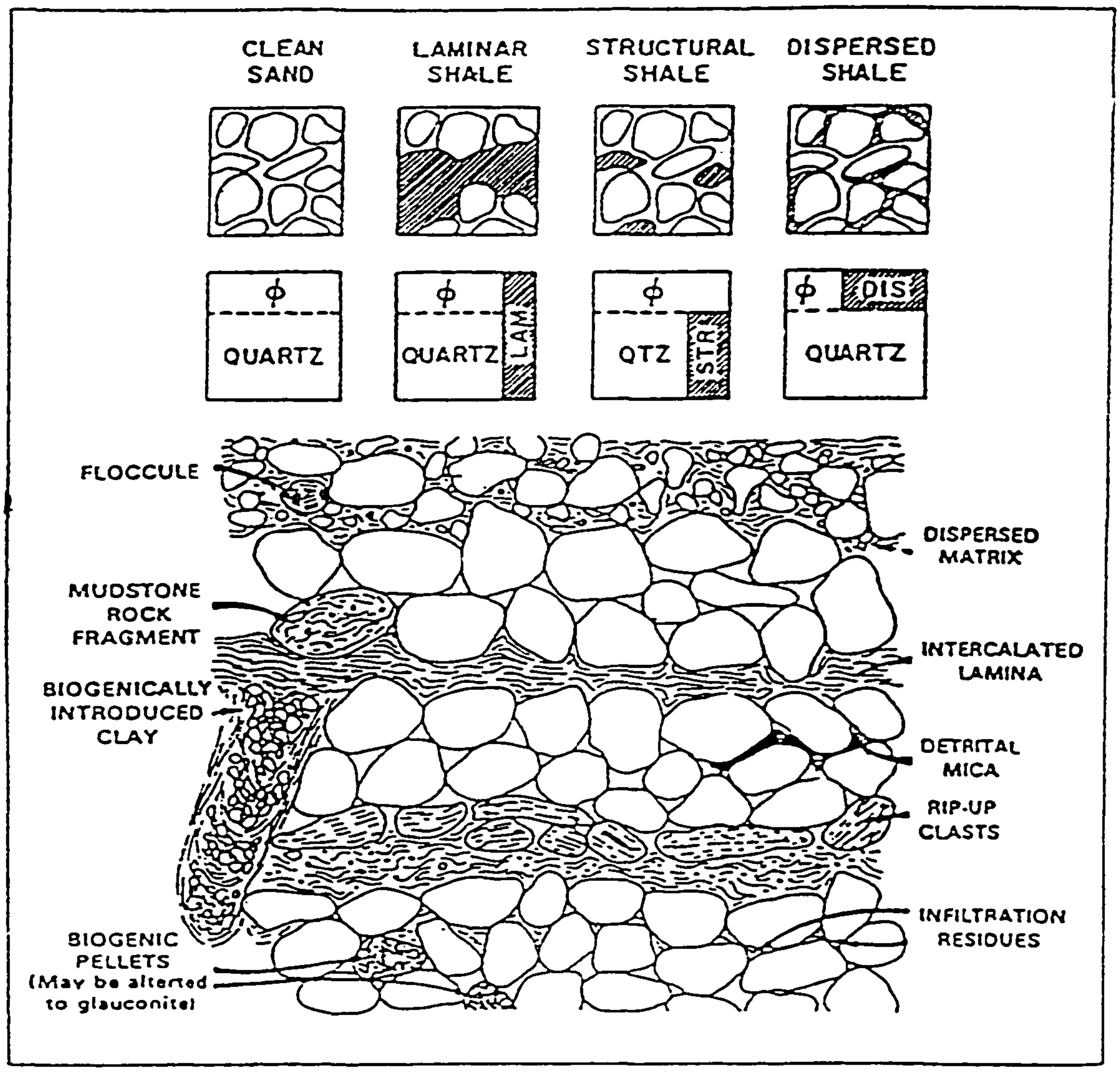

Fig. 3. 3 - Forms of shale distribution in sediments, [Dewan, 1983]

Neasham (1977), studied the effect of clay on permeability. He showed that the maximum amount of dispersed shale (which the sand reservoir can produce) is in the range of 15 to 40 % of the sand pore volume. Dispersed shale contains an authigenic clay which has been characterized as a discrete-particle, pore-lining, and pore-bridging type, based on scanning electron microscopes (SEM). Fig. 3. 4 shows the different forms of authigenic clay. Neasham (1977), also showed that the porosity-permeability relationship varies corresponding to the constituents of dispersed shale. Figs. 3. 4 and 3. 5 show the three categories described as follows:

(a) Discrete Particle clays reflect the typical mode of kaolinite occurrence in sandstones.

(b) Pore lining clays are attached to the walls of the pores and form continuous and thin clay mineral coating, and

(c) Pore bridging clays due to extensive growth of clay crystal within the pore system, lead to micro-porosity and tortuous fluid flow pathways.

Without considering shale distribution in the formation rocks, water saturation and effective porosity of a shaly sand can be determined by correcting the parameters involved in Archie's equation for the shaliness of the formation. This requires calculation of the volume of shale (V_{sh}).

3. 2. Shale Content Evaluation (Mixed Lithology)

It is important to determine the overall shale content of shaly formations for accurate calculation of porosity, using wireline log data such as neutron, density and sonic

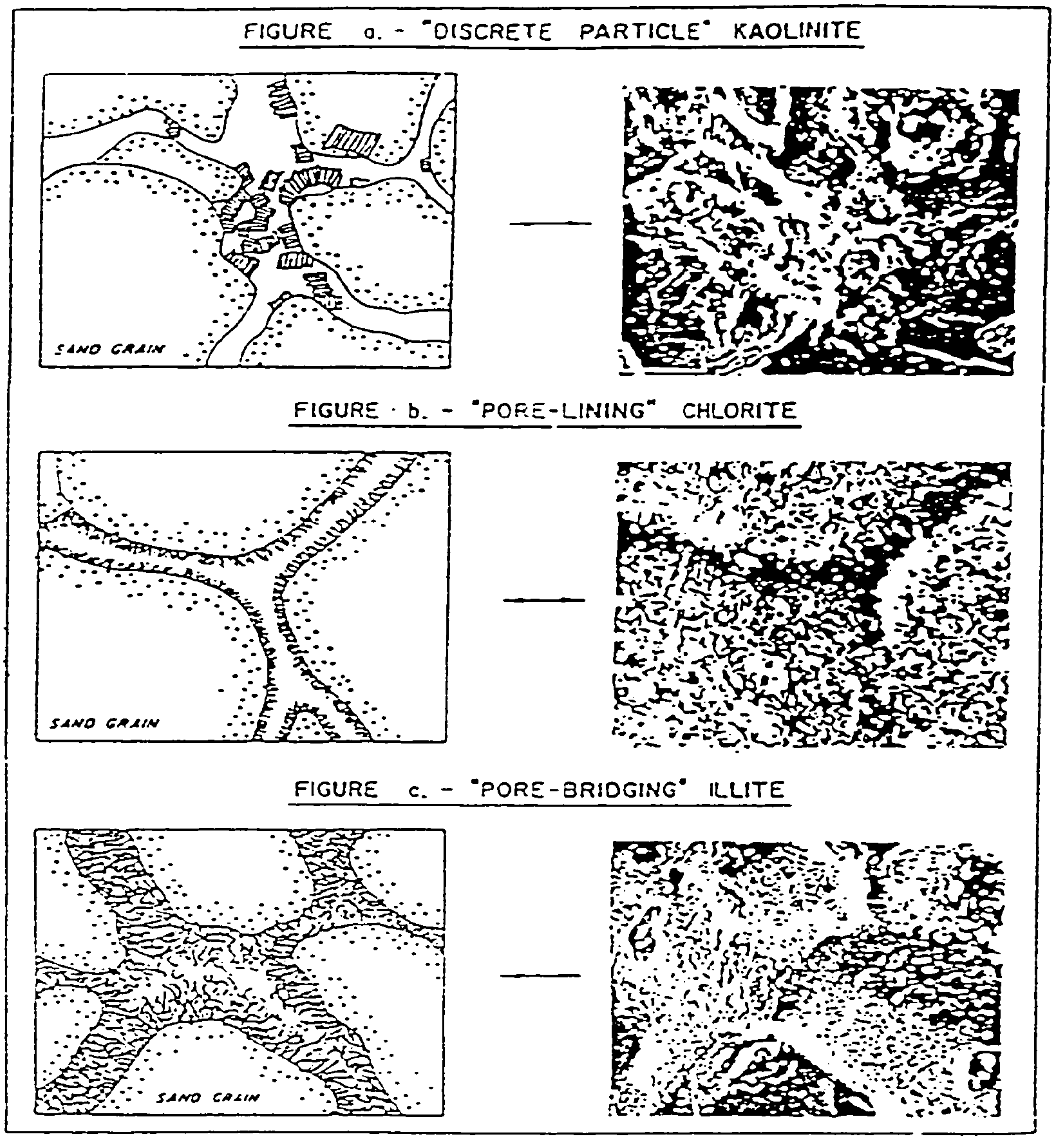

Fig. 3. 4 - Forms of Authigenic Clay in Sandstone Pore Space, [Neasham, 1977].

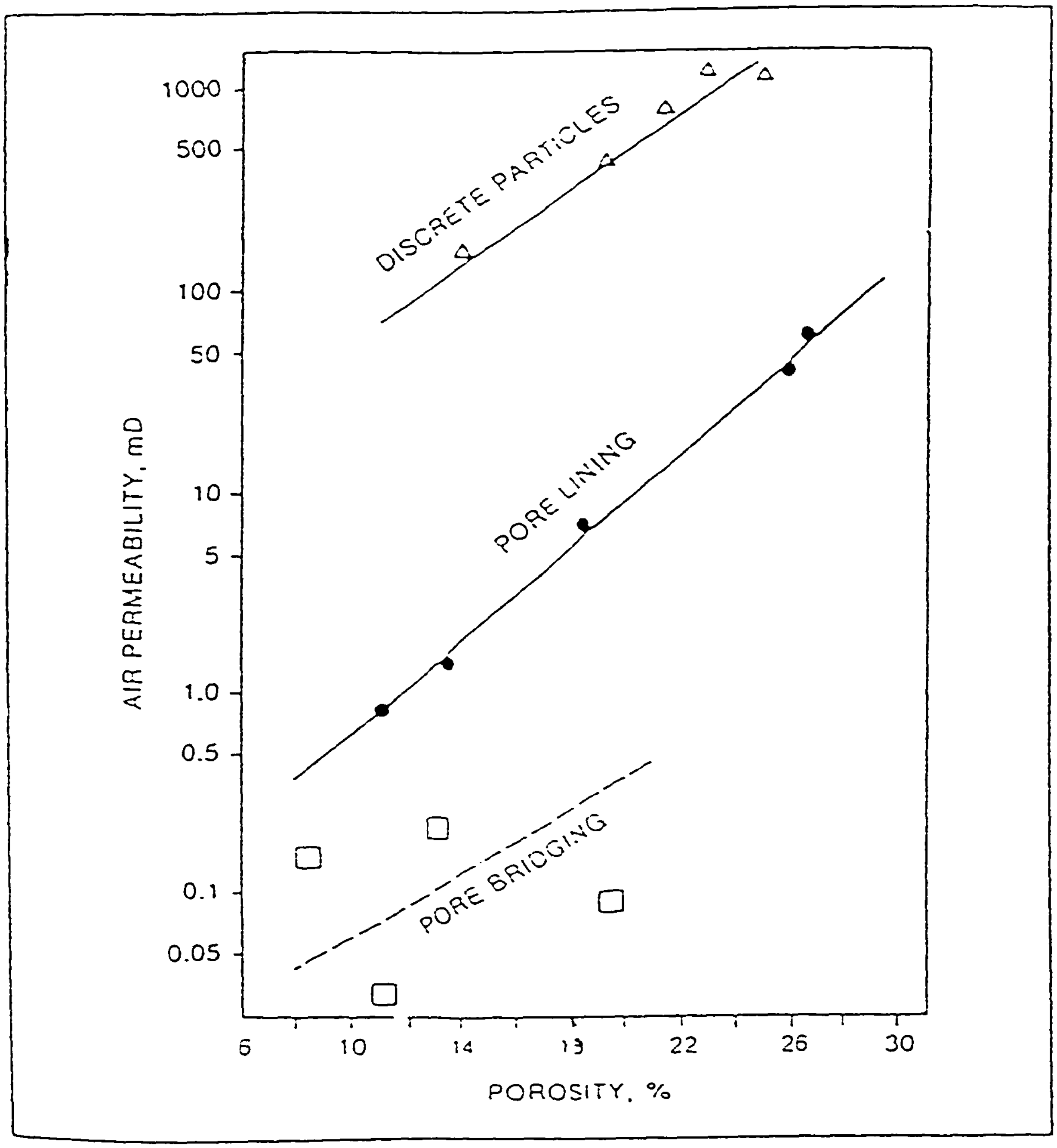

Fig. 3. 5 - Effect of clay type on permeability,[Neasham, 1977].

logs. Neglecting the effect of shale on calculated porosity (from neutron and/or sonic logs) will lead to higher values of porosity, and also erroneous estimation of permeability and oil-in-place (OIP). Several tools have appeared in the literature that can be used for evaluating shaly formations. These tools may be listed as follows:

1. Gamma Ray Log,
2. Spectralog Total Counts
3. Spectralog Potassium,
4. Spectralog Thorium,
5. Spontaneous Potential (SP),
6. Resistivity Logs,
7. Neutron Log,
8. Density-Neutron Crossplot,
9. Neutron-Acoustic Crossplot,
10. Density-Acoustic Crossplot.

A comprehensive review of equations that are currently used for shale-volume determination was done by the Society of Petroleum Well Log Analysts (SPWLA, 1982). At the end of the study, other models were added as shown in Table 3. 1. Twenty six equations have been included with the definition of the parameters and some conditions for their applications in order to calculate shale volume in mixed lithology.

Calculation of the shale volume is one of the most important keys to correct the shaliness of the formation. Therefore, reliable data must be obtained so that correct shale

Table 3.1 - Equations for shale volume determination

Logging tool	Equation for shale volume calculation	Remarks
Gamma Ray	(1) $V_{sh} = \dfrac{GR_L - GR_{min}}{GR_{max} - GR_{min}}$	Linear Approximation
	(2) $V_{shc} = \dfrac{2^{(V_{sh} * GCUR)-1}}{2^{GCUR-1}}$	V_{sh} from equation (1) V_{shc} = Corrected V_{sh} GCUR=2, older rocks. GCUR=3.7, Tertiary rocks.
	(3) $V_{shc} = X * V_{sh}$	X = Local Correction Factor V_{sh} from equation (1)
	(4) $V_{sh} = \dfrac{GR_L - A}{B}$	A, B = Geological Area Coefficients
	(5) $V_{sh} = \dfrac{\rho_B . GR - B_o}{\rho_{sh} * GR_{max} - B_o}$	ρ_B, ρ_{sh} = Correction Factors for Formation Density
	(6) $V_{sh} = \dfrac{(\rho_B * GR)^M * A}{B * \left(\dfrac{SI}{1 - SI}\right) + C}$	SI = statistical Index for Slit-shale A, B, C, M = Coefficients
Spectralog Total Counts	(7) $V_{sh} = \dfrac{CTS_L - CTS_{min}}{CTS_{max} - CTS_{min}}$	Linear Approximation
	(8) $V_{shc} = \dfrac{2^{(V_{sh} * GCUR)-1}}{2^{GCUR-1}}$	V_{sh} from equation (7) V_{shc} = Corrected V_{sh} GCUR=2, older rocks. GCUR=3.7, Tertiary rocks.
Spectralog Potassium	(9) $V_{shc} = \dfrac{2^{(V_{sh} * GCUR)-1}}{2^{GCUR-1}}$	V_{sh} from equation (1) V_{shc} = Corrected V_{sh} GCUR=2, older rocks. GCUR=3.7, Tertiary rocks.

Table 3.1 - Equations for shale volume determination (contd.)

Logging tool	Equation for shale volume calculation	Remarks
Spontaneous Potential (SP)	(10) $V_{sh} = 1.0 - \frac{SP}{SSP}$	
	(11) $1.0 - \frac{SP}{SSP} = \frac{Log(R_t / R_{xo})}{Log\left(\frac{(R_t / R_{xo} - V_{sh} R_t / R_{sh})}{1 - V_{sh} R_t / R_{sh}}\right)}$	Requires R_t, R_w, R_{sh}
	(12) $1.0 - \frac{SP}{SSP} = \frac{K_1 * V_{sh} * W_{sh}}{(K_1 * V_{sh} * W_{sh}) + \varphi * S_{xo}}$	W_{sh} = water content/shale vol.
Resistivity	(13) $V_{sh} = \left(\frac{R_{sh}}{R_{Log}}\right)^{1/b}$	b = 1.0 - 2.0
	(14) $V_{sh} = \left(\frac{R_{sh} * (R_{Lim} - R_t)}{R_{Log} * (R_{Lim} - R_t)}\right)^{1/b}$	R_{Lim} = Maximum Resistivity in Clean Formation
	(15) $\frac{1}{R_t} = \frac{V_{Wirr}}{\varphi} x \frac{V_{sh}}{R_{sh}} + \frac{V_{wirr}^2}{0.8 R_w}$	V_{wirr} = f (clean + shale)
Neutron	(16) $V_{sh} = \left(\frac{\varphi_N}{\varphi_{Nsh}}\right)$	Works for low porosity
	(17) $V_{sh} = \frac{\varphi_N - \varphi_{N\min}}{\varphi_{N\max} - \varphi_{N\min}}$	High in porous zone
Acoustic	(18) $V_{sh} = \frac{\varphi_{acoustic}}{(\varphi_{acoustic})_{sh}}$	High in porous zone

Table 3.1 - Equations for shale volume determination (contd.)

Logging tool	Equation for shale volume calculation	Remarks
DEN-NEU Crossplot	(19) $V_{sh} = A / B$ $A = \rho_B * (\varphi_{ma} - 1.0) - \varphi_N * (\rho_{ma} - \rho_f) - \rho_f * \varphi_{Nma} + \rho_{ma}$ $B = (\rho_{sh} - \rho_f) * (\varphi_{Nma} - 1.0) - (\varphi_{Nsh} - 1.0) * (\rho_{ma} - \rho_t)$	Can be too clean in gas formation
NEU-AC Crossplot	(20) $V_{sh} = A / B$ $A = \varphi_N * (\Delta t_{ma} - \Delta t_f) - \Delta t * (\varphi_{Nma} - 1.0) - \Delta t_{ma} + \varphi_{Nma} * \Delta t_f$ $B = (\Delta t_{ma} - \Delta t_f) * (\varphi_{Nsh} - 1.0) - (\varphi_{Nma} - 1.) * (\Delta t_{sh} - \Delta t_f)$	Dependent on assumed clean matrix
DEN-AC Crossplot	(21) $V_{sh} = A / B$ $A = \rho_B * (\Delta t_{ma} - \Delta t_f) - \Delta t * (\varphi_{Nma} - \rho_f) - \rho_f * \Delta t_{ma} + \rho_{Nma} * \Delta t_f$ $B = (\Delta t_{ma} - \Delta t_f) * (\rho_{sh} - \rho_f) - (\varphi_{Nma} - \rho_{f}.) * (\Delta t_{sh} - \Delta t_f)$	Sensitive to rugose borehole
Models using GR Models	(22) $I_{sh} = \dfrac{GR_L - GR_{\min}}{GR_{\max} - GR_{\min}}$	I_{sh} = Shale Index
	(23) $V_{sh} = 0.083 * (2^{3.7 I_{sh}} - 1.0)$	For Tertiary Rocks
	(24) $V_{sh} = I_{sh} / (3 - 2 * I_{sh})$	Stieber Equation
	(25) $V_{sh} = 1.7 - \sqrt{3.38 - (I_{sh} + 0.70)^2}$	Clavier et al Equation
	(26) $V_{sh} = 0.33 * (2^{2 I_{sh}} - 1.0)$	For Older Rocks

models can be used for the interpretation and calculation of fluid saturations and other parameters within the reservoir of interest.

3. 3. Electrical and Cation Exchange Capacity Properties of Shaly Sands

Since Shale is rich in clay minerals, the terms "Clayey" or " Shaly" has been used interchangeably in well logging and petroleum engineering. Clays are the sediments with grain diameter less than 0.004 mm. Also, clays are essentially composed of hydrous aluminum silicates and alumina. On the other side, shale is a sediment composed of clays and other variety of other fine-grained compounds. The distribution of shale in sand formation is shown in Fig. 3. 6 for laminated, dispersed and structural shales.

For clean or relatively clean sands, the relationship between resistivity or the formation resistivity factor and porosity is well known. However, the same relationship for shaly sands is much more complicated. Fig. 3. 7 shows the relationship between the rock conductivity and the formation water conductivity (C_w) which is not linear. At a certain value of water conductivity (C_w), the rock conductivity is much higher in comparison to that of clean (non-shaly) formation as explained by Worthington (1985).

Winsaur et al (1953) studied the ionic conductivity in double layers in reservoir rocks and introduced the model in Fig. 3. 8 for charge distribution in shaly sands. He explained that the increase of the apparent conductivity of shale is due to the fact that clays contribute to the total conductivity of the rock while the rock matrix is non conductive. The principal building elements of clays are:

(a) a sheet of silicon (Si) and oxygen (O) atoms in a tetrahedral arrangement, and

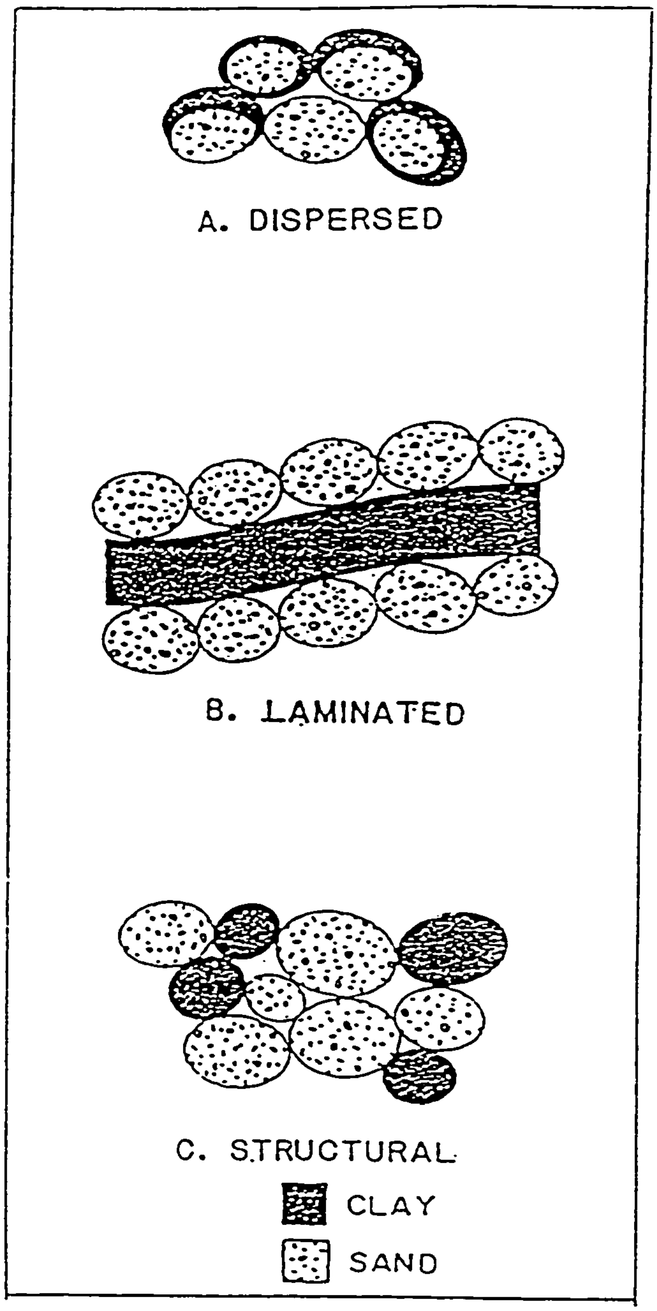

Fig. 3. 6 - Clay distribution modes, [Bassiouni, 1994]

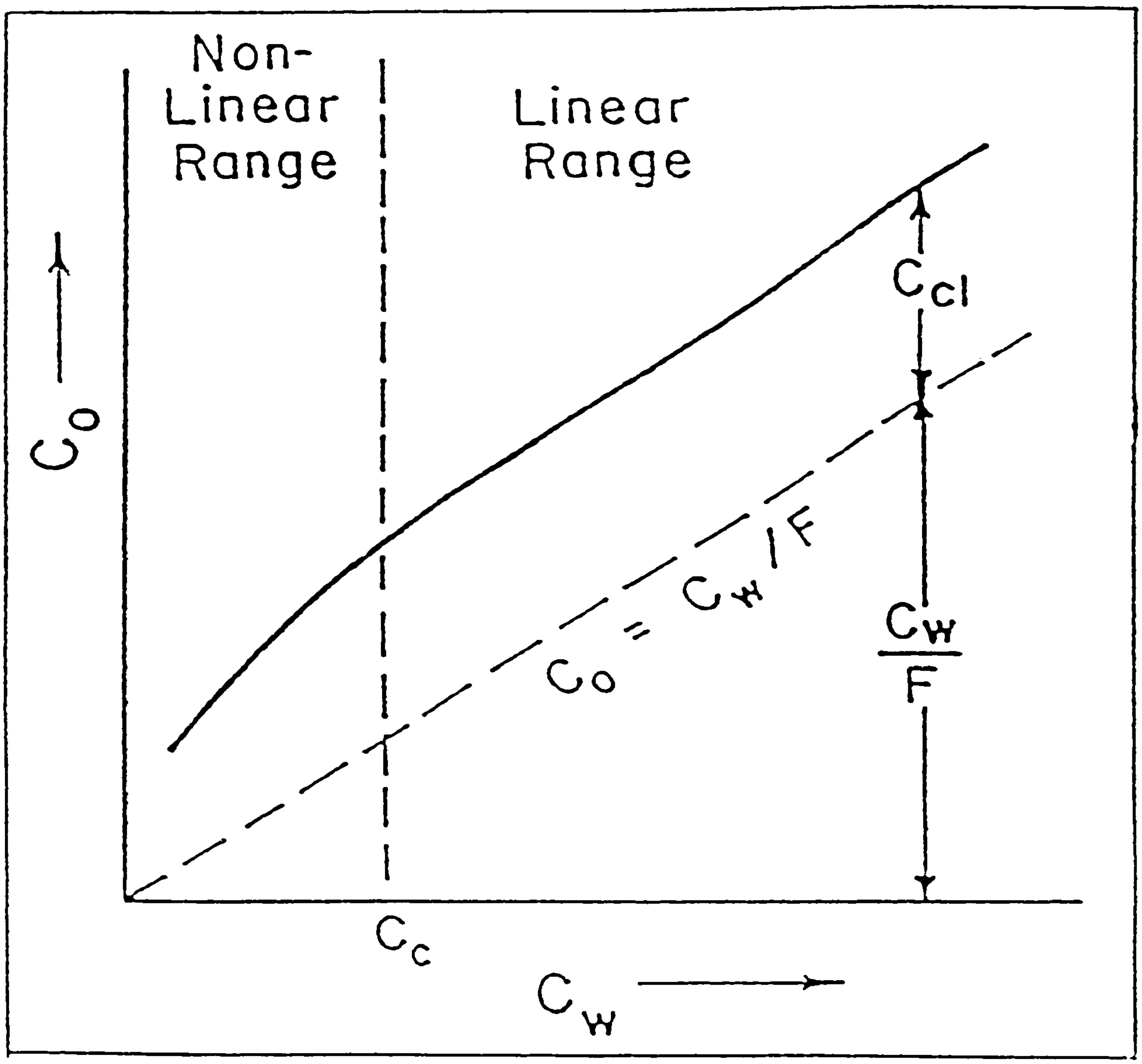

Fig. 3. 7 - Conductivity of shaly sand as a function of formation water conductivity,[Worthington, 1985]

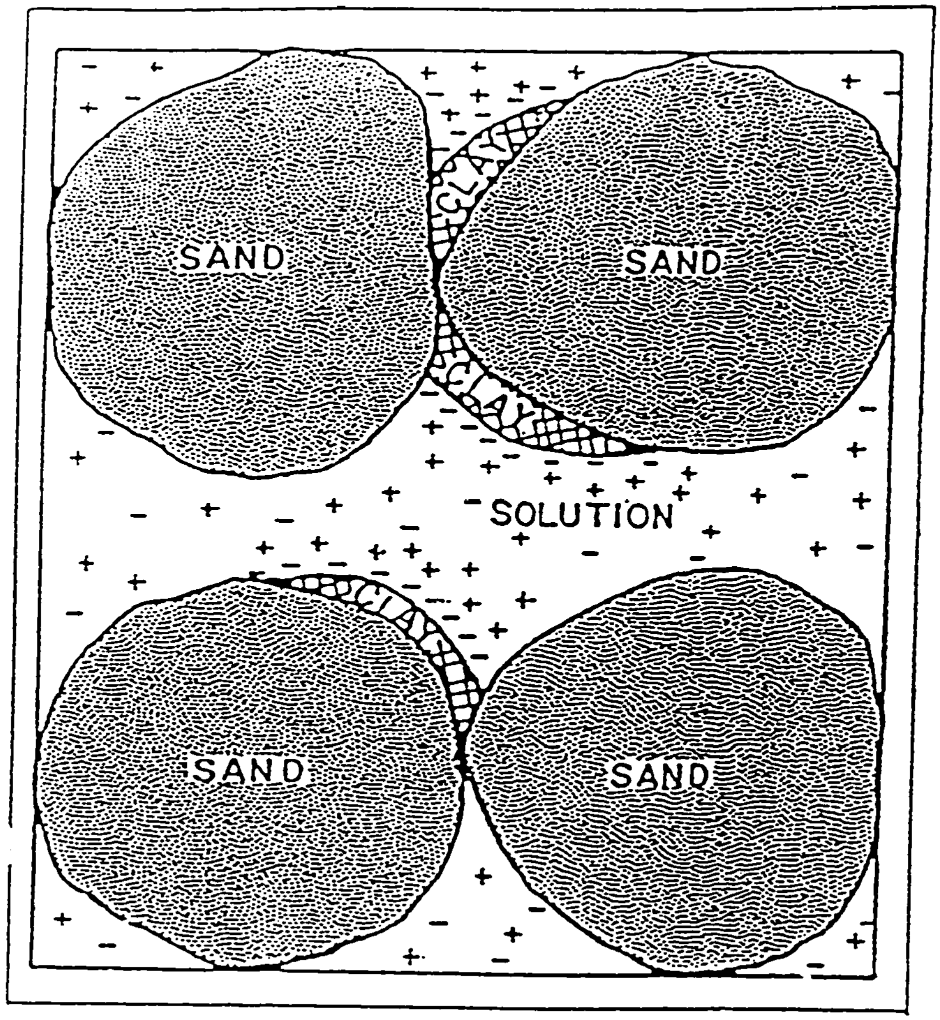

Fig. 3. 8 - Schematic of charge distribution in shaly sands, [Winsaur, 1953]

(b) a sheet of aluminum (Al), oxygen (O), and hydroxyl (OH) arrangement in an octahedral.

In the presence of water, the compensating cations, such as Ca, Mg, and Na, on the layer surface may be exchanged by other cations when available in solution; hence, they are called exchange cations. This property is called cation exchange capacity (CEC) and the number of these cations can be measured by Q_{CEC} expressed in meq/cc.

Swelling is one of the most important problems of shaly formations. When shale is contacted with water, shale is capable of absorbing certain amount of water. The water molecules penetrate the unit between the unit layers and the interlayer cation become hydrated. Some clay particles have a negative charges, and are balanced by the nearest cations to these shale particles. The diffusion characteristics of the counter-ions has been recognized, as shown in Fig. 3. 9. The diffusion layer thickness depends mainly on the salt concentration. In general, it decreases with increase in the salt concentration.

3. 4. Shaly Sand Interpretation Models

The interpretation of shaly sands is still not completely understood. Several models have been introduced for calculating water saturation with shaly formations. Recently, Worthington (1985) showed that the determination of water saturation in shaly formations still lacks a satisfactory solution. The use of the available shaly models provides significantly-different values of water saturation. Therefore, no universally-accepted model exists for log analysts. A real need then arises for a sound, scientific theory to yield a water-saturation model capable of providing a consistent and predictive performance.

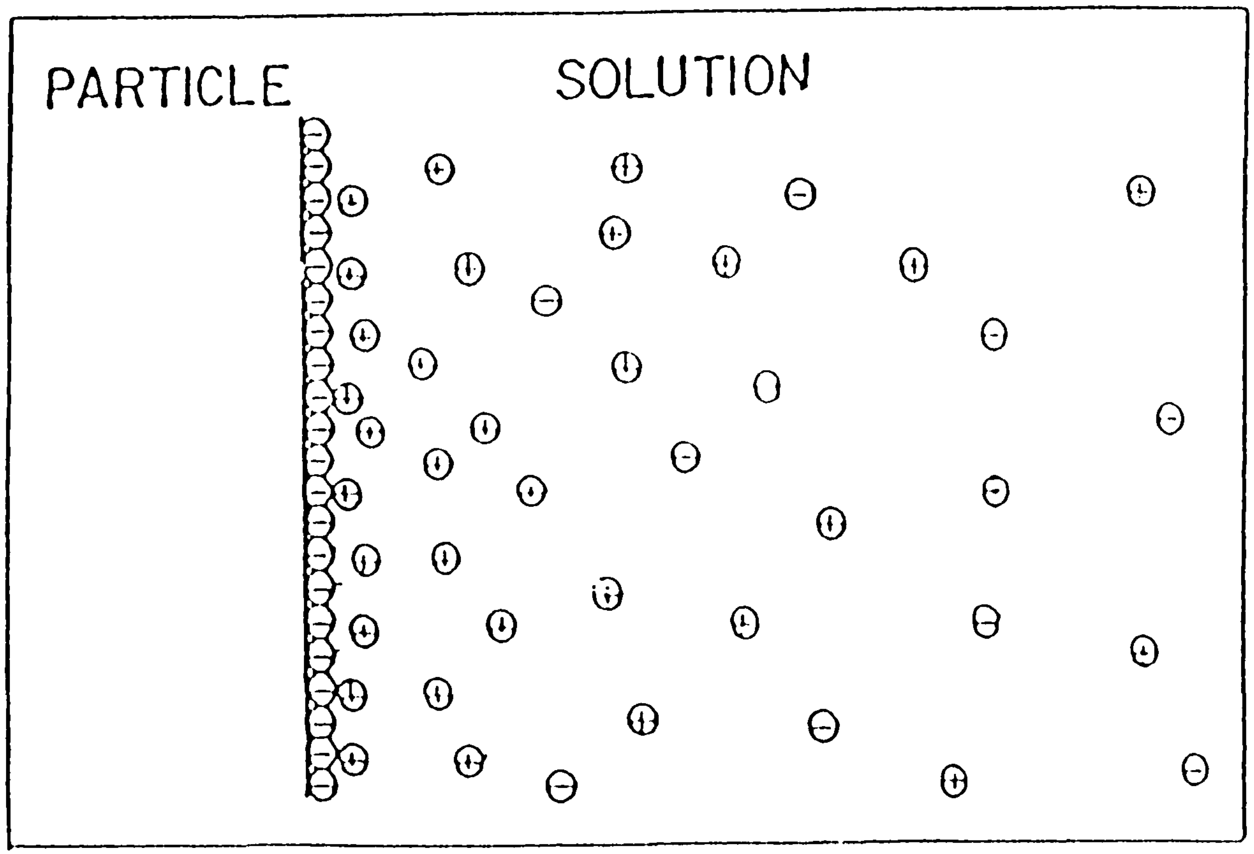

Fig. 3. 9 - Diffuse electric double-layer model,[Bassiouni, 1994 from Gouy, 1910]

Dewan (1983), reviewed the following methods used to interpret shaly sands:

1. The automatic compensation method, in which the sonic porosity and induction resistivity are directly used in the Archie equation along with compensating effects. This is a simple approach that provides good results in medium to high porosity sands containing dispersed shales,
2. The dispersed model used sonic and density porosities. The difference between sonic and density readings is used as an indication of the degree of shaliness of the formation under investigation. This method provides good results for shaly sands having authigenic clay. However, this method also gives good results with laminated shaly sands,
3. The Simandoux model (1963) uses neutron and density logs for porosity and self-potential (SP), gamma-ray (GR), or other shale indicators to get the shale volume. This method is applicable for laminated or dispersed shales,
4. The Waxman-Smith (W-S) Model (1968): This model uses the cation exchange capacity (CEC) of the shale rather than the usual shale fraction. The CEC of shale represents the most important property of shale for log interpretation, because it represents the source of the excess conductivity. In this model, the cation conduction and the conduction of the normal sodium chloride electrolyte are assumed to act independently in the pore space, and
5. Dual-Water (D-W) Model: The dual-water model assumes that the counterion conduction is restricted to the bound water and the normal electrolyte conductions confined to the free-water. Consequently, the D-W model predicts that shales, which

contain only bound water, should have water conductivities dependent only on temperature and essentially independent of salinity in adjacent water sands.

The Waxman-Smith (W-S) and Dual Water (D-W) models are the most recent models available in oil industry. Other shaly formation models have been reviewed by Fertl (1987) and some of these models are listed in Appendix A. Appendix A contains only the models used for determination of water saturation in shaly formations.

3. 5. Determination of Well Logging Parameters in Shaly Sands

With respect to the clean formations, the Archie's equation was used for the determination of water saturation and other well known relations discussed in the previous chapter. However, this is not the case with shaly formations. Evaluation of shaly formations requires determination of several parameters, including cementation factor (m), the Archie equation coefficient (a), porosity (φ), resistivity of shaly formation (R_{sh}), resistivity of true formation (R_t), and shale volume(V_{sh}).

Pickett plot (1966, 1973), has been successfully used to calculate the required parameters (a and m) for the clean formation. For the case of clean formations, modification of Archie's equation yields the following equation

$$-LogR_t = mLog\varphi - Log(aR_w) + nLogS_w \qquad (3\text{-}1)$$

A log-log plot of true formation resistivity (R_t) versus porosity (φ) shows that a clean water saturation line can be drawn for water bearing zone (S_w = 1.0). Therefore, the slope of that line provides the value of the cementation exponent (m). Also, at φ = 1.0, the intercept of water line provides the value of (aR_w), from which the value of the coefficient

(a) can be derived. These concepts were introduced by Pickett (1966, 1973) in the well-known, "Pickett plot", a very useful tool in well logging for obtaining the above parameters for clean formations.

Miyairi and Itoh (1978) used Poupon et al model (1971) for shaly sands to introduce a technique that can be used to obtain shaly sand parameters: a, n, and m. This technique may be explained through using several crossplots, including formation resistivity factor versus porosity (F vs φ), true formation resistivity versus porosity (R_t vs φ) and true formation resistivity versus porosity of shaly formation (R_t vs φ_{sh}). Their equation was given in the following form:

$$-LogR_t = mLog\varphi + nLogS_w + 2Log\left(1+\sqrt{\frac{aR_w}{\varphi^m}\frac{V_{sh}^2}{R_{sh}}}\right) \quad (3\text{-}2)$$

In water bearing zone, in equation (3-2), formation water resistivity (R_w) will be replaced by resistivity of 100 % saturated formation water (R_o), and the porosity (φ) by shaly-sand porosity which is given by $(\varphi_\tau = \varphi + V_{sh} * \varphi_{\tau sh})$. Then, the same procedure as for clean formation is followed. Fig. 3. 10. Table 3. 2 shows schematic explanation of resistivity-porosity crossplot introduced by Miyairi and Itoh (1978).

Later, a more sophisticated procedure was introduced by Aguilera (1990) for extending Pickett plot for the analysis of shaly formations from well logs. Aguilera (1990), developed new shale models by mathematical manipulated some of the water saturation model equations listed in Appendix A. He developed a generalized equation of the form:

$$\frac{R_t}{A_{sh}} = aR_w * \varphi^{-m} * S_w^{-n} \quad (3\text{-}3)$$

TYPES	$Rt - \phi D$
USES	m, aRw, Quick look
EQUATIONS Clean water bearing Clean hydrocarbon bearing Shaly water bearing	$-\log Rt = m\log\phi D - \log aRw$ $-\log Rt = m\log\phi D - \log aRw + \log\frac{Sw^n}{(1+Shr\phi Dh)^n}$ $-\log Rt = m\log\phi D - \log aRw + 2\log\frac{(\phi D - Vsh\phi Dsh)^{m/2} + Vsh^{b/2}(aRw/Rsh)^{1/2}}{\phi D^{m/2}}$
ASSUMED TERMS	Single mineral & known lithology
CRITERIA	$\phi Dsh > \sqrt{\frac{aRw}{Rsh}}$
PRESENTATION & EFFECT of SHALE and HYDROCARBON	m : Slop $m = \frac{\log(Rt2/Rt1)}{\log(\phi D1/\phi D2)}$ aRw = Rt when ϕD = 100 %

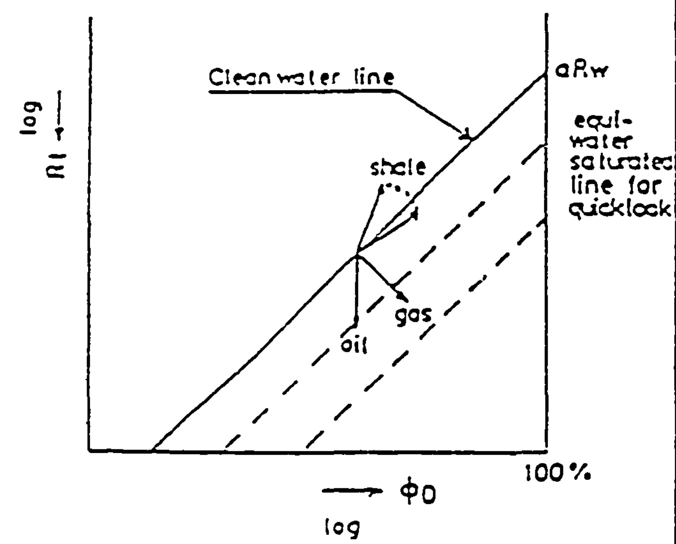

Table 3. 2 - Schematic explanation of porosity-resistivity crossplot, [Miyairi and Itoh, 1978]

Table 3. 3 - Different definitions of (A_{sh}) group for equation (3-3), [Aguilera,1990]

Used Shale Model	Shale Resistivity (A_{sh}) Group
Laminated Shale Model	$A_{sh} = A_{Lam} = \frac{(R_{sh} - R_t V_{Lam})(1 - V_{Lam})}{R_{sh}}$
Dispersed Shale Model	$A_{sh} = A_{dis} = 1 + \frac{\varphi^m R_t}{aR_w}\left(B_{dis} - \sqrt{\frac{aR_w}{\varphi^m R_t} + B_{dis} * C_{dis+C_{dis}^2}}\right)$
	where $B_{dis} = \frac{V_{dis}(R_{dis} - R_w)^2}{2\varphi R_{dis}}$, and
	$C_{dis} = \frac{V_{dis}(R_{dis} - R_w)}{2\varphi R_{dis}}$.
Total Shale Model	$A_{sh} = A_{tsh} = 1 + \frac{\varphi^m R_t}{aR_w}\left(2B_{tsh} - 2B_{tsh\sqrt{\frac{aR_w}{\varphi^m R_t} + B_{tsh}^2}}\right)$
	where $B_{tsh} = \frac{aR_w}{2\varphi^m} x \frac{V_{tsh}}{R_{tsh}}$
Dual Water Model	$Ash = \frac{R_t \varphi_t^2}{aR_w}\left(2B_{sh}^2 + 2B_{sh}\sqrt{B_{sh}^2 + \frac{aR_w}{R_t \varphi_t^2}}\right) + 1$
	where $B_{sh} = S_b\left(\frac{1 - (R_w / R_b)}{2}\right)$
	b = bound-water
Indonesian Model	$Ash = \left[\frac{V_{sh}^{(1-V_{sh})/2}(aR_w)^{1/2}}{R_{sh}^{1/2} * \varphi^{m/2}}\right]^{-2}$
Hossin Model	$Ash = \frac{R_{sh} - R_t V_{sh}^2}{R_{sh}}$

More than thirty models have been proposed for calculating the overall water saturation in shaly-sandstone reservoirs. Some of these models are shown in Appendix A. These models can generally be classified as models describing the laminated, dispersed, total, and cation exchange capacity (CEC) of shale.

Poupan et al (1971), proposed a model describing laminated shale, while deWitte (1950), introduced his model for dispersed shale considering very shaly formations. This model can be simplified to describe low shaly formations containing low values of water resistivities. Based on laboratory investigations and field experience, Schlumberger (1967), a model was developed for total shaliness of the formation independent of shale distribution. This total shale model can be applied over a practical range of water saturation values encountered in real cases. In addition, Waxman and Smits (1968) then developed a model to relate the resistivity contribution of the shale to its cation exchange capacity (CEC).

The purpose of this study is to develop models both for characterizing and identifying flow units when considering different types of shaly sands. These models are primarily based on the previously-mentioned shale models (Appendix A) in combination with permeability correlation proposed by Timur (1968). Timur (1968), made careful laboratory measurements of 155 sandstone cores from the Gulf Coast, Colorado and California, and correlated porosity (φ), irreducible water saturation (S_{wirr}) and absolute permeability of the rock (K) by equation (2-26).

Amaefule et al (1993) proposed the definition for Reservoir Quality Index (RQI) as given by equation (2-6).

The effective porosity is correlated to total porosity in shaly formation by the following equation:

$$\varphi_e = \varphi(1 - V_{sh}) \qquad (3\text{-}6)$$

where

φ_e = effective porosity of the rock, (fraction)

φ = total porosity of the rock, (fraction)

V_{sh} = shale volume of the formation, (fraction)

This study modified the Reservoir Quality Index (RQI) to "Shaly Reservoir Quality Index"(SRQI) by substituting equation (3-6) into equation (2-6). This substitution results in the following equation:

$$SRQI(\mu m) = 0.0314\sqrt{\frac{K}{\varphi_t(1 - V_{sh})}} \qquad (3\text{-}7)$$

where,

SRQI = shaly reservoir quality index, (μm)

In this study, a complete derivation of four flow unit identification, covering laminated, dispersed, total, and CEC models of shales, are included. In addition, a systematic technique, and step-by-step example calculations, showing the application of these flow unit models for shaly formations are given.

3. 6. 1. Development of New Flow Unit Model for Laminated Shale

For laminated shale, thin-shale laminations from one to many inches, are interspersed in clean sand. These laminated shale laminae have almost zero values of permeability and effective porosity. Therefore, the overall permeability and porosity of the whole interval is reduced in proportion to the fractional volume of the shale. Using Poupan et al model (1971) for laminated shale which is given by the following equation:

$$\frac{1}{R_t} = \frac{\varphi^2 S_w^2}{aR_w(1 - V_{lam})} + \frac{V_{Lam}}{R_{sh}} \tag{3-8}$$

where

a = coefficient of Archie's equation

R_t = true formation resistivity in the direction of the bedding planes, (ohm-m)

R_w = formation water resistivity, (ohm-m)

R_{sh} = resistivity of laminated shale, (ohm-m)

S_w = water saturation in laminated shaly formation, (fraction)

V_{Lam} = bulk volume fraction of the shale, distributed in laminae, each of uniform thickness, (fraction)

φ = total porosity of the formation, (fraction)

Solving equation (3-10) for water saturation (S_w) gives

$$S_w^2 = \frac{aR_w(1 - V_{Lam})}{\varphi^2}\left(\frac{1}{R_t} - \frac{V_{Lam}}{R_{sh}}\right) \tag{3-9}$$

Substituting the cementation exponent (m) for the coefficient (2) for porosity to make the model more general and applying the condition of irreducible water saturation on equation (3-9), the following equation is obtained:

$$S_{wirr}^2 = \left\{\frac{aR_w(1 - V_{Lam})}{\varphi^m}\left(\frac{1}{R_t} - \frac{V_{Lam}}{R_{sh}}\right)\right\}_{wirr} \tag{3-10}$$

Bassiouni (1994) showed that effective porosity (φ_e), which represents pore space containing only free-water and possible hydrocarbon, can be expressed as:

$$\varphi_e = \varphi_t(1 - S_{WB}) \qquad (3\text{-}11)$$

where

S_{WB} = saturation of the bound water, (fraction)

The saturation of the bound water (S_{WB}) can be expressed as follows:

$$S_{WB} \approx V_{sh} \qquad (3\text{-}12)$$

Therefore, equation (3-11) can be expressed as shown before in equation (3-6) as follows:

$$\varphi_e = \varphi_t(1 - V_{sh}) \qquad (3\text{-}6)$$

The total porosity of the formation can be obtained from neutron-density (N-D) crossplot or as $\varphi_t = (\varphi_{DC} + \varphi_{DN})/2$, where φ_{DC} and φ_{NC} are density and neutron porosities respectively, corrected for shaliness of the formation where there is no gas.

Substituting equation (3-10) into the permeability, equation (2-26), yields the following equation:

$$K_{sh} = \frac{(93)^2 * \varphi^{m+4.4}}{aR_w(1 - V_{Lam})}\left(\frac{R_{sh}R_t}{R_{sh} - V_{Lam}R_t}\right)_{wirr} \qquad (3\text{-}13)$$

where

K_{sh} = permeability of laminated shaly formations, (md)

Equation (3-13) can be used for predicting permeability for laminated shale since there is no available permeability equation for this purpose currently. All of the available permeability equations are almost developed for clean (shale-free) formations.

Substituting equation (3-13) into equation (3-7) results in an equation for shaly reservoir quality index for laminated shaly formation $(SRQI)_{Lam}$ as follows:

$$SRQI_{Lam} = \frac{2.92 * \varphi^{[1.7+(m/2)]}}{(1 - V_{Lam})\sqrt{aR_w\left(\frac{1}{R_t} - \frac{V_{Lam}}{R_{sh}}\right)_{Wirr}}} \qquad (3\text{-}14)$$

Defining a shale flow unit factor for laminated shale $(SFUF)_{Lam}$ as follows:

$$(SFUF)_{Lam} = \frac{2.92}{(1 - V_{Lam})\sqrt{aR_w\left(\frac{1}{R_t} - \frac{V_{Lam}}{R_{sh}}\right)_{Wirr}}} \qquad (3\text{-}15)$$

Then, equation (3-14) can be expressed in a simple form as follows:

$$(SRQI)_{Lam} = \varphi^{[1.7+(m/2)]} * (SFUF)_{Lam} \qquad (3\text{-}16)$$

Taking the logarithm of both sides of equation (3-16) provides a flow unit model for laminated shaly formations as follows:

$$Log(SRQI)_{Lam} = [1.7 + (m/2)]Log\varphi + Log(SFUF)_{Lam} \qquad (3\text{-}17)$$

where

m = cementation factor of the rock, (from Pickett plot)

$(SRQI)_{Lam}$ = shaly reservoir quality index for laminated shale

$(SFUF)_{Lam}$ = shaly flow unit factor for laminated shale

This model, equation (3-17), provides an effective tool for identifying flow units residing in laminated-shaly formations. It reveals that each set of data points (representing a flow unit of laminated shale) can be represented by a straight line of a unique slope equals [1.7 + (m/2)], and specific intercept, equals $(SFUF)_{Lam}$, with a Y-axis at porosity φ = 1.0

on a log-log plot of $(SRQI)_{Lam}$ versus porosity (φ). Therefore, different flow units of laminated shale can be represented by different straight lines having the same slope of [1.7 + (m/2)], and also different intercepts which represent different values of the Archie's equation coefficient (a), formation water resistivity (R_w), laminated shale resistivity (R_{sh}), and shale volume (V_{sh}) involved in $(SFUF)_{Lam}$.

3. 6. 2. Development of New Flow Unit Model for Dispersed Shale

Dispersed shale may exist in the form of accumulations adhering to (or coating) the sand grains, or even partially filling the smaller-pore channels. This type of shale is very damaging to porosity and permeability, because a relatively small amount of clay can choke the pores of the formations. Using the deWitte model (1950) for dispersed shale,

$$\frac{1}{R_t} = \frac{\varphi_{im}^2 * S_{im}}{a}\left(\frac{q}{R_{dis}} + \frac{S_{im} - q}{R_w}\right) \qquad (3\text{-}18)$$

where,

φ_{im} = intermatrix porosity, which includes the entire space occupied by fluids and dispersed shale, (fraction)

S_{im} = fraction of the intermatrix porosity (φ_{im}) occupied by the formation water, dispersed shale matrix mixture, (fraction)

q = fraction of intermatrix porosity (φ_{im}) occupied by dispersed shale

R_{disp} = resistivity of the dispersed shale, (ohm-m)

Based on the previous definitions, water saturation can be written as follows:

$$S_w = \left(\frac{S_{im} - q}{1 - q}\right) \quad (3\text{-}19)$$

Substituting equation (3-19) into equation (3-18) and solving for water saturation (S_w):

$$S_w = \frac{\sqrt{\frac{aR_w}{\varphi_{im}^2 R_t} + \left(\frac{q\left(R_{disp} - R_w\right)^2}{2R_{disp}}\right)} - \left(\frac{q\left(R_{disp} + R_w\right)}{2R_{disp}}\right)}{(1-q)} \quad (3\text{-}20)$$

where φ_{im} can be obtained from sonic log directly, and q can be obtained, for dispersed shale, from sonic and density logs as follows:

$$q = \left(\frac{\varphi_S - \varphi_D}{\varphi_S}\right) \approx \frac{\varphi_{disp}}{\varphi_{im}} \quad (3\text{-}21)$$

Case (1) Very Shaly Dispersed Shale Model

Expressing equation (3-20) at irreducible water saturation (S_w) and using it in equation (2-26) provides the permeability equation for very shaly formation which is substituted in SRQI equation, equation (3-7). The final model equation for the flow units of very dispersed shaly formations containing dispersed shale is as follows:

$$(SRQI)_{Disp} = \frac{2.92 * \varphi^{1.7} * (1-q)}{\sqrt{(1-V_{sh})}\left\{\sqrt{\frac{aR_w}{\varphi_{im}^2 R_t} + \left(\frac{q\left(R_{disp} - R_w\right)^2}{2R_{disp}}\right)} - \left(\frac{q\left(R_{disp} + R_w\right)}{2R_{disp}}\right)\right\}_{Wirr}}$$

(3-22)

Defining very shale flow unit factor for laminated shale $(VSFUF)_{Disp}$ as follows:

$$(VSFUF)_{Disp} = \frac{(1-q)}{\sqrt{(1-V_{sh})}\left\{\sqrt{\frac{aR_w}{\varphi_{im}^2 R_t}+\left(\frac{q(R_{disp}-R_w)^2}{2R_{disp}}\right)}-\left(\frac{q(R_{disp}+R_w)}{2R_{disp}}\right)\right\}_{Wirr}} \tag{3-23}$$

where

a = coefficient depending upon the rock type (a = 1.0 for sandstone, a = 0.8 for carbonate)

q = the fraction of clean sand intergranular space occupied by clay

R_t = true formation resistivity, (ohm-m)

R_{sh} = resistivity of shale, (ohm-m)

R_w = formation water resistivity, (ohm-m)

V_{sh} = shale content of the formation, (fraction)

R_{Disp} = resistivity of dispersed shale, (ohm-m)

Then, equation (3-22) can be expressed in a simple form as follows:

$$(SRQI)_{Disp} = \varphi^{[1.7]} * (VSFUF)_{Disp} \tag{3-24}$$

Taking the logarithm of both sides of equation (3-24) provides a flow unit model for very shaly formation having dispersed shale as follows:

$$Log(SRQI)_{Disp} = 1.7 * Log\varphi + Log(VSFUF)_{Disp} \tag{3-25}$$

where

$(SRQI)_{Disp}$ = shale reservoir quality index for very dispersed shale

$(VSFUF)_{Disp}$ = very shaly flow unit factor for dispersed shale

Case (2) Low Shaly Dispersed Shale Model

If the sands are not very shaly and formation water resisitivity (R_w) is very small compared to resistivity of dispersed shale (R_{Disp}), then equation (3-20) can be simplified to:

$$S_w = \frac{\sqrt{\frac{aR_w}{\varphi_{im}^2 R_t} + \left(\frac{q^2}{4}\right)} - \left(\frac{q}{2}\right)}{(1-q)} \qquad (3\text{-}26)$$

Following the same procedure as shown in case (1), the following flow unit model for low shaly formation of dispersed shale is obtained:

$$(SRQI)_{Disp} = \frac{2.92 * \varphi^{1.7} * (1-q)}{\sqrt{(1-V_{sh})}\left\{\sqrt{\frac{aR_w}{\varphi_{im}^2 R_t} + \left(\frac{q^2}{2}\right)} - \left(\frac{q}{2}\right)\right\}_{Wirr}} \qquad (3\text{-}27)$$

Defining the low shaly flow unit factor for dispersed shale $(LSFUF)_{Disp}$ as follows:

$$(LSFUF)_{Disp} = \frac{(1-q)}{\sqrt{(1-V_{sh})}\left\{\sqrt{\frac{aR_w}{\varphi_{im}^2 R_t} + \left(\frac{q^2}{2}\right)} - \left(\frac{q}{2}\right)\right\}_{Wirr}} \qquad (3\text{-}28)$$

Then, equation (3-27) can be expressed in a simple form as follows:

$$(SRQI)_{Disp} = \varphi^{[1.7]} * (LSFUF)_{Disp} \qquad (3\text{-}29)$$

Taking the logarithm of both sides of equation (3-29) provides a flow unit model for low shaly formation having dispersed shale as follows:

$$Log(SRQI)_{Disp} = 1.7 * Log\varphi + Log(LSFUF)_{Disp} \qquad (3\text{-}30)$$

where

$(SRQI)_{Disp}$ = shale reservoir quality index for low dispersed shale

$(LSFUF)_{Disp}$ = low shaly flow unit factor for dispersed shale

As shown by equations (3-25) and (3-30), a log-log plot of $(SRQI)_{Disp}$ versus porosity (φ) provides a straight line (of unique slope equal to 1.7) for dispersed shale for both cases of low and very shaly formations. Through each set of data points representing the characteristics of each flow unit in dispersed shaly formations, a straight line can then be drawn (with a unique slope equal to 1.7) and an intercept equal to $(LSFUF)_{Disp}$ or $(VSFUF)_{Disp}$.

3. 6. 3. Development of New Flow Unit Model for Total Shale Model

Schlumberger (1972) introduced the total shale model which is given by the following equation:

$$\frac{1}{R_t} = \frac{V_{sh}}{R_{sh}} + \frac{S_w^n}{FR_w} \qquad (3\text{-}31)$$

where

n = water saturation exponent (usually n = 2)

F = formation resistivity factor

V_{sh} = shale volume of the formation (independent of shale type), (fraction)

R_{sh} = resistivity of shale, (ohm-m)

The formation resistivity factor (F) proposed by Archie is given by the following equation:

$$F = \frac{a}{\varphi^m} \qquad (3\text{-}32)$$

where

a = coefficient of Archie equation (a = 1.0 for sandstone, a = 0.81 for carbonate)

m = cementation exponent (also called porosity exponent).

Substituting equation (3-32) into equation (3-31) and assuming that water saturation exponent (n) = 2 in equation (3-31), then solving the resultant equation for water saturation results in:

$$S_w^2 = \frac{aR_w}{\varphi^m}\left(\frac{1}{R_t} - \frac{V_{sh}}{R_{sh}}\right) \tag{3-33}$$

where

φ = bulk porosity of the formation.

Applying equation (3-33) at irreducible water saturation condition and using the resultant (S_{wirr}) in equation (2-26) provides a new permeability equation independent of shale type and distribution in the shaly formation. This equation is given as:

$$K_{sh} = \frac{(93)^2 \varphi^{4.4+m}}{aR_w}\left(\frac{1}{R_t} - \frac{V_{sh}}{R_{sh}}\right)_{Wirr} \tag{3-34}$$

Substituting equation (3-34) into SRQI equation, equation (3-7), yields shaly reservoir quality index for total shale model as follows:

$$(SRQI)_{tot} = \frac{2.92 * \varphi^{[1.7+(m/2)]}}{\sqrt{aR_w(1-V_{sh})\left(\frac{1}{R_t} - \frac{V_{sh}}{R_{sh}}\right)_{wirr}}} \tag{3-35}$$

The flow unit factor for total shale model $(SFUF)_{tot}$ as follows:

$$(SFUF)_{tot} = \frac{2.92}{\sqrt{aR_w(1-V_{sh})\left(\frac{1}{R_t} - \frac{V_{sh}}{R_{sh}}\right)_{wirr}}} \tag{3-36}$$

Then, the flow unit model can be formulated in a simple form as follows:

$$(SRQI)_{tot} = \varphi^{[1.7+(m/2)]} * (SFUF)_{tot} \qquad (3\text{-}37)$$

Taking the logarithm of both sides of equation (3-37) provides a flow unit model based on total shale model as follows:

$$Log(SRQI)_{tot} = [1.7 + (m/2)] * Log\varphi + Log(SFUF)_{tot} \qquad (3\text{-}38)$$

where

$(SRQI)_{tot}$ = shale reservoir quality index based on total shale model

$(SFUF)_{tot}$ = shaly flow unit factor for total shale model

Independent of the type of the shale in the formation, a flow unit can then be identified by drawing a straight line through each group of data points. This straight line should have a slope equal to [1.7 +(m/2)], i. e. equation (3-38) on a log-log plot of $(SRQI)_{tot}$ versus total porosity (φ).

3. 6. 4. Development of New Flow Unit Model for Cation Exchange Capacity (CEC) of Shale

The Waxman and Smits (W-S) model (1968) is based on the cation exchange capacity (CEC) of a shale, which is considered as one of the most important property of shale. One major objection to the application of the W-S model by Dewan (1983) is that of water sands of constant conductivity, but increasing shaliness, will have increasing effective water conductivities to the point that the shale should appear to contain quite saline water. Despite this fact, a good amount of evidence exists. The CEC is proportional to the shale content of the formation, but also depends on the type of clay.

Using Waxman and Smits model, their "Cation Exchange capacity (CEC)" model is given by the following equation:

$$S_w^2 = \frac{R_w F^*}{R_t\left(1+\frac{R_w B Q_v}{S_w}\right)} \qquad (3\text{-}39)$$

where

S_w = water saturation in shaly formation based on CEC model, (fraction)

R_w = formation water resistivity, (ohm-m)

B = coefficient which may be made variable with formation water resistivity (R_w) in order to fit the experimental data for very high values of R_w.

F^* = limiting formation resistivity factor introduced by Waxman and Smits (1968)

Q_v = the cation-exchange concentration in milliequivalents of exchange sites for Na ions per cm^3 of pore-volume as defined by Waxman and Smits (1968)

The limiting formation resistivity factor (F^*) is approximately the same as for a clean formation with the same porosity. But the porosity of shaly formation is, however, expected to be considerably different from that of clean formations. Therefore, this study suggests modifying (F^*) to be more representative to shaly formation as follows:

$$F^* = \frac{a}{\varphi^m (1-V_{sh})^m} \qquad (3\text{-}40)$$

The term (BQ_v/F^*) represents the excess conductivity contributed by shaliness. Solving equation (3-39) for water saturation (S_w), the positive term will be:

$$S_w = \frac{F^* R_w}{2}\left\{\left(\frac{-BQ}{F^*}\right)+\sqrt{\left(\frac{-BQ}{F^*}\right)^2-\left(\frac{4}{F^* R_w R_t}\right)}\right\} \qquad (3\text{-}41)$$

Substituting equation (3-40) into equation (3-41) and applying irreducible water saturation condition produces equation for (S_{wirr}). Using S_{wirr} in equation (2-26) to obtain the permeability equation for shaly formation obeys CEC model. This equation is then substituted in SRQI equation, equation (3-7), to obtain the following flow unit model based on the cation exchange capacity (CEC) of the formation as follows:

$$(SRQI)_{CEC} = \frac{2.92 * \varphi^{(1.7+m)}(1-V_{sh})^{(m-0.5)}}{\left(\frac{aR_w}{2}\right)\left\{\left(\frac{-BQ}{F^*}\right)+\sqrt{\left(\frac{-BQ}{F^*}\right)^2-\left(\frac{4}{F^* R_w R_t}\right)}\right\}_{wirr}} \qquad (3\text{-}42)$$

where

B = specific concentration conductivity, (mho/m per meq/cc)

F^* = formation resistivity factor for shaly formation

Q_v = cation exchange capacity, (meq/cc)

Taking logarithm of both sides of equation (3-42) provides shaly flow unit model as follows:

$$Log(SRQI)_{CEC} = [1.7+m] * Log\varphi + Log(SFUF)_{CEC} \qquad (3\text{-}43)$$

where

$(SFUF)_{CEC}$ = shaly flow unit factor based on W-S model, which is defined by:

$$(SFUF)_{CEC} = \frac{(2.92) * (1-V_{sh})^{(m-0.5)}}{\left(\frac{aR_w}{2}\right)\left\{\left(\frac{-BQ}{F^*}\right)+\sqrt{\left(\frac{-BQ}{F^*}\right)^2-\left(\frac{4}{F^* R_w R_t}\right)}\right\}_{wirr}} \qquad (3\text{-}44)$$

Based on the W-S model for CEC of shale, a new flow unit model is obtained, equation (3-43). This model shows that a straight line of slope [1.7 + m] can be drawn through each set of data points representing a single flow unit in shaly sand reservoirs.

In the derivation of the previously described flow unit models, the water saturation exponent (n) is considered equals 2 based on Archie's equation.

Serra (1986) then showed that the cementation factor (m) varies as a function of grain size and distribution, or as a function of the complexity of the channels linking the pores. For this reason, this study suggests determining the value of (m) using the so called "Pickett plot" to better (and more accurately) representative of the reservoir, especially in the case of shaly formations. Using the previously-derived four models to identify flow units in shaly formations, a log-log plot of $(SRQI)_{CEC}$ versus porosity (φ) provides an effective method to both characterize and identify the flow units of interest.

3. 6. 5. Development of Generalized Flow Unit Model for Shaly Formations

Using the total shale model for water saturation, equation (3-33), and the generalized form of permeability, equation (2-37), the following equation of permeability for shaly formation is obtained as follows:

$$K_{sh}(md) = \left(\frac{C_1 A_{sh}}{aR_w}\right) * \varphi^{(C_2+1)m} \tag{3-45}$$

where

A_{sh} = shale group from total shale model, given as:

$$A_{sh} = \left(\frac{R_{sh} - V_{sh}R_t}{R_{sh}R_t}\right) \tag{3-46}$$

Substituting equation (3-45) into the equation of SRQI, equation (3-7) yields

$$SRQI(\mu m) = 0.0314 * \varphi^{0.5*[(C_2+1)m-1]} * \sqrt{\left(\frac{C_1 A_{sh}}{aR_w}\right)} \qquad (3\text{-}47)$$

Applying logarithm on both sides of equation (3-47) yields

$$Log(SRQI) = \left(\frac{(C_2+1)m-1}{2}\right) Log\varphi + Log\left\{0.0314 * \sqrt{\left(\frac{C_1 A_{sh}}{aR_w}\right)}\right\} \qquad (3\text{-}48)$$

Equation (3-48) is a generalized flow unit model. This model works for any shaly formation that obeys permeability equation which is a function of porosity and irreducible water saturation. It reveals that a single flow unit can be represented by a straight line with slope equal to {[(C_2 + 1)m-1]/2} and an intercept equal to $\left\{0.0314 * \sqrt{\left(\frac{C_1 A_{sh}}{aR_w}\right)}\right\}$. This model can be used to develop the required flow unit model for a new shaly reservoir by substituting the permeability equation coefficients (C_1 and C_2) and the shale group (A_{sh}).

The most important aspect of this generalized model, equation (3-48) is that it works also for clean stress-insensitive formations. A comparison of Archie's equation for water saturation in clean formation and total shale model for shaly formation leads to a conclusion that the shale group (A_{sh}) can be replaced by (R_{tt}). This replacement reduces equation (3-48) to the generalized flow unit model derived in chapter 2, equation (2-41).

It is found that these newly-developed models possess a common feature in that each flow unit in any shaly reservoir can be represented by a straight line on a log-log plot of shaly reservoir quality index (SRQI) versus porosity (φ). This straight line (representing the flow unit) yields a unique slope of : [1.7 + (m/2)] for laminated shaly formation, [1.7] for dispersed shaly formation, [1.7 + (m/2)] for shaly formations obey total shale model, [1.7 + m] for shaly formations obey cation exchange capacity (CEC) model, and {[(C_2 + 1)m - 1]/2} for flow unit model bsaed on general permeability equation. In addition, each flow unit should have a characteristic intercept, on the previously mentioned log-log plot, at $\varphi = 1.0$ equal to shaly flow unit factor (SFUF). These five flow unit models can be used effectively to identify shale type and define flow units consitituting the reservoir under investigation. Table 3. 4 summaries four flow unit models developed in this chapter to identify shale type and flow units residing in heterogeneous shaly reservoirs.

3. 7. Generalized Systematic Technique to Identify Flow Units in Shaly Sand Reservoirs

This study recommends the following steps for identification of flow units in shaly formations using the previously-derived flow unit models, which are accordingly based on laminated, dispersed, total, and W-S model. This technique may be described as follows:

1. Using conventional well log-derived data, calculate the shaliness of the formation, Table 3. 5, at different depths of shaly-pay zone,
2. Calculate the porosity of the formation at the same chosen depths in step (1) through the pay zone, using such conventional porosity logs as neutron, and density logs. The porosity values obtained should then be corrected for shale and hydrocarbon effects,
3. Calculate the irreducible water saturation (S_{wirr}) from well logs at pay zone, use the value of S_{wirr} with the values of porosity to get the permeability of the formation,

Table 3. 4 - List of the newly-developed flow unit models for characterization of shaly formations

#	Used Shale Model	Slope of Flow Unit Model	Shaly Flow Unit Factor (SFUF)
1.	Laminated	[1.7 + (m/2)]	$(SFUF)_{Lam} = \dfrac{2.92}{(1-V_{Lam})\sqrt{aR_w\left(\dfrac{1}{R_t}-\dfrac{V_{Lam}}{R_{sh}}\right)}_{Wirr}}$
2.	Dispersed Model		
	(A) Very Shaly	1.7	$(VSFUF)_{Disp} = \dfrac{(1-q)}{\sqrt{(1-V_{sh})}\left\{\sqrt{\dfrac{aR_w}{\varphi_{im}^2 R_t}+\left(\dfrac{q(R_{disp}-R_w)^2}{2R_{disp}}\right)}-\left(\dfrac{q(R_{disp}+R_w)}{2R_{disp}}\right)\right\}_{Wirr}}$
	(B) Low Shaly	1.7	$(LSFUF)_{Disp} = \dfrac{(1-q)}{\sqrt{(1-V_{sh})}\left\{\sqrt{\dfrac{aR_w}{\varphi_{im}^2 R_t}+\left(\dfrac{q^2}{2}\right)}-\left(\dfrac{q}{2}\right)\right\}_{Wirr}}$
3.	Total Shale	[1.7 +(m/2)]	$(SFUF)_{tot} = \dfrac{2.92}{\sqrt{aR_w(1-V_{sh})\left(\dfrac{1}{R_t}-\dfrac{V_{sh}}{R_{sh}}\right)}_{wirr}}$
4.	Cation Exchange Capacity (CEC)	[1.7 + m]	$(SFUF)_{CEC} = \dfrac{(2.92)*(1-V_{sh})^{(m-0.5)}}{\left(\dfrac{aR_w}{2}\right)\left\{\left(\dfrac{-BQ}{F^*}\right)+\sqrt{\left(\dfrac{-BQ}{F^*}\right)^2-\left(\dfrac{4}{F^* R_w R_t}\right)}\right\}_{wirr}}$

equation (2-26), and use it in combination with the previously calculated values of porosity and shaliness (V_{sh}) to calculate (SRQI), equation (3-7),

4. Read true formation resistivity (R_t) from electric logs (Induction log), calculate shale group (A_{sh}) and then plot (R_t/A_{sh}) versus corrected porosity on a log-log plot "Pickett Plot", Fig. 3. 12. Calculate the coefficient (a) and the cementation exponent (m) from "Pickett Plot" (assuming that R_w is known, from SP or another source of measurements),
5. Plot (SRQI) versus porosity on a log-log plot and draw a straight line having a consistent characteristics of reservoir properties. Calculate the slope of the straight line, Figs. 3. 13 and 3. 14,
6. Compare the slope of the straight line obtained with slopes of the derived flow unit models, Table 3. 4. The closest value of the slope of the straight using field data to the slope of the flow unit model, Table 3. 4, defines the shale type in the reservoir because it shows the shale model that field data of interest obeys. For instance, if the slope of the straight line using field data is 1.7 i. e., close to the slope of 1.7 in Table 3. 4, the shale type in the formation is dispersed since the flow unit model for dispersed shale, equation (3-25) or (3-30),
7. Draw another straight line through another set of data points and repeat steps 1-6 to define other flow units within the formation,
8. It should be noted at this point that it is very possible for one pay zone in the reservoir to have different shale types and, of course, different flow units models,

Table 3. 5 Simulated Data for Shaly Sand Flow Unit Models.

Irreducible Water saturation (Swirr) = 23.58 %
Formation Water Resistivity (Rw) = 0.0531 oh-m
Coefficients : a = 1.0 . n = 2 , and m = 1.89 (Pickett Plot, Fig. 3. 12)
Maximum GR = 120, Minimum GR = 8

Interval #	GR (API)	Ish=V(sh (%)	Neutron Porosity (%)	Density Porosity (%)	Average Porosity (%)	SRQI (um)
1	65	50.8929	21	16.6	18.8	1.031252006
2	63.5	49.5536	16.5	12.5	14.5	0.654303415
3	71.5	56.6964	19.5	14.2	16.85	0.911647146
4	100	82.1429	23	20.5	21.75	2.191005933
5	97	79.4643	21.2	17	19.1	1.638213926
6	57	43.75	13.5	12	12.75	0.497937514
7	11	2.67857	24	21.5	22.75	1.013054803
8	8	0	28.5	22.2	25.35	1.201244284
9	12	3.57143	31	24.5	27.75	1.426635439
10	12	3.57143	28.5	23.6	26.05	1.281265306
11	66	51.7857	27.5	22.5	25	1.689580708
12	70	55.3571	24	20.5	22.25	1.440302887
13	49	36.6071	16.6	15.5	16.05	0.693675244
14	60	46.4286	24	18.5	21.25	1.21594063
15	73	58.0357	27.5	23.5	25.5	1.873040573
16	78	62.5	29	25	27	2.183592335
17	79	63.3929	31	28.5	29.75	2.606235931
18	103	84.8214	26	21	23.5	2.710620462
19	108	89.2857	28.5	23	25.75	3.768846772
20	113	93.75	30.5	28.5	29.5	6.217649184
21	9	0.89286	22.5	19	20.75	0.858513423
22	8	0	22.5	19.5	21	0.872251243
23	8	0	21	18	19.5	0.769002294
24	8	0	17.5	15	16.25	0.564052485

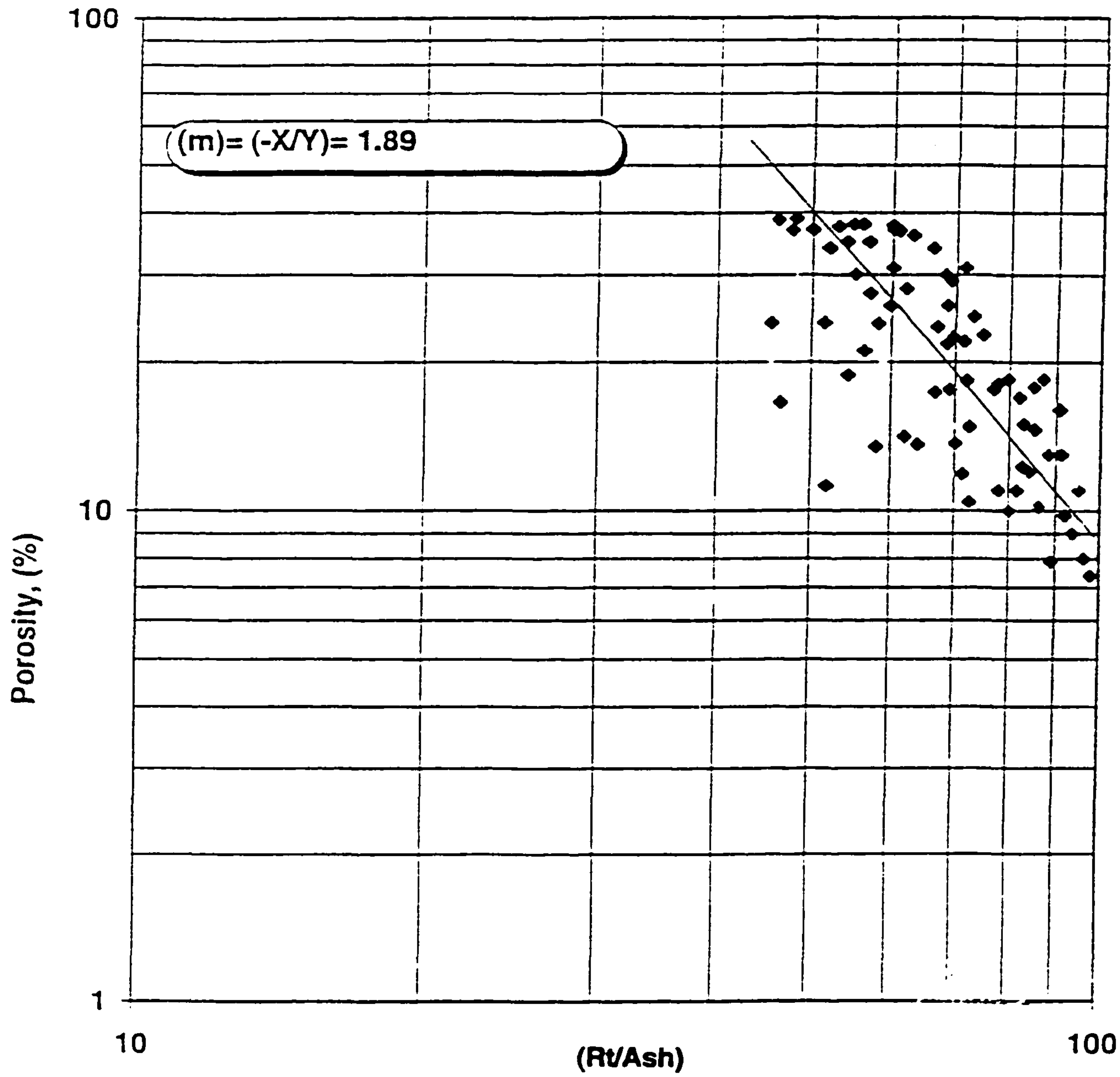

Fig. 3. 12 - Pickett Plot Log (Rt/Ash) Vs Log Porosity

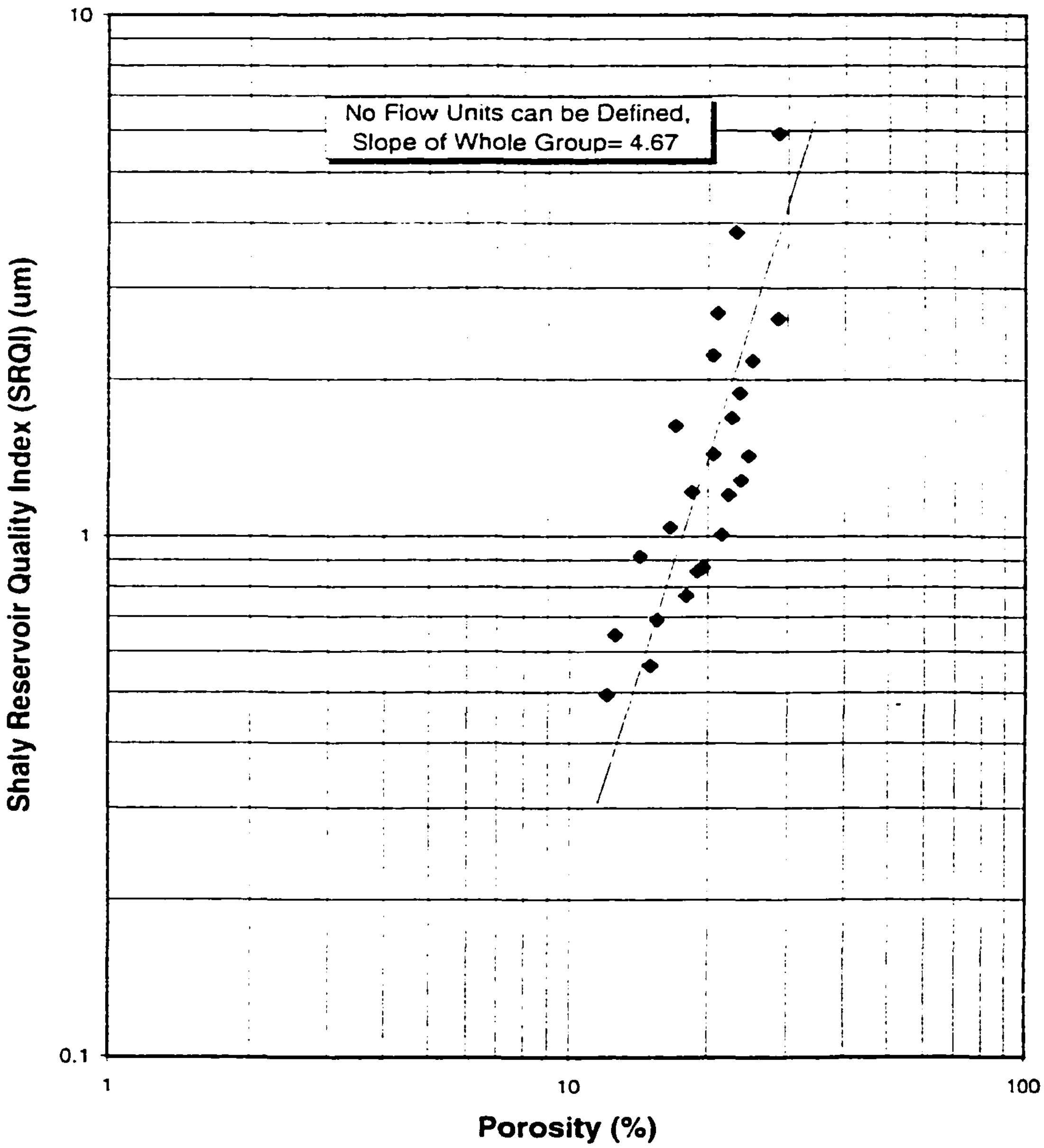

Fig. 3. 13 - Shaly Reservoir Quality Index (SRQI) Versus Porosity, using all of data points as one group, [slope has no meaning]

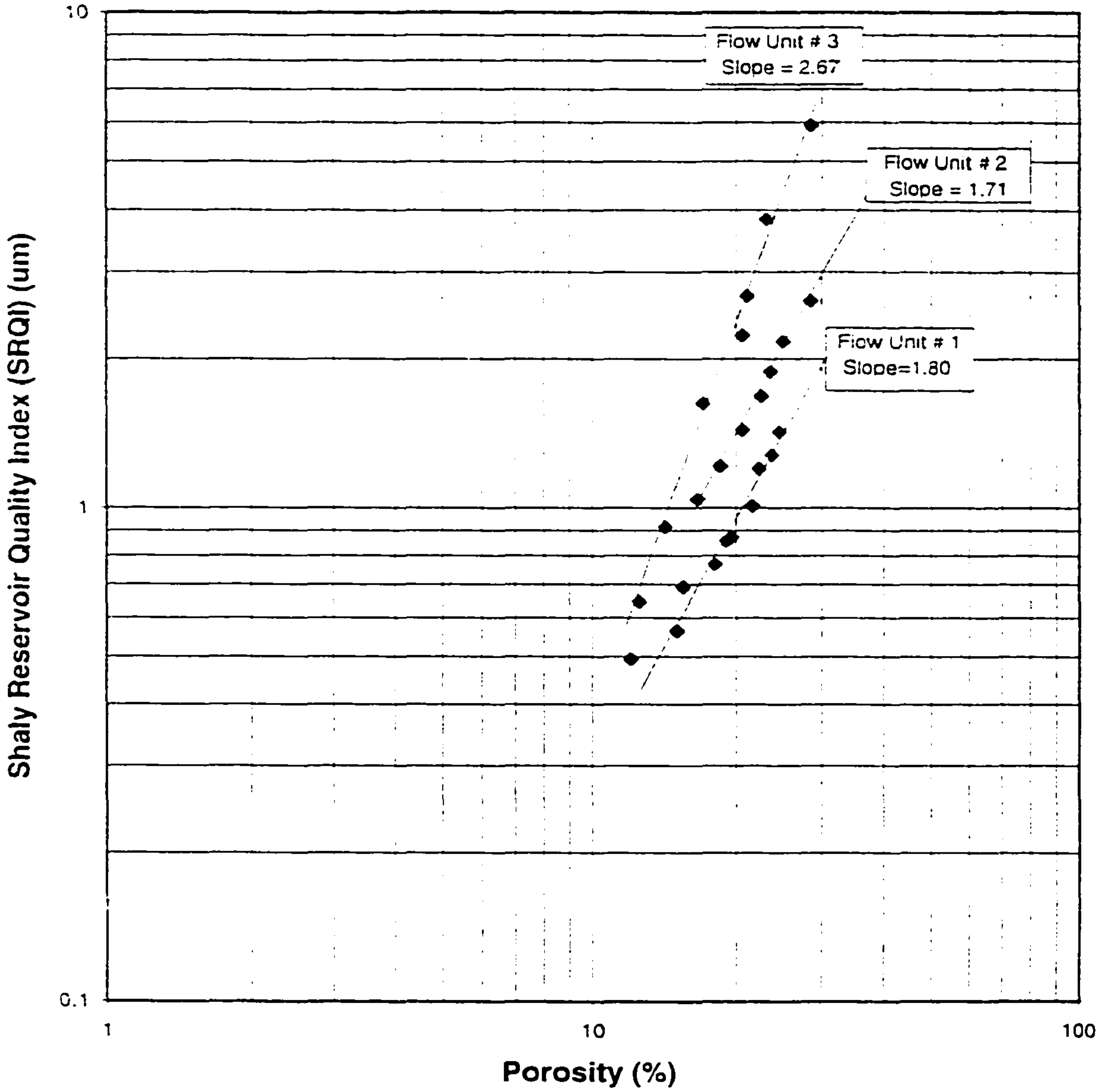

Fig. 3. 14 - Shaly Reservoir Quality Index (SRQI) Versus Porosity

9. Difference in the slope of the straight line defining the flow unit, on a log-log plot of SRQI versus porosity (φ), results mainly from the shaly model used to develop the flow unit model. Each shale model was derived to represent a specific shale type. Therefore, for dispersed shale type, a flow unit model having a slope equal to 1.7 is obtained while a slope equal to [1.7 + m] is obtained for shaly formation obeys CEC model. These two flow unit models, resulted from using dispersed and CEC shale models, have unique slopes that can be used effectively to identify shale type and flow units in these shale types. With respect to flow unit using laminated shale and total shale models, the slopes of the derived flow unit models are similar. The reason is that total shale model is derived independent of shale type while laminated shale model provides its unique slope of the straight line representing the flow unit. Therefore, the slope of [1.7 + (m/2)] can be used mainly for describing laminated shale. However, this total flow unit model can also be used to describe shaly formation obeys total shale model.

A simulated data is used to test these newly-developed flow unit models for shaly formations, Table 3. 5. Also, the data is used to draw Figs. 3. 12, 3. 13, and 3. 14 for the identification of both the shale type and the number of flow units involved.

For the purpose of validation of the previously-developed models for shaly-sand reservoirs, an assumed conventional well log data is used, Table 3. 5. For the interval of interest of shaly sand, the following readings are generated: Gamma Ray (GR), Neutron porosity, Density porosity, and true formation resistivity. Using these data, Table 3. 5, Pickett plot is obtained, Fig. 3. 12, and the shaly reservoir quality index (SRQI) is calculated and plotted versus porosity, Fig. 3. 13 and Fig. 3. 14. Fig. 3. 13 shows a slope of

4.67 (when all of the data points is used a one group) which has no meaning while application of the derived shaly sand models defines 3 flow units, Fig. 3. 14, and the shale types are dispersed and laminated shale. A detailed description of the procedure followed is included in the following section showing a step by step example of calculation.

The newly developed flow unit models introduce unique parameters include: Shaly Reservoir Quality Index (SRQI) and Shaly Flow Unit Factor (SFUF). When applied with the prescribed technique presented herein, these flow unit models represent an effective, economical tool (due to their inherent use of conventional well-log derived data) to enhance reservoir description, which will prove of significant assistance in future in reservoir development.

EXAMPLE OF CALCULATIONS

The purpose of this section is to introduce a step-by-step example of calculation for facilitating the application of the newly-developed flow unit models for shaly reservoirs.

This solved example will show in details how to apply these flow unit models to identify flow units and shale type of each flow unit residing in the formation of interest. let us assume that the following values of the given reservoir are known:

Equation coefficient (a)	=	1.0
Cementation exponent (m)	=	1.89
Irreducible water saturation (S_{wirr})	=	23.58 %

The following steps are suggested for application the flow unit models

1. Select zone of the interest for the reservoir under investigation and divide it into intervals depending upon the change in well logs readings through each interval. For our example, the zone of interest has been divided into 24 intervals.

2. Read maximum and minimum reading of Gamma Ray (GR) through the whole given log. These values are assumed as:

   Maximum GR (GR_{Max}) = 120 API,

   Minimum GR (GR_{Min}) = 62 API

3. For each interval, read Gamma Ray (GR) and use it to calculate shale volume of the formation. Interval # 6 is selected for showing the calculation (GR of interval # 6 = 87 API) as follows:

   GR of interval # 6 = 87 API

$$V_{Sh} = \frac{GR_{Log} - GR_{min}}{GR_{Max} - GR_{min}} = \frac{87 - 62}{120 - 62} = 0.431$$

4. Read Neutron and density porosity values for each interval. For interval # 6, the following values are assume as follows:

   Neutron porosity = 13.5 %,

   Density porosity = 12 %

5. Calculate the average porosity (assuming oil zone, no gas saturation)

$$\varphi_t = \frac{\varphi_N + \varphi_D}{2} = \frac{135 + 12}{2} = 12.75 \ \%$$

6. Calculate the permeability of the interval (interval # 6) using Tiumr's permeability equation as follows:

$$K(md) = \frac{\left(93*\varphi^{2.2}\right)^2}{S_{wirr}^2} = \frac{\left(93*(0.1275)^{2.2}\right)^2}{(0.2358)^2} = 18.0 \quad \text{md}$$

7. Calculate Shaly Reservoir Quality Index (SRQI) as follows:

$$SRQI(\mu m) = 0.0314 * \sqrt{\frac{K}{\varphi_{tot}(1-V_{sh})}} = 0.0314 * \sqrt{\frac{(18)}{0.1275*(1-0.431)}} = 0.49 \ \mu m$$

8. Repeat all of the previously describes steps for all the selected intervals of the formation under investigation to get values of porosity and Shaly Reservoir Quality Index (SRQI).

9. Read true formation resistivity (R_t) from Induction log (or other conventional electric log) and plot it versus porosity on a log-log plot ."Pickett Plot". Fig. 3. 12. to determine the cementation exponent (m = 1.89) and use it to get an accurate values of slopes in shaly sand model in Table 3. 4.

10. Plot Shaly Reservoir Quality Index (SRQI) versus porosity. Fig. 3. 14. to obtain different sets of data points. each set of them can be used to plot a straight line to define a separate flow unit. Two shale types can be identified as laminated and dispersed. In addition. three flow units have been defined.

This chapter reviewed shale distribution in shaly sands. shale content evaluation (mixed lithology). and the electrical and cation exchange capacity properties of shale. In addition. shale sand interpretation models for calculating water saturation in shaly formations are covered. A step-by-step derivation of five models are developed in this chapter to characterize and identify shale type and flow units constituting shaly heterogeneous reservoirs. The flow unit models are validated and showed that shale type (laminated and dispersed) and a number of flow units (three) can be recognized, based on the used simulated data. Table 3. 6 lists the assumptions and limitations of the newly-developed flow unit models. This chapter also involved a generalized technique showing the application of these new models. This technique was followed by example calculations for the sake of showing how to apply and to use these models to identify shale type and flow units in shaly formations. The important aspects of these newly-developed flow unit models is that it provides an effective tool to determine which shale model can be selected to determine water saturation in shaly formation. This can be achieved by identification shale type using flow unit models and use it to choose the suitable shale model for the reservoir under investigation.

Table 3. 6 List of assumptions and limitations of the newly-developed flow unit models for shaly formations

Flow Unit Model Based on	Assumption(s) and Limitation(s)	
Laminated Shale Model Model given by equation (3-16)	C_1 = 8649 and C_2 = 2.2	Laminated Shaly formations
Dispersed Shale Models Model given by equations (3-25) and (3-30)	C_1 = 8649 and C_2 = 2.2	Dispersed Shaly
Total Shale Model Model given by equation (3-38)	C_1 = 8649 and C_2 = 2.2	Formations obey total shale model
Cation Exchange Capacity (CEC) Model, Model given by eq. (3-43)	C_1 = 8649 and C_2 = 2.2	Formations obey CEC model
Generalized Perm. Equation Model given by equation (3-48)	Perm Equation is function of porosity and Swirr.	

CHAPTER 4

INFLUENCE OF STRESS ON THE CHARACTERIZATION OF FLOW UNITS IN CLEAN FORMATIONS

When the hydrocarbon reservoir pressure declines due to oil production, reservoir rock will be compacted because the load on the formation grains increases causing changes in the characteristics of flow units. When the reservoir pore-volume decreases, the overburden shifts as well, causing variation in fluid flow paths through that porous rock.

Hydrocarbon and mineral production may cause collapse or subsidence of the local geo-structures in certain geological environments. Significant subsidence causes casing failure, either in the overburden or in the producing zone. In severe cases, subsidence may be transmitted to the surface through the overburden causing significant problems such as platform collapse or pipeline failure, especially in soft and fractured formations having high porosity and permeability properties.

Green (1991) introduced a technique using existing downhole wireline tools configured to provide high-resolution measurements to detect the onset of a subsidence. These measurements could be used to detect small shifts in the formation or casing which indicate the onset of a subsidence problem. The tool uses a radioactive marker for subsidence detection is shown in Fig. 4. 1. Assuming constant rock properties during the extended life of the hydrocarbon reservoir can cause serious problems and errors in determining the reservoir rock transmissibility and storativity.

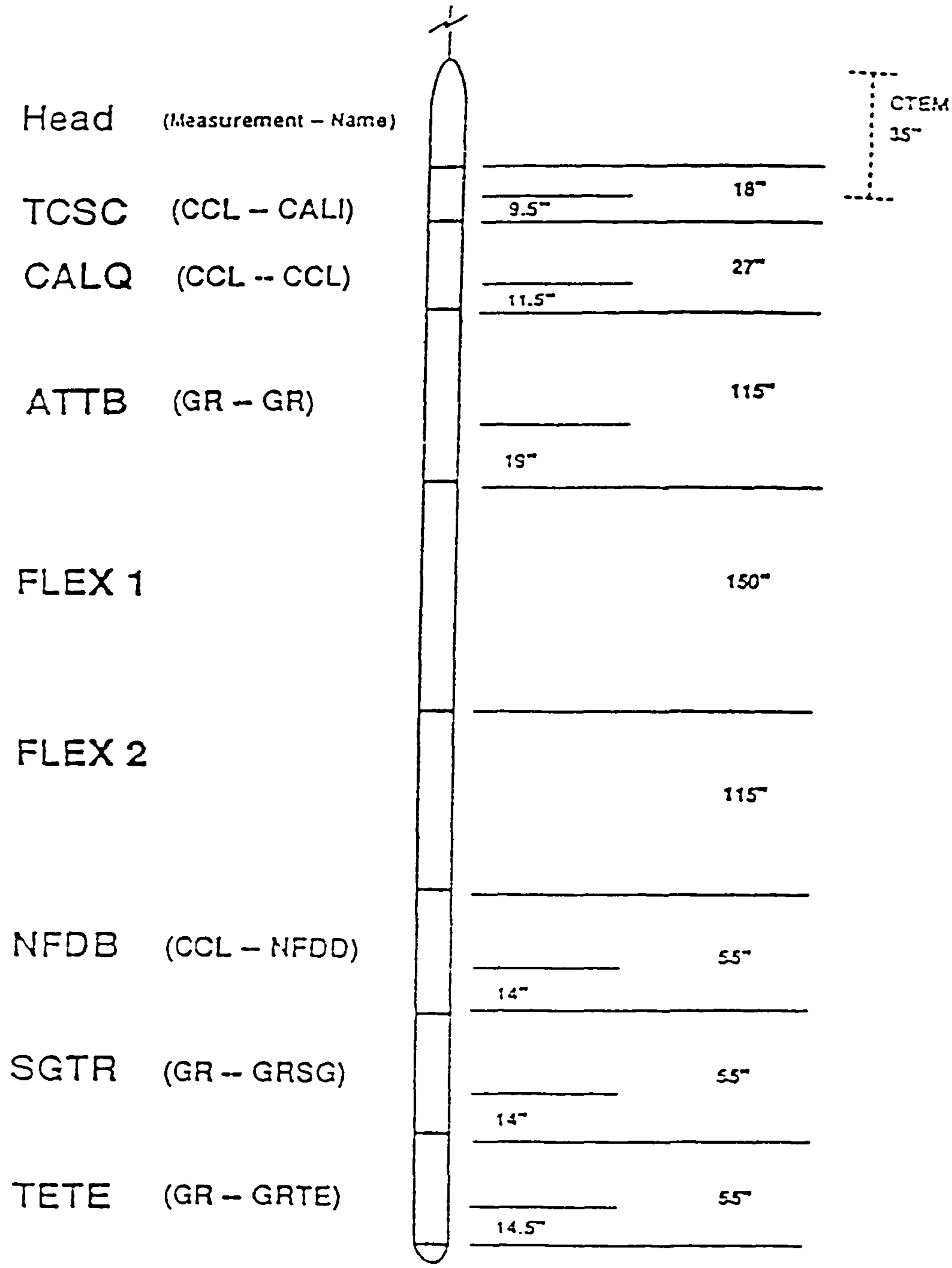

Fig. 4. 1- Subsidence compaction monitoring tool, [Green, 1991]

Klkanl and Pedrosa (1991) showed that reduction in the pore pressure in tight formations leads to increase in effective rock stresses. This increase is counterbalanced by the reduction on pore diameter which causes increase in the resistance to fluid flow and then reduced fluid storage. Klkanl and Pedrosa (1991), also, investigated the effect of wellbore storage on the pressure behavior. This study showed that assuming constant rock properties in pressure transient analysis provides good results in several situations. but on the other side, for fractured and tight formations. this assumption should be re-evaluated. The reason is that reduction in the pore pressure leads to the increase in effective rock stress. Therefore, subsidence (stress) sensitivity in a variety of reservoir situations could be important and needs to be taken into account.

Morita et al (1984) studied rock property change during reservoir compaction. They proved that the occurrence of change in rock properties such as deformation, absolute permeability, electrical resistivity, pore volume, and seismic wave velocity. This study introduced some semi-analytical equations simulating these rock properties under various loading conditions up to rock failure. Considering complex rock properties, Berea sandstone, under various loading paths, five different phases have been observed experimentally. These paths include: initial, non-linear portion, a linear volume change in rock matrix due to pore fluid pressure, and a linear volume change in rock matrix due to temperature change.

Arising problems in well drilling and production have created the need for more research about the effect of stress (subsidence) on the petrophysical properties of the reservoir rocks.

Three types of equations have appeared in the literature to express rock properties variation under stress effect. These equations are: purely analytical expressions, semi-analytical equations, and curve fitting equations to experimental data equations. The analytical method uses a simplified model for constructing the equation. Therefore, it is not preferred to be used because it is not accurate enough for practical use. On the other side, curve fitting methods give accurate values if sufficient data points exist around the point to be evaluated and also, if this equation can be proven theoretically. For these reasons, this current study will use equations produced by curve fitting and validated by a theoretical proof.

The results of several investigations showed that rock properties at subsurface stress conditions can have significant difference from those measured at normal laboratory conditions. Stress effect on rock body has been described using the stress tensor (σ) whose components represent the total force applied on the face of a unit cube of porous rock and by the pore pressure. Average stress is obtained as

$$\sigma = \frac{\sigma_{xx} + \sigma_{yy} + \sigma_{zz}}{3} \tag{4-1}$$

where

σ_{xx}, σ_{yy}, and σ_{zz} are the components of the stress in x, y, and z directions respectively.

The principle stress direction in oil fields (σ_{zz}), due to the weight of the overburden, is given by

$$\sigma_{zz} = \int_0^h g\left[\rho_w \varphi + \rho_r (1-\varphi)\right] dh \tag{4-2}$$

where

g = gravity acceleration.

h = thickness of the formation above the rock.

ρ_r = matrix rock density.

ρ_w = formation water density.

φ = porosity. (fraction)

The importance of the effect of sub-surface stress conditions on reservoir rock to the reservoir engineer is based mainly on the following two reasons:

1. evaluating the reservoir pore volume from porosity data obtained under laboratory atmospheric conditions, and
2. evaluating the variation of the reservoir pore volume with the decline of reservoir fluid pressure resulting from reservoir depletion.

Rock, bulk, fluid, and pore compressibility have been expressed mathematically as follows:

$$C_r = \frac{-1}{V_r}\left(\frac{\partial V_r}{\partial \sigma}\right)_{(\sigma - P)} \tag{4-3}$$

$$C_b = \frac{-1}{V_r}\left(\frac{\partial V_r}{\partial \sigma}\right)_P \tag{4-4}$$

$$C_f = \frac{1}{V_p}\left(\frac{\partial V_r}{\partial \sigma}\right)_\sigma \tag{4-5}$$

$$C_r = \frac{-1}{V_p}\left(\frac{\partial V_r}{\partial \sigma}\right)_P \quad (4\text{-}6)$$

where

C_r, C_b, C_f and C_p = rock, bulk, fluid, and pore compressibilities, respectively.

V = volume

P = pressure.

4. 1. Effect of Stress on Petrophysical Properties of Reservoir Rocks

Characterization of reservoir rocks during subsidence requires quantitative and qualitative interpretation of changes in porosity, permeability, density, and velocity of elastic waves with stress. Dobrynin (1962) and other researchers studied the effect of overburden pressure on several physical properties of sandstone and other geologic formations. These rock properties include: pore compressibility, porosity, formation resistivity factor, and permeability. Almost all of these researchers come up with a common conclusion of the importance of considering the overburden pressure in oil reservoir on the petrophysical properties of the rocks.

4. 1. 1. Effect of Stress on Rock Pore Compressibility

Dobrynin (1962) used the following sandstone rock samples: (1) Torpedo sandstone from Kansas, and (2) Medina sandstone from Ohio. each of these sandstone sample contains almost 5 % clay mineral.

A standard definition of rock pore-compressibility is given above by equation (4 - 6). According to Dobrynin (1962), Fig. 4. 2 shows the increase of net overburden pressure leads to the decrease in the pore compressibility. Also, Fig. 4. 2 shows that within a certain interval between P_{min} (between 150 and 300 psi) and P_{max} (between 30,000 and 35,000 psi), the relation between rock compressibility and logarithm of pressure can be approximated by a straight line. Using these data of this straight line portion, the following mathematical equation can be written as follows:

$$C_b = \frac{C_{P_{max}}}{Log(P_{max} / P_{min})} Log\left(\frac{P_{max}}{P}\right) \tag{4-7}$$

where

C $=$ rock compressibility, (1/psi)

P_{max} $=$ certain maximum pressure for straight line portion of C_p vs P,

P_{min} $=$ certain minimum pressure for straight line portion of C_p vs P,

P $=$ pore pressure.

Bulk compressibility (C_b) can be expressed as

$$C_b = \varphi C_p + (1-\varphi) * C_r \tag{4-8}$$

where

C_b, C_p, and C_r $=$ bulk, pore, and rock compressibility, respectively.

φ $=$ porosity, (fraction)

Combining equations (4-7) and (4-8) yields the relationship between bulk compressibility and pressure as follows:

$$C_b = \varphi * \frac{C_{P_{max}}}{Log(P_{max} / P_{min})} Log\left(\frac{P_{max}}{P}\right) + (1-\varphi) * C_r \tag{4-9}$$

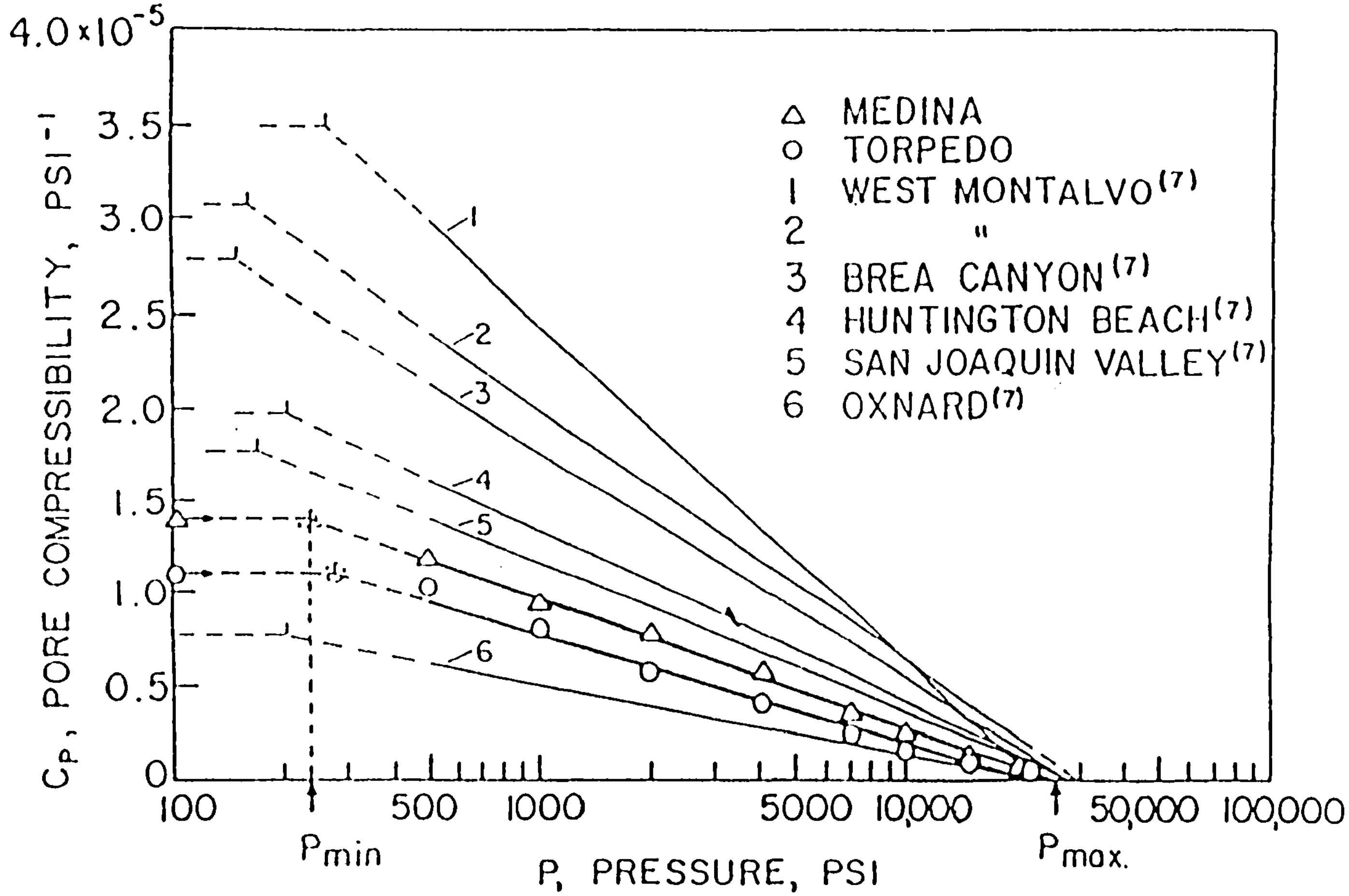

Fig. 4. 2 - Pore-compressibility as a function of net overburden pressure, [Dobrynin, 1962].

4. 1. 2. Effect of Stress on Porosity

Mathematically, the relative change in porosity can be expressed as

$$\frac{\Delta\varphi}{\varphi} = 1 - \frac{(V_p - \Delta V_p)/(V - \Delta V)}{(V_p / V)} = 1 - \frac{\left(1 - (\Delta V_p / V_p)\right)}{\left(1 - (\Delta V / V)\right)} \tag{4-10}$$

where

V, V_P = bulk and pore volume, respectively,

Δ V, Δ V_p = change in bulk and pore volume, respectively,

Neglecting the effect of the rock matrix compressibility yields

$$\frac{\Delta V}{V} = \varphi \frac{\Delta V_p}{V_p} \tag{4-11}$$

and equation (4-10) becomes

$$\frac{\Delta\varphi}{\varphi} = 1 - \frac{\left(1 - (\Delta V_p / V_p)\right)}{\left(1 - \varphi * (\Delta V / V)\right)} \tag{4-12}$$

As proven experimentally by Dobrynin (1962), through the range of $0 < P < P_{max}$. It is possible to assume that pore compressibility is independent of pressure. Therefore, relative change in pore volume can be expressed as follows:

$$\frac{\Delta V}{V} = C_{P_{max}} * F(P) \tag{4-13}$$

where F(P) is expressed by the following equation

$$F(P) = \left\{ P_{\min} + \frac{P}{Log(P_{\max} / P_{\min})} \left[Log\left(\frac{P_{\max}}{P} + 0.434\right) - \frac{P_{\min}}{P}\left(Log\left(\frac{P_{\max}}{P_{\min}}\right) - 0.434\right)\right]\right\}$$

(4-14)

Using equation (4-13) into equation (4-12) yields

$$\frac{\Delta\varphi}{\varphi} = 1 - \frac{1 - C_{P_{max}} * F(P)}{1 - \varphi * C_{P_{max}} * F(P)} \tag{4-15}$$

Fig. 4. 3 demonstrates the relative change in porosity under the effect of pressure for different values of minimum pore compressibility, calculated using equation (4-15). In addition, Fig. 4. 4 was constructed for determination changes in porosity and density as a function of net overburden pressure.

Recently, McKee et al (1988) laid the foundation for the theoretical relationship between stress-dependent permeability and porosity for coals and other geologic formations. This relationship eliminates the need for variable compressibility in the range of interest, and therefore, is simpler to use and not limited by maximum stress. The resultant formulas are shown fitting both laboratory and field data. Considering the volume of solid grains is given by

$$V_s = A * \Delta z(1 - \varphi) \tag{4-16}$$

where

V_s = volume of solid grains,

A = cross-sectional area of the rock,

Δz = difference in the height of the rock,

φ = porosity of the rock.

Assuming that the compressibility of individual grains in solid is negligible in comparison to the change in porosity is a valid assumption. Also, assuming constant pore compressibility is a good assumption. The reason is pore compressibility is independent on pressure in the range of 0.0 to 20,000 psi.

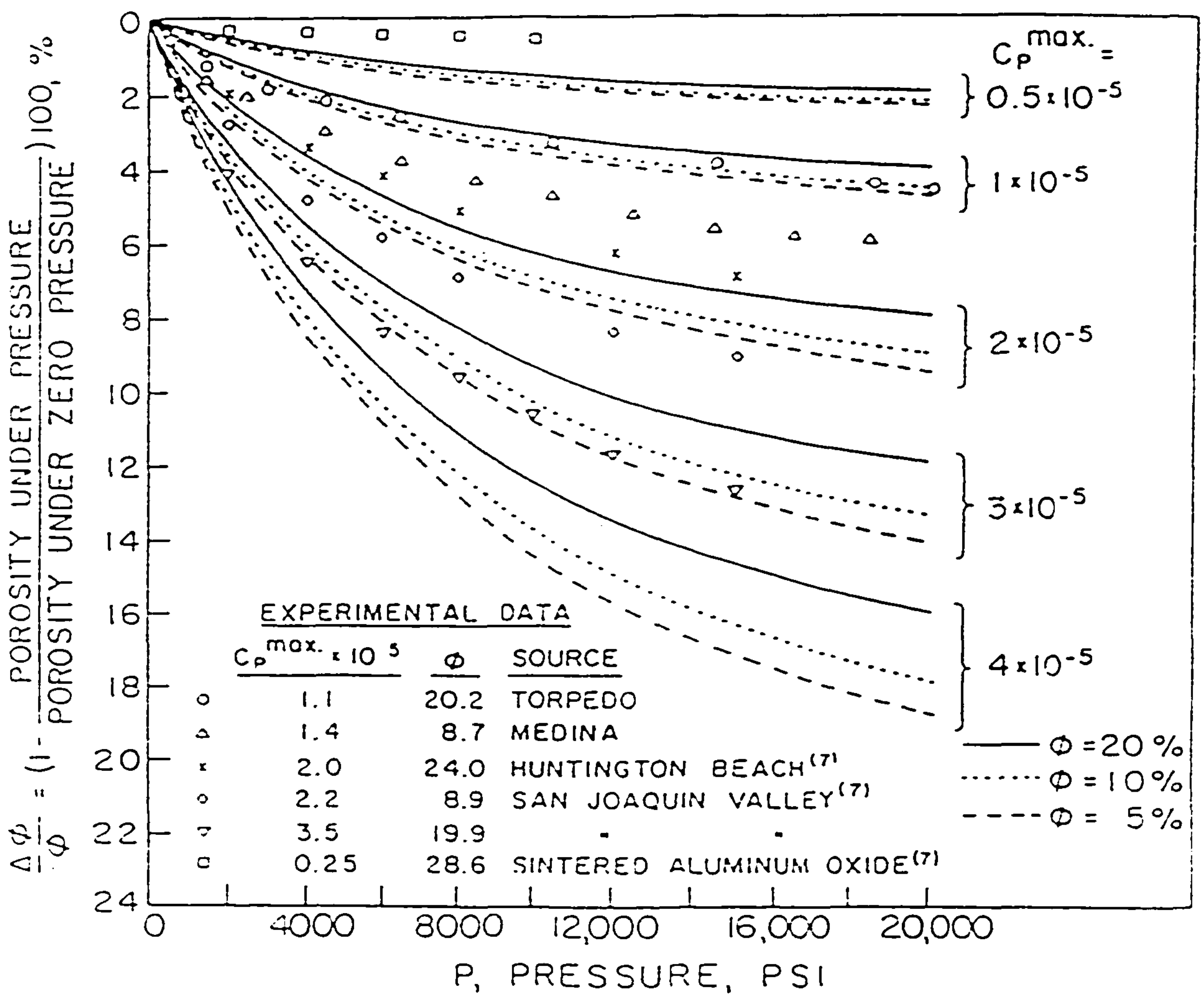

Fig. 4. 3 - Calculated curves of changes in porosity versus net overburden pressure compared with experimental data, [Dobrynin, 1962].

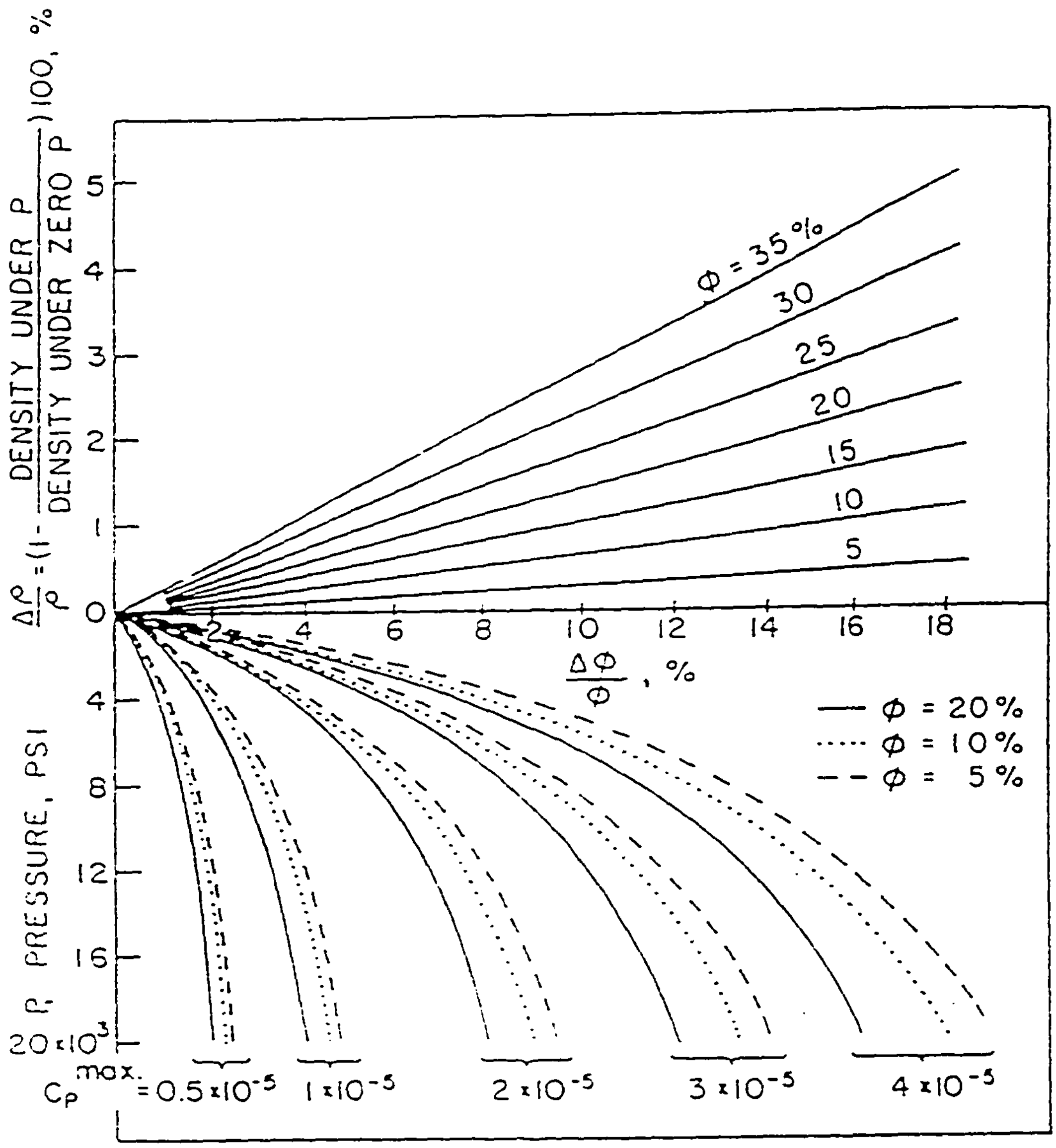

Fig. 4. 4 - Graph for determining changes in porosity and density as a function of net overburden pressure, [Dobrynin, 1962]

Hantush (1964) derived the following relationship holds for the change in porosity, with respect to the change in effective (compressive) stress:

$$d\varphi = -C_m(1-\varphi)d\sigma \qquad (4\text{-}17)$$

where

C_m = bulk matrix compressibility,

$d\varphi$ = change in porosity,

$d\sigma$ = change in effective stress = $\sigma - \sigma_o$

Equation (4-17) assumes that all stress relief is the result of pore space comprising the effective interconnected porosity. Since bulk matrix compressibility is related to pore compressibility by porosity as follows:

$$C_m = \varphi * C_p \qquad (4\text{-}18)$$

Combining equations (4-17) and (4-18) results in:

$$d\varphi = -\varphi(1-\varphi) * C_p d\sigma \qquad (4\text{-}19)$$

Integrating of equation (4-19) yields:

$$\varepsilon = \frac{\varphi}{(1-\varphi)} = \frac{\varphi_o}{(1-\varphi_o)}\exp\left[\int_{\sigma_o}^{\sigma} C_p d\sigma\right] \qquad (4\text{-}20)$$

where

ε = void to grain ratio of the rock,

C_p = average pore compressibility,

φ = effective interconnected porosity under stress condition,

φ_o = effective interconnected porosity under initial conditions.

By definition, average pore compressibility will be:

$$\bar{C}_p = \frac{1}{\sigma - \sigma_o} \int_{\sigma_o}^{\sigma} C_p d\sigma \tag{4-21}$$

At this point, equation (4-20) can be written as:

$$\varepsilon = \frac{\varphi}{(1-\varphi)} = \frac{\varphi_o}{(1-\varphi_o)} * e^{-\bar{C}_p \Delta\sigma} \tag{4-22}$$

Assuming that pore compressibility is constant, then equation (4-22) can be formulated as follows:

$$\varphi_s = \varphi_o * \frac{e^{-\bar{C}_p \Delta\sigma}}{\left[1 - \varphi_o\left(1 - e^{-\bar{C}_p \Delta\sigma}\right)\right]} \tag{4-23}$$

where

φ_s = porosity under stress condition, (fraction)

φ_o = porosity under zero (or initial) stress condition, (fraction)

$\Delta\sigma$ = change in effective stress, (psi)

$\bar{C}_p$ = average rock compressibility, (1/psi)

This equation, (4-23), represents a real new foundation for accounting for the effect of effective stress on porosity. It is important to emphasize that equation (4-23) is not only supported by strong assumptions and theoretical base, but its results also fit both laboratory and field data for different geologic formations. Eight laboratory core tests using two sandstone, one granite, four coal, and one clay have been used for testing this equation, (4-23), and the correlation coefficient ranged from 0.82 to 0.92. In addition, porosity data using well logs yielded excellent curve fitting. For all of the previously mentioned reasons, equation (4-23) has been chosen by this study to consider the stress effect on porosity during characterization and identification of flow units in clean reservoirs.

4. 1. 3. Effect of Stress on Rock Density

Change of rock density with increasing stress is dependent upon the change in pore volume, and the changes in the density of mineral grains and the contained fluids. For oil fields where rocks above producing formations is completely saturated with brine and subjected to overburden pressure (almost less than 20,000 psi in several cases), the change in rock density is mainly expected to be from a change in pore volume.

Dobrynin (1962) showed that the effect of overburden pressure on the change in density of porous rocks. Density of porous rock can be expressed as follows:

$$\rho = \rho_r - (\rho_r - \rho_f) * \varphi \qquad (4\text{-}24)$$

where

ρ, ρ_r, ρ_f = density of porous rock, rock matrix, and fluid, respectively.

Considering the change in porosity, as discussed in the previous section. Then, the relative change in porous rock density can be written as follows

$$\frac{\Delta\rho}{\rho} = \left[\frac{(\rho_r - \rho_f)}{(\rho_r / \varphi) - (\rho_r - \rho_f)}\right] * \left[1 - \frac{C_{p_{max}} F(P)}{1 - \varphi C_{p_{max}} F(P)}\right] \qquad (4\text{-}25)$$

Using rock density = 2.65 gm/cc and fluid density = 1.0 gm/cc, equation (4-25) is used to plot Fig. 4. 4. This figure shows change in porosity and density as a function of net overburden pressure.

Recently, McKee et al (1988) studied the effect of effective stress on the density of the porous rock and developed an equation for correlating the ratio of the pore-volume to grain volume with the effective stress as follows: writing the specific density of a rock in terms of specific density of its matrix can be made by the following equation:

$$\rho = \rho_g * (1-\varphi) \tag{4-26}$$

where

ρ = specific density of the rock, (gm/cc)

ρ_g = specific density of the matrix of the rock, (gm/cc)

φ = total porosity of the rock, (fraction)

Porosity can be substituted from equation (4-23) into equation (4-26) to get

$$\rho = \frac{\rho_g(1-\varphi)}{\left[1-\varphi_o\left(1-e^{-\bar{C}_p \Delta\sigma}\right)\right]} \tag{4-27}$$

Solving equation (4-26) for porosity as a function of specific density of the rock yields

$$\varphi = \frac{\rho_g - \rho}{\rho_g} \tag{4-28}$$

Therefore,

$$\frac{\varphi}{1-\varphi} = \frac{\rho_g - \rho}{\rho_g} = e^{-\bar{C}_p \Delta\sigma} \tag{4-29}$$

Equation (4-29) indicates that a semi-log plot of $[(\rho_g - \rho)/\rho_g]$ versus effective stress will provide a straight line for constant pore compressibility.

4. 1. 4. Effect of Stress on Formation Resistivity Factor

Formation resistivity factor is well-defined by the following equation for clean formations and without considering the effect of stress (subsidence):

$$F = \frac{1}{\varphi^m} \tag{4-30}$$

where

m = cementation factor depending upon the amount and distribution of cementing materials between sand grains.

Equation (4-30) assumes (a=1.0). Considering the effect of overburden pressure on the rock will reduce the porosity by a factor of ($\Delta\varphi$). Fatt (1957) shows that the cementation factor (m) is increased by a factor (Δ m) with increasing the overburden pressure. Therefore, equation (4-30) can be written as

$$F_p = \frac{1}{(\varphi - \Delta\varphi)^{m+\Delta m}} \tag{4-31}$$

Dividing equation (4-30) by equation (4-31) provides the relative change in formation resistivity factor as

$$\frac{F_p}{F} = \frac{1}{\left(1 - \frac{\Delta\varphi}{\varphi}\right)^m \left(1 - \frac{\Delta\varphi}{\varphi}\right)^{\Delta m} * \varphi^{\Delta m}} \tag{4-32}$$

For simplicity, it is possible to assume that $(1 - (\Delta\varphi / \varphi))^{\Delta m} = 1.0$ is a good approximation and for "m" greater than or equal to 2.0, $(\Delta\varphi / \varphi))^2 = 0.0$, then equation (4-32) becomes

$$\frac{F_p}{F} = \frac{1}{(1 - \frac{\Delta\varphi}{\varphi})^m * \varphi^{\Delta m}} \tag{4-33}$$

Dobrynin (1962) proved that the value of (Δ m) can be expressed as a function of pressure and lithology, and the maximum change in (Δ m) depends upon the number of small conductivity channels in the rock. Assuming that shale content expressed as a percentage of total pore space $(\varphi/(\varphi+c))$, where "c" is the pore volume occupied by shale. Fig. 4. 5 shows ratio of shale content to total bulk volume as a function of change of (Δ m) with pressure. Finally, the ratio of the formation resistivity factor under overburden pressure to formation resistivity factor can be expressed by:

$$\frac{F_p}{F} = \frac{1}{\left(\frac{2(1-C_{P_{max}})}{(1-C_P)} - 1\right) * \varphi^{f(P,(c/c+\varphi))}} \tag{4-34}$$

A comparison between the calculated and experimentally measured formation resistivity factor has been plotted in Fig. 4. 6.

Dobrynin (1962) compared the experimental data with calculated data of relative change of formation resistivity factor, Fig. 4. 6, which shows a very good matching and agreement between the two.

4. 1. 5. Effect of Stress on Permeability

Change of permeability under pressure may be assumed depending mainly upon the reduction of the pore channels. Using Marshall's equation of permeability to study the effect of overburden pressure on permeability. The study, conducted by Dobrynin (1962), showed that increasing overburden pressure leads to a reduction in rock permeability, Fig. 4. 7.

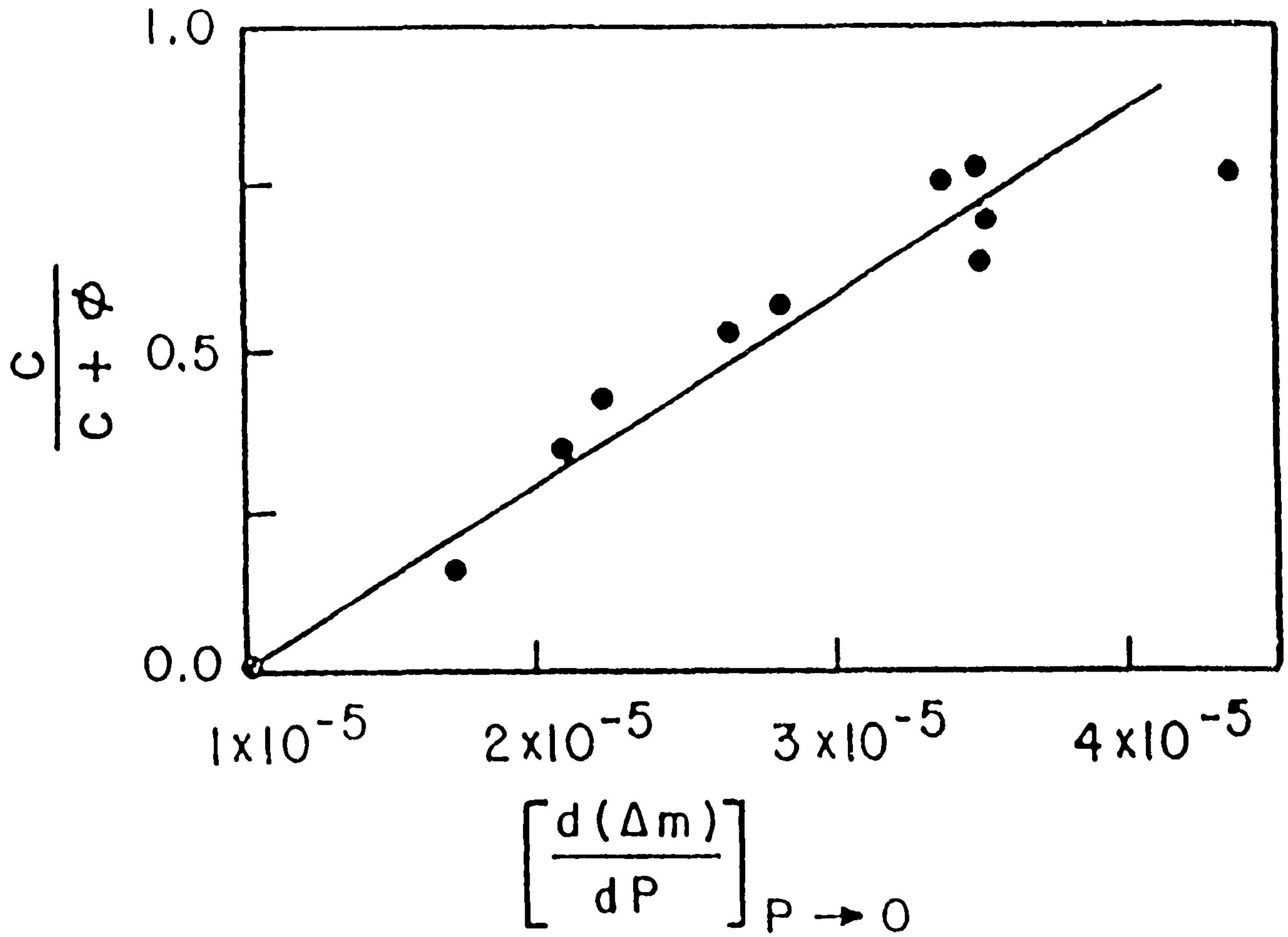

Fig. 4. 5 - Relative clay content (c) versus change in formation-resistivity factor exponent (m) under net overburden pressure, [Dobrynin, 1962].

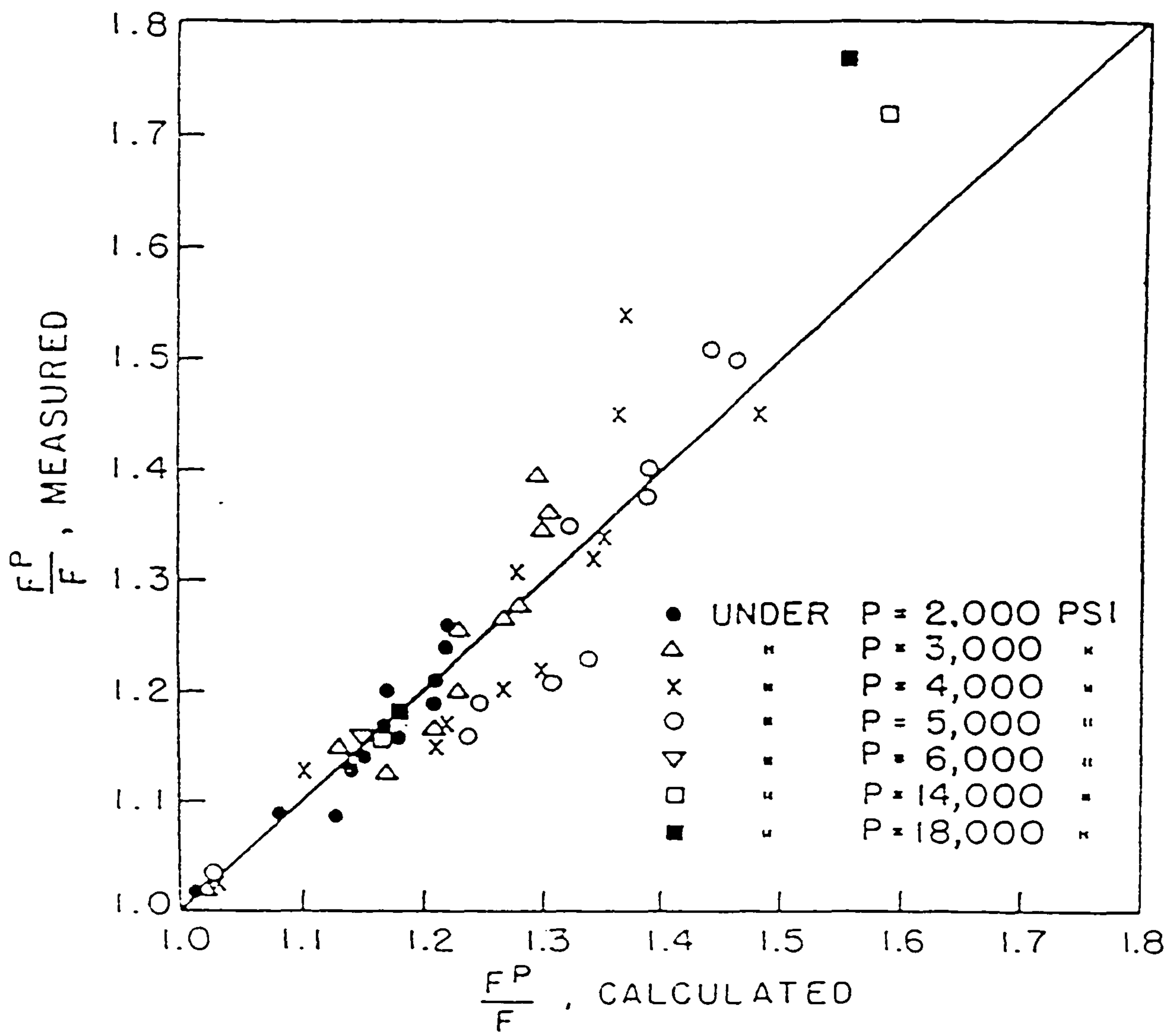

Fig. 4. 6 - Comparison of calculated values of (F_P/F) and measured values of (F_P/F), [Dobrynin, 1962].

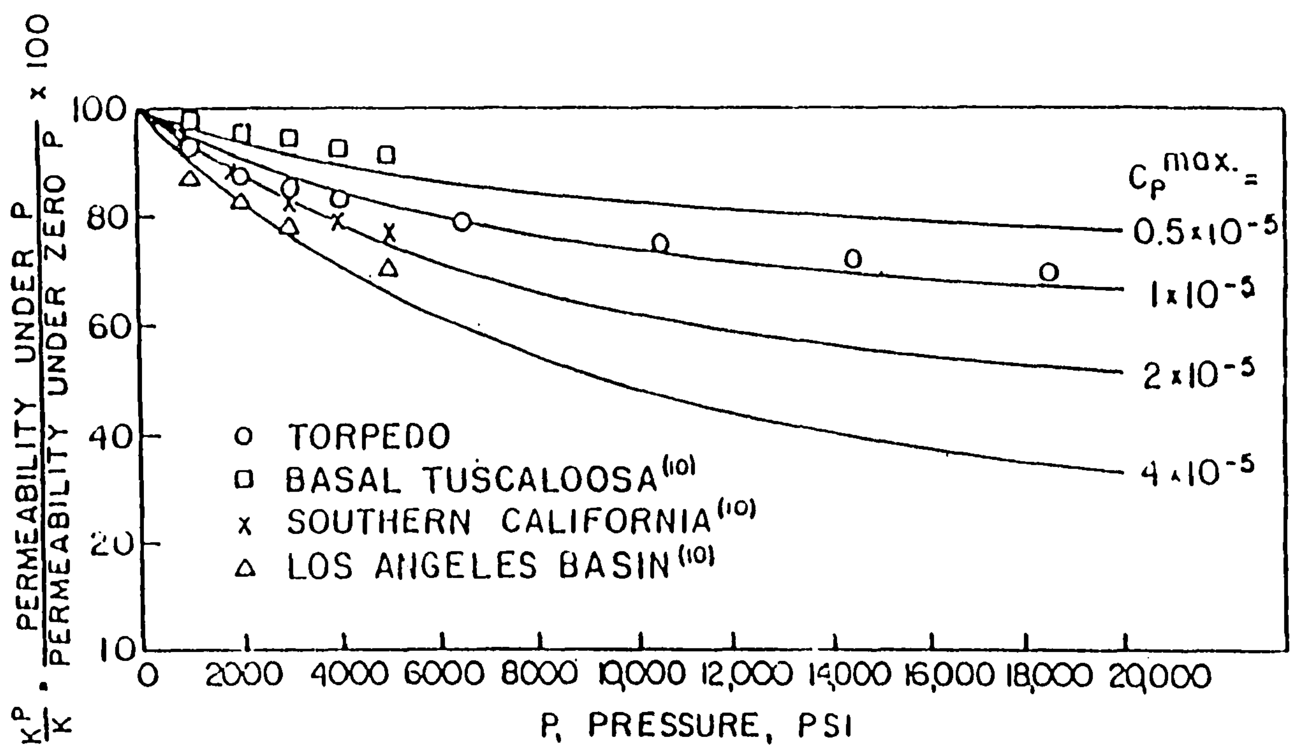

Fig. 4. 7 - Calculated curve showing changes in permeability of sandstones as a function of net overburden pressure, [Dobrynin, 1962]

Fig. 4. 7 shows the relative change in rock permeability as a function of net overburden pressure for different pore compressibilities. Next, Gary and Fatt (1963) studied the effect of stress on permeability of sandstone and proved that not only the rock permeability but also the permeability anisotropy of several sandstones is a function of overburden pressure.

In addition, Gary and Fatt showed that the permeability reduction due to stress effect is also a function of the ratio of radial to axial stress. Fig. 4. 8 shows the effect of applied stress on actual horizontal permeability and absolute permeability of Berea sandstones. Fig. 4. 9 shows the effect of the applied stress on the actual horizontal and vertical permeability of Roise sandstone. Fatt (1952) has shown also that the permeability of reservoir sandstones are decreased by application of overburden pressure. Fatt (1953) proved the reduction in relative permeability by application the overburden pressure on sanstones. The same result have been confirmed by Fertl et al (1962).

The overburden pressure of the rock is approximately 0.56 psi/ft of depth for shaly sandstone having density 2.3 gm/cc and liquid density = 1.0 gm/cc.

Recently, Jones (1988) defined net stress as the difference between isostatic (hydrostatic) confining stress and the average pore pressure. Jones (1988) introduced several empirical equations describing change in permeability, pore volume and porosity with net confining stress. This equation for permeability is given by:

$$K_S = K_O * EXP\left\{\frac{a_K\left[EXP\left(-\sigma / \sigma^{*}\right)-1\right]}{\left(1-C*\sigma\right)}\right\} \tag{4-35}$$

where

a_k, a_v, and c = curve fitting constants

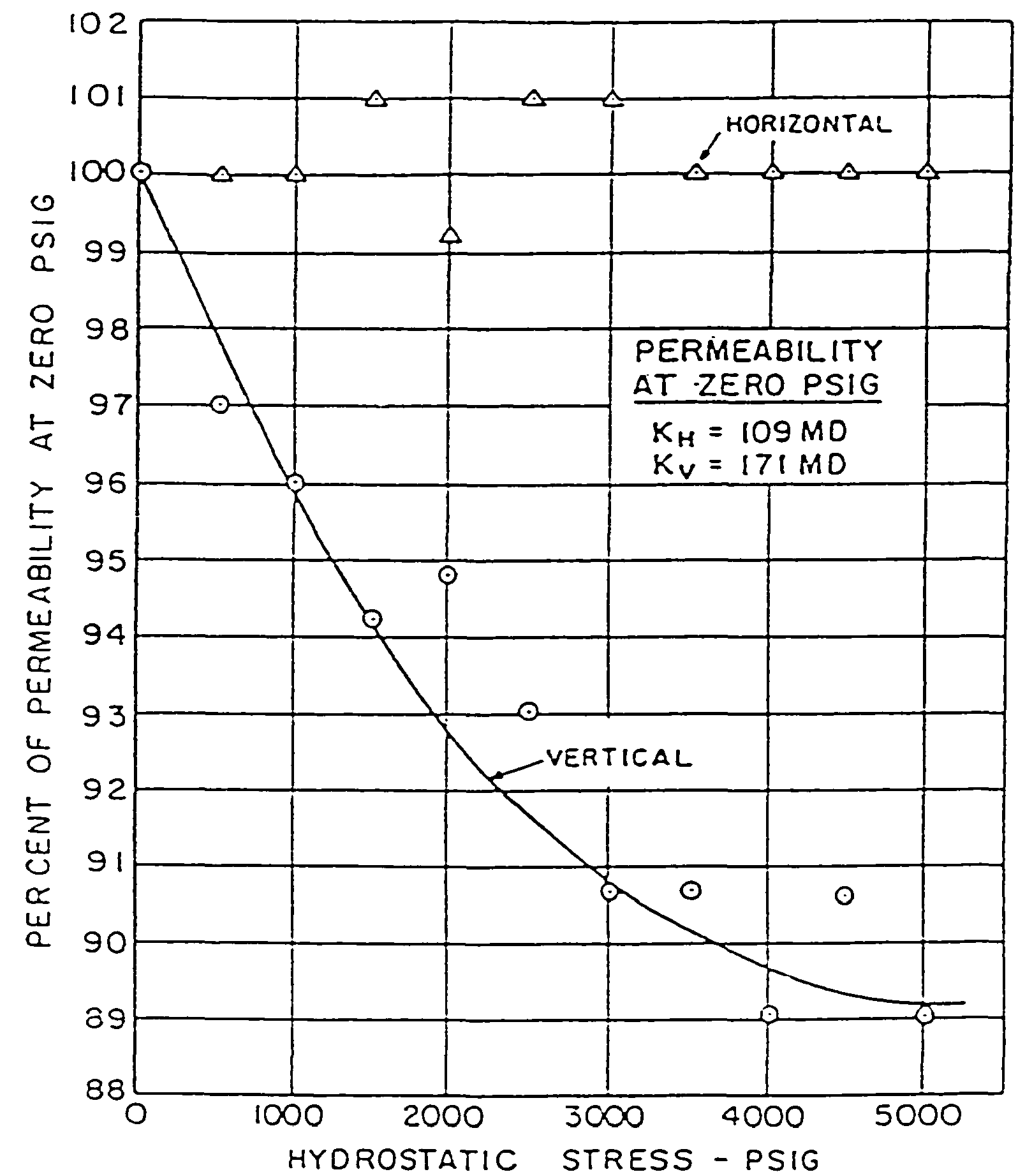

Fig. 4. 8 - The effect of the applied stress on the actual horizontal and vertical permeabilities of Roise sandstone, [Gary and Fatt, 1963]

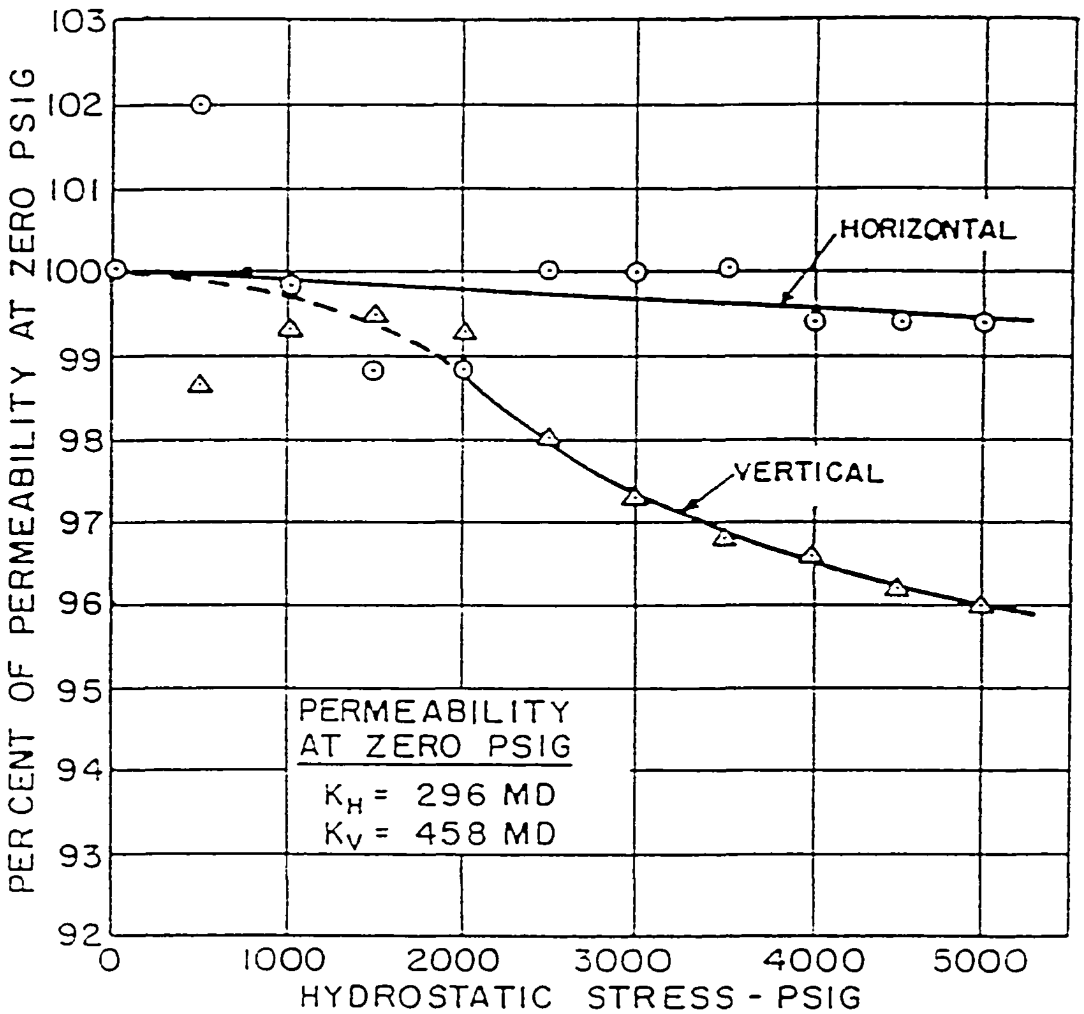

Fig. 4. 9 - The effect of the applied stress on the actual horizontal and vertical permeabilities of Berea sandstone, [Fatt, 1953].

σ = net isostatic stress, (psi)

σ^* = decay constant.

This equation, and other equations for porosity and pore compressibility suffer from:

1. requirement the determination of four adjustable parameters which have to be determined experimentally, and
2. these equations have been determined using only two confining stresses (1,500 and 5,000 psi) which is not enough for getting accurate curve fitting. Fig.4. 10 shows data used for getting equation (4-35).

McKee et al (1988) used the equation of porosity, equation (4-23), and assumed that Carmen-Kozeny equation is valid to get the following equation correlating porosity and permeability as follows:

$$K \alpha \frac{\varphi^3}{(1-\varphi)^2} \tag{4-36}$$

Combining equations (4-23) and (4-30) yields:

$$K_s = K_o \frac{e^{-3 \cdot \bar{C}_p \Delta\sigma}}{\left[1-\varphi_o\left(1-e^{-\bar{C}_p \Delta\sigma}\right)\right]} \tag{4-37}$$

Equation (4-37) shows the effect of effective stress on permeability assuming constant pore compressibility. This equation, in combination with equation (4-23), will be used to consider the effect of stress while characterizing and identification the hydraulic (flow) units in the clean formations.

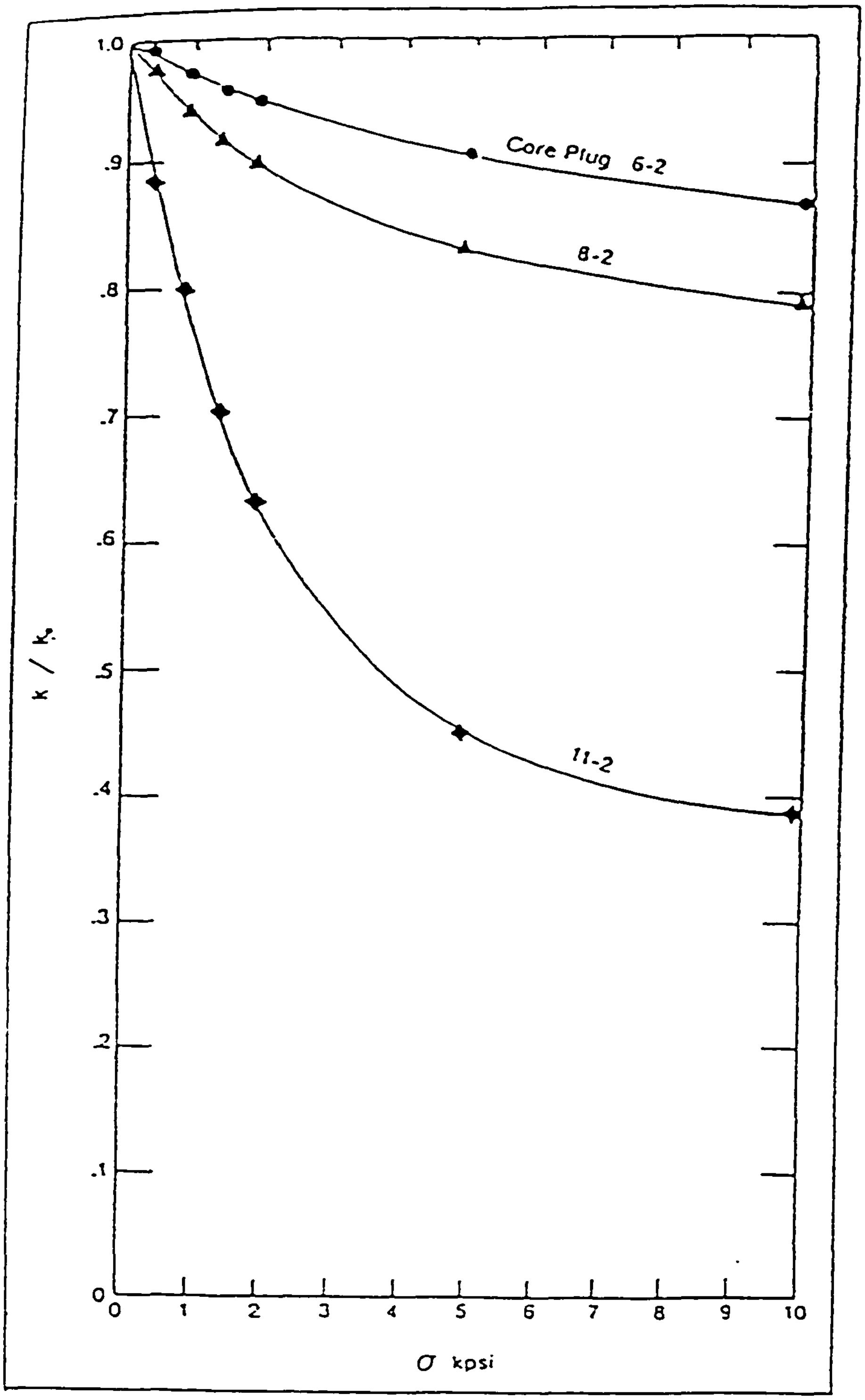

Fig. 4. 10 - Permeability versus stress data with best fit of equation (4-35), [Jones, 1988]

4. 1. 6. Effect of Fluid Pressure on Permeability

Hantush (1964) noted that a change in effective stress, if the water pressure is assumed to act effectively throughout the elemental volume under investigation. The relation between the pressure and the effective stress was formulated as follows:

$$dP = -d\sigma \tag{4-38}$$

Walsh (1981) introduced a general relationship between the effective and the total stresses as follows

$$\sigma = \sigma_t - \alpha P \tag{4-39}$$

where

σ = effective stress, (psi)

σ_t = total stress, (psi)

α = constant, correlating change in pore pressure to change in effective stress

Integrating equation (4-38) over the stress range yields

$$\Delta\sigma = \sigma - \sigma_o = \alpha(P_o - P) = \alpha\Delta P \tag{4-40}$$

where

σ_o = initial stress, (psi)

P_o = initial reservoir pore-pressure, (psi)

ΔP = pressure drop, (psi)

$\Delta\sigma$ = increase in effective stress, (psi)

Using equation (4-40) in equation (4-37) yields an equation for permeability considering pore pressure as follows:

$$K_s = K_o \frac{e^{-3 \cdot \alpha \bar{C}_p \Delta p}}{\left[1-\varphi_o\left(1-e^{-\alpha \bar{C}_p \Delta p}\right)\right]} \tag{4-41}$$

Equation (4-41) is a very important tool for predicting the effect of pressure drop on reservoir permeability.

4. 2. Effect of Stress on Reservoir Quality Index (RQI)

Characterization of clean formations under subsidence (stress) creates a need for developing new expression for reservoir quality index (RQI). McKee et al (1988) derived relationship between porosity at original condition (without stress effect) and porosity under stress, equation (4-23), which is given by

$$\varphi_s = \varphi_o * \frac{e^{-\bar{C}_p \Delta\sigma}}{\left[1-\varphi_o\left(1-e^{-\bar{C}_p \Delta\sigma}\right)\right]} \tag{4-23}$$

Rearranging equation (4-23) results in the following form

$$\frac{e^{-\bar{C}_p \Delta\sigma}}{\left[1-\varphi_o\left(1-e^{-\bar{C}_p \Delta\sigma}\right)\right]} = \frac{\varphi_s}{\varphi_o} \tag{4-43}$$

Again, McKee et al (1988) introduced another equation for permeability, equation (4-37) as follows:

$$K_s = K_o \frac{e^{-3 \cdot \bar{C}_p \Delta\sigma}}{\left[1-\varphi_o\left(1-e^{-\bar{C}_p \Delta\sigma}\right)\right]} \tag{4-37}$$

Rearranging equation (4-37) in a similar form as for porosity equation, equation (4-23), yields

$$\frac{e^{-\bar{C}_p \Delta\sigma}}{\left[1-\varphi_o\left(1-e^{-\bar{C}_p \Delta\sigma}\right)\right]} = \frac{K_s}{K_o} * e^{-2\bar{C}_p \Delta\sigma} \qquad (4\text{-}44)$$

Equating equations (4-43) and (4-44) results in

$$\frac{K_o}{\varphi_o} = \frac{K_s}{\varphi_s} e^{-2\bar{C}_p \Delta\sigma} \qquad (4\text{-}45)$$

where

K_o = permeability at initial condition (without stress effect), (md)

φ_o = porosity at initial condition (without stress effect), (fraction)

K_s = permeability under stress, (md)

φ_s = porosity under stress, (fraction)

$\Delta\sigma$ = change in effective stress, (psi)

$\bar{C}_p$ = average pore compressibility, (1/psi)

Amaefule et al (1993) introduced RQI definition as

$$RQI_o(\mu m) = 0.0314 * \sqrt{\frac{K_o}{\varphi_o}} \qquad (4\text{-}46)$$

Let us define the RQI of formation under stress (RQIs) by the following equation:

$$RQI_S(\mu m) = 0.0314 * \sqrt{\frac{K_S}{\varphi_s}} \qquad (4\text{-}47)$$

where

RQIs = Reservoir Quality Index for formation under stress. (μm)

Ks = Permeability of the rock under stress conditions. (md)

φ_s = Porosity of the rock under stress conditions. (fraction)

Based on the definition of RQI. the values of porosity and permeability at the original conditions (even. if it is under certain stress) should be used. For that reason. substituting equations (4-46) and (4-47) into equation (4-45) yields

$$RQI_S(\mu m) = 0.0314 * \sqrt{\frac{K_o}{\varphi_o}} * e^{-\bar{C}_p \Delta\sigma} \qquad (4\text{-}48)$$

Applying natural log on both sides of equation (4-48) provides

$$Ln(RQI_S) = -\bar{C}_P * \Delta\sigma + Ln(RQI_O) \qquad (4\text{-}49)$$

Equation (4-48) represents a valuable tool for correlating Reservoir Quality Index at zero stress condition (RQIo) measured under laboratory conditions and Reservoir Quality Index under stress condition (RQIs) (using well-logging data). Fig. 4. 11A using data in Table 4. 1. A shows the effect of change in effective stress on the Reservoir Quality Index under stress (RQIs) for different values of Reservoir Quality Index under zero stress condition (RQIo), using equation (4-48). This Figure. 4. 11A. proves the importance of considering stress effect while characterizing and identifying flow units in clean formations. It shows that the increase of stress from 0.0 to 1,800 psi causes a severe reduction in Reservoir Quality Index (RQI) value. Equation (4-49) represents a linear relationship between Ln (RQIs) and the product of pore compressibility and change of

Table 4. 1.A - Simulated data for studying the effect of stress on the newly-developed Reservoir Quality Index (RQIs).

Sandstone formations
Average Cp = 0.000144 (1/psi) (from Bolivar Oil Field, Venezuela)

del stress	RQIs=0.1	RQIs=0.5	RQIs=1	RQIs= 5
0	0.1	0.5	1	5
500	0.093054	0.4652689	0.9305378	4.65268921
1000	0.08659	0.4329503	0.8659007	4.32950338
1500	0.080575	0.4028767	0.8057533	4.02876674
2000	0.074978	0.374892	0.749784	3.74891991
2500	0.06977	0.3488512	0.6977024	3.48851184
3000	0.064924	0.3246192	0.6492385	3.24619228
3500	0.060414	0.3020705	0.604141	3.02070476
4000	0.056218	0.281088	0.562176	2.81088009
4500	0.052313	0.261563	0.5231261	2.6156303
5000	0.048679	0.2433943	0.4867886	2.43394297
5500	0.045298	0.2264876	0.4529752	2.26487604
6000	0.042151	0.2107553	0.4215106	2.10755287

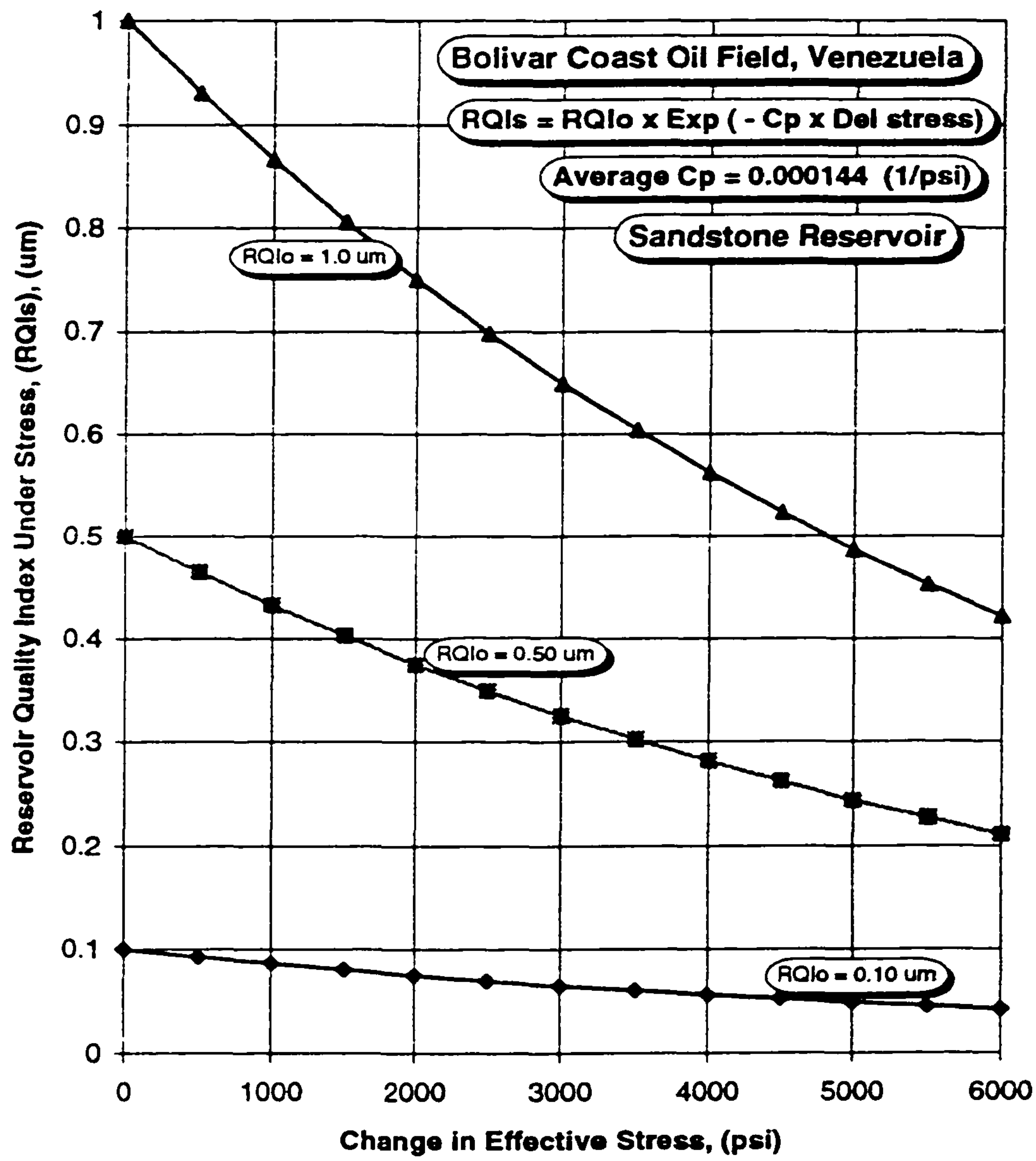

Fig. 4.11A-Effect of stress on Reservoir Quality Index of formation under stress (RQIs)

effective stress. Data in Table 4.1B is used to study the effect of stress on the RQI. The results shows that increasing the change ineffective stress reduces the values of RQIs. Also, the increase in the change in effective stress causes a more reduction in RQIs at smaller values of RQIo than in larger values.

Fig. 4.11B shows a graphical representation of equation (4-49). It shows the change in reservoir quality index under stress (RQIs) under different values of effective stress, and for different values of reservoir quality index under zero stress conditions (RQIs). This figure, 4.11B, shows that an increase in change in effective stress leads to a decrease in RQIs, assuming a constant rock compressibility.

From equation (4-49), the ratio of reservoir quality index with and without stress effect (RQIs/RQIo) can be written as follows:

$$\frac{RQI_S}{RQI_O} = e^{-\bar{C}_p * \Delta\sigma} \qquad (4\text{-}50)$$

Applying natural log on both sides of equation (4-50) yields

$$Ln(RQI_S \; / \; RQI_O) = -\bar{C}_P * \Delta\sigma \qquad (4\text{-}51)$$

Equation (4-50) is very useful for showing and studying the effect of stress on RQI. Also, it can be used effectively for characterizing and identifying flow units in clean formation under stress effect.

A plot of the ratio of RQIs and RQIo versus change in effective stress is given in Fig. 4.12A, using simulated data in Table 4.2 assuming constant average pore compressibility (average Cp = 0.000144 1/psi). Figure 4. 12A shows that (RQIs/RQIo)

Table 4. 1. B - Simulated data for studying the effect of stress on Reservoir Quality Index under Stress (RQIs).

Sandstone formations
Average Cp = 0.000144 (1/psi) (from Bolivar Oil Field, Venezuela)

del stress	Cp*del(stress)	RQIs=1	RQIs=2	RQIs= 3	RQIs=4	RQIs=5	RQIs=10
0	0	1	2	3	4	5	10
500	0.2	0.930538	1.861076	2.791614	3.722151	4.652689	9.305378
1000	0.4	0.865901	1.731801	2.597702	3.463603	4.329503	8.659007
1500	0.6	0.805753	1.611507	2.41726	3.223013	4.028767	8.057533
2000	0.8	0.749784	1.499568	2.249352	2.999136	3.74892	7.49784
2500	1	0.697702	1.395405	2.093107	2.790809	3.488512	6.977024
3000	1.2	0.649238	1.298477	1.947715	2.596954	3.246192	6.492385
3500	1.4	0.604141	1.208282	1.812423	2.416564	3.020705	6.04141
4000	1.6	0.562176	1.124352	1.686528	2.248704	2.81088	5.62176
4500	1.8	0.523126	1.046252	1.569378	2.092504	2.61563	5.231261
5000	2	0.486789	0.973577	1.460366	1.947154	2.433943	4.867886
5500	2.2	0.452975	0.90595	1.358926	1.811901	2.264876	4.529752
6000	2.4	0.421511	0.843021	1.264532	1.686042	2.107553	4.215106

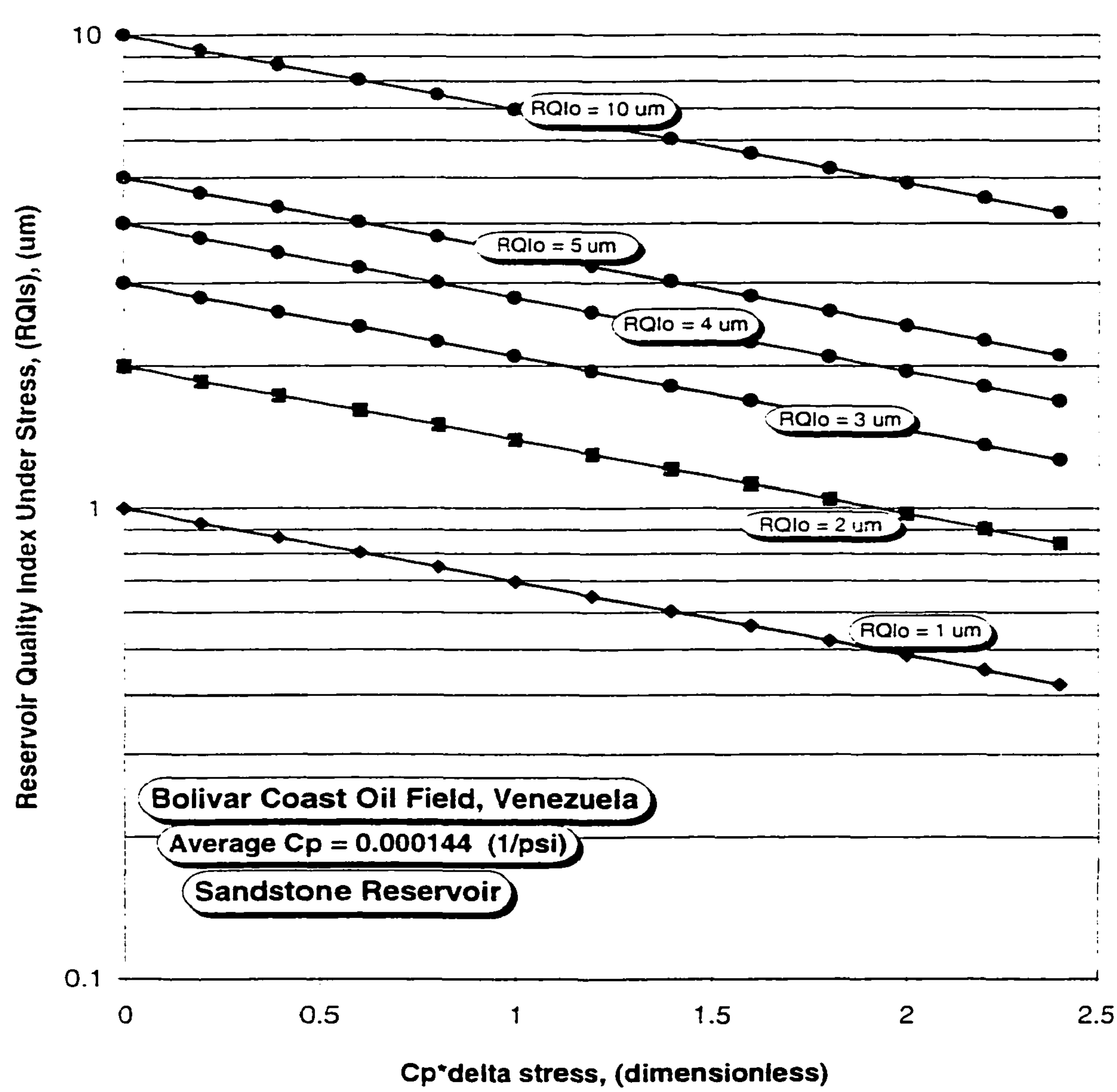

Fig. 4.11. B- Semi-Log Plot of the Effect of Change in Effective Stress on Reservoir Quality Index Under Stress

decreases with increase in ($\bar{C}_p * \Delta\sigma$). This confirms the importance of considering the effect of stress. Ignoring this effect may lead to serious mistakes due to a markable reduction in RQIs with increase in change in effective stress.

A graphical presentation of equation (4-51) is shown in Fig. 4. 12. B. This figure shows a linear relationship between RQIs/RQIo and the change in effective stress. It shows that increasing the change in effective stress decreases the ratio of RQIs to RQIo. It also shows that the reduction in (RQIs/RQIo) is larger at higher values of change in effective stress than at smaller ones because the slope of curve increases with increasing the values of change in effective stress.

The most important aspect of equations (4-50) and (4-51) is their elimination of the need for measuring rock porosity and permeability under stress conditions. Laboratory measurements (at zero stress condition) of porosity and permeability can be used to calculate conventional Reservoir Quality Index (RQIo) and use it only with the expected stress values in the field. Again, equation (4-50) can be used with well-logging derived data because the porosity and permeability values are generally estimated under stress. Then, the use of equation (4-50) does not require laboratory measurements of porosity and permeability in order to get the conventional RQI (RQIo) values.

Table 4. 2 - Simulated data for studying the effect of stress on (RQIs/RQIo)

Sandstone formations

Average Cp = 0.000144 (1/psi) (from Bolivar Oil Field, Venezuela)

cp*del(stress)	porosity	Perm.	RQIo	change in effective stress	RQIs	RQIs/RQIo
	(%)	(md)	(um)	(psi)	(um)	
0	0	0	-	0	-	1
-0.2	13	0.17	0.035907	500	0.033413	0.930538
-0.4	26	6.17	0.152963	1000	0.132451	0.865901
-0.6	13	4.29	0.180379	1500	0.145341	0.805753
-0.8	14	9.74	0.261906	2000	0.196373	0.749784
-1	17	23.74	0.371061	2500	0.25889	0.697702
-1.2	18	39.76	0.466677	3000	0.302985	0.649238
-1.4	22	82.96	0.609751	3500	0.368376	0.604141
-1.6	25	142.63	0.750007	4000	0.421636	0.562176
-1.8	23	155.06	0.815297	4500	0.426503	0.523126
-2	21	161.45	0.870641	5000	0.423818	0.486789
-2.2	19	161.48	0.915403	5500	0.414655	0.452975
-2.4	17	155.03	0.948229	6000	0.399688	0.421511

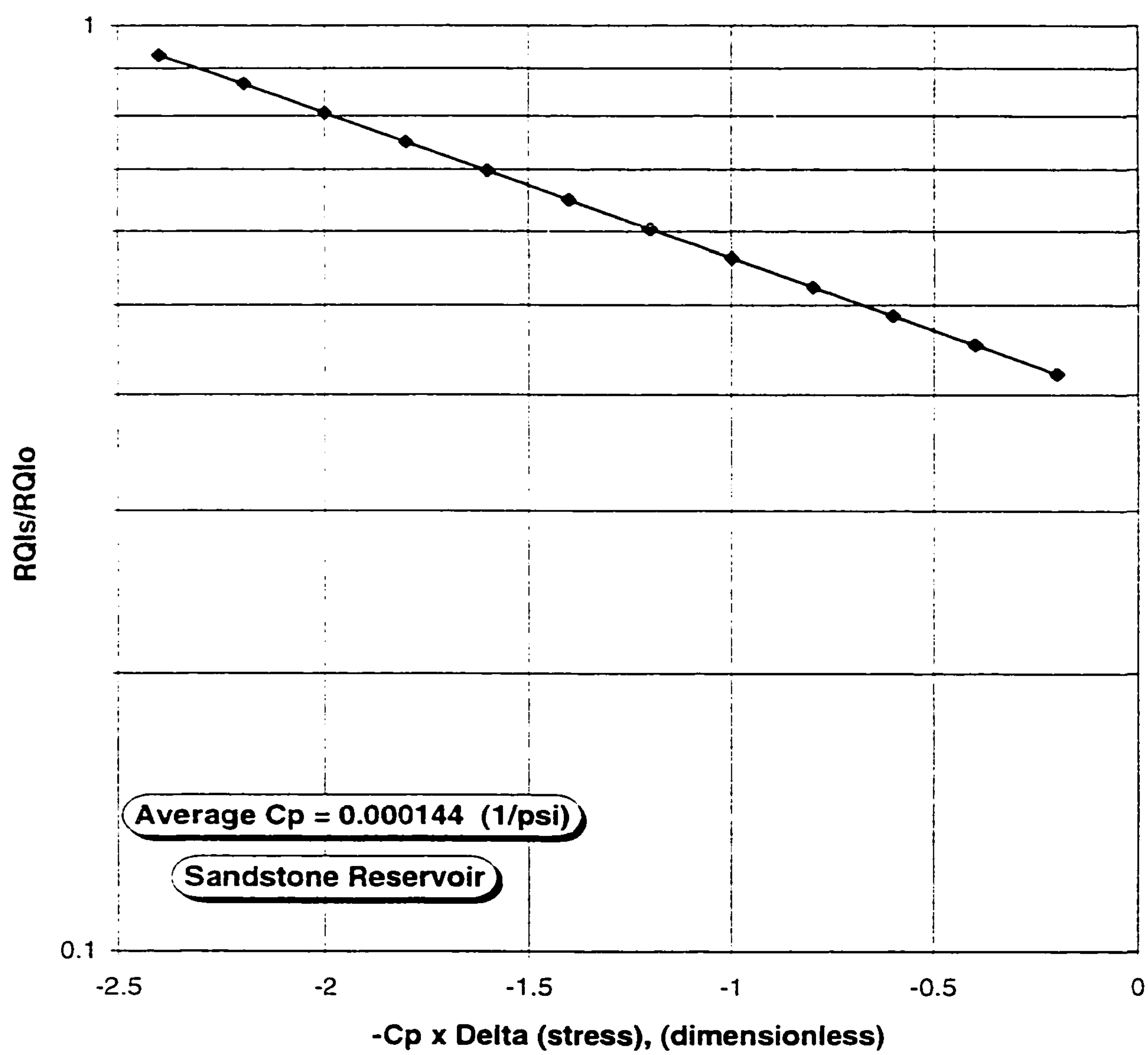

Fig. 4. 12. A- Semi-Log plot of (RQIs/RQIo) versus [-Cp * del (stress)].

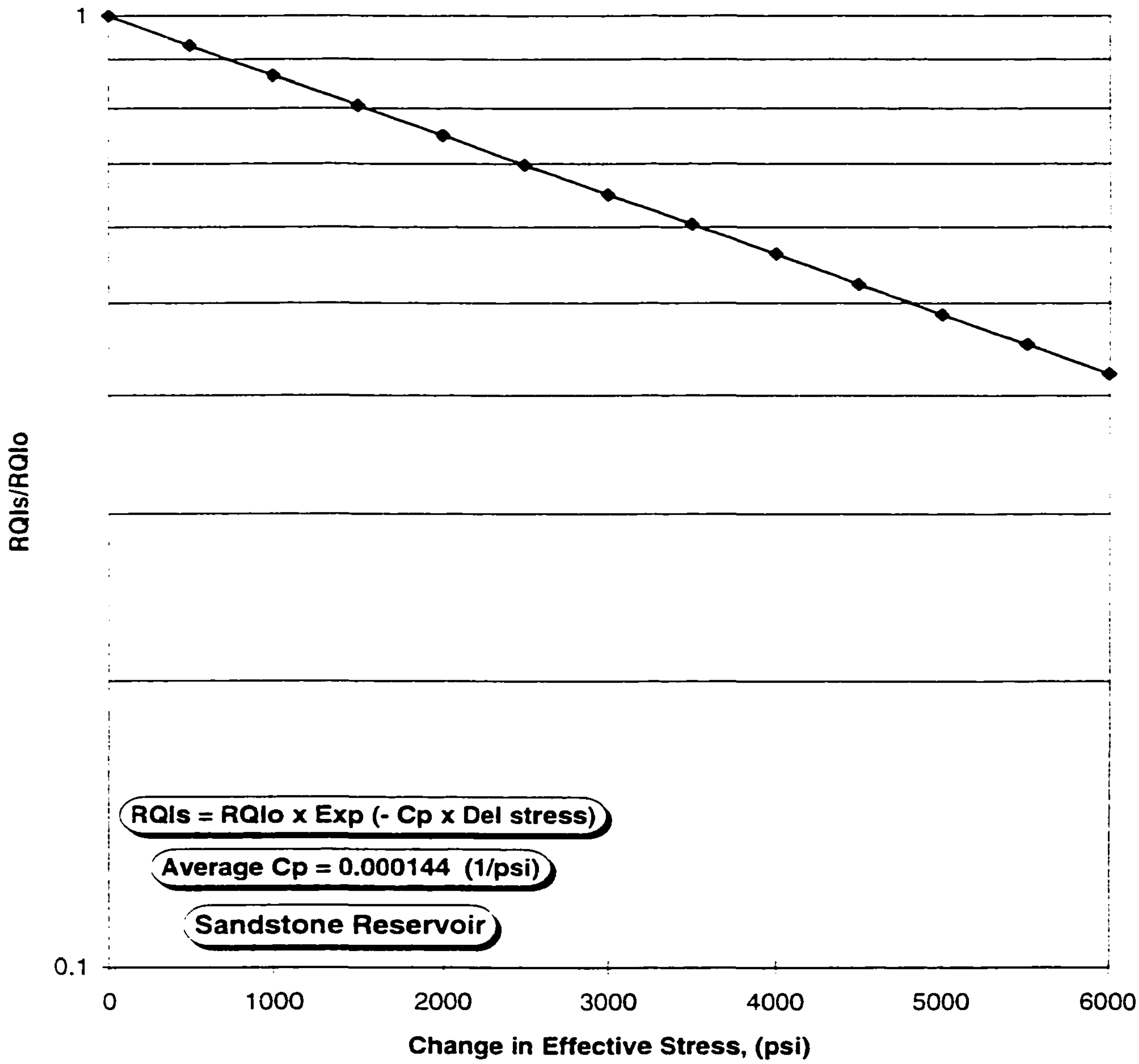

Fig. 4. 12. B- (RQIs/RQIo) versus change in effective stress

4. 3. Effect of Stress on Several Newly-Developed Flow Unit Models for Clean Formations

4. 3. 1. New Flow Unit Model with Effect of Stress on the Characterization of Clean Formations Using Wyllie and Rose Equation

Wyllie and Rose (1950) introduced an equation for permeability using porosity and irreducible water saturation as follows:

$$K_o = 62500\frac{\varphi_o^6}{S_{wi}^2} \tag{2-21}$$

where

K_o = permeability of the reservoir rock at zero stress, (md)

S_{wir} = irreducible water saturation, (fraction)

φ_o = porosity at initial condition (zero stress), (fraction)

Calculation of irreducible water saturation (S_{wir}) is difficult, if not impossible especially in old reservoirs or developed reservoir where irreducible condition does not exist anymore. This difficulty of determining irreducible water saturation (S_{wir}) limits the use of Wyllie and Rose equation and other permeability equations having similar feature.

Archie's equation for water saturation under irreducible water condition can be written as follows:

$$S_{wirr}^n = \frac{aR_w}{\varphi^m R_{ti}} \tag{4-52}$$

Substituting equation (4-52) into equation (2-21) results in

$$K_o = 62500\left(\frac{R_{ti}}{aR_w}\right) * \varphi^{m+6} \tag{4-53}$$

Equation (4-53) eliminates the irreducible water saturation condition. It can be used as a new model of estimating permeability independent of irreducible water saturation which may vary from top to the bottom of the pay zone.

Using equation (4-53) into the equation of the ratio of conventional Reservoir Quality Index (RQIo) to Reservoir Quality Index under stress (RQIs), equation (4-48) can be written as follows:

$$RQI_S(\mu m) = 7.85 * \varphi_o^{(m/2+2.5)} * e^{-\bar{C}_p \Delta\sigma} * \sqrt{\left(\frac{R_{ti}}{aR_w}\right)} \tag{4-54}$$

Substituting porosity at zero stress condition (φ_o) from equation (4-23) into equation (4-54) yields:

$$RQI_S = 7.85 * \varphi_s^{(m/2+2.5)} * e^{(m/2+1.5)*\bar{C}_p*\Delta\sigma}\left[1-\varphi_o\left(1-e^{-\bar{C}_p\Delta\sigma}\right)\right]^{(m/2+2.5)}\sqrt{\frac{R_{ti}}{aR_w}} \tag{4-55}$$

Arranging equation (4-55) and applying logarithm on both sides yields

$$Log(RQI_S) = \left(\frac{m}{2}+2.5\right)Log\varphi_S + Log\left\{7.85 * e^{(m/2+1.5)*\bar{C}_p*\Delta\sigma}\left[1-\varphi_o\left(1-e^{-\bar{C}_p\Delta\sigma}\right)\right]^{(m/2+2.5)}\sqrt{\frac{R_{ti}}{aR_w}}\right\} \tag{4-56}$$

Equation (4-56) represents a new flow unit model that could be used for the characterization and identification of flow units in formations under stress conditions. It reveals that a log-log plot of reservoir quality index under stress (RQIs) versus porosity under stress (φ_s) yields a straight line (assuming constant average pore compressibility) for each flow unit under the same condition of stress. This straight line representing the flow unit, also has two unique features: (1) the slope equal to [m/2 +2.5] and (2) the intercept that is called Flow Unit Factor $(FUF)_{S-WR}$ and written as:

$$(FUF)_{S\text{-}WR} = \left\{7.85 * e^{(m/2+1.5) * \bar{C}_p * \Delta\sigma}\left[1-\varphi_o\left(1-e^{-\bar{C}_p\,\Delta\sigma}\right)\right]^{(m/2+2.5)}\sqrt{\frac{R_{ti}}{aR_w}}\right\} \quad (4\text{-}57)$$

where

$FUF_{S\text{-}WR}$ = flow unit factor of clean stress-sensitive formation using Wyllie and Rose permeability equation, (dimensionless)

This model can also be used to predict flow units at different time intervals (during the life of the reservoir). This new model can be transformed to involve pressure drop instead of change of effective stress, using equation (4-39), as follows

$$\Delta\sigma = \alpha \Delta P \quad (4\text{-}39)$$

where

α = constant relating change in pore pressure to change in effective stress, and depends on rock and fluid type.

Substituting equation (4-39) into equation (4-56) results in

$$Log(RQI_S) = \left(\frac{m}{2}+2.5\right)Log\varphi_S + Log\left\{7.85 * e^{(m/2+1.5) * \alpha\bar{C}_p * \Delta P}\left[1-\varphi_o\left(1-e^{-\alpha\bar{C}_p\,\Delta P}\right)\right]^{(m/2+2.5)}\sqrt{\frac{R_{ti}}{aR_w}}\right\}$$

(4-58)

Pore compressibility can be assumed constant and (α) is constant, then equation (4-58) reveals that a log-log plot of reservoir quality index under stress condition versus porosity under stress yields a straight line having a unique slope equals [m/2+ 2.5] and a unique intercept. This flow unit can be represented by drawing a straight line passing through each set of data points and having a slope = 3.5 (assuming m = 2).

The new flow unit model is validated using simulated data of porosity values under zero stress conditions, Table 4. 3. The simulated values of porosity are used to estimate permeability (under zero stress conditions) using Wyllie and Rose equation, equation (2-21). Then porosity and permeability are used to obtain RQIo. The values of permeability and porosity are subjected to two different effective stresses (2,500 and 5,000 psi) and used to estimate the corresponding values of Reservoir Quality Index under these values of (RQIs). Fig. 4. 13 shows a comparison between these two values of Reservoir Quality Index under these effective stresses (RQIs) versus porosity under stress. The result shows that a change in effective stress from 2,500 psi to 5,000 psi causes a change in the position of the predicted flow unit in the direction of reducing both the porosity (φ_s) and the RQIs. This reduction may lead to serious errors in description and characterization of the flow units in stress-sensitive reservoirs.

According to Fig. 4. 13, the position of the flow unit is a function of change in effective stress (or pressure drop) of the reservoir. Therefore, the flow units constituting the producing zone should be evaluated regularly.

Table 4. 3 - Simulated data for characterization of stress-sensitive clean formations using the newly-developed flow unit model based on Wyllie and Rose permeability equation

Rock Coefficient (Alpha) = 0.50
Pore Compressibility (cp) = 0.000144 (1/psi) (sandstone formation)
Irreducible Watre Saturation = 20 %
Cementation Coefficient (m) = 2.0 (assumed)

(phi)o (fract.)	Ko (md	RQIo (um)	(phi)s 2,500 psi (fract.)	(phi)s 5,000 psi (fract.)	RQIs 2,500 psi (um)	RQIs 5,000 psi (um)
0.4	6400	3.971821	0.317469	0.2360558	2.77114874	1.933437
0.36	3401.222	3.05208	0.2818453	0.2080334	2.12944344	1.4857177
0.32	1677.722	2.273603	0.2471753	0.1811525	1.5862981	1.1067639
0.28	752.9536	1.628301	0.2134214	0.1553446	1.13606959	0.7926384
0.24	298.5984	1.107561	0.1805476	0.1305468	0.77274813	0.5391482
0.2	100	0.702125	0.1485199	0.106701	0.48987452	0.3417866
0.16	26.2144	0.40192	0.1173062	0.0837532	0.28042054	0.1956501
0.12	4.6656	0.195791	0.0868758	0.0616539	0.13660386	0.0953088
0.08	0.4096	0.07105	0.0571995	0.0403566	0.04957182	0.0345864
0.04	0.0064	0.01256	0.0282497	0.0198186	0.00876314	0.0061141

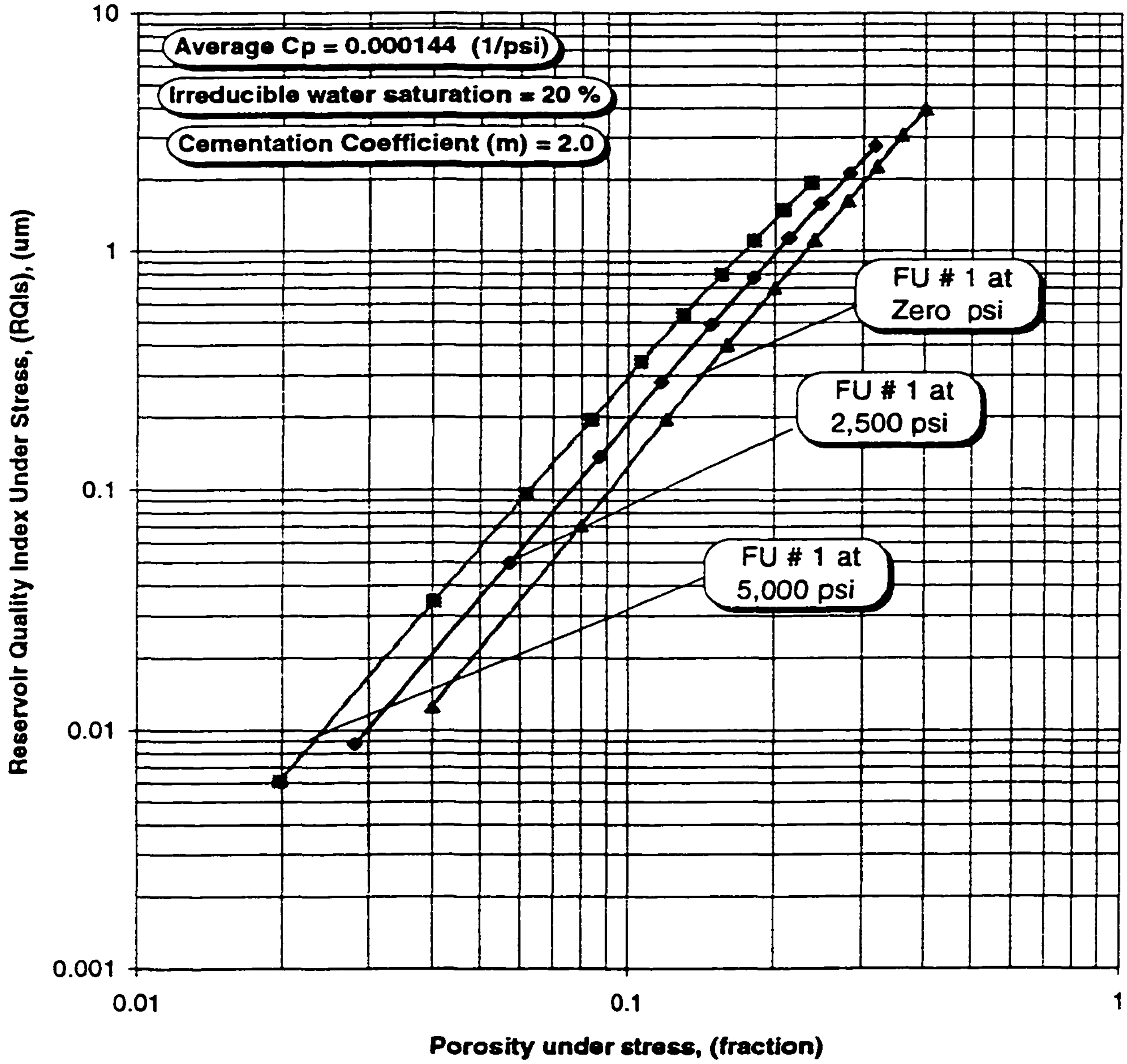

Fig. 4. 13- New flow unit model for stress-sensitive clean formations using Wyllie and Rose permeability equation

4. 3. 2. New Flow Unit Model with Effect of Stress on the Characterization of Clean Formations Using Jorgensen Equation

Jorgensen (1986) developed the following empirical equation for calculating the permeability:

$$K_o = 84105\frac{\varphi_o^{\,m+2}}{(1-\varphi_o)^2} \tag{2-35}$$

where

K_o = permeability at original (laboratory) conditions, (md)

φ_O = porosity at original (laboratory) conditions, (fraction),

m = cementation factor depending on the rock type.

Substituting equation (2-35) into equation (4-48) results in the following equation:

$$RQIs(\mu m) = 9.11 * e^{-\bar{C}_p \Delta\sigma}\left(\frac{\varphi_o^{(m/2+0.5)}}{(1-\varphi_o)}\right) \tag{4-59}$$

Substituting porosity at zero stress condition $\left(\varphi_o^{(m/2+0.5)}\right)$ from equation (4-23) into equation (4-59) yields

$$RQIs(\mu m) = 9.11 * \varphi_s^{(m/2+0.5)} * e^{(m/2-0.5)\cdot\bar{C}_p \Delta\sigma} * \left\{\frac{\left[1-\varphi_o\left(1-e^{-\bar{C}_p \Delta\sigma}\right)\right]^{\left(\frac{m}{2}+0.5\right)}}{(1-\varphi_o)}\right\} \tag{4-60}$$

Arranging equation (4-60) and applying logarithm on both sides yields

$$Log(RQI_s) = \left(\frac{m}{2}+0.5\right)Log(\varphi_s) + Log\left\{9.11 * e^{(m/2-0.5)*\bar{C_p}\,\Delta\sigma} * \left\{\frac{\left[1-\varphi_o\left(1-e^{-\bar{C_p}\,\Delta\sigma}\right)\right]^{\left(\frac{m}{2}+0.5\right)}}{(1-\varphi_o)}\right\}\right\}$$

(4-61)

Equation (4-61) reveals that a log-log plot of reservoir quality index under stress (RQIs) versus porosity under the effect of stress (φ_s) yields a straight line having a slope equal to [(m/2) + 0.5] and a unique intercept that can be determined graphically. This intercept is given as:

$$(FUF)_{S-J} = \left\{9.11 * e^{(m/2-0.5)*\bar{C_p}\,\Delta\sigma} * \left\{\frac{\left[1-\varphi_o\left(1-e^{-\bar{C_p}\,\Delta\sigma}\right)\right]^{\left(\frac{m}{2}+0.5\right)}}{(1-\varphi_o)}\right\}\right\} \qquad (4\text{-}62)$$

where

FUF_{S-J} = flow unit factor of clean stress-sensitive formation using Jorgensen permeability equation, (dimensionless).

Fig. 4. 14 shows a graphical representation of this newly-developed model and how it can effectively be used to define and characterize flow units in the reservoir under investigation, and to study the effect of stress on the predicted flow units. This can be achieved by drawing a straight line having a slope = [(m/2) + 0.5] through each set of data points on a log-log plot of RQIs versus φ_s .

Simulated values of porosity under laboratory condition (zero stress) are used, Table 4. 4, and subjected to different changes in effective stress such as 2,500 and 5,000 psi. Then, the simulated porosity values at zero stress condition are used to estimate permeability (K_o) using Jorgensen equation. Finally, RQIo values are calculated. In addition, the values of reservoir quality index under zero stress (RQIo) are used to obtain reservoir quality index under stress (RQIs) under 2,500 and 5,000 psi. Then RQIs is plotted versus porosity under stress (φ_s) for effective stress values of 2,500 and 5,000 psi, Fig. 4. 14.

For the purpose of validating this flow unit model (Equation (4-61)) and of studying the effect of stress on flow units, simulated data of Reservoir Quality Index (RQI) and porosity under different stress conditions are used, Table 4. 4. The result shows that a single flow unit is identified since a straight line can be drawn through the resulting set of data points. However, change of stress condition leads to shifting the position of this flow unit on a log-log plot of RQIs versus porosity under stress, Fig. 4. 14. Again, this new flow unit model provides an effective tool for using well logging data (porosity and permeability under stress) to characterize clean stress-sensitive formations. In addition, this figure shows the importance of evaluating stress-sensitive formations regularly since the position of these flow units have been proven to be a function of effective stress (or oil production).

Table 4. 4-Simulated data for characterization of stress-sensitive clean formations using the newly-developed flow unit model based on Jorgensen permeability equation

Rock Coefficient (Alpha) = 0.50
Rock Compressibility (cp) = 0.000144 (1/psi)
Irreducible Watre Saturation = 20 %
Cementation Coefficient (m) = 2.0 (assumed)

(phi)o	Ko	RQIo	(phi)s	(phi)s	RQIs	RQIs
			2,500 psi	5,000 psi	2,500 psi	5,000 psi
(fract.)	(md	(um)	(fract.)	(fract.)	(um)	(um)
0.4	2563.2	2.51357	0.31747	0.24501	1.753723	1.22358
0.36	1622.98	2.10831	0.28185	0.21496	1.470974	1.0263
0.32	982.514	1.7399	0.24718	0.18638	1.213932	0.84696
0.28	560.934	1.40542	0.21342	0.15917	0.980565	0.68414
0.24	296.095	1.10291	0.18055	0.13324	0.769502	0.53688
0.2	140.175	0.83128	0.14852	0.10849	0.579989	0.40466
0.16	56.5672	0.59041	0.11731	0.08485	0.411929	0.2874
0.12	17.6948	0.3813	0.08688	0.06225	0.266031	0.18561
0.08	3.46713	0.20671	0.0572	0.04061	0.144225	0.10063
0.04	0.21565	0.07291	0.02825	0.01988	0.050868	0.03549

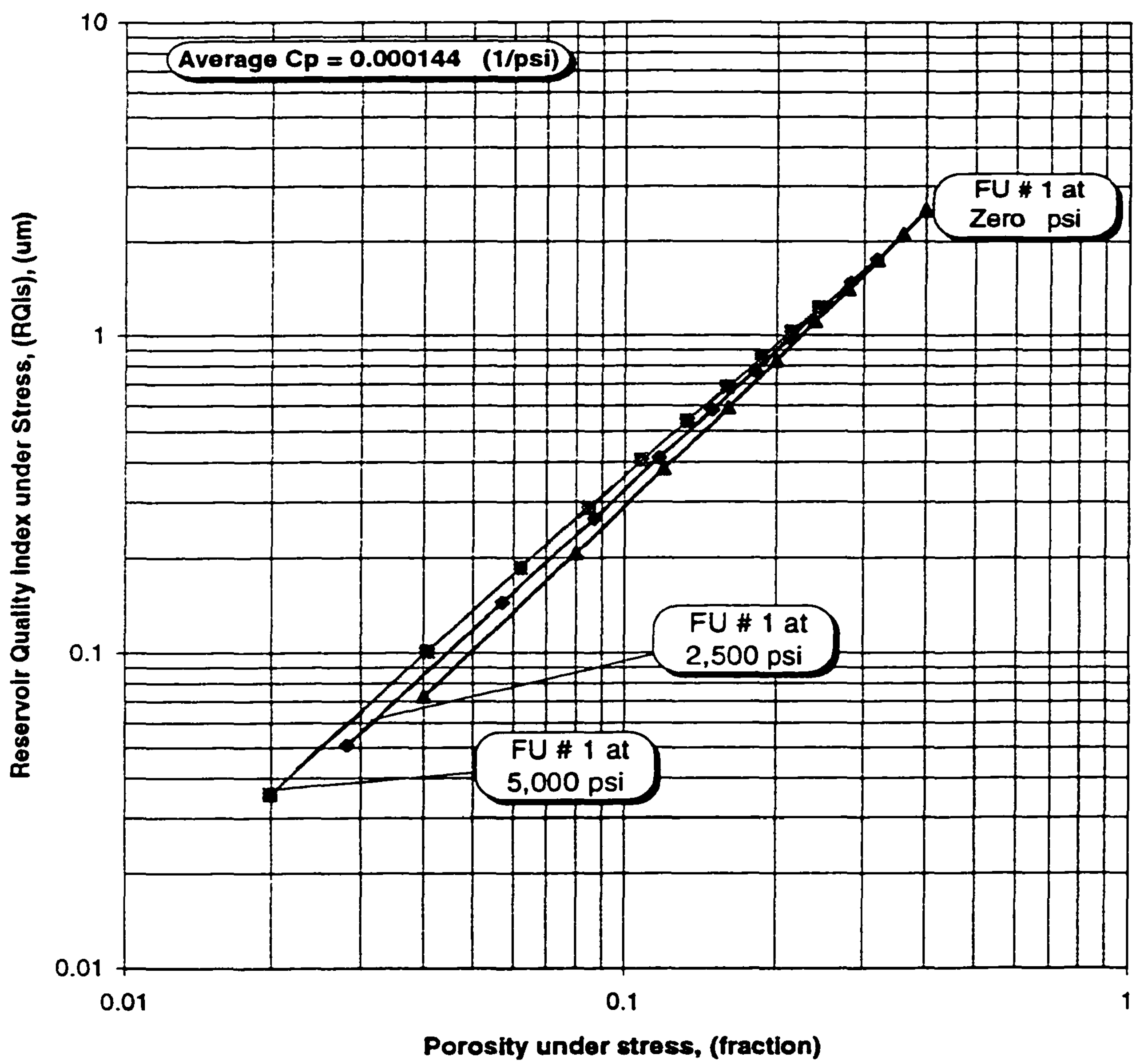

Fig. 4.14-New flow unit model for stress-sensitive clean formations using Jorgensen permeability equation

4. 3. 3. New Flow Unit Model with Effect of Stress on the Characterization of Clean Formations Using Timur Equation

Timur (1968) made careful laboratory measurements of absolute permeability, porosity and irreducible water saturation on 155 sandstone cores from Gulf coast, Colorado and California. These measurements were used to obtain the following correlation:

$$K_o = (93)^2\left(\frac{\varphi_o^{4.4}}{S_{wirr}^2}\right) \tag{2-30}$$

Timur's permeability equation has been developed using laboratory measurements which means the effect of subsidence (stress) has not been taken into account. Therefore, this equation should be corrected for the stress effect before using it to develop a model to characterize reservoir flow units.

Using Archie's equation

$$S_W^2 = \frac{aR_W}{\varphi_o^m R_t} \tag{4-63}$$

and applying irreducible water condition on equation (4-63). Then substitution into equation (2-30) yields

$$K_o = (93)^2\left(\frac{R_{ti}}{aR_w}\right) * \varphi_o^{4.4} \tag{4-64}$$

where

R_{ti} = true formation resistivity at irreducible water condition, (ohm-m)

Substituting equation (4-64) into equation of the ratio of RQIs to RQIo, equation (4-48) results in the following equation:

$$RQI_s(\mu m) = 2.92 * \varphi_o^{(m/2)+1.7} * e^{-\bar{C}_p \Delta\sigma} * \sqrt{\left(\frac{R_{ti}}{aR_w}\right)} \tag{4-65}$$

Substituting porosity at zero stress condition $\left(\varphi_o^{(m/2+1.7)}\right)$ from the equation of porosity under stress, equation (4-23), results in

$$RQI_s(\mu m) = 2.92 * \varphi_s^{(m/2)+1.7} * e^{(m/2+0.7)\bar{C}_p \Delta\sigma} * \sqrt{\left(\frac{R_{ti}}{aR_w}\right)} * \left[1 - \varphi_o\left(1 - e^{-\bar{C}_p \Delta\sigma}\right)\right]^{(m/2+1.7)} \tag{4-66}$$

Taking logarithm on both sides of equation (4-66) yields

$$Log(RQI_s) = \left(\frac{m}{2} + 1.7\right) Log(\varphi_s) + Log(FUF)_{S-TM} \tag{4-67}$$

where

$(FUF)_{S\text{-}TM}$ = flow unit factor of clean stress-sensitive formation using Timur permeability equation, (dimensionless)

$$(FUF)_{S-TM} = \left\{2.92 * e^{(m/2+0.7)\bar{C}_p \Delta\sigma} * \sqrt{\left(\frac{R_{ti}}{aR_w}\right)} * \left[1 - \varphi_o\left(1 - e^{-\bar{C}_p \Delta\sigma}\right)\right]^{(m/2+1.7)}\right\} \tag{4-68}$$

Equation (4-67) reveals that a log-log plot of reservoir quality index under stress (RQIs) versus porosity under stress effect (φ_S) would yield a straight line having a slope equal to [(m/2) + 1.7] and a specific intercept equal to $(FUF)_{S\text{-}TM}$, for a single flow unit having the same pore-throat/pore-size distribution and under the same condition of stress.

This model is validated using simulated data in Table 4. 5. The values of porosity under zero stress condition (φ_O) are simulated and used to calculate the permeability (K_o) using Timur's equation. Then, values of porosity and permeability at zero stress conditions are used for estimating (RQIo) values. Finally, calculated values of RQIo

Table 4. 5 - Simulated data for characterization of stress-sensitive clean formations using the newly-developed flow unit model based on Timur permeability equation

Rock Compressibility (cp) = 0.000144 (1/psi)
Irreducible Watre Saturation = 20 %
Cementation Coefficient (m) = 2.0 (assumed)

(phi)o (fract.)	Ko (md	RQIo (um)	(phi)s 2500 psi (fract.)	(phi)s 5,000 psi (fract.)	RQIs 2500 psi (um)	RQIs 5,000 psi (um)
0.4	3806.65	3.06317	0.31747	0.24501	2.13436	1.48718
0.36	2394.47	2.560845	0.28185	0.21496	1.78435	1.2433
0.32	1426.06	2.096158	0.24718	0.18638	1.46056	1.01769
0.28	792.454	1.670466	0.21342	0.15917	1.16395	0.81102
0.24	402.169	1.28537	0.18055	0.13324	0.89562	0.62405
0.2	180.306	0.942801	0.14852	0.10849	0.65693	0.45773
0.16	67.5471	0.645168	0.11731	0.08485	0.44954	0.31323
0.12	19.0492	0.395619	0.08688	0.06225	0.27566	0.19207
0.08	3.19945	0.198574	0.0572	0.04061	0.13836	0.09641
0.04	0.15155	0.061118	0.02825	0.01988	0.04259	0.02967

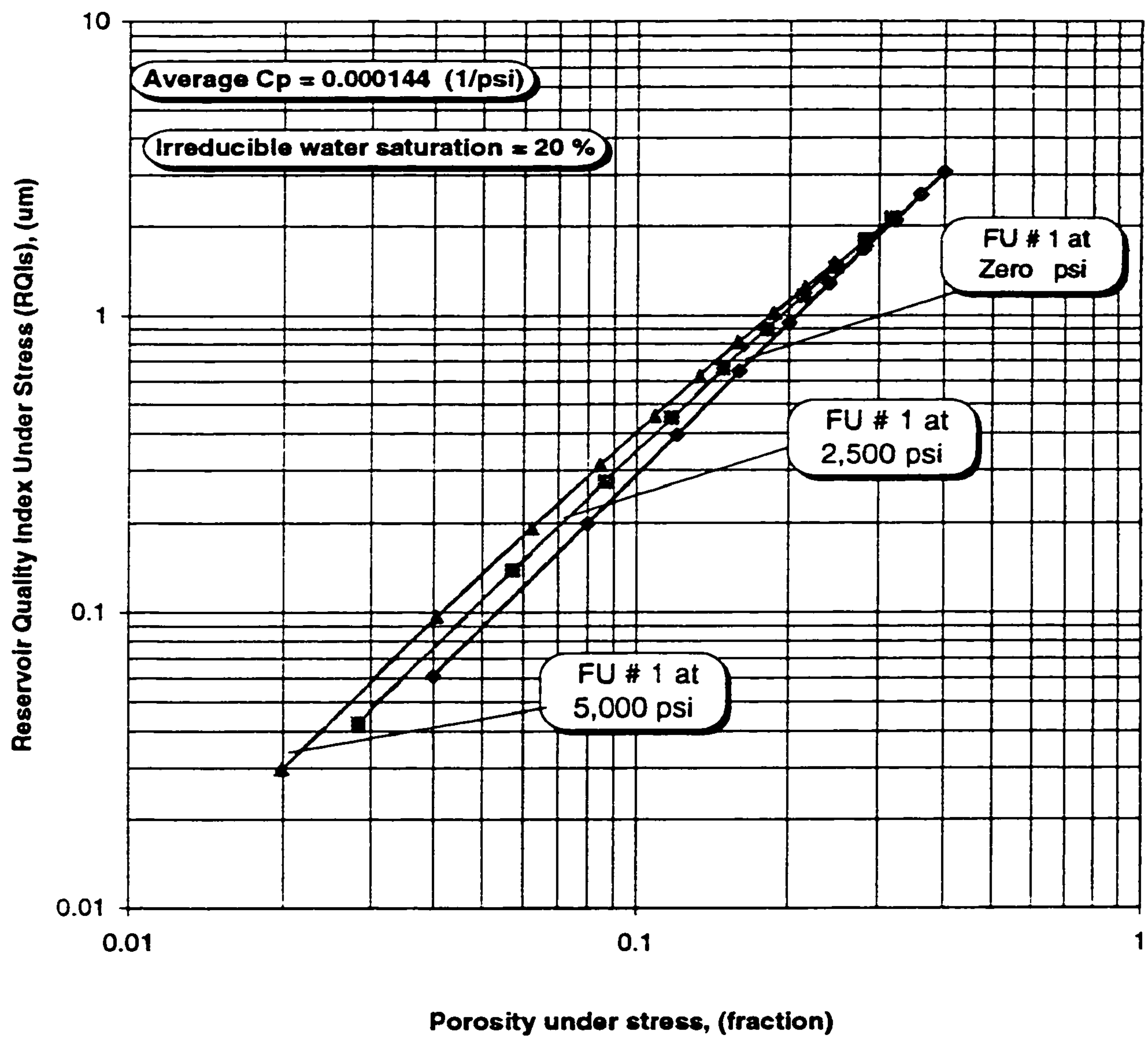

Fig. 4.15-New flow unit model for stress-sensitive clean formations using Timur's permeability equation

are used to estimate the corresponding values of RQIs. Then, simulated values of porosity under zero stress (φ_o) are subjected to two different changes of effective stress (2,500 and 5,000 psi). The RQIs is plotted versus porosity under stress for the same change in effective stress, Fig. 4. 15.

According to the new flow unit model, equation (4-67), a plot of RQIs versus porosity under stress can be used for flow unit identification, Fig. 4. 15. This figure shows that the flow unit model defines a single flow unit successfully and the position of that flow unit depends mainly upon the applied stress values which cause a shift of the predicted flow unit in the direction of decreasing porosity and RQIs.

4. 3. 4. Generalized Flow Unit Model with Effect of Stress on the Characterization of Clean Formations

Substituting irreducible water saturation equation, equation (2-20), into the general form of permeability equation under zero stress, equation (2-37), results in a new permeability equation which is independent on irreducible water saturation, equation (2-39). Substituting permeability under zero stress condition from equation (2-39) into equation of permeability under stress, equation (4-37), yields permeability equation for stress-sensitive formation which is given as follows:

$$K_s = \left(\frac{C_1 R_{tt}}{a R_w} \right) * \varphi_o^{(C_2+1)m} * \frac{e^{-3\bar{C}_p \Delta\sigma}}{\left[1 - \varphi_o \left(1 - e^{-\bar{C}_p \Delta\sigma} \right) \right]} \tag{4-48}$$

Substituting porosity under zero stress from equation (4-23) into equation (4-38) yields

$$K_s = \left(\frac{C_1 R_{ti}}{aR_w}\right) * \varphi_s^{(C_2+1)m} * \left[1-\varphi_o\left(1-e^{-\bar{C_p}\,\Delta\sigma}\right)\right]^{(C_2+1)m} * e^{((C_2+1)m-3)\bar{C_p}\,\Delta\sigma} \qquad (4\text{-}49)$$

Substituting equation (4-49) into Reservoir Quality Index under stress (RQIs) equation, equation (4-47) results in the following equation:

$$RQIs = \left(0.0314\sqrt{C_1}\right)\varphi_s^{\left\{\frac{(C_2+1)m-1}{2}\right\}}\left\{\left[1-\varphi_o\left(1-e^{-\bar{C_p}\,\Delta\sigma}\right)\right]^{[(C_2+1)m-1]/2} e^{\left(\frac{(C_2+1)m-3}{2}\right)\bar{C_p}\,\Delta\sigma}\sqrt{\left(\frac{R_{ti}}{aR_w}\right)}\right\}$$

(4-50)

Applying logarithm on both sides of equation (4-50) yields

$$LogRQIs = \left\{\frac{(C_2+1)m-1}{2}\right\}Log\varphi_s + Log\left\{\left(0.0314\sqrt{C_1}\right)\left[1-\varphi_o\left(1-e^{-\bar{C_p}\,\Delta\sigma}\right)\right]^{[(C_2+1)m-1]/2} * e^{\left(\frac{(C_2+1)m-3}{2}\right)\bar{C_p}\,\Delta\sigma}\sqrt{\left(\frac{R_{ti}}{aR_w}\right)}\right\} \qquad (4\text{-}51)$$

Equation (4-51) is a generalized flow unit model which can be used for flow unit identification and reservoir characterization of clean stress-sensitive formations. The model shows that a single flow unit in a clean stress-sensitive reservoir can be represented by a straight line having slope equal to {[(C_2 + 1)m - 1] / 2 } and an intercept equal to the following flow unit factor which is given as follows:

$$FUF_{G-S} = \left\{\left(0.0314\sqrt{C_1}\right)\left[1-\varphi_o\left(1-e^{-\bar{C_p}\,\Delta\sigma}\right)\right]^{[(C_2+1)m-1]/2} e^{\left(\frac{(C_2+1)m-3}{2}\right)\bar{C_p}\,\Delta\sigma}\sqrt{\left(\frac{R_{ti}}{aR_w}\right)}\right\}$$

(4-52)

where

$FUF_{G\text{-}S}$ = Flow Unit Factor of clean stress-sensitive formation using general permeability equation, (dimensionless)

At zero stress condition $(\Delta\sigma = 0.0)$, the following equations can be written as follows:

$\varphi_s \rightarrow \varphi_o$ from equation (4-23)

$RQIs \rightarrow RQIo$ from equation (4-48)

$\left\{ e^{-\frac{(C_2-1)m-3}{2}\bar{C}_p \Delta\sigma} \right\} = 1.0$ from equation (4-23)

$\left[1 - \varphi_o \left(1 - e^{-\bar{C}_p \Delta\sigma} \right) \right]$ has to be equal unity from equation (4-23)

Substituting all of these previous conditions into equation (4-51), the model reduces to the flow unit model for clean stress-insensitive formation which was derived before in Chapter 2, equation (2-41).

Table 4. 6 summarizes all of the newly-developed flow unit models for clean stress-sensitive formations. Also, a comparison of these models is achieved using data in table 4. 7. The table compares the values of RQIs calculated using Wyllie and Rose, Jorgensen, and Timur permeability equations under 2,500 psi. The comparison shows that the use of Timur'e equation provides the highest RQIs values while the use of Jorgensen equation produces the lowest ones. Also, the limitations and assumptions of these models are shown in Table 4. 8.

Table 4. 6 - List of newly-developed models for characterization and identification of flow units in clean stress-sensitive formations

Used Permeability Equation	Newly-Developed Flow Unit Model for Clean Stress-Sensitive Formations

Wyllie and Rose Equation

$$Log(RQI_S) = \left(\frac{m}{2} + 2.5\right) Log\varphi_S + Log\left\{7.85 * e^{(m/2+1.5)*\bar{C}_p*\Delta\sigma}\left[1 - \varphi_o\left(1 - e^{-\bar{C}_p\Delta\sigma}\right)\right]^{(m/2+2.5)}\sqrt{\frac{R_t}{aR_w}}\right\}$$

Jorgensen Equation

$$Log(RQI_s) = \left(\frac{m}{2} + 0.5\right) Log(\varphi_s) + Log\left\{9.11 * e^{(m/2-0.5)*\bar{C}_p\Delta\sigma} * \left\{\frac{\left[1 - \varphi_o\left(1 - e^{-\bar{C}_p\Delta\sigma}\right)\right]^{\left(\frac{m}{2}+0.5\right)}}{(1 - \varphi_o)}\right\}\right\}$$

Timur Equation

$$Log(RQI_s) = \left(\frac{m}{2} + 1.7\right) Log(\varphi_s) + Log\left\{2.92 * e^{(m/2+0.7)\bar{C}_p\Delta\sigma} * \sqrt{\left(\frac{R_t}{aR_w}\right)} * \left[1 - \varphi_o\left(1 - e^{-\bar{C}_p\Delta\sigma}\right)\right]^{(m/2+1.7)}\right\}$$

Generalized Permeability Equation

$$LogRQIs = \left\{\frac{(C_2 + 1)m - 1}{2}\right\} Log\varphi_s + Log\left\{\left(0.0314\sqrt{C_1}\right)\left[1 - \varphi_o\left(1 - e^{-\bar{C}_p\Delta\sigma}\right)\right]^{[(C_2+1)m-1]/2} * e^{\left(\frac{(C_2+1)m-3}{2}\right)\bar{C}_p\Delta\sigma}\sqrt{\left(\frac{R_{ti}}{aR_w}\right)}\right\}$$

Table 4. 7 Comparison the results of different flow unit models for clean stress-sensitive formations.

Av. Rock Compressibility = 0.000144 (1/psi)
Irreducible Water Saturation = 20 %
Cementation Coefficient (m) = 2.0 (assumed)

	RQIs at 2.500 psi using permeability equation of		
	Wyllie and Rose	Jorgensen	Timur
(Phi)s	RQIs	RQIs	RQIs
2.500	2.500	2.500	2.500
(fract.)	(um)	(um)	(um)
0.3086	2.771	1.754	2.134
0.2738	2.129	1.471	1.784
0.2398	1.586	1.214	1.461
0.2067	1.136	0.981	1.164
0.1747	0.773	0.770	0.896
0.1435	0.490	0.580	0.657
0.1132	0.281	0.412	0.450
0.0838	0.137	0.266	0.276
0.0551	0.049	0.144	0.138
0.0272	0.009	0.050	0.043

Table 4. 8- List of assumptions and limitations of the newly-developed flow unit models for clean formations using in-situ measurements.

Flow Unit Model Based on	Assumption(s) and Limitation(s)
Wyllie and Rose Perm Equation Model given by equation (4-56)	In-situ values of porosity and perm. - clean formations assumes P_c is inversely proportional to SQRT(K) $C_1 = 62500$ and $C_2 = 3$
Jorgensen's Equation, Model given by equation (4-61)	In-situ values of porosity - clean formations assumes that perm. if function of porosity only
Timur Perm Equation Model given by equation (4-66)	In-situ values of porosity and perm. - clean formations $C_1 = 8649$ and $C_2 = 2.2$ applicable for (a) Gulf Coast field (depth 9,000-12,000 ft) (b) Colorado field (depth 6,000-7,000 ft), and (c) California field (depth 9,000 ft - 10,000 ft),
Generalized Perm. Equation Model given by equation (4-51)	In-situ values of porosity and perm. - clean formations

Finally, it is important to emphasize that the selection of a flow unit model for application is mainly based on the locality of the oil reservoir. Therefore, a plot of permeability versus porosity should be constructed for the field under study. This plot is expected to produce a permeability equation (having coefficients C_1 and C_2) representing this formation. If this permeability equation is close to one of the permeability equations used in this study, then, the flow unit model developed in this study can be applied directly. If not, the same approach developed for the generalized flow unit model to identify flow units can be used.

EXAMPLE CALCULATIONS

The purpose of this example of calculations is to show how the previously developed models can be used to identify flow units and study the effect of stress on these flow units. The flow unit model using Wyllie and Rose permeability equation is selected to show a step-by-step example to define flow unit and study the effect of stress on this flow unit. The following steps of calculations are suggested by this study:

1. Assuming that the field data obeys Wyllie and Rose permeability equation which is given as follows:

$$K_o = 62500\frac{\varphi_o^{3m}}{S_{wi}^2} \tag{4-68}$$

2. Knowing the values of porosity from laboratory measurements (at zero stress conditions), these values of porosity are simulated in Table 4. 3. Then porosity values at different stress conditions can be obtained using equation (4-37) as follows:

$$\varphi_s = \varphi_o * \frac{e^{-\bar{C}_P \Delta\sigma}}{\left[1-\varphi_o\left(1-e^{-\bar{C}_P \Delta\sigma}\right)\right]} \tag{4-37}$$

3. The value of porosity at zero stress condition is selected to be 0.24 as shown in Table 4. 3. This value of porosity at change in effective stress = 2,500 psi can be calculated, using equation (4-37), as follows:

   Porosity (zero psi) = 0.24

$$\varphi_s(2{,}500psi) = \varphi_o * \frac{e^{-\bar{C}_P \Delta\sigma}}{\left[1-\varphi_o\left(1-e^{-\bar{C}_P \Delta\sigma}\right)\right]} = \frac{(0.24) * e^{-(0.000144)*(2,500)}}{\left[1-(0.24)\left(1-(2.718)^{-(0.000144)*(2,500)}\right)\right]}$$

   porosity (2,500 psi) = 0.181

4. By the same procedure in step # 3, porosity values at different stress values can be calculated.

5. If the field data obeys Wyllie and Rose permeability equation, then rock permeability can be calculated as follows:

   Assuming the values of cementation exponent (m) and irreducible water saturation (S_{wirr}) are measured to be as follows:

   cementation exponent (m) = 2.0

   irreducible water saturation (S_{wirr}) = 20 %

Then, permeability (at zero stress condition) can be calculated using equation (4-68) as follows

$$K_o = 62500 * \left(\frac{\varphi_o^{3m}}{S_{wirr}^2}\right) = 62500 * \left(\frac{(0.24)^{3x2}}{(0.2)^2}\right) = 298.6 \text{ md}$$

7. Repeat all the steps for all of the given data points of porosity at zero stress conditions to get porosity at different stress conditions and calculate the Reservoir Quality Index under zero stress conditions (RQIo) using the previously assumed values of porosity and calculated values of permeability by using Amaefule's equation, equation (4-6).
8. Calculate the corresponding reservoir quality index under stress (RQIs) using equation (4-48). Then, plot the obtained values of RQIs versus porosity values at 2,500 psi. This provides a clear single flow unit. The reason for the best fitting of the data points is that all of the data points assumed obey the permeability equation. This flow unit model at 2,500 psi has two unique parameters

   (1) slope (2,500 psi) = [(m/2) + 2.5] = [1.0 + 2.5] = 3.5, and

   (2) intercept (2,500 psi) = 51, from Fig. 4. 13.

This chapter reviewed the effect of stress on petrophysical properties that include pore compressibility, porosity, rock density, and permeability. In addition, a new Reservoir Quality Index for clean stress-sensitive formations (RQIs) was developed. The RQIs was used to study the effect of stress on Reservoir Quality Index at zero stress condition (RQIo). In this chapter, four models were developed for characterization and identification of flow units in clean stress-sensitive reservoirs. These models were derived using permeability equations of Wyllie and Rose, Jorgensen, Timur, and a generalized model. The flow unit models were found to have a common feature in that each flow unit can be represented by a straight line of a unique slope and intercept. The intercept of the straight line defining the flow unit is a function of stress (or pressure drop).

CHAPTER 5

INFLUENCE OF STRESS ON THE CHARACTERISTICS OF FLOW UNITS IN SHALY FORMATIONS

Characterization of shaly formations has been a difficult task for several reasons. One key factor of this difficulty is that conventional core tests on reservoir core samples simply does not work. Special equipment or procedures are required to determine the low permeabilities and porosities. Serious and more fundamental problem related to studying shaly formations is that of the very heterogeneous nature of shales. In addition to the previously summarized reasons for dealing with shaly formations, stress effect will make investigation and characterization of shaly formations much more difficult.

This chapter is devoted to developing relationships for interpreting the combined effect of stress and shale on petropysical properties of reservoir rocks. These new relationships are used to characterize and identify flow units in stress-sensitive shaly formations, also to study the effect of stress on reservoir quality index for shaly formation (SRQIo). Four flow unit models have been developed for characterizing shaly formations under stress. These models are laminated, dispersed, total, and cation exchange capacity model.

The development of these models required modification of Mckee et al (1988) porosity equation for clean formation to work for shaly formations. Permeability equations also have been modified to consider shaliness of the formation. Using these modified equations of porosity and permeability in combination with conventional reservoir Quality

Index (RQIo) by Amafulae et al (1993), a new reservoir Quality Index for shaly formation under stress (SRQIs) is developed.

5. 1. Effect of Stress on Porosity and Water Saturation Exponents

Electrical properties of reservoir rocks have long been used for calculating fluid saturations. Information from well logging have been used for interpreting the results of different well logs. It is important to establish the basic relationships between rock properties under different conditions before applying them. For instance, the relationship between water saturation and resistivity may not be applicable to formations under stress conditions.

Guyod (1948), Dunlap (1948), and Keller (1953) proved that the water saturation exponent "n" could be substantially different from 2.0. Dunlap (1948) found that the water saturation exponent "n" may range from 1.18 to 2.90 depending upon core rock type and different saturation techniques.

Keller (1953) conducted electrical resistivity experiments using treated sandstones. The study showed that the water saturation exponent "n" varied from 1.5 to 11.7, depending upon how the cores were treated.

With respect to the stress effect, Hilchie (1964) used six brine saturated porous samples under simulated conditions of overburden and temperature. The simulated overburden pressure used was up to 10,000 psi and the simulated temperature conditions were up to 450 °F. The results showed that the increase of stress caused increase of the formation resistivity factor, Fig. 5. 1.

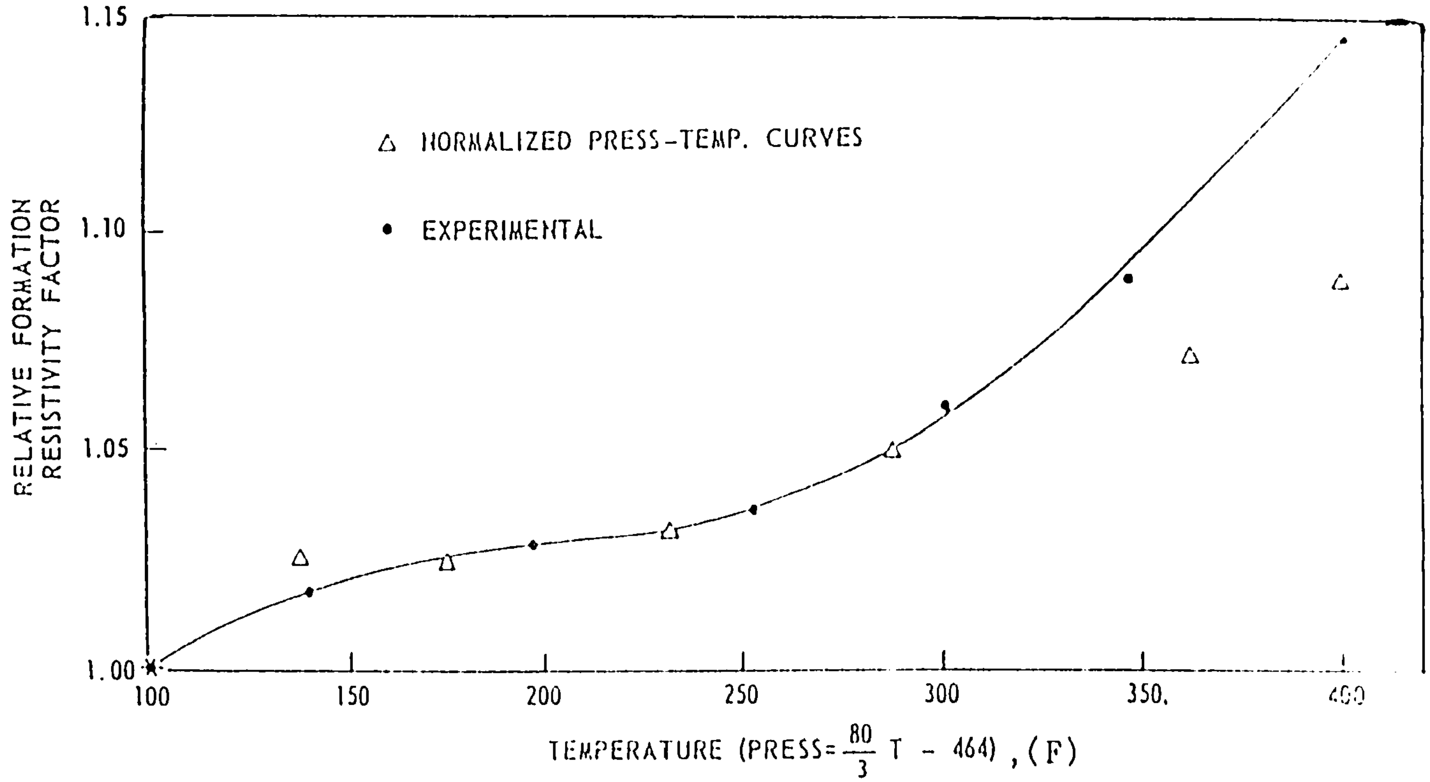

Fig. 5. 1 - Effects of pressure and temperature on Berea sandstones, [Hilchie, 1964].

Longeron (1986) investigated the effect of overburden pressure on the electrical properties of sandstones and carbonates. The results showed that formation resistivity factor increased by about 15 % for sandstones when stress range from 400 psi to 2,900 psi was applied, Fig. 5.2 and Fig. 5.3.

Lewis et al (1988) investigated the effects of stress and wettability on the water saturation exponent "n" and the cementation exponent "m". The results showed that changes in stress have a relatively minor effect upon the water saturation exponent "n" and the cementation exponent "m", but trends having an increase in these exponents with increasing stress levels have been observed. Lewis et al (1988) data also showed that a slight decrease in these exponents with decreasing stress, Figs. 5.4 and 5.5. But the effect of stress on the water saturation exponent "n", Fig. 5.6, was less clear that of the cementation exponent "m". Therefore, changes in the cementation and water saturation exponents are probably small enough that can be neglected. The reason was that the maximum observed change in the cementation exponent "m" was 2.0 %, when the stress was altered from 300 psi to 5000 psi.

5. 2. Effect of Stress on Porosity and Permeability in Shaly Formations

5. 2. 1. Effect of Stress on Porosity in Shaly Formations

Characterization and identification of flow units in shaly formations creates a heavily need for extending the stress effect on petrophysical properties, especially porosity and permeability, in shaly formation.

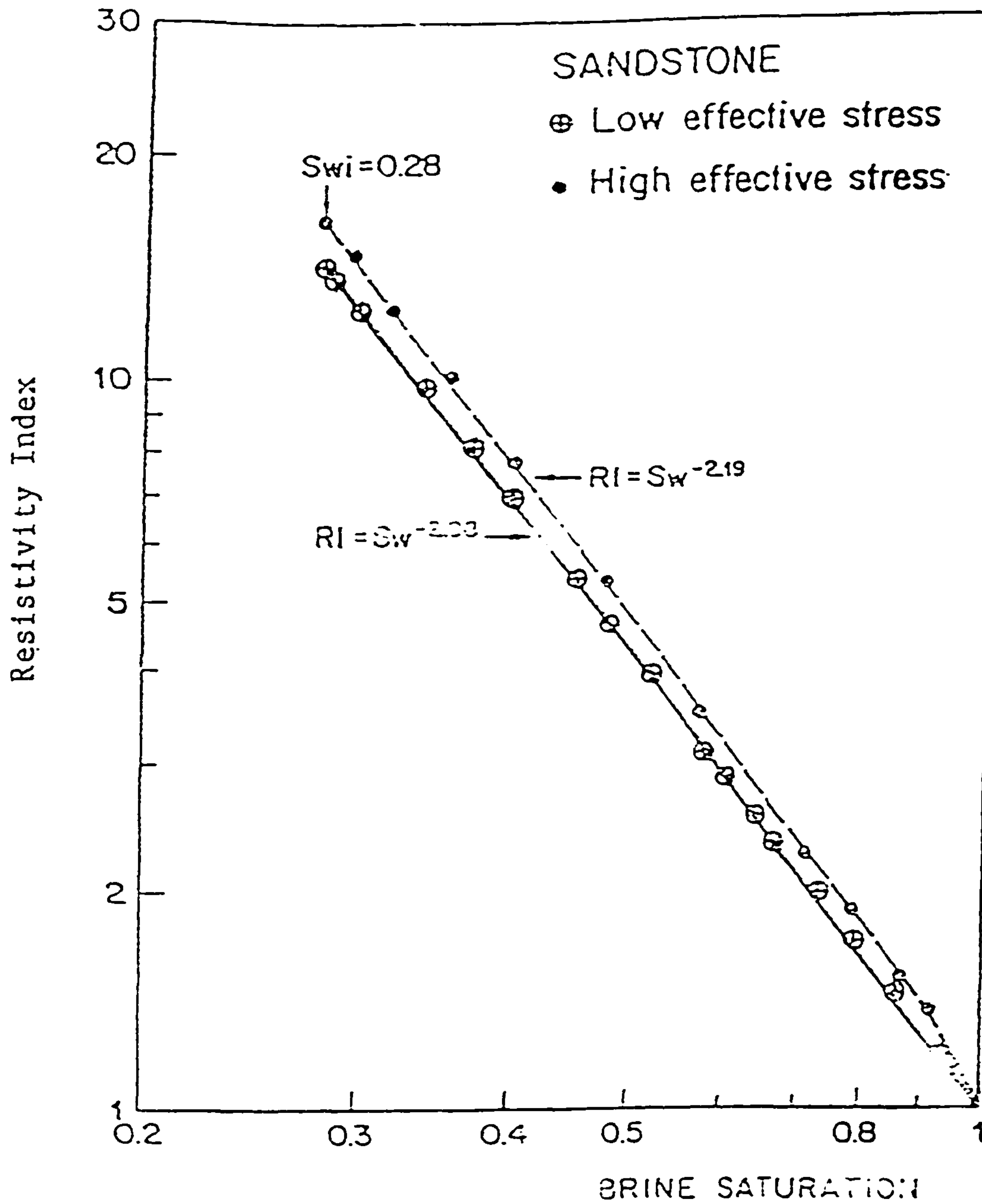

Fig. 5.2 -Effect of stress on resistivity index-drainage curve-sandstone, [Longeron, 1986]

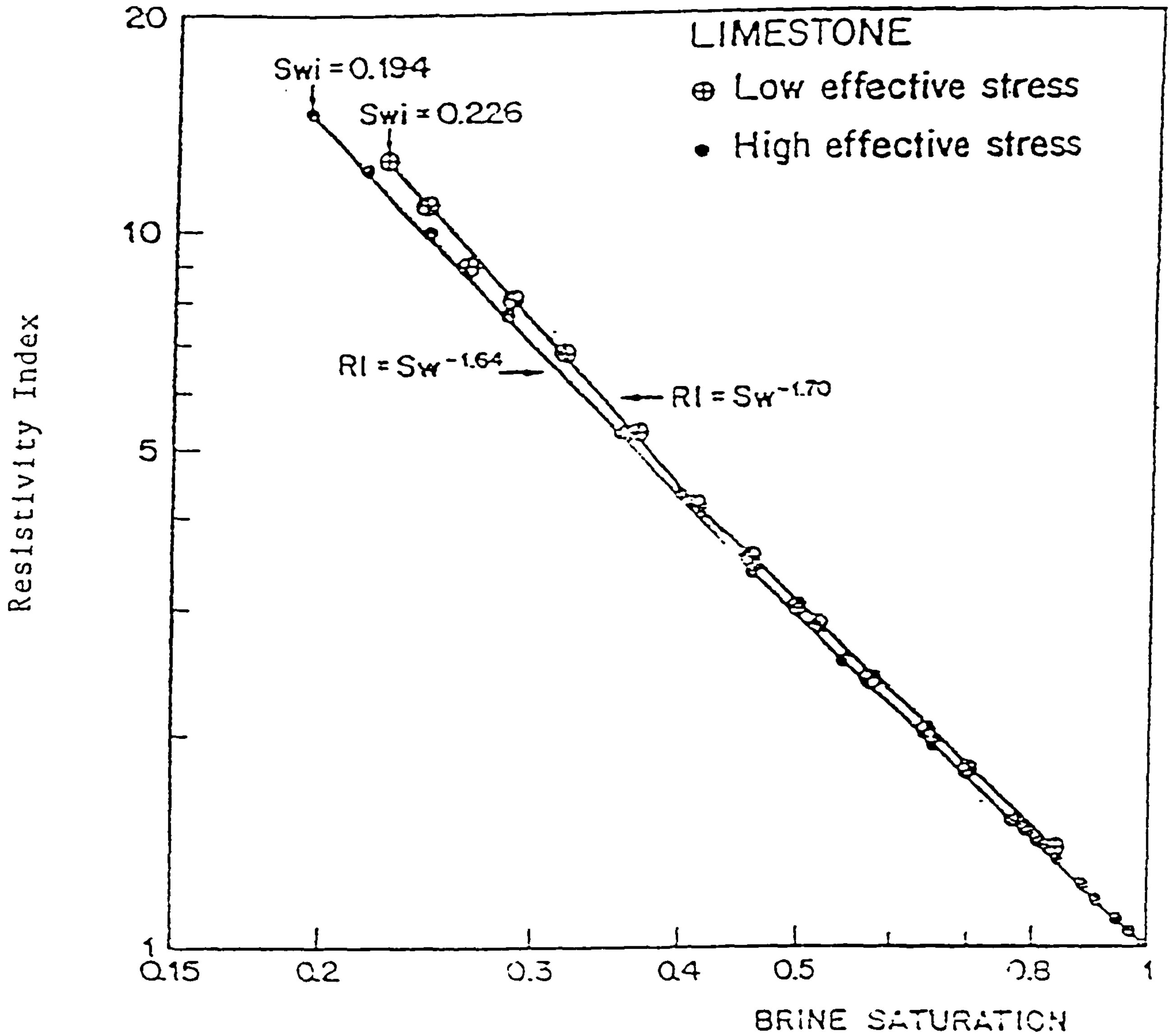

Fig. 5. 3-Effect of stress on resistivity index-drainage curve-limestone, [Longeron, 1986]

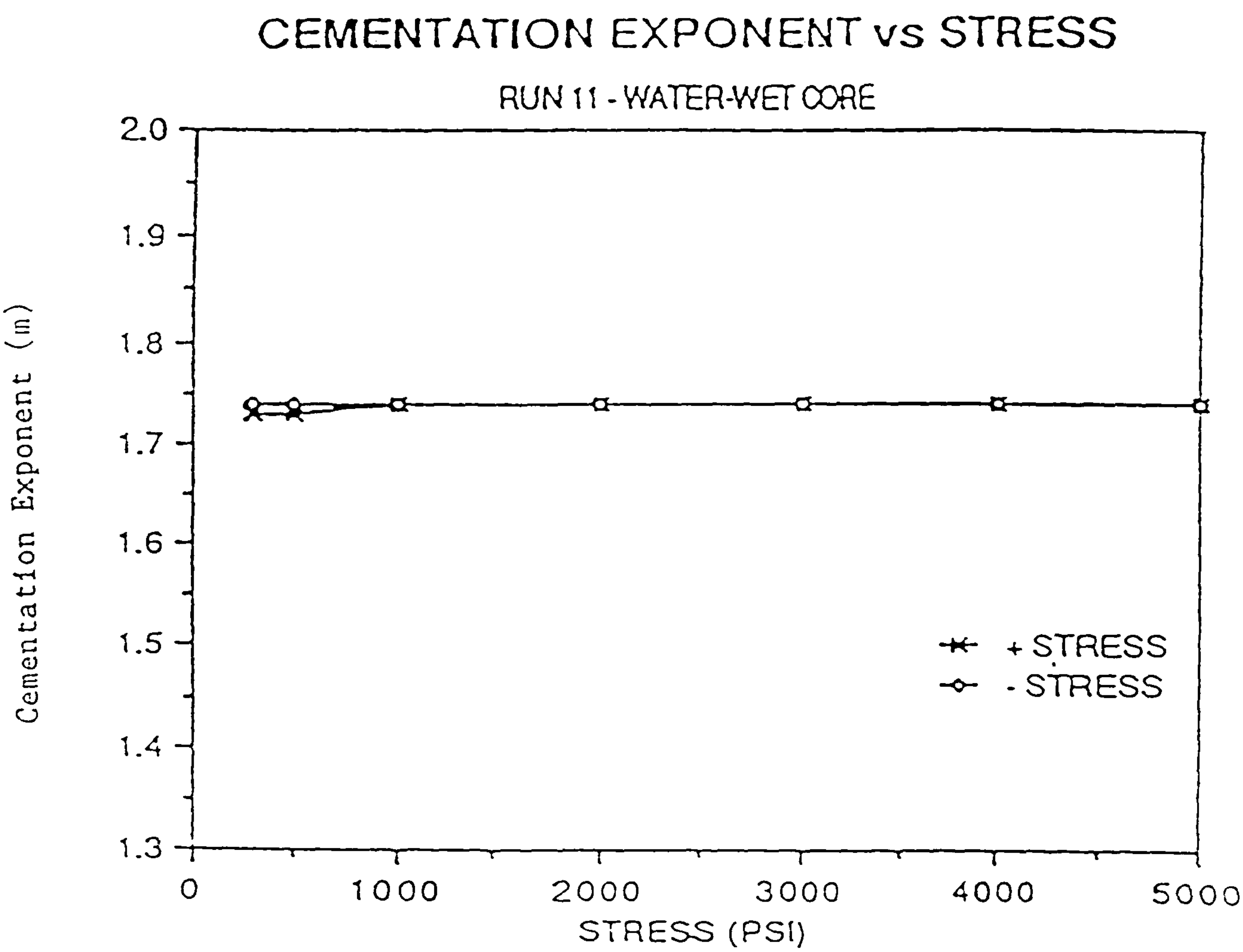

Fig. 5. 4 - Influence of stress on the cementation exponent for water-wet cores, [Lewis et al, 1988]

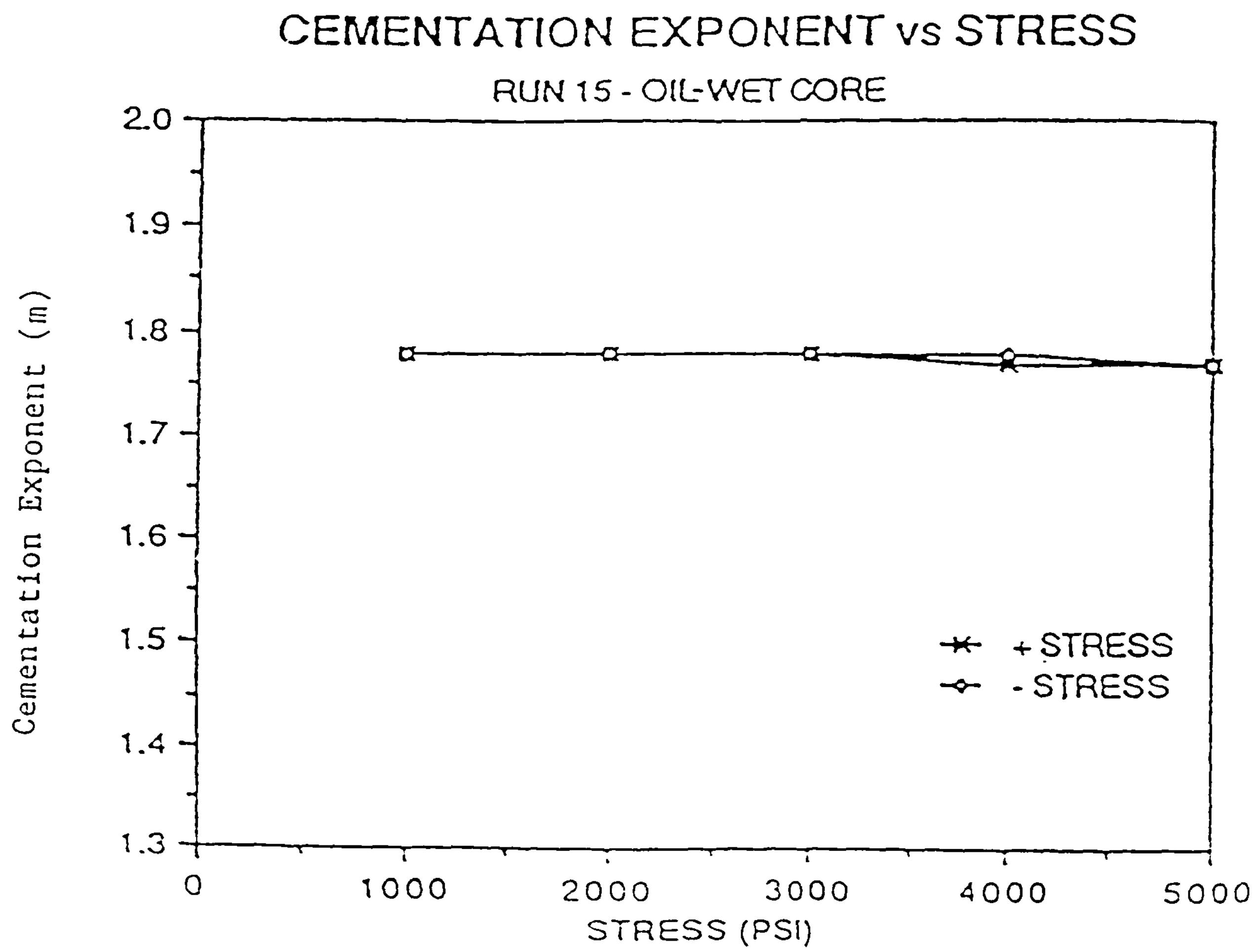

Fig. 5. 5 - Influence of stress on the cementation exponent for oil-wet cores, [Lewis et al, 1988]

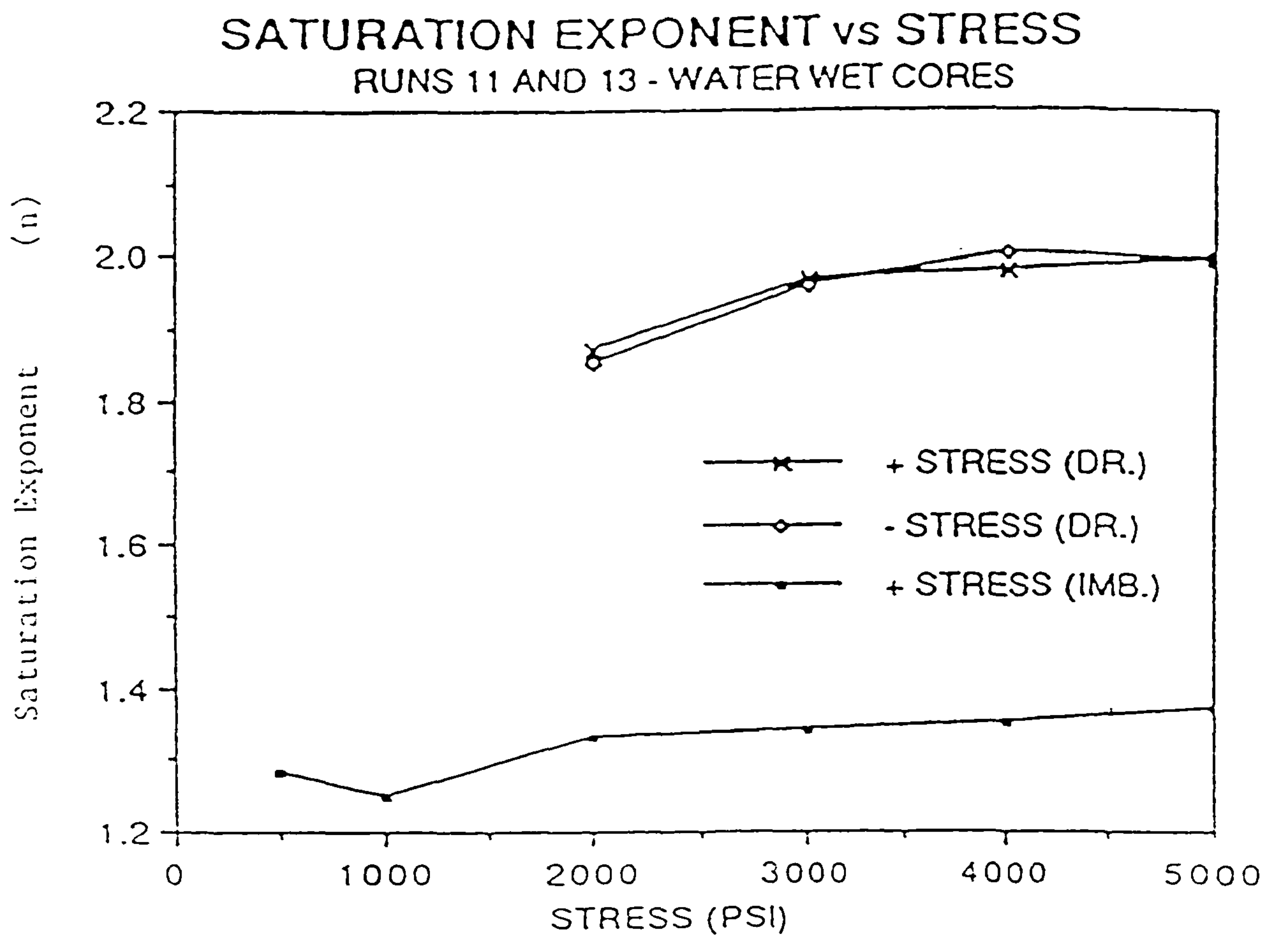

Fig. 5. 6 - Influence of stress on the saturation exponent for water-wet cores during drainage and imbibition saturation, [Lewis et al, 1988]

Since petroleum engineers used to deal with pressure drop in the reservoir. change in effective stress ($\Delta\sigma$) can be expressed in terms of pressure drop as follows

$$\Delta\sigma = \alpha * \Delta P \tag{5-1}$$

where

$\Delta\sigma$ = change in effective stress, (psi)

ΔP = drop in pore pressure of the reservoir. (psi)

α = constant relating pore pressure to change in effective stress. depending upon rock type and its contained fluids. [alpha =0.572 for coal beds. McKee et al (1988). no values in the literature for sandstones and shales]

Bassiouni (1994) showed that effective and total porosity of shaly formations are related by the following equation

$$\varphi_o = \varphi_{to} * (1 - V_{sh}) \tag{5-2}$$

where

φ_o = effective porosity, (fraction)

φ_{to} = total porosity, (fraction)

V_{sh} = shale content of the formation, (fraction).

Substituting equation (5-2) into equation (4-37) for porosity under stress, one obtains

$$\varphi_{s-sh} = \varphi_{to} * (1 - V_{sh}) * \frac{e^{-\bar{C}_p \Delta\sigma}}{\left[1 - \varphi_o\left(1 - e^{-\bar{C}_p \Delta\sigma}\right)\right]} \tag{5-3}$$

where

φ_{s-sh} = porosity of shaly formation under stress effect, (fraction)

Sunstituting equation (5-1) into equation (5-3) results in

$$\varphi_{s-sh} = \varphi_{to} * (1 - V_{sh}) * \frac{e^{-\alpha \bar{C}_p \Delta p}}{\left[1 - \varphi_o\left(1 - e^{-\alpha \bar{C}_p \Delta P}\right)\right]} \tag{5-4}$$

Equation (5-4) can be expressed as

$$\varphi_{s-sh} = \varphi_{to} * S_{s-po} \tag{5-5}$$

where

S_{s-po} = stress correction factor for porosity in shaly formation, (dimensionless).

Hence, stress correction factor for porosity in shaly formation (S_{s-po}) is given by

$$S_{s-po} = \frac{(1 - V_{sh}) * e^{-\alpha \bar{C}_p \Delta P}}{\left[1 - \varphi_o\left(1 - e^{-\alpha \bar{C}_p \Delta P}\right)\right]} \tag{5-6}$$

Table 5.1 shows the effect of reservoir pressure drop (or stress) on effective porosity of shaly formations using equation (5-4). Simulated values of porosity at laboratory conditions (zero stress conditions) were used to investigate the assumption of using constant porosity values over the extended life of the reservoir.

Fig. 5.7 is a plot of effective porosity versus pressure drop of the reservoir for shaly formation. This figure shows that assuming a constant porosity in shaly stress-sensitive formation is not a good assumption and may lead to serious errors in predicting reservoir performance.

Table 5. 1 - Simulated data for studying the effect of pore-pressure on porosity for shaly formations

Av. Pore Compressibility (Cp) = 0.000147 (1/psi)
Rock Coefficient (alpha) = 0.47
Porosity (zero psi and Vsn=0.0%) = 24 %

	Effective porosity				
Delta (P) (psi)	Vsh=0.0 (fract.)	Vsh=0.10 (fract.)	Vsh=0.25 (fract.)	Vsh=0.40 (fract.)	Vsh=0.60 (fract.)
0	0.24	0.216	0.18	0.144	0.096
500	0.23376	0.2103807	0.1753173	0.1402538	0.0935025
1000	0.22763	0.2048638	0.1707198	0.1365759	0.0910506
1500	0.22161	0.1994498	0.1662081	0.1329665	0.0886443
2000	0.21571	0.1941388	0.1617823	0.1294259	0.0862839
2500	0.20992	0.1889311	0.1574426	0.1259541	0.0839694
3000	0.20425	0.1838268	0.153189	0.1225512	0.0817008
3500	0.1987	0.1788257	0.1490214	0.1192171	0.0794781
4000	0.19325	0.1739276	0.1449396	0.1159517	0.0773011

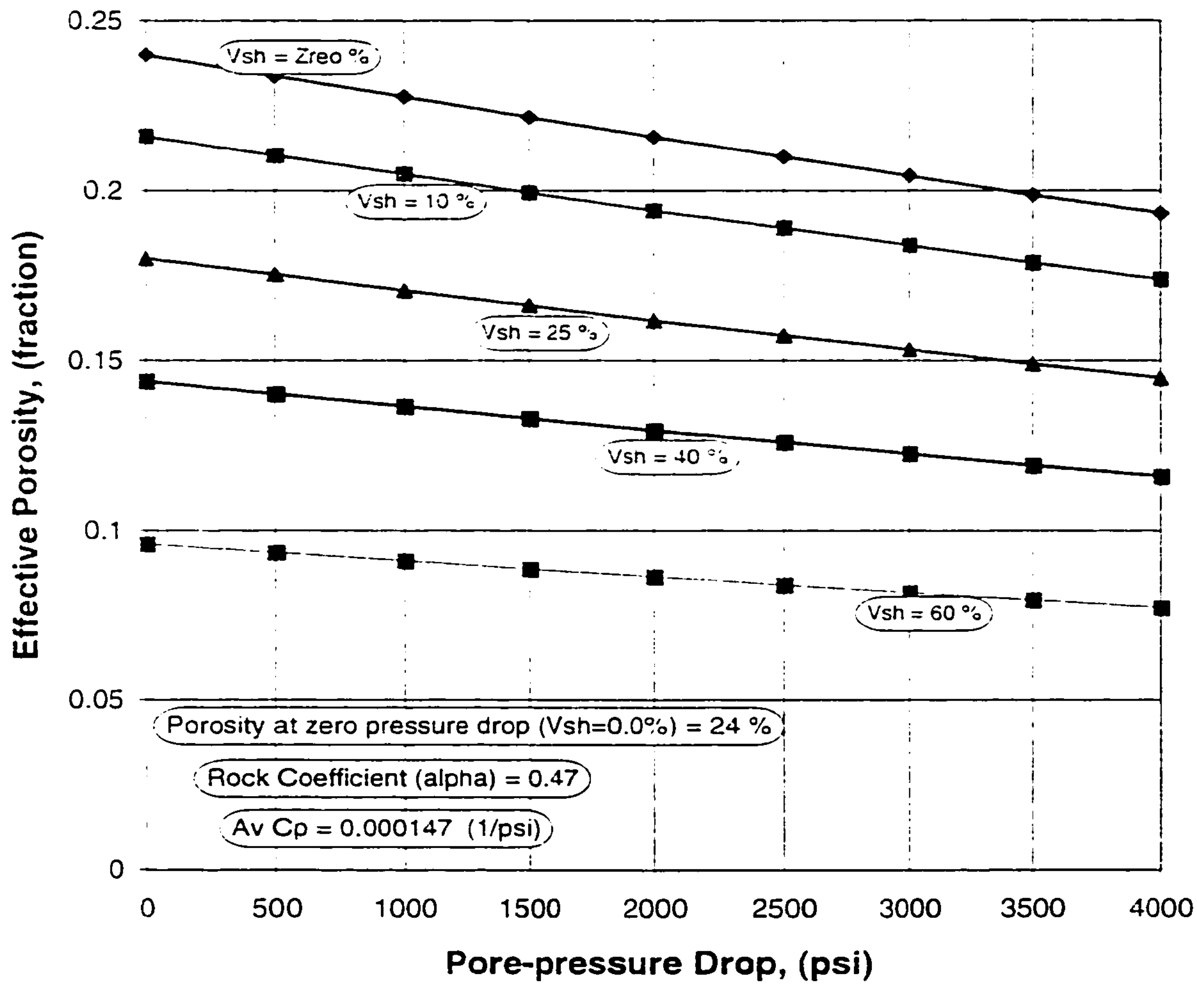

Fig. 5. 7 - Effect of pore-pressure drop on porosity of shaly formations

Fig. 5. 7 shows that increasing the pressure drop decrearses the value of porosity of shaly formations. In addition, for shaly formations, the higher the shale content of the formation leads to more reduction in porosity under the effect of stress. Also, the reduction in porosity of shaly formation under stress decreases at higher values of pressure drops, specially when pressure drop is higher than 3,000 psi.

5. 2. 2. Effect of Stress on Permeability In Shaly Formations

Water saturation in shaly formation can be obtained using several models. Total shale model, Schlumberger (1977), is selected for that purpose because it does not depend upon shale type and shale distribution. According to this model, the water saturation is given by the following equation

$$S_w^2 = \frac{aR_w}{\varphi^m}\left(\frac{1}{R_t} - \frac{V_{sh}}{R_{sh}}\right) \qquad (5\text{-}7)$$

Applying equation (5-7) for irreducible water saturation condition and substituting it into Timur's permeability equation, (2-26), gives

$$K_o(md) = (93)^2 * \frac{\varphi_{to}^{m+4.4}}{aR_w\left(\frac{1}{R_t} - \frac{V_{sh}}{R_{sh}}\right)_{Wirr}} \qquad (5\text{-}8)$$

Using equation (5-8) into permeability equation under stress (4-37) yields an equation for describing the permeability of shaly formation under stress effect as follows:

$$K_{s-sh}(md) = (93)^2 * \frac{\varphi_{to}^{m+4.4}}{aR_w\left(\frac{1}{R_t} - \frac{V_{sh}}{R_{sh}}\right)_{Wirr}} * \frac{e^{-3\alpha \bar{C}_p \Delta p}}{\left[1 - \varphi_o\left(1 - e^{-\alpha \bar{C}_p \Delta P}\right)\right]} \qquad (5\text{-}9)$$

where

K_{s-sh} = permeability of shaly formation under stress effect, (md).

The development of equation (5-9) depends mainly upon three equations: (1) Timur's permeability equation but other equations can also be used, (2) equation considering stress effect on the formation, and (3) total shale model.

5. 3. Effect of Stress on The Reservoir Quality Index for Shaly Formations

The literature does not show any definition for the reservoir quality index (RQI) for shaly formation under stress. This study develops new mathematical expression for shaly formation under stress in order to enhance its description and characterization. Also, this expression will be used to study the effect of stress on reservoir quality index in shaly formations. In the previous section, two equations were developed to extend stress effect (or pore-pressure drop) on porosity (equation 5-4) and on permeability (equation 5-9). Dividing equation (5-9) by equation (5-4) results in

$$\frac{K_{s-sh}}{\varphi_{s-sh}} = \frac{(93)^2 * \varphi_{to}^{m+3.4} * e^{-2\alpha \bar{C_p} * \Delta P}}{aR_w(1-V_{sh})\left(\frac{1}{R_t} - \frac{V_{sh}}{R_{sh}}\right)_{Wirr}} \qquad (5\text{-}10)$$

Taking square root of equation (5-10) results in

$$\sqrt{\frac{K_{s-sh}}{\varphi_{s-sh}}} = \frac{93 * \varphi_{to}^{(m/2)+1.7} * e^{-\alpha \bar{C_p} * \Delta P}}{\sqrt{aR_w(1-V_{sh})\left(\frac{1}{R_t} - \frac{V_{sh}}{R_{sh}}\right)_{Wirr}}} \qquad (5\text{-}11)$$

Multiplying equation (5-11) by (0.0314), the constant included in RQI definition, results in a definition for reservoir quality index of shaly formations under stress effect (SRQIs).This SRQIs s given by the following equation:

$$SRQI_s(\mu m) = \frac{2.92 * \varphi_{to}^{(m/2)+1.7} * e^{-\alpha \bar{C}_p * \Delta P}}{\sqrt{aR_w(1 - V_{sh})\left(\frac{1}{R_t} - \frac{V_{sh}}{R_{sh}}\right)}} \qquad \text{(5-12-A)}$$

A shale group (A_{sh}) can be wriiten as follows:

$$A_{sh} = (1 - V_{sh})\left(\frac{1}{R_t} - \frac{V_{sh}}{R_{sh}}\right) \qquad \text{(5-12-B)}$$

This SRQIs is based on (1) Timur permeability equation and (2) total shale model for water saturation in shaly formation. Equation (5-12-A) provides a definition for the reservoir quality index of shaly formations under stress effect (SRQIs) when both Timur's equation for permeability and total shale model for water saturation calculations are valid and represent the reservoir under investigation.

Equation (5-12-A) and the simulated data in Table 5.2 are used to study the effects of reservoir pressure drop and formation shaliness on the reservoir quality index of shaly formations under stress. The results show that reservoir pressure drop has a remarkable effect of causing a reduction of the values of reservoir quality index of shaly formations under stress effect (SRQIs), Fig. 5.8. For reservoirs with 3,500 psi pressure drop, a severe reduction in SRQIs values is indicated with constant formation shaliness. The effect of formation shalinees diminishes after almost 4,000 psi pressure drop of the reservoir. In addition, increasing formation shaliness from 10 % to 60 % leads to almost 60 % increment in SRQIs values at a constant reservoir pressure drop of 3,500 psi.

Table 5.2-Simulated data for studying the effects of reservoir pore-pressure drop (or stress) and formation shaliness on Shaly Reservoir Quality Index Under Stress (SRQI), (um)

Rock Coefficient (a) = 0.90
Rock Coefficient (alpha) = 0.47
Cementation Exponent (m) = 2.0
Shale Formation Resistivity (Rsh) = 35 ohm-m
Formation Water Resistivity (Rw) = 0.053 ohm-m
Average Pore Compressibility (Cp) = 0.000147 1/psi
Porosity (at zero pressure Drop and Vsh = 0.0 %) = 20 %

		Ash Group			SRQI		
delta (P) (psi)	Rt (ohm-m)	Vsh=0.10 (fract)	Vsh=0.40 (fract)	Vsh=0.60 (fract)	Vsh=0.10 (um)	Vsh=0.40 (um)	Vsh=0.60 (um)
0	18.4	0.04634	0.02575	0.01488	0.848785	1.39453	2.2467
500	18	0.04743	0.02648	0.01537	0.810517	1.32862	2.13602
1000	17	0.05037	0.02844	0.01667	0.759795	1.23847	1.98096
1500	15.6	0.05512	0.0316	0.01878	0.701652	1.13488	1.80293
2000	14.5	0.0595	0.03452	0.02073	0.652423	1.049	1.65798
2500	14	0.06171	0.036	0.02171	0.618849	0.99237	1.56493
3000	13.5	0.0641	0.03759	0.02277	0.586629	0.93821	1.47626
3500	13	0.06666	0.0393	0.02391	0.555706	0.88643	1.39174
4000	12	0.07243	0.04314	0.02648	0.515014	0.81727	1.27773
4500	11	0.07925	0.04769	0.02951	0.475644	0.75095	1.16925
5000	10	0.08743	0.05314	0.03314	0.437467	0.68722	1.06578

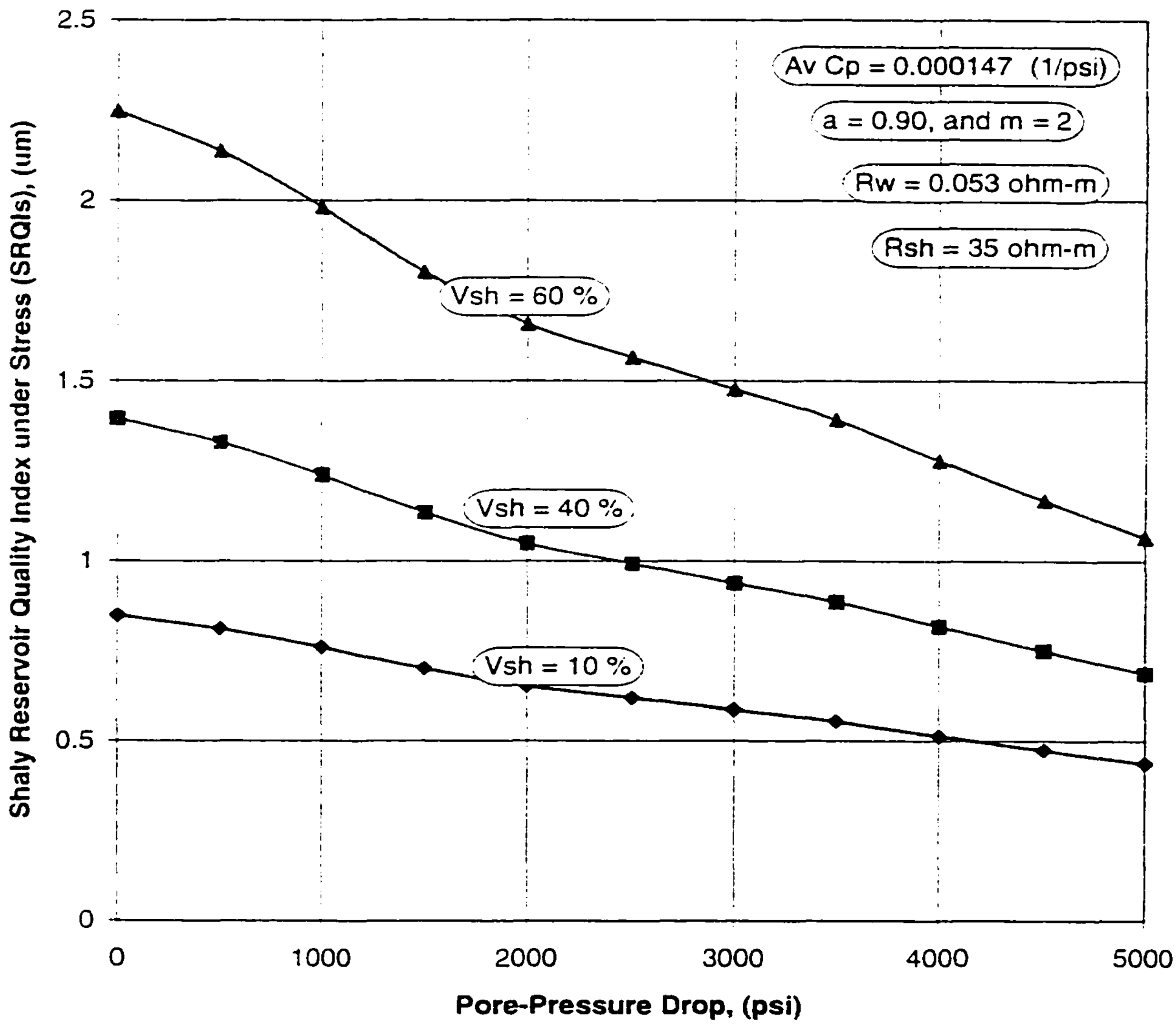

Fig. 5. 8 - Effect of pore-pressure drop on shaly reservoir quality index under stress (SRQIs) for different formation shaliness

Seeking a more general formulation for reservoir quality index of shaly formations under stress effect (SRQIs), the following procedure is followed

Dividing equation (5-9) by equation (5-4) results in

$$\frac{K_{s-sh}}{\varphi_{s-sh}} = \frac{K_{o-sh}}{\varphi_{0-sh}} * e^{-2\alpha \bar{C}_p * \Delta P} \tag{5-13}$$

where

K_{s-sh} = permeability of shaly formation under stress, (md)

K_{o-sh} = permeability of shaly formation under zero stress condition, (md)

φ_{s-sh} = porosity of shaly formation under stress, (fraction)

φ_{o-sh} = porosity of shaly formation under zero stress, (fraction)

ΔP = drop in pore pressure of the reservoir, (psi)

α = constant relating pore pressure to change in effective stress, depending upon rock type and its contained fluids, (a =0.572 for coal beds, McKee et al (1988))

Inserting the term (K_0 / φ_o) into the definition of (RQIo), introduced by Amaefule et al (1993), yields shaly reservoir quality index at zero stress condition (SRQIo) as follows

$$SRQI_o(\mu m) = 0.0314 * \sqrt{\frac{K_{s-sh}}{\varphi_{ts}(1 - V_{sh})}} * e^{-\alpha \bar{C}_p \Delta P} \tag{5-14}$$

where

φ_{ts} = total porosity under stress effect, (fraction)

Defining the following general definition for reservoir quality index of shaly formations under stress effect (SRQIs) as follows:

$$SRQI_s(\mu m) = 0.0314 * \sqrt{\frac{K_{s-sh}}{\varphi_{ts}(1-V_{sh})}} \tag{5-15}$$

Then, equation (5-14) can be expressed as follows

$$SRQI_o = SRQI_s * e^{\alpha \bar{C_p} \bullet \Delta P} \tag{5-16}$$

Ratio of (SRQIs) to (SRQIo) can be expressed as follows

$$RSRQI = \left(\frac{SRQI_s}{SRQI_o}\right) = e^{-\alpha \bar{C_p} \bullet \Delta P} \tag{5-17}$$

Equation (5-17) is similar to the equation of the ratio of RQIs and RQIo, developed in chapter 4, except that permeability and porosity in equation (5-17) should be for shaly formations under stress.

Porosity decreases to a large extent because of shaliness of the formations, Fig. 5.8. This reduction in porosity will be more severe if stress effect is considered plus shale effect. The final result will be a large reduction in porosity that leads to a similar reduction in the Reservoir Quality Index of shaly formation under stress (SRQIs). Figure 5.8 shows that the reduction in shaly reservoir quality index under stress (SRQIs) is smaller at the begining of oil production (small presure drop) than after reservoir developement (higher pressure drop).

Table 5.3 and Fig. 5.9 show the effect of pore pressure drop on shaly formations for different values of reservoir quality index of shaly formation under zero stress (SRQIo). This figure shows the importance of the effect of stress on shaly formations while characterizing them.

Table 5. 3 - Simulated data for studying the effect of reservoir pore pressure drop on Shaly Reservoir Quality Index under Stress (SRQIs) and on (SRQIs/SRQIo).

Rock Coefficient (alpha) = 0.47
Average Pore Compressibility (Cp) = 0.000147 1/psi

delta P (psi)	SRQIo=0.6 (um)	SRQIo=1.2 (um)	SRQIo=1.8 (um)	SRQIo=2.4 (um)	SRQIs/SRQIo
0	0.6	1.2	1.8	2.4	1
500	0.579628996	1.159257992	1.73888699	2.31851598	0.966048327
1000	0.559949622	1.119899244	1.67984887	2.23979849	0.93324937
1500	0.540938395	1.081876791	1.62281519	2.16375358	0.901563992
2000	0.522572632	1.045145263	1.5677179	2.09029053	0.870954386
2500	0.504830417	1.009660833	1.51449125	2.01932167	0.841384028
3000	0.487690579	0.975381159	1.46307174	1.95076232	0.812817632
3500	0.471132668	0.942265336	1.413398	1.88453067	0.785221114
4000	0.455136926	0.910273852	1.36541078	1.8205477	0.758561543
4500	0.439684266	0.879368531	1.3190528	1.75873706	0.732807109
5000	0.424756249	0.849512498	1.27426875	1.699025	0.707927082
5500	0.410335064	0.820670128	1.23100519	1.64134026	0.683891773
6000	0.396403502	0.792807004	1.18921051	1.58561401	0.660672503

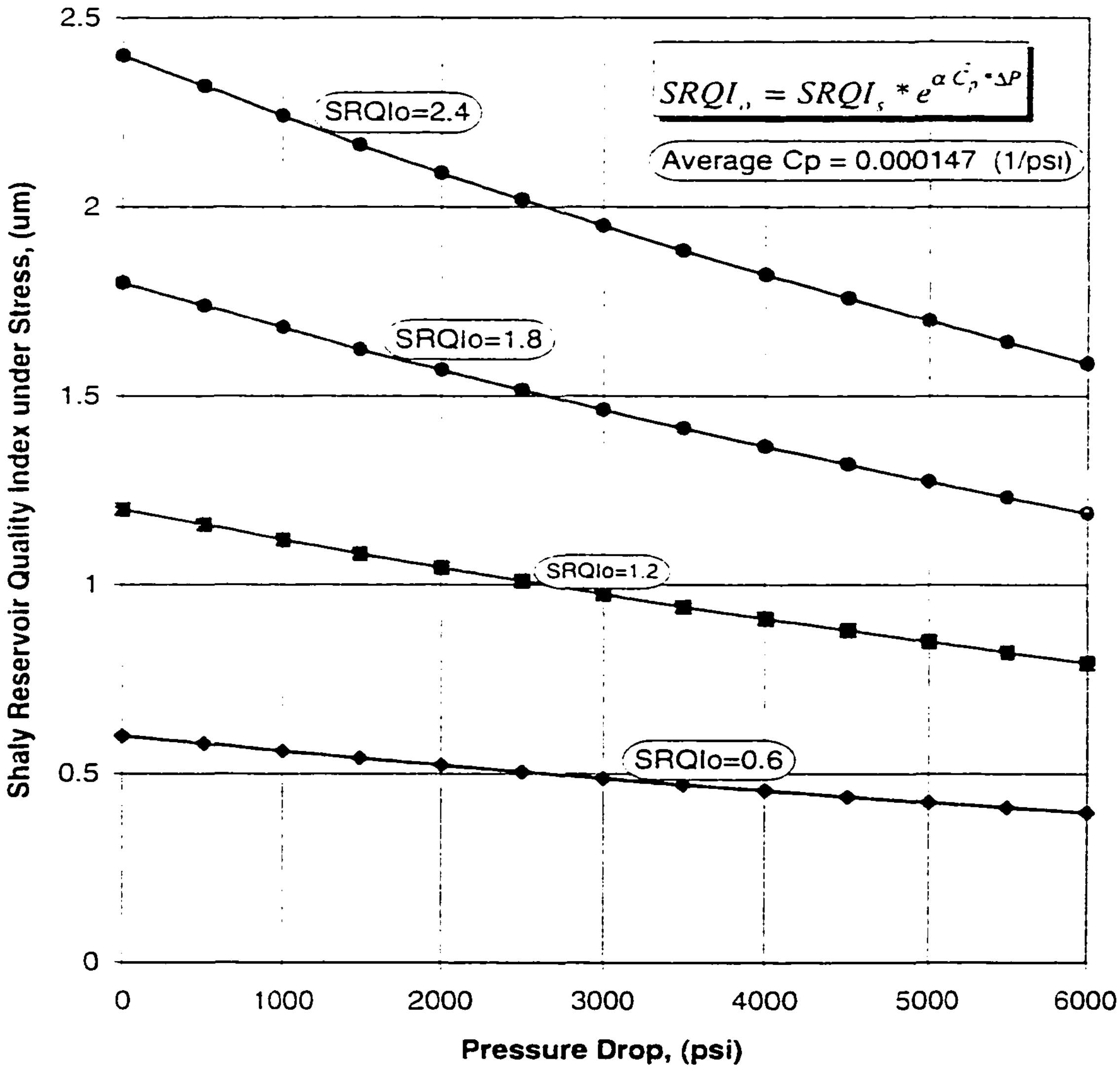

Fig. 5. 9 - Effect of pore-pressure drop on the newly-developed Shaly Reservoir Quality Index Under Stress (SRQIs)

Fig. 5. 9 shows that (SRQIs) decreases with increase in reservoir pressure drop for different values of (SRQIo). For reservoirs with 3,500 psi pressure drop, a severe reduction in shaly reservoir quality index under stress (SRQIs) value is indicated with constant SRQIo. The reduction in (SRQIs) is smaller at higher values of pressure drop than at the early stage of the reservoir.

Furthermore, Fig. 5.10 shows a semi-log plot of (SRQIs/SRQIo) versus reservoir pore-pressure drop. This graph shows a general trend of reduction of (SRQIs/SRQIo) with increasing oil production (increasing pore-pressure drop). The slope of this graph decreases gradually with increasing pore-pressure drop.

5. 4. Effect of Stress on the Newly-Developed Flow Unit Models for Characterizating Shaly Formations

This study will modify some of the existing shaly models to consider stress effect before using them to characterize and identify flow units in shaly formations. Also the modified models will be used to study the effect of stress on petrophysical properties of flow units. Consideration of the effect of stress on these shaly models is expected to enhance their accuracy and provide more accurate values of water saturation in shaly formations.

Several models have been introduced to calculate water saturation in shaly formations, Fertl (1987). The reason for the several models is that there is no universal model available for obtaining water saturation for different shale types and in different reservoir conditions. These shale models do not consider several important factors such as stress effect and local characteristics of each reservoir. Hence, the shale models often

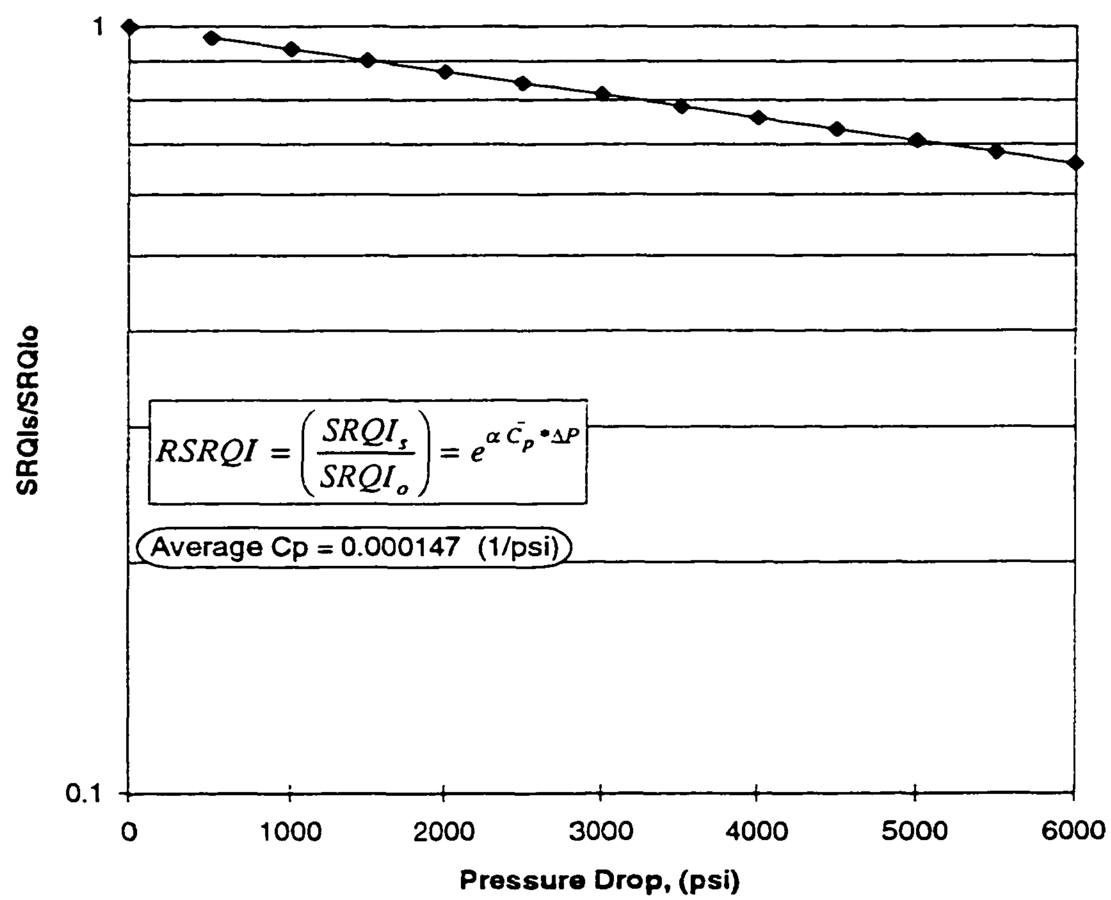

Fig. 5. 10 - Semi-Log Plot of (SRQIs/SRQIo) versus Reservoir Pressure Drop

provide over or underestimated values of water saturation in shaly formations. This leads to serious errors in calculating oil saturation and estimation of the initial oil-in-place.

In this study, four shale models for calculating water saturation in shaly formations have been selected to investigate the effect of of stress on the characterization and identification of flow units in stress-sensitive shaly formations.

5.4.1 Effect of Stress on The Newly-Developed Flow Unit Model For Characterizating Laminated Shaly Formations

Poupan and Leveaux (1971) developed a model to determine water saturation in laminated shaly formations. This model is given by

$$\frac{1}{R_t}=\frac{\varphi^2 S_w^2}{aR_w(1-V_{lam})}+\frac{V_{lam}}{R_{sh}} \tag{5-18}$$

where

a = equation coefficient,

V_{lam} = laminated shale volume in the formation, (fraction)

φ = total porosity of the formation, (fraction)

R_t = true resistivity of the formation, (ohm-m),

R_{sh} = resistivity of laminated shale, (ohm-m),

S_w = water saturation in shaly formations, (fraction).

This model represents a relationship (between true formation resistivity and water saturation) which expresses the conductivity of the formation which is made-up of three factors: two of these involve the conductivities of shale and formation water network. The third term represents the additional conductivity resulting from the cross-linking of the two networks. Rearranging equation (5-18) and using (m) exponent for porosity instead of (2) results in the following equation

$$S_w^2 = \frac{aR_w(1-V_{sh})}{\varphi^m}\left(\frac{R_{sh}-V_{Lam}R_t}{R_tR_{sh}}\right) \tag{5-19}$$

Subjecting equation (5-19) to irreducible water saturation condition and substituting into Wyllie and Rose equation of permeability, equation (2-21), one obtains

$$K_{0-sh} = \frac{62500*\varphi_{to}^{m+6}}{aR_w(1-V_{Lam})\left(\frac{R_{sh}-V_{Lam}R_t}{R_tR_{sh}}\right)} \tag{5-20}$$

where

$K_{o\text{-}sh}$ = permeability of shaly formation under zero stress conditions, (md)

Substituting total porosity from equation (5-4) into equation (5-20) results in the following equation

$$K_{s-sh} = \frac{62500*\varphi_{s-sh}^{m+6}*\left[1-\varphi_o\left(1-e^{-\alpha\bar{C}_p\Delta P}\right)\right]^{m+5}}{aR_w(1-V_{Lam})^{m+6}\left(\frac{R_{sh}-V_{Lam}R_t}{R_tR_{sh}}\right)_{Wirr}} * e^{(m+3)\alpha\bar{C}_p\Delta p} \tag{5-21}$$

Rearranging equation (5-21) an taking the square root of the resultant equation yields

$$\sqrt{\frac{K_{s-sh}}{\varphi_{s-sh}}} = \frac{250*\varphi_{s-sh}^{\frac{m}{2}+2.5}*\left[1-\varphi_o\left(1-e^{-\alpha\bar{C}_p\Delta P}\right)\right]^{\left(\frac{m}{2}+2.5\right)}}{(1-V_{Lam})^{\frac{m}{2}+3.0}\sqrt{aR_w\left(\frac{R_{sh}-V_{Lam}R_t}{R_tR_{sh}}\right)_{Wirr}}} * e^{\left(\frac{m}{2}+1.5\right)\alpha\bar{C}_p\Delta p} \tag{5-22}$$

Substituting equation (5-22) into SRQIs equation (5-15), one obtains

$$SRQI_s(\mu m) = \frac{7.85 * \varphi_{s-sh}^{\frac{m}{2}+2.5} * \left[1-\varphi_o\left(1-e^{-\alpha \bar{C}_p \Delta P}\right)\right]^{\left(\frac{m}{2}+1.5\right)}}{\left(1-V_{Lam}\right)^{\frac{m}{2}+3.0}\sqrt{aR_w\left(\frac{R_{sh}-V_{Lam}R_t}{R_t R_{sh}}\right)_{Wirr}}} * e^{\left(\frac{m}{2}+1.5\right)\alpha \bar{C}_p \Delta p} \tag{5-23}$$

Taking logarithm on both sides of the equation, (5-23) results in the following equation

$$Log(SRQI_s) = \left(\frac{m}{2}+2.5\right)Log(\varphi_{s-sh}) + Log\left\{\frac{7.85 * \left[1-\varphi_o\left(1-e^{-\alpha \bar{C}_p \Delta P}\right)\right]^{\left(\frac{m}{2}+2.5\right)}}{\left(1-V_{Lam}\right)^{(m/2+3)}\sqrt{aR_w\left(\frac{R_{sh}-V_{Lam}R_t}{R_t R_{sh}}\right)_{Wirr}}} * e^{\left(\frac{m}{2}+1.5\right)\alpha \bar{C}_p \Delta p}\right\} \tag{5-24}$$

Equation (5-24) is a new model that can be used for the characterization and identification of flow units for laminared shaly formation under stress effect. This model is also used to study the effect of stress on petrophysical properties of flow units.

This model has two main unique characteristics for each flow unit. The characteristics are: (1) the slope of the straight line defining the flow unit is equal to [(m/2) +2.5], and (2) the straight line defines each flow unit with an intercept (at φ_{s-sh} = 1.0) equal to stress factor for laminated shaly formation (σ_{Lam}) which is given by

$$\sigma_{Lam} = \left\{\frac{7.85 * \left[1-\varphi_o\left(1-e^{-\alpha \bar{C}_p \Delta P}\right)\right]^{\left(\frac{m}{2}+2.5\right)}}{\left(1-V_{Lam}\right)^{\frac{m}{2}+3.0}\sqrt{aR_w\left(\frac{R_{sh}-V_{Lam}R_t}{R_t R_{sh}}\right)_{Wirr}}} * e^{\left(\frac{m}{2}+1.5\right)\alpha \bar{C}_p \Delta p}\right\} \tag{4-25}$$

These two unique characteristics are very useful for identifying and characterizing laminated shaly formation using a log-log plot of (SRQIs) versus porosity of laminated shale under stress (φ_{z-sh}). This is achieved by drawing a straight line through each set of data points of log-log plot. Each straight line defines a single flow unit in stress-sensitive shaly formation and the slope defines the shale type. This new flow unit model for laminated shaly formation will be used to study the effect of stress (or reservoir pressure drop) on petrophysical properties of these flow unit.

5.4.2 Effect of Stress on The Newly-Developed Flow Unit Model For Characterizating Dispersed Shaly Formations

Dewitte (1950) developed a model for estimating water saturation in dispersed shaly formations. This model is well-known as the clay slurry model. The model consists of a clean sand pore structure with the clay dispersed within the pore space. In other words, the clay minerals in the formations are assumed to exist in a slurry with the formation fluid. This model is given by the following equation

$$S_w = \sqrt{\frac{aR_w}{\varphi^2 R_t} + \left(\frac{V_{disp}\left(R_{disp} - R_w\right)}{2\varphi R_{disp}}\right)} - \left(\frac{V_{disp}}{\varphi}\frac{\left(R_{disp} - R_w\right)}{2R_{disp}}\right) \qquad (5\text{-}26)$$

Squaring equation (5-26) yields

$$S_w^2 = \left\{\frac{aR_w}{\varphi^2 R_t} + \left(\frac{V_{disp}\left(R_{disp} - R_w\right)}{2\varphi R_{disp}}\right)\right\} - \left\{2 * \left(\frac{V_{disp}}{\varphi}\frac{\left(R_{disp} - R_w\right)}{2R_{disp}}\right)\sqrt{\frac{aR_w}{\varphi^2 R_t} + \left(\frac{V_{disp}\left(R_{disp} - R_w\right)}{2\varphi R_{disp}}\right)}\right\}$$
$$+\left(\frac{V_{disp}^2}{\varphi^2}\frac{\left(R_{disp} - R_w\right)^2}{4R_{disp}^2}\right) \qquad (5\text{-}27)$$

Equation (5-26) can be expressed in the following simple form:

$$S_w^2 = \frac{A_{disp}}{\varphi^2} \qquad (5\text{-}28)$$

where

A_{disp} = dispersed shale group, (dimensionless), which is given by the following equation

$$A_{disp} = \left\{ \left(\frac{aR_w\varphi + B_{disp}}{R_t} \right) - \left(2 * C_{disp} \sqrt{\left(\frac{aR_w\varphi + B_{disp}}{R_t} \right)} \right) - C_{disp} \right\} \qquad (5\text{-}29)$$

where

B_{disp} = dispersed shale sub-group, (ohm-m), which is formulated by the following equation

$$B_{disp} = \frac{V_{disp}\left(R_{disp} - R_w\right)^2}{2R_{disp}} \qquad (5\text{-}30)$$

where

C_{disp} = dispersed shale sub-group, (dimensionless), which is formulated by the following equation

$$C_{disp} = \frac{V_{disp}\left(R_{disp} + R_w\right)}{2R_{disp}} \qquad (5\text{-}31)$$

where

a = equation coefficient

V_{disp} = dispersed shale volume in the formation, (fraction)

φ = total porosity of the formation, (fraction)

R_t = true resistivity of the formation, (ohm-m)

R_{disp} = resistivity of dispersed shale, (ohm-m)

S_w = water saturation in dispersed shaly formations, (fraction).

Subjecting equation (5-28) to irreducible water condition, and substituting it into Wyllie and Rose permeability equation, equation (2-21), yields

$$K_{o-sh}(md) = 62500 * \frac{\varphi_{to}^{8}}{A_{disp}} \tag{5-32}$$

Substituting total porosity at initial conditions (φ_{to}) from equation (5-4) into equation (5-32) provides an equation for permeability of shaly formations under stress effect (K_{s-sh}) as follows

$$K_{s-sh}(md) = \frac{62500 * \varphi_{s-sh}^{8} * e^{5\alpha \bar{C}_p \Delta P} * \left(1 - \varphi_o\left(1 - e^{-\alpha \bar{C}_p \Delta P}\right)\right)^{7.0}}{A_{disp}\left(1 - V_{disp}\right)^{8}} \tag{5-33}$$

Rearranging equation (5-33) and taking the square root of the resultant equation yields

$$\sqrt{\frac{K_{s-sh}}{\varphi_{s-sh}}} = \frac{250 * \varphi_{s-sh}^{3.5} * e^{2.5\alpha \bar{C}_p \Delta P} * \left(1 - \varphi_o\left(1 - e^{-\alpha \bar{C}_p \Delta P}\right)\right)^{3.5}}{\left(1 - V_{disp}\right)^{4}\sqrt{A_{disp}}} \tag{5-34}$$

RQI for shaly formations under the effect of stress (SRQIs) has been driven before by this study, equation (5-15). Substituting equation (5-34) into equation (5-15) yields

$$SRQI_s(\mu m) = \frac{7.85 * \varphi_{s-sh}^{3.5} * e^{2.5\alpha \bar{C}_p \Delta P} * \left(1 - \varphi_o\left(1 - e^{-\alpha \bar{C}_p \Delta P}\right)\right)^{3.5}}{\left(1 - V_{disp}\right)^{4}\sqrt{A_{disp}}} \tag{5-35}$$

Taking logarithm of both sides of equation (5-35) results in

$$Log(SRQI_s) = 3.5Log(\varphi_{s-sh}) + Log\left\{\frac{7.85 * e^{2.5\alpha \bar{C}_p \Delta P} * \left(1 - \varphi_o\left(1 - e^{-\alpha \bar{C}_p \Delta P}\right)\right)^{3.5}}{\left(1 - V_{disp}\right)^{4}\sqrt{A_{disp}}}\right\} \quad (5\text{-}36)$$

Equation (5-36) reveals that a log-log plot of shaly reservoir quality index under stress (SRQIs) versus porosity of dispersed shale under stress (φ_{s-sh}) will have a unique slope equal to [3.5] and a unique intercept which is given by (σ_{disp}) as follows:

$$\sigma_{disp} = \left\{\frac{7.85 * e^{2.5\alpha \bar{C}_p \Delta P} * \left(1 - \varphi_o\left(1 - e^{-\alpha \bar{C}_p \Delta P}\right)\right)^{3.5}}{\left(1 - V_{disp}\right)^{4}\sqrt{A_{disp}}}\right\} \quad (5\text{-}37)$$

where

σ_{disp} = shaly flow unit factor for dispersed shale under stress, (dimensionless)

The most important feature of this new flow unit model is that it can be used not only to identify shale type (when slope equals to 3.5) but also to identify several flow units within shaly formation. These goals are achieved by drawing straight lines through the set of data points. If the slope of the straight line is close to 3.5, then the shale type is dispersed. Each straight line defines a single flow unit in shaly stress-sensitive formations. Knowing the shale type from the slope of the straight line, the shale model can be selected, which can then be used to estimate the water saturation in shaly formation.

5.4.3. Effect of Stress on The Newly-Developed Flow Unit Model For Characterizating Shaly Formation Using Total Shale Model

Using total shale model which is given by the following equation

$$\frac{1}{R_t} = \frac{V_{sh}}{R_{sh}} + \frac{S_w^2}{FR_w} \qquad (5\text{-}38)$$

where

R_t = true resistivity of the formation, (ohm-m)

R_{sh} = resistivity of shale, (ohm-m)

V_{sh} = shale volume in the reservoir rock, (fraction)

S_w = water saturation in shaly formations, (fraction).

R_w = formation water resistivity, (ohm-m)

F = formation resistivity factor

Writing equation (5-38) in terms of water saturation after substitution formation resisitivity factor into it, one obtains

$$S_w^2 = \frac{aR_w}{\varphi^m}\left(\frac{R_{sh} - V_{sh}R_t}{R_{sh}R_t}\right) \qquad (5\text{-}39)$$

Applying irreducible water condition on equation (5-39) and inserting it into Wyllie and Rose equation, equation (4-68), results in

$$K_{0-sh}(md) = \frac{62500 * \varphi_{to}^{m+6}}{aR_w\left(\frac{R_{sh} - V_{sh}R_t}{R_{sh}R_t}\right)_{wirr}} \qquad (5\text{-}40)$$

Substituting ($K_{0\text{-}sh}$) from equation (5-40) into permeability equation under stress, equation (5-9), yields an equation for permeability of shaly formation under stress as follows:

$$K_{s-sh} = \frac{62500 * \varphi_{to}^{m+6}}{aR_w\left(\frac{R_{sh} - V_{sh}R_t}{R_t R_{sh}}\right)_{Wirr}} * \frac{e^{-3\alpha \bar{C}_p \Delta P}}{\left[1 - \varphi_o\left(1 - e^{-\alpha \bar{C}_p \Delta P}\right)\right]} \tag{5-41}$$

Using total porosity from equation (5-4) into equation (5-41) results in the following equation

$$K_{s-sh} = \frac{62500 * \varphi_{s-sh}^{m+6} * e^{(m+3)\alpha \bar{C}_p \Delta P} * \left[1 - \varphi_o\left(1 - e^{-\alpha \bar{C}_p \Delta P}\right)\right]^{m+5}}{aR_w * (1 - V_{sh})^{m+6}\left(\frac{R_{sh} - V_{sh}R_t}{R_t R_{sh}}\right)_{Wirr}} \tag{5-42}$$

Rearranging equation (5-42) in the following form yields

$$\sqrt{\frac{K_{s-sh}}{\varphi_{s-sh}}} = \frac{250 * \varphi_{s-sh}^{(m/2)+2.5} * e^{(m/2+1.5)\alpha \bar{C}_p \Delta P} * \left(1 - \varphi_o\left(1 - e^{-\alpha \bar{C}_p \Delta P}\right)\right)^{\frac{m}{2}+2.5}}{(1 - V_{sh})^{(m/2)+3}\sqrt{aR_w * \left(\frac{R_{sh} - V_{sh}R_t}{R_t R_{sh}}\right)_{Wirr}}} \tag{5-43}$$

Substituting equation (5-43) into SRQIs equation, equation (5-15), provides

$$SRQI_s(\mu m) = \frac{7.85 * \varphi_{s-sh}^{(m/2)+2.5} * e^{(m/2+1.5)\alpha \bar{C}_p \Delta P} * \left(1 - \varphi_o\left(1 - e^{-\alpha \bar{C}_p \Delta P}\right)\right)^{\frac{m}{2}+2.5}}{(1 - V_{sh})^{(m/2)+3}\sqrt{aR_w * \left(\frac{R_{sh} - V_{sh}R_t}{R_t R_{sh}}\right)_{Wirr}}} \tag{5-44}$$

Taking logarithm of both sides of equation (5-44) provides the following equation

$$Log(SRQI_s) = \left(\frac{m}{2} + 2.5\right) Log(\varphi_{s-sh}) + Log\left\{ \frac{7.85 * e^{(m/2+1.5)\alpha \bar{C_p} \Delta P} * \left(1 - \varphi_o\left(1 - e^{-\alpha \bar{C_p} \Delta P}\right)\right)^{\frac{m}{2}+2.5}}{(1 - V_{sh})^{(m/2)+3} \sqrt{aR_w * \left(\frac{R_{sh} - V_{Lam}R_t}{R_t R_{sh}}\right)_{Wirr}}} \right\}$$

(5-45)

Equation (5-45) reveals that a log-log plot of shaly reservoir quality index under stress (SRQIs) versus porosity of shaly formation under stress effect (φ_{s-sh}) provides a straight line for each flow unit. This straight line has two unique characteristics: (l) its slope equal to *(m/2 + 2.5)* and (2) its intercept, which is given by

$$\sigma_{tot} = \left\{ \frac{7.85 * e^{(m/2+1.5)\alpha \bar{C_p} \Delta P} * \left(1 - \varphi_o\left(1 - e^{-\alpha \bar{C_p} \Delta P}\right)\right)^{\frac{m}{2}+2.5}}{(1 - V_{sh})^{(m/2)+3} \sqrt{aR_w * \left(\frac{R_{sh} - V_{Lam}R_t}{R_t R_{sh}}\right)_{Wirr}}} \right\} \qquad (5\text{-}46)$$

where

σ_{tot} = stess factor of shaly formation obeying total shale model, (dimensionless)

5. 4. 4. Effect of Stress on Flow Unit Model Using Cation Exchange Capacity (CEC) of Shaly Formations

Waxman and Smits (1968) developed a model based on the cation exchange capacity (CEC) of shale. The cation exchange capacity (CEC) is considered as one of the most important properties of shale. The cation exchange capacity (CEC) is expressed in milliequivalent unit pore volume of pore fluids, Qv (meq/cc).

Dewan (1983) had one objection to the application of Waxman-Smits model for water sands of constant conductivity. He observed that increasing shale content will have increasing effective water conductivities to the extent that shale could appear to contain saline water. The cation exchange capacity (CEC) is proportional to the formation shaliness but also depends on shale type.

Using Waxman-Smits Model, which is given by

$$S_w^2 = \frac{F^* R_w}{R_t\left(1 + \frac{R_w B Q_v}{S_w}\right)} \tag{5-47}$$

where

S_w = water saturation (using CEC model) in shaly formation, (fraction)

R_t = true formation resistivity, (ohm-m),

R_w = formation water resistivity, (ohm-m),

B = specific concentration conductivity, (mho/m per meq/cc),

Q_v = cation exchange capacity of shaly formation, (meq/cc),

F^* = a limiting formation factor, which is approximately the same factor of clean formation (but the porosity of shaly formation is, however, expected to be considerably different from that of clean formations).

Rearranging equation (5-47) in the following form results in the following equation

$$\frac{S_w^2}{F^* R_w} + \left(\frac{BQ_v}{F^*}\right) * S_w - \frac{1}{R_t} = 0 \tag{5-48}$$

The term (BQ_v / F^*) in equation (5-48) represents the excess conductivity contributed by shaliness. Equation (5-48) is a quadratic equation which can be solved easily and the positive root of the solution will be given by

$$S_w = \frac{F^* R_w}{2}\left\{\left(\frac{-BQ_v}{F^*}\right) + \sqrt{\left(\frac{-BQ_v}{F^*}\right) - \left(\frac{4}{F^* R_w R_t}\right)}\right\} \tag{5-49}$$

Squaring equation (5-49) and subjecting the resultant equation to irreducible water saturation, and substituting the final equation into Wyllie and Rose equation, equation (2-21), yields

$$K_{0-sh} = \frac{62500 * \varphi_{to}^6}{\left(\frac{F^* R_w}{2}\right)^2 \left[\left(\frac{-BQ_v}{F^*}\right) + \sqrt{\left(\frac{-BQ_v}{F^*}\right) - \left(\frac{4}{F^* R_w R_t}\right)}\right]^2_{Wirr}} \tag{5-50}$$

Equation (5-50) is a permeability equation for shaly formation under zero stress condition. Subjecting equation (5-50) to stress condition requires substituting it into permeability equation which obeys cation-exchange capacity (CEC) model under stress, equation (5-9). This yields the following equation

$$K_{s-sh} = \frac{62500 * \varphi_{to}^6}{\left(\frac{F^* R_w}{2}\right)^2 \left[\left(\frac{-BQ_v}{F^*}\right) + \sqrt{\left(\frac{-BQ_v}{F^*}\right) - \left(\frac{4}{F^* R_w R_t}\right)}\right]^2_{Wirr}} \frac{e^{-3\alpha \bar{C}_p \Delta P}}{\left[1 - \varphi_o (1 -) e^{-3\alpha \bar{C}_p \Delta P}\right]} \tag{5-51}$$

Substituting total porosity from porosity under stress equation, equation (5-4), into equation (5-51) results in

$$K_{s-sh} = \frac{62500 * \varphi_{s-sh}^{6} * e^{3\alpha \bar{C_p} \Delta P \left[1-\varphi_o(1-)e^{-3\alpha \bar{C_p} \Delta P}\right]^5}}{(1-V_{sh})^6 \left(\frac{F^* R_w}{2}\right)^2 \left\{\left(\frac{-BQ_v}{F^*}\right) + \sqrt{\left(\frac{-BQ_v}{F^*}\right) - \left(\frac{4}{F^* R_w R_t}\right)}\right\}^2_{Wirr}} \tag{5-52}$$

Rearranging equation (5-52) in the follwoing form

$$\sqrt{\frac{K_{s-sh}}{\varphi_{s-sh}}} = \frac{250 * \varphi_{s-sh}^{2.5} * e^{1.5\alpha \bar{C_p} \Delta P} * \left[1-\varphi_o(1-)e^{-3\alpha \bar{C_p} \Delta P}\right]^{2.5}}{(1-V_{sh})^3 \left(\frac{F^* R_w}{2}\right) \left\{\left(\frac{-BQ_v}{F^*}\right) + \sqrt{\left(\frac{-BQ_v}{F^*}\right) - \left(\frac{4}{F^* R_w R_t}\right)}\right\}_{Wirr}} \tag{5-53}$$

Using equation (5-53) into SRQIs equation developed by this study, (5-15), yields

$$SRQI_s(\mu m) = \frac{7.85 * \varphi_{s-sh}^{2.5} * e^{1.5\alpha \bar{C_p} \Delta P} * \left[1-\varphi_o(1-)e^{-3\alpha \bar{C_p} \Delta P}\right]^{2.5}}{(1-V_{sh})^3 \left(\frac{F^* R_w}{2}\right) \left\{\left(\frac{-BQ_v}{F^*}\right) + \sqrt{\left(\frac{-BQ_v}{F^*}\right) - \left(\frac{4}{F^* R_w R_t}\right)}\right\}_{Wirr}} \tag{5-54}$$

Taking logarithm on both sides of equation (5-54) provides

$$Log(SRQI_s) = 2.5 * Log(\varphi_{s-sh}) + Log\left\{\frac{7.85 * e^{1.5\alpha \bar{C_p} \Delta P} * \left[1-\varphi_o(1-)e^{-3\alpha \bar{C_p} \Delta P}\right]^{2.5}}{(1-V_{sh})^3 \left(\frac{F^* R_w}{2}\right) \left\{\left(\frac{-BQ_v}{F^*}\right) + \sqrt{\left(\frac{-BQ_v}{F^*}\right) - \left(\frac{4}{F^* R_w R_t}\right)}\right\}_{Wirr}}\right\} \tag{5-55}$$

Equation (5-55) represents a new model which has the capability to identify shale type and flow units in shaly formations. This newly-developed model has two unique characteristics including: (1) a unique slope equals [2.5] which is different from the slopes of other previously-developed models, and (2) a unique intercept which is given by

$$\sigma_{CEC} = \left\{ \frac{7.85 * e^{1.5\alpha \bar{C}_p \Delta P} * \left[1 - \varphi_o (1 -) e^{-3\alpha \bar{C}_p \Delta P} \right]^{2.5}}{(1 - V_{sh})^3 \left(\frac{F^* R_w}{2} \right) \left\{ \left(\frac{-BQ_v}{F^*} \right) + \sqrt{\left(\frac{-BQ_v}{F^*} \right) - \left(\frac{4}{F^* R_w R_t} \right)} \right\}_{Wirr}} \right\} \qquad (5\text{-}56)$$

where

σ_{CEC} = stress factor for shaly formation obeying CEC model, (ohm-m)

This intercept (σ_{CEC}) is very useful to distinguish one flow unit from another since each flow unit has a certain value under a specific effective stress.

Table 5.4 summarizes the newly-developed flow unit models for shaly formations. The four models can be used for the following purposes:

1. Reservoir characaterization and flow unit identification of shaly stress-sensitive reservoirs,
2. Studying the effect of stress on Shaly Reservoir Quality Index of stress-sensitive formations (SRQIs),
3. Studying the effect of stress on petrophysical properties of flow unit in shaly stress-sensitive formation, and
4. Selection of the shale model for calculation of water saturation in shaly formation. This can be achieved by defining shale type.

All the flow unit models for shaly stress sensitive formations were found to have a common feature. A single flow unit can be represented by a straight line with a specific slope (depending on shale type) and a unique intercept (depending upon stress and shale volume).

Table 5.4 - List of flow unit models for the characaterization and identification of flow units in stress-sensitive shaly formations.

Used Shale Model	Newly-Developed Flow unit Model
1. Laminated Shale	$Log(SRQI_s) = \left(\frac{m}{2} + 2.5\right) Log(\varphi_{s-sh}) + Log(\sigma_{Lam})$ $\sigma_{Lam} = \left\{ \frac{7.85 * \left[1 - \varphi_o\left(1 - e^{-\alpha \bar{C_p} \Delta P}\right)\right]^{\left(\frac{m}{2}+2.5\right)}}{(1 - V_{Lam})^{(m/2+3)} \sqrt{aR_w \left(\frac{R_{sh} - V_{Lam} R_t}{R_t R_{sh}}\right)_{Wirr}}} * e^{\left(\frac{m}{2}+1.5\right)\alpha \bar{C_p} \Delta p} \right\}$
2. Dispersed Shale	$Log(SRQI_s) = 3.5\, Log(\varphi_{s-sh}) + Log(\sigma_{Disp})$ $\sigma_{Disp} = \left\{ \frac{7.85 * e^{2.5\alpha \bar{C_p} \Delta P} * \left(1 - \varphi_o\left(1 - e^{-\alpha \bar{C_p} \Delta P}\right)\right)^{3.5}}{(1 - V_{disp})^4 \sqrt{A_{disp}}} \right\}$

Table 5.4 -List of flow unit models for the characaterization and identification of flow units in stress-sensitive shaly formations (contd.)

Used Shale Model	Newly-Developed Flow unit Model
3. Total Shale Model	$$Log(SRQI_s) = \left(\frac{m}{2} + 2.5\right) Log(\varphi_{s-sh}) + Log(\sigma_{tot})$$ $$\sigma_{tot} = \left\{ \frac{7.85 * e^{(m/2+1.5)\alpha \bar{C_p} \Delta P} * \left(1 - \varphi_o\left(1 - e^{-\alpha \bar{C_p} \Delta P}\right)\right)^{\frac{m}{2}+2.5}}{(1 - V_{sh})^{(m/2)+3} \sqrt{aR_w * \left(\frac{R_{sh} - V_{Lam} R_t}{R_t R_{sh}}\right)_{Wirr}}} \right\}$$
4. Cation Exchange Capacity (CEC) Model	$$Log(SRQI_s) = 2.5 * Log(\varphi_{s-sh}) + Log(\sigma_{CEC})$$ $$\sigma_{CEC} = \left\{ \frac{7.85 * e^{1.5\alpha \bar{C_p} \Delta P} * \left[1 - \varphi_o (1 -) e^{-3\alpha \bar{C_p} \Delta P}\right]^{2.5}}{(1 - V_{sh})^3 \left(\frac{F^* R_w}{2}\right) \left\{ \left(\frac{-BQ_v}{F^*}\right) + \sqrt{\left(\frac{-BQ_v}{F^*}\right) - \left(\frac{4}{F^* R_w R_t}\right)} \right\}_{Wirr}} \right\}$$

5.5. Development of Generalized Flow Unit Model for Shaly Stress-Sensitive Formations

Using total shale model for water saturation, equation (5-39), and the generalized form of permeability equation, equation (2-39), the following permeability equation for shaly formation under zero stress is obtained and given as follows:

$$K_{o-sh} = \left(\frac{C_1}{aR_w}\right) * \varphi_{to}^{(C_2+1)m} * \left(\frac{R_{sh} - V_{sh}R_t}{R_{sh}R_t}\right)_{wirr} \tag{5-57}$$

Substituting equation (5-57) into the equation of permeability under stress, equation (4-37), yields an equation for shaly formation under stress effect as follows:

$$K_{s-sh} = \left(\frac{C_1}{aR_w}\right) * \varphi_{to}^{(C_2+1)m} * \frac{e^{-3\bar{C}_p \Delta\sigma}\left(\frac{R_{sh} - V_{sh}R_t}{R_{sh}R_t}\right)_{wirr}}{\left[1 - \varphi_o\left(1 - e^{-\bar{C}_p \Delta\sigma}\right)\right]} \tag{5-58}$$

Equation (5-58) can be written in the following simple form

$$K_{s-sh} = \left(\frac{C_1}{aR_w}\right) * \varphi_{to}^{(C_2+1)m} * \frac{e^{-3\bar{C}_p \Delta\sigma} * A_{sh}}{S} \tag{5-59}$$

where

A = shale group, given as follows

$$A_{sh} = \left(\frac{R_{sh} - V_{sh}R_t}{R_{sh}R_t}\right)_{wirr} \tag{5-60}$$

S = stress correction factor for porosity and permeability, given as follows

$$S = \left[1 - \varphi_o\left(1 - e^{-\bar{C}_p \Delta\sigma}\right)\right] \tag{5-61}$$

Substituting total porosity under zero stress (φ_{to}) from the equation of porosity of shaly formation under stress, equation (5-4), into equation (5-58) results in

$$K_{s-sh} = \left(\frac{C_1}{aR_w}\right) * \varphi_{s-sh}^{(C_2+1)m} * \frac{e^{[(C_2+1)m-3]\bar{C_p}\Delta\sigma} * S^{(C_2+1)m-1} * A_{sh}}{(1-V_{sh})^{(C_2+1)m}} \tag{5-62}$$

Using equation (5-62) into SRQIs equation, equation (5-15) yields

$$SRQIs = (0.0314\sqrt{C_1})\varphi_{s-sh}^{[(C_2+1)m-1]/2} * \frac{e^{0.5[(C_2+1)m-3]\bar{C_p}\Delta\sigma} * S^{0.5[(C_2+1)m-1]} * \sqrt{A_{sh}}}{\sqrt{aR_w(1-V_{sh})^{(C_2+1)m}}} \tag{5-63}$$

Applying logarithm on both sides of equation (5-63) yields

$$Log(SRQIs) = \left[\frac{(C_2+1)m-1}{2}\right] Log\varphi_{s-sh} + Log\left\{(0.0314\sqrt{C_1})\frac{e^{0.5[(C_2+1)m-3]\bar{C_p}\Delta\sigma} * S^{0.5[(C_2+1)m-1]} * \sqrt{A_{sh}}}{\sqrt{aR_w(1-V_{sh})^{(C_2+1)m}}}\right\}$$

(5-64)

Equation (5-64) reveals that a flow unit in shaly stress-sensitive formation can be represented by a straight line having slope equal to {[(C_2 + 1)m - 1]/2}and intercept equal to flow unit factor which is given as follows:

$$FUF_{G-S-Sh} = \left\{(0.0314\sqrt{C_1})\frac{e^{0.5[(C_2+1)m-3]\bar{C_p}\Delta\sigma} * S^{0.5[(C_2+1)m-1]} * \sqrt{A_{sh}}}{\sqrt{aR_w(1-V_{sh})^{(C_2+1)m}}}\right\} \tag{5-65}$$

where

FUF_{G-S-Sh} = flow unit factor of shaly stress-sensitive formation based on generalized permeability equation, ($1/\sqrt{ohm-m}$)

This generalized flow unit model, equation (5-64), can be used to identify flow units in several cases including

(a) clean stress-insensitive formations,

(b) shaly stress-insensitive formations,

(c) clean stress-sensitive formations, and

(d) shaly stress-insensitive formations.

Case (a) clean stress-insensitive formations

Several models are derived and validated in Chapter 2 for reservoir characterization and for flow unit identification of formation types. For the purpose of proving that the generalized flow unit model, equation (5-64), works for clean stress-insensitive formations, the following conditions are applied to the generalized model, equation (5-64), as follows:

1. For clean formation, $V_{sh} = 0$ so that A_{sh} can be replaced by R_{ti}. This is obtained by comparing Archie equation for water saturation, equation (2-27), and total shale model, equation (3-33). In addition, porosity of shaly formation under stress can be replaced by porosity under stress as follows: $\varphi_{s-sh} \rightarrow \varphi_s$.
2. For clean insensitive formation, change in effective stress can be considered negligible ($\Delta\sigma = 0$). Then, the following equality equation can be written $\varphi_s = \varphi_o$.
3. Combining steps 1 and 2 leads to $\varphi_{s-sh} \rightarrow \varphi_o$,
4. At $V_{sh} = 0$ and $\Delta\sigma = 0$, SRQIs can be reduced to RQIo from equation (5-17),
5. $\left\{ e^{-\left(\frac{(C_2+1)m-3}{2}\right)\bar{C}_p \Delta\sigma} \right\} = 1.0$ at $\Delta\sigma = 0$, and

6. $\left[1-\varphi_o\left(1-e^{-\bar{C}_p \Delta\sigma}\right)\right]$ has to be equal unity from equation (4-23).

Finally, the generalized flow unit model, equation (5-64) can be reduced to the same model for clean stress-insensitive formation, developed in chapter 2, equation (2-41).

Case (b) shaly stress-insensitive formations

For shaly stress-insensitive formations, the following conditions can be written as follows:

1. At $\Delta\sigma = 0$, $SRQIs \rightarrow SRQIo$

$$\varphi_{s-sh} \rightarrow \varphi\text{, and} \quad \left\{ e^{-\left(\frac{(C_2+1)m-3}{2}\right)\bar{C}_p \Delta\sigma} \right\} = 1.0$$

3. $\left[1-\varphi_o\left(1-e^{-\bar{C}_p \Delta\sigma}\right)\right]$ has to be equal unity from equation (4-23)

Substituting the above three condition in equation (5-64) leads to the generalized flow unit model for shaly stress-insensitive formation developed in chapter 3, equation (3-48).

Case (c) clean stress-sensitive formations

For clean stress-sensitive formations, the following conditions are applied on the generalized flow unit model, equation (5-64), as follows:

1. at $V_{sh} = 0$, $\varphi_{s-sh} \rightarrow \varphi_s$ from equation (5-3).

$SRQIs \rightarrow RQIs$ from equations (4-48) and (5-16).

2. for clean formation, $V_{sh} = 0$, A_{sh} can be replaced by R_{ti} as shown in case (a).

This leads to the reduction of equation (5-64) to equation (4-51).

5. 6. Effect of Stress on the Flow Unit Models for Shaly Formations Under Stress

With respect to the illustration of the newly-developed flow unit models for shaly formations under the effect of stress, porosity and permeability data (under zero psi) are simulated, Table 5.5. Values of Gamma-Ray (GR) are simulated and used to calculate shale volume. The simulated values of porosity and permeability (at zero change in effective stress) are then used to calculate the corresponding values of porosity (at 1,000 psi and 5,000 psi) and permeability (at 1,000 and 5,000 psi) using equations (5-4) and (4-37) respectively. Shaly Reservoir Quality under zero stress effect (SRQIo) is used to calculated Shaly Reservoir Quality under stress effect (at 1,000 and 5, 000 psi) using equation (5-17).

A plot of shaly reservoir quality under stress effect (SRQIs) versus porosity under stress (φ_{s-sh}), Fig. 5.11, shows that three flow units can be identified. These three flow units are defined using three straight lines. Each straight line represents one flow unit having a consistent characteristics of reservoir properties. Calculating the slope of each straight line and comparing it to slopes of flow unit models in Table 5.4 shows that one flow unit obeys dispersed shale model (slope ~ 3.5) while the other two flow units obey cation-exchange-capacity (CEC) model dispersed shale model (slope ~ 2.5). The same simulated data as shown in Table 5.5 is used to illustrate the effect of stress on

- Flow unit models characterizing shaly formations,
- Shaly Reservoir Quality Index under Stress (SRQIs), and
- Porosity of shaly formations under stress.

Table 5.5 -Simulated Data For Validating the Newly Developed Flow Unit Models and for Studying the Effect Of Stress on Characteristics of Flow Units

Irreducible water saturation (Swirr) = 26 %
Formation water resistivity (Rw) = 0.0531 ohm-m
Coefficients a = 0.9, n = 2, and m = 2.2
Maximum GR = 130 API, and Minimum GR = 58 API

GR (API)	Vsh (%)	(Phi)o (%)	(Ko-sh) (md)	(Phi)s 1000 psi (fract)	(Phi)s 5,000 psi (fract)	(Ks-sh) 1,000 psi (md)	(Ks-sh) 5,000 psi (md)	SRQIo Zero psi (um)	SRQIs 1000 psi (um)	SRQIs 5,000 psi (um)
92	47.2222	0.166	47.3691	0.146636	0.08713	31.1859	5.718	0.73	0.6303	0.3501
90	44.4444	0.125	13.5964	0.109789	0.06411	8.90029	1.604	0.439	0.3793	0.2107
110	72.2222	0.142	23.828	0.125016	0.07353	15.635	2.837	0.772	0.6663	0.3701
120	86.1111	0.205	119.877	0.18208	0.11005	79.3553	14.8	2.037	1.7589	0.977
125	93.0556	0.23	198.894	0.205006	0.12529	132.127	24.92	3.504	3.025	1.6803
110	72.2222	0.12	11.361	0.105325	0.06138	7.43183	1.336	0.58	0.5005	0.278
63	6.94444	0.215	147.825	0.191231	0.11609	97.9939	18.36	0.854	0.7368	0.4093
62	5.55556	0.222	170.205	0.197652	0.12037	112.941	21.22	0.895	0.7724	0.429
64	8.33333	0.245	262.633	0.218839	0.13466	174.839	33.19	1.074	0.927	0.5149
64	8.33333	0.236	222.757	0.210532	0.12902	148.105	28	1.008	0.8699	0.4832
92	47.2222	0.225	180.56	0.200408	0.12221	119.863	22.55	1.224	1.057	0.5872
94	50	0.205	119.877	0.18208	0.11005	79.3553	14.8	1.074	0.927	0.5149
83	34.7222	0.155	35.0331	0.136709	0.08085	23.029	4.202	0.584	0.5044	0.2802
89	43.0556	0.185	76.3088	0.163855	0.09817	50.3726	9.312	0.845	0.7296	0.4053
96	52.7778	0.235	218.634	0.20961	0.1284	145.343	27.47	1.394	1.2032	0.6684
98	55.5556	0.25	287.048	0.223463	0.13782	191.228	36.39	1.596	1.3778	0.7653
99	56.9444	0.285	510.901	0.256016	0.16047	342.05	66.15	2.026	1.7491	0.9716
111	73.6111	0.21	133.286	0.186652	0.11306	88.2936	16.5	1.54	1.3294	0.7385
121	87.5	0.23	198.894	0.205006	0.12529	132.127	24.92	2.612	2.2547	1.2524
125	93.0556	0.285	510.901	0.256016	0.16047	342.05	66.15	5.045	4.3553	2.4193
62	5.55556	0.19	85.8094	0.168402	0.10111	56.6839	10.5	0.687	0.5928	0.3293
62	5.55556	0.195	96.1992	0.172955	0.10407	63.5917	11.81	0.718	0.6195	0.3441
62	5.55556	0.18	67.6423	0.159315	0.09524	44.6204	8.23	0.626	0.5407	0.3004
58	0	0.15	30.3264	0.132207	0.07802	19.9211	3.627	0.446	0.3854	0.2141

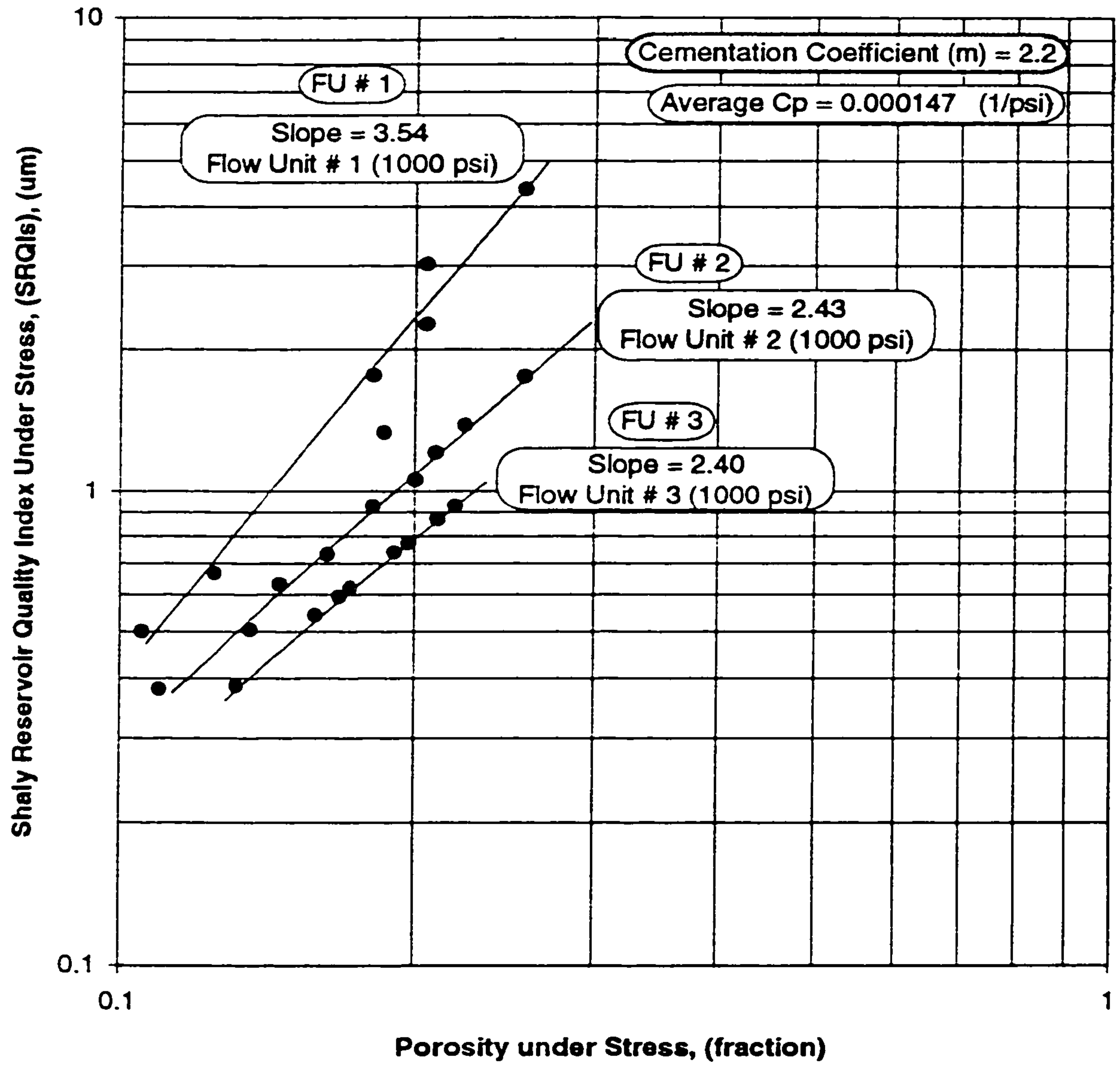

Fig. 5.11-Validation of flow unit models for shaly formations under stress

The effect of stress on the characteristics of flow units is shown in Fig. 5.12. Data in Table 5.5 is used to plot shaly reservoir quality under stress effect (SRQIs) versus porosity of shaly formation under stress (φ_{s-sh}) at 1,000 psi and 5,000 psi change in effective stress. This plot shows that increasing change in effective stress from 1,000 psi to 5,000 psi leads to reduction in both porosity of shaly formation and Shaly Reservoir Quality Index under Stress (SRQIs). Also, increasing change in effective stress causes flow units to be shifted, on a log-log plot of SRQIs versus porosity under stress, in the direction of reduced values of both SRQI and porosity. This shift may lead, in some cases, to errors in definition of flow units and characterizing stress-sensitive reservoirs. Change in effective stress causes shifting the flow units residing in shaly stress-sensitive formations.

EXAMPLE CALCULATIONS

The purpose of this section is to introduce a step-by-step example of calculation for facilitating the application of the newly-developed flow unit models for shaly reservoirs under the effect of stress. This example shows how to apply these flow unit models to identify flow units and shale type of each flow unit residing in the formation of interest. The following values are simulated for the reservoir under study

Equation coefficient (a) = 0.90

Cementation exponent (m) = 2.20

Water saturation Exponent (n) = 2.0

Irreducible water saturation (Sinw) = 26 %

Here, this study suggests the following steps for application the flow unit models

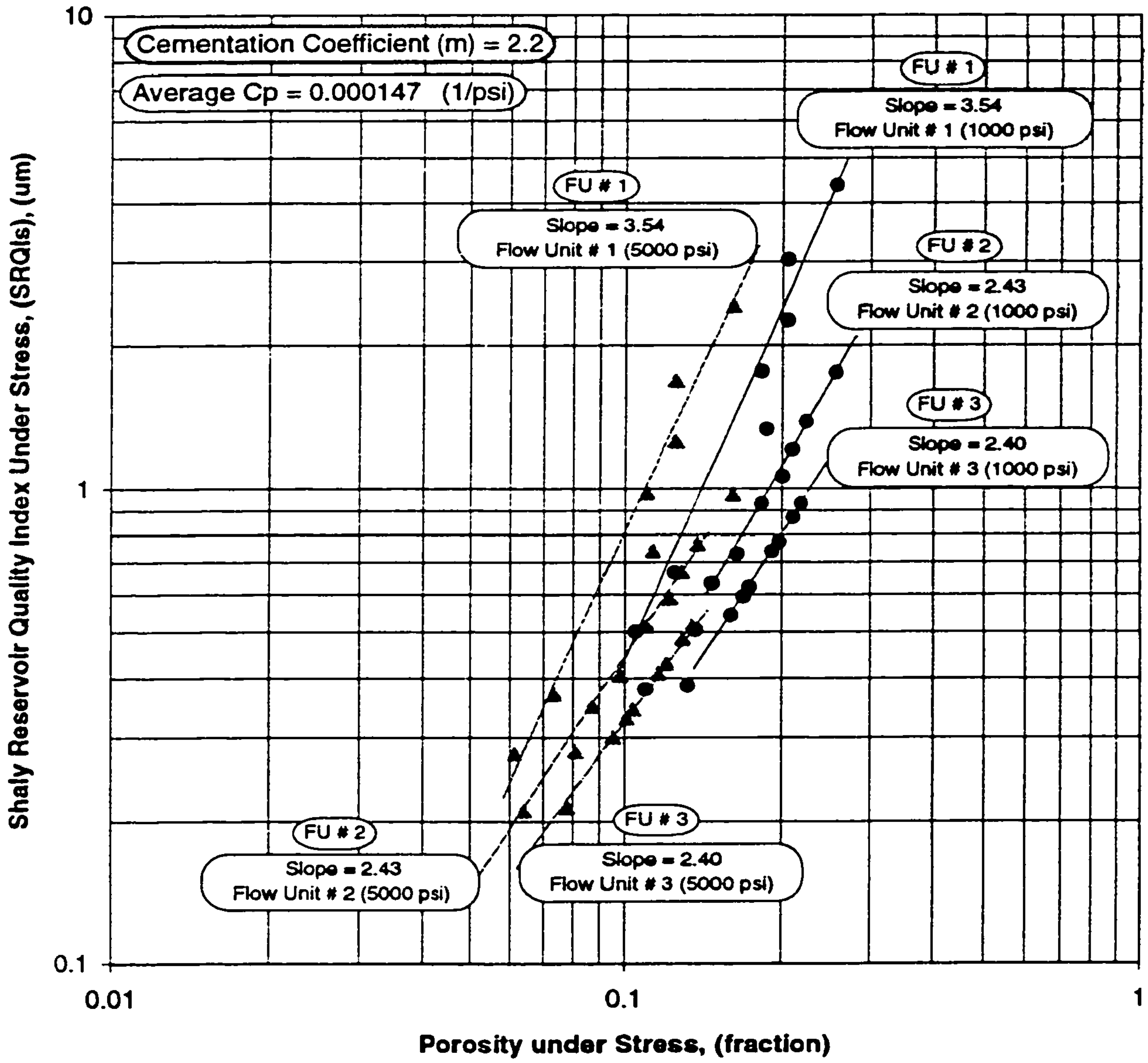

Fig. 5.12 - Effect of stress on Flow Unit Models of Shaly Formations under Stress

1. Select zone of the interest for the reservoir under investigation and divide it into intervals depending upon the change in well log readings through each interval. For our example, the zone of interest has been divided into 24 intervals.
2. Read maximum and minimum reading of Gamma Ray (GR) through the whole given log. These values are simulated as

   $GR_{max} = 130$ API

   $GR_{min} = 58$ API
3. For each interval, read Gamma Ray (GR) and use it to calculate shale volume. Interval # 1 is selected for showing the calculation (GR of interval # 1 = 92 API) as follows

   GR of interval # 1 = 92 API

$$V_{sh} = \frac{GR_{\log} - GR_{\min}}{GR_{\max} - GR_{\min}}$$

$$V_{sh}(\text{interval}\#1) = \frac{92-58}{130-58} = 0.4722$$

4. Measure the porosity at laboratory condition (zero psi). For interval # 1, the porosity is simulated to be 16.60
5. Calculate the permeability of the interval # 1(at zero psi) using Timur's equation as follows

$$K(md) = \frac{\left(93 * \varphi^{2.2}\right)^2}{S_{wirr}^2} = \frac{\left[93 * (0.166)^{2.2}\right]^2}{(0.26)^2} = 47.37 \text{ md}$$

6. Calculate shaly reservoir quality index under zero stress (SRQIo) as follows:

$$SRQI_o(\mu m) = 0.0314\sqrt{\frac{K}{\varphi_{io}(1-V_{sh})}} = 0.0314 * \sqrt{\frac{(47.37)}{0.166(1-0.4722)}} = 0.73\mu m$$

7. Calculate porosity and permeability at effectrive stress =1,000 psi (assuming that average rock compressibility (C_p) = 0.000147 1/psi) by using the following two equations respectively

$$\varphi_s = \frac{\varphi_o * e^{-\bar{C}_p \Delta\sigma}}{\left[1-\varphi_o\left(1-e^{-\bar{C}_p \Delta\sigma}\right)\right]} = \frac{(0.166)\left[(2.718)^{-(0.000147)x(1,000)}\right]}{\left[1-(0.166)\left(1-(2.718)^{-(0.000147)x(1,000)}\right)\right]} = 0.15$$

$$K_s = \frac{K_o * e^{-3\bar{C}_p \Delta\sigma}}{\left[1-\varphi_o\left(1-e^{-\bar{C}_p \Delta\sigma}\right)\right]} = \frac{(47.37)\left[(2.718)^{-(0.000147)x(1,000)}\right]}{\left[1-(0.166)\left(1-(2.718)^{-(0.000147)x(1,000)}\right)\right]} = 31.19 \text{ md}$$

8. Calculate shaly reservoir quality index under stress (at 1000 psi) using the following equation

$$\text{SRQIs(um)} = \text{SRQI (um)} * e^{-\bar{C}_p \Delta\sigma} = (0.73) *(2.718)^{-(0.000147) \times (1,000)}$$

SRQIs (1000 psi) = 0.63 μm

9. Repeat all the previously described steps for all the selected interval of the formation under investigation to calculate values of porosity and shaly reservoir quality index under stress (SRQIs) for different values of effective stress.

10. Plot SRQIs versus porosity under stress on a log-log plot such as shown in Fig. 5.11,

11. Draw straight lines passing through each group of data points. The straight lines define various flow units. Calculate the slope of each straight line and compare it to porosity exponents of shaly sand models under stress effect from Table 5. 4. For instance, two straight lines (defining flow units # 2 and 3) are recognized with a slope very close to 2.4 so that the shale obeys cation exchange capacity (CEC) model

because slope of CEC shale model equals 2.5. Also, another straight line was drawn (defining flow unit # 1) with slope close to $(1.7 + (m/2)) = 3.54$ to show that shale type of that flow unit is a dispersed shale.

12. Calculate porosity and SRQIs at another expected effective stress (depending upon the depth of pay zone, or after expected pressure drop in the reservoir). For example, for an effective stress of 5,000 psi as shown in Table 5.5, construct a log-log plot of SRQIs versus porosity under stress, Fig. 5.12. Change in effective stress from 1,000 psi to 5,000 psi leads to change in the position of the previously defined flow units in Fig. 5.11. This shows the shifting of the flow units constituting the reservoir under study after a specific period of time and/or certain expected pressure drop due to oil production.

This chapter reviews the effect of stress on porosity, permeability, and water saturation exponent. In this chapter, porosity and permeability equations under stress effect are extended to shaly formations. This chapter also includes the development of new reservoir quality index for shaly stress-sensitive formation (SRQIs). Shaly Reservoir Quality Index under stress (SRQIs) is used to study the effect of stress on SRQIo and on the petrophysical properties of flow units in shaly stress-sensitive reservoirs. In addition, this chapter includes a step by step development of five models which are used to identify flow units and define shale type in shaly formations under stress. These flow unit models can also be used to select the shale model suitable to calculate the water saturation in this type of formation. Limitations and assumptions of these newly-developed flow unit models are listed before in Table 3.5 except that $C_1 = 62500$ and $C_2 = 3$.

CHAPTER 6

NEW APPROACH FOR OBTAINING J-FUNCTION IN CLEAN AND SHALY RESERVOIRS USING IN-SITU MEASUREMENTS

6. 1. Introduction

Leverett's capillary pressure J-function has been widely used in the petroleum industry as an effective tool for correlating capillary pressure data. Capillary pressure data is very useful since it reflects the pore size distribution, the radius of the largest pore, the rock wettability, and the interfacial tension of fluids involved in the system. The possibility to normalize these data using J-function has also been proven.

Fundamental behavior of flowing mixtures in sands has resulted in the development of a theory explaining the capillary pressure behavior. However, the application of this theory to the behavior of oil wells or oil fields has proven too complicated. Leverett (1940) developed the basic theory for the behavior of mixtures of fluids in reservoir rocks. He used well established thermodynamic and physical principles in the development of his theory. Leverett (1940) divided the problems into two groups:

1. Static problems, involving only the static balance between capillary forces and those due to the difference in densities of the fluids; gravitational forces, and
2. Dynamic problems, involving analysis of the motion of the mixtures of immiscible fluids in porous media under the effect of gravity, capillary, external differential pressure forces.

Using J-function as a correlation tool is expected to be useful for correlating capillary pressure data and provides an effective tool for better description of reservoir rock and the behavior of the capillary retention of the wetting fluid.

6. 2. The Concept of J-Function

Leverett (1940) established the theory for capillary behavior in porous solids. Leverett conducted several experiments using unconsolidated clean and clayey sands for development a dimensionless group called "Leverett J-function" to correlate capillary pressure (Pc), interfacial tension (σ), in addition to permeability (K) and porosity (φ) of the porous rock. Leverett (1940) found that the results of his experiments in dimensionless form of the dimensionless group ($\frac{P_c}{\sigma} * \sqrt{\frac{K}{\varphi}}$) versus water saturation (S_w) provides a satisfactory near two curves, one for imbibition of water and the other for drainage.

Leverett's data (1940) showed that a plot of this dimensionless group versus the wetting-phase saturation (S_w) yielded a unique curve describing the capillary retention of the wetting liquid existing in the clean, unconsolidated sands, when capillary forces were at equilibrium, Fig. 6. 1.

Later, Leverett (1941) proved theoretically, using dimensionless analysis technique, that capillary pressure is proportional to the interfacial tension, to the radical $\left(\sqrt{K / \varphi}\right)$, and to the dimensionless function of the water saturation $J(S_W)$.

The term $\left(\sqrt{K / \varphi}\right)$ according to the equalization of Poiseuille and Darcy equations, can be proven to be equal to the "average pore radius" of porous rock.

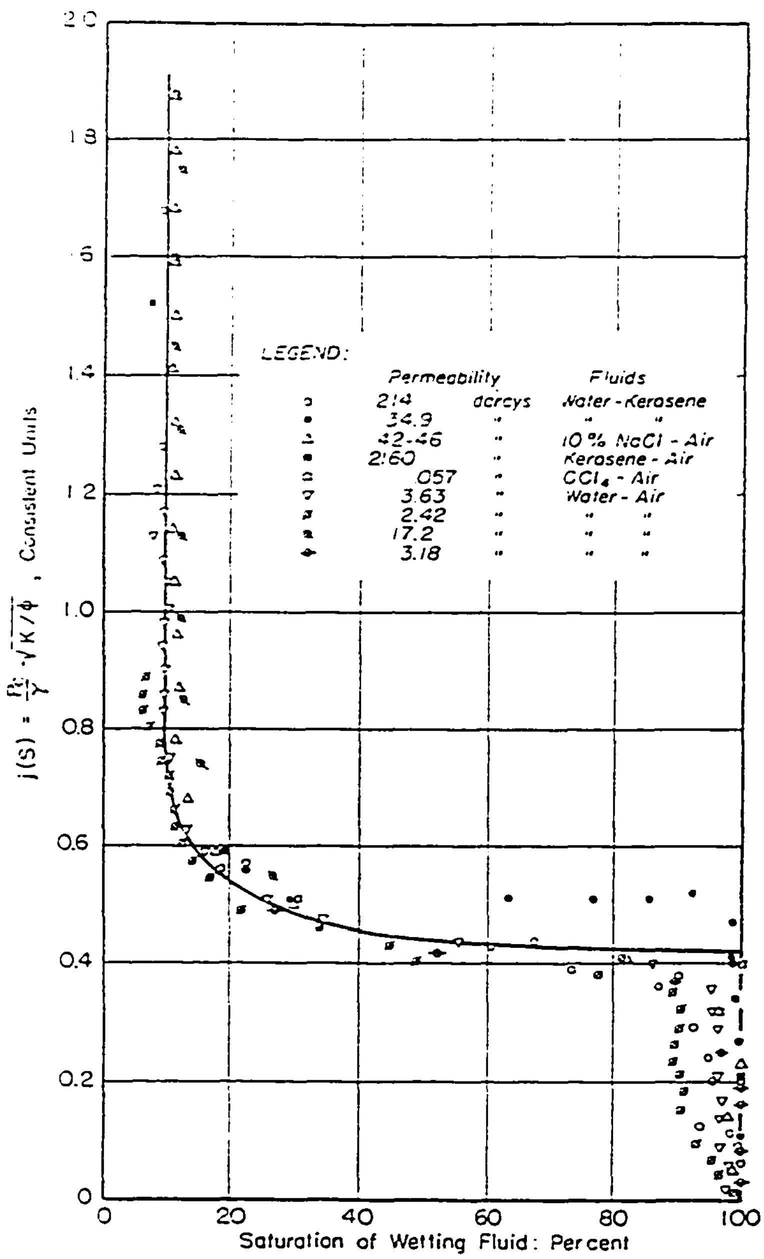

Fig. 6. 1 - J-Function versus water saturation for clean unconsolidated sands [Leverett, 1940]

The results of Leverett's studies showed that a plot of the capillary function, $J(S_w)$, versus saturation of the wetting phase (S_w) resulted in a unique curve describing the behavior of the capillary retention of the wetting phase. Normalization of the capillary pressure data to a universal curve was originally proposed using J-function as follows

$$J(S_w) = \frac{P_c}{\sigma_{ow}} * \sqrt{\frac{K}{\varphi}} \qquad (6\text{-}1)$$

where

$J(S_w)$ = function of water saturation, (dimensionless)

P_c = capillary pressure, (dyne/cm)

S_w = saturation of the wetting-phase (water), (fraction)

K = rock permeability, (cm^2)

σ_{ow} = interfacial tension between wetting (water) and non-wetting (oil) phases, (dyne/em)

φ = rock porosity, (fraction)

Rose and Bruce (1949) used improved apparatus, methods, and experimental techniques for better determination the capillary pressure-saturation of the wetting phase correlation. The results of their study showed that the basic theory concerning the Leverett J-function was extended and was given some practical applications. Rose and Bruce (1949) extended Leverett's work by introducing the contact angle into Leverett capillary pressure function to yield the well-known J-function which is given by the following equation

$$J(S_w) = \frac{P_c}{\sigma_{ow} Cos\theta_c} * \sqrt{\frac{K}{\varphi}} \qquad (6\text{-}2)$$

where

θ_c = contact angel between the interface separating the two fluids (wetting and non-wetting) and the rock surface, (degree)

A plot of $J(S_w)$ calculated using equation (6-2) versus wetting-phase (water) saturation showed a constant curve for clean unconsolidated sands, Fig. 6.1. However, it has been observed that the existence of significant differences in correlating the J-function and water saturation form formation to another, Fig. 6.2. This implies that the J-function is not universal but it could be used as a correlative tool. Also, this shows that the J-function may vary from one hydraulic (flow) unit to another within the same producing formation of the reservoir. Therefore, this study suggests that the J-function be used as a tool for reservoir characterization and flow unit identification in clean and shaly reservoirs.

The usefulness of the J-function for obtaining pore-size distribution has been proven by Brown (1951) who used core samples from the Edwards limestone in Jourdanton field, Texas, USA. Fig. 6.3 shows the behavior of the J-function in the Jourdanton Field, illustrated by Brown (1951). Fig. 6.3-a shows all of the data points accumulated to define one flow unit. Fig. 6.3-b through Fig. 6.3-e explain that the scattering degree of the data points suggests the presence of several zones having different textures, different rock types (dolomite and limestones), and different grain sizes. Each flow zone (unit) can be described by a group of data points defining a single J-function curve.

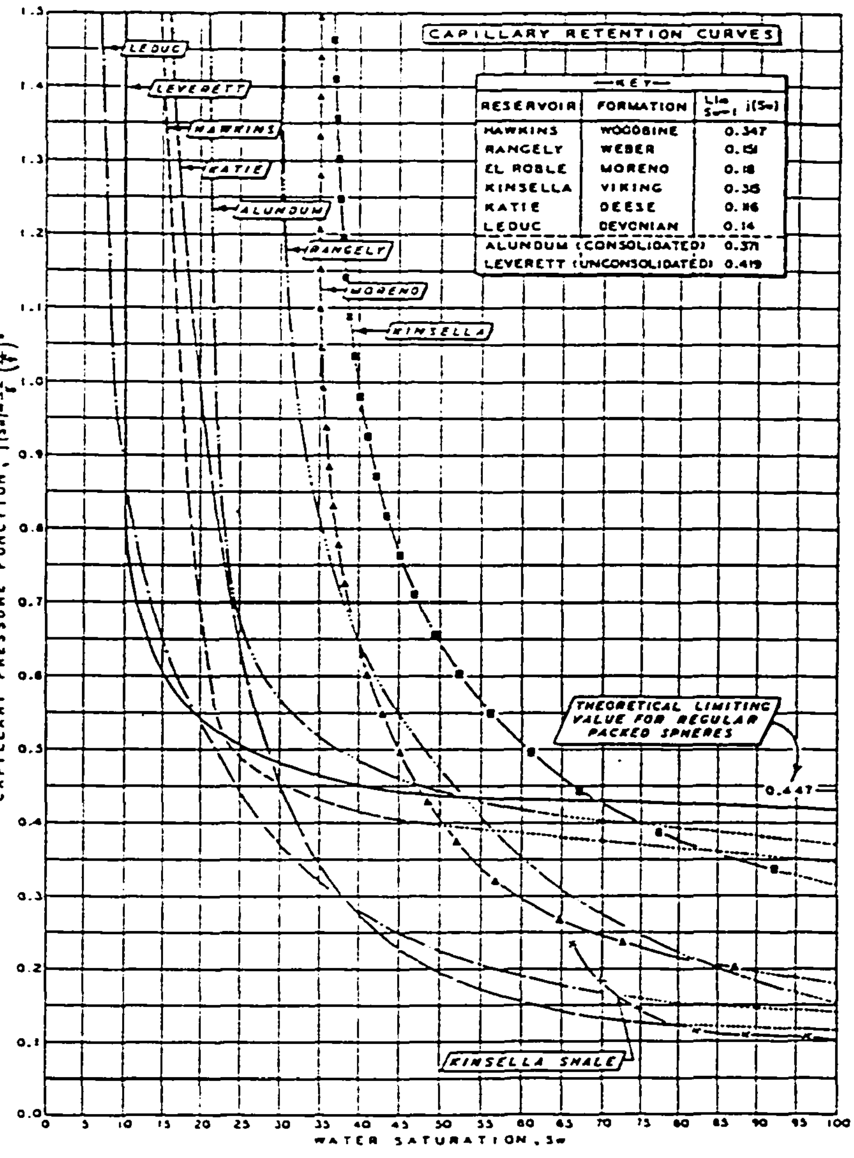

Fig. 6. 2 - Capillary retention curves, [Rose and Bruce, 1940]

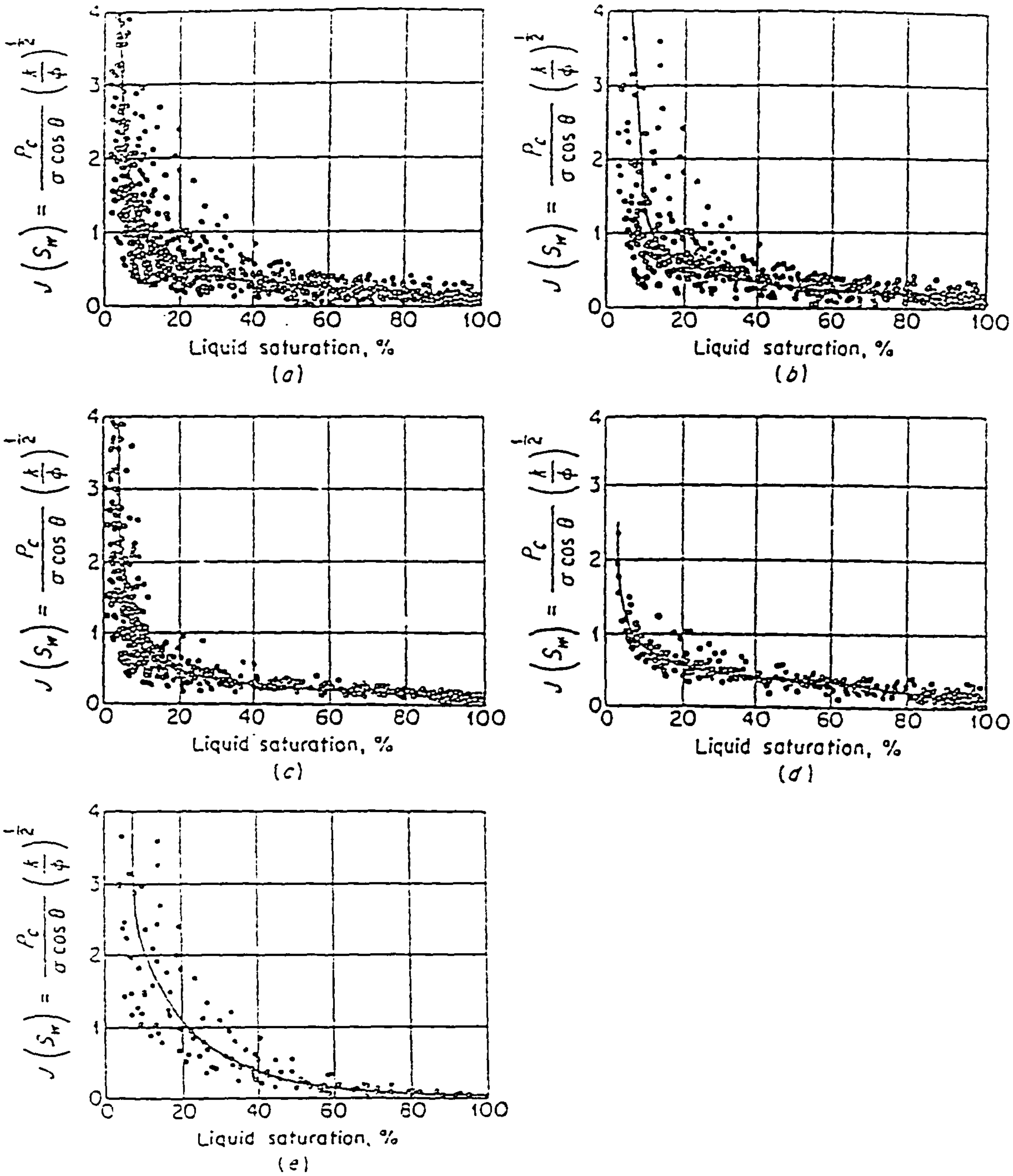

Fig. 6. 3 - J-Function correlation on capillary-pressure data in Edwards formation, Jourdanton Field, [Brown, 1951]

Rose and Bruce (1949), also, developed a monograph for correlating this J-function to the capillary pressure data since these data reflected the pore-size distribution, the radius of the largest pore, the rock wettability, and the interfacial tension of the fluid pair involved in the system.

One of the major goals of this study is to investigate the effect of stress on the calculated values of the J-function and to eliminate the need for several laboratory measurements involved in the J-function such as capillary pressure, porosity and permeability. Another goal of the study is to show how log-derived values of resistivity gradient may be used to estimate the J-function in both clean and shaly reservoirs.

6. 3. The Effect of Stress on J-Function

Literature review shows that wherever the J-function is used, laboratory measurements (at zero stress conditions) such as porosity, permeability, and capillary pressure are used for interpreting the J-function. This study suggests the development of a new correlation capable of transforming the laboratory measurements into field conditions under the effect of stress and vice versa. Achieving this goal requires corrected values of porosity, permeability, and other parameters involved in the J-function and are assumed to be independent of stress.

The behavior of the J-function is primarily governed by porosity, permeability, and capillary pressure and secondary by interfacial tension and contact angel. Therefore, porosity and permeability under the stress effect can be expressed by equations (4-23) and (4-37).

Relative permeability and capillary pressure curves both depend on pore size distribution. Fatt (1953), Wilson (1956) and Cherici (1967) showed that capillary pressure curves are slightly modified by the applied stresses. Fatt (1953) conducted several experiments in oil-gas system in the imbibition direction at atmospheric pore fluid pressure and effective stresses equal to 3000 psi. The results showed that within that range of stress values, relative permeability of the gas became constant. Wilson (1956) measured relative permeabilities of oil and water in the imbibition direction on a sandstone samples with pore fluid pressure up to 5,000 psi and effective stresses in x, y, and z directions of up to 10,000 psi. The results indicated that relative permeability curves are only slightly modified by applied stress and the effective stress was found to be the only variable causing the small changes of the relative permeability curves. Cherici (1967), also conducted a set of experiments to study the effect of stress on capillary pressure curves. He concluded that capillary pressure curve is considerably affected by the stress tensor only at low capillary pressure values, while the irreducible water saturation is only slightly affected by the overburden pressure.

Based on the previously mentioned review, it is clear enough that porosity and permeability are the most important parameters affected by the stress effect and influencing the values of the J-function. Furthermore, capillary pressure measurements will be eliminated by using the newly-developed J-functions in clean and shaly formations. In addition, interfacial tension and contact angle of the fluid pair involved in the system are suggested to be measured at reservoir conditions of pressure and temperature. Dividing equation (4-37) by equation (4-23) results in

$$\frac{K_o}{\varphi_o} = \frac{K_s}{\varphi_s} * e^{2 * \bar{C}_p * \Delta\sigma} \qquad (6\text{-}3)$$

Taking the square root of equation (6-3) and inserting the resultant equation into the J function, equation (6-2), one obtains

$$J_s(S_w) = \frac{P_c}{\sigma_{ow} Cos\theta_c} * \sqrt{\frac{K_o}{\varphi_o}} * e^{\bar{C}_p * \Delta\sigma} \qquad (6\text{-}4)$$

where

$J_s(S_w)$ = J-function under stress effect, (dimensionless)

K_s = permeability under stress, (md)

φ_s = porosity under stress, (fraction)

$\bar{C}_P$ = average rock compressibility, (1/psi)

$\Delta\sigma$ = change in effective stress, (psi)

Equation (6-4) shows clearly that assuming constant J-function for a reservoir rock is not a valid assumption, and may lead to erroneous results in reservoir characterization and flow unit identification. Using equation (6-4) with actual data from Rose and Bruce (1949), the effect of stress on the J-function was demonstrated. Fig. 6. 4, using data in Table 6. 1, show data for Hawkins Reservoirs (Woodbine Formation). This set of data has been subjected to different changes in effective stress (zero, 1,000, 3000, and 5,000 psi) using equation (6-4) for J-function under stress effect. The results show that increasing

Table 6.1 - Data for studying the effect of stress on J-function, [Rose and Bruce, 1949]

Average (Cp) = 0.000144 1/psi

S_W (%)	$Js(S_W)$ 0 psi	Js(Sw) 1,000 ps	$Js(S_W)$ 3,000 psi	$Js(S_W)$ 5,000 psi
15	1.4	1.21	0.9089	0.6815
20	0.7	0.61	0.4545	0.3408
25	0.49	0.42	0.3181	0.2385
30	0.45	0.39	0.2922	0.2191
35	0.43	0.37	0.2792	0.2093
40	0.415	0.36	0.2694	0.202
45	0.4	0.35	0.2597	0.1947
50	0.39	0.34	0.2532	0.1898
55	0.38	0.33	0.2467	0.185
60	0.374	0.32	0.2428	0.1821
70	0.372	0.32	0.2415	0.1811
80	0.365	0.32	0.237	0.1777
90	0.36	0.31	0.2337	0.1752
100	0.354	0.31	0.2298	0.1723

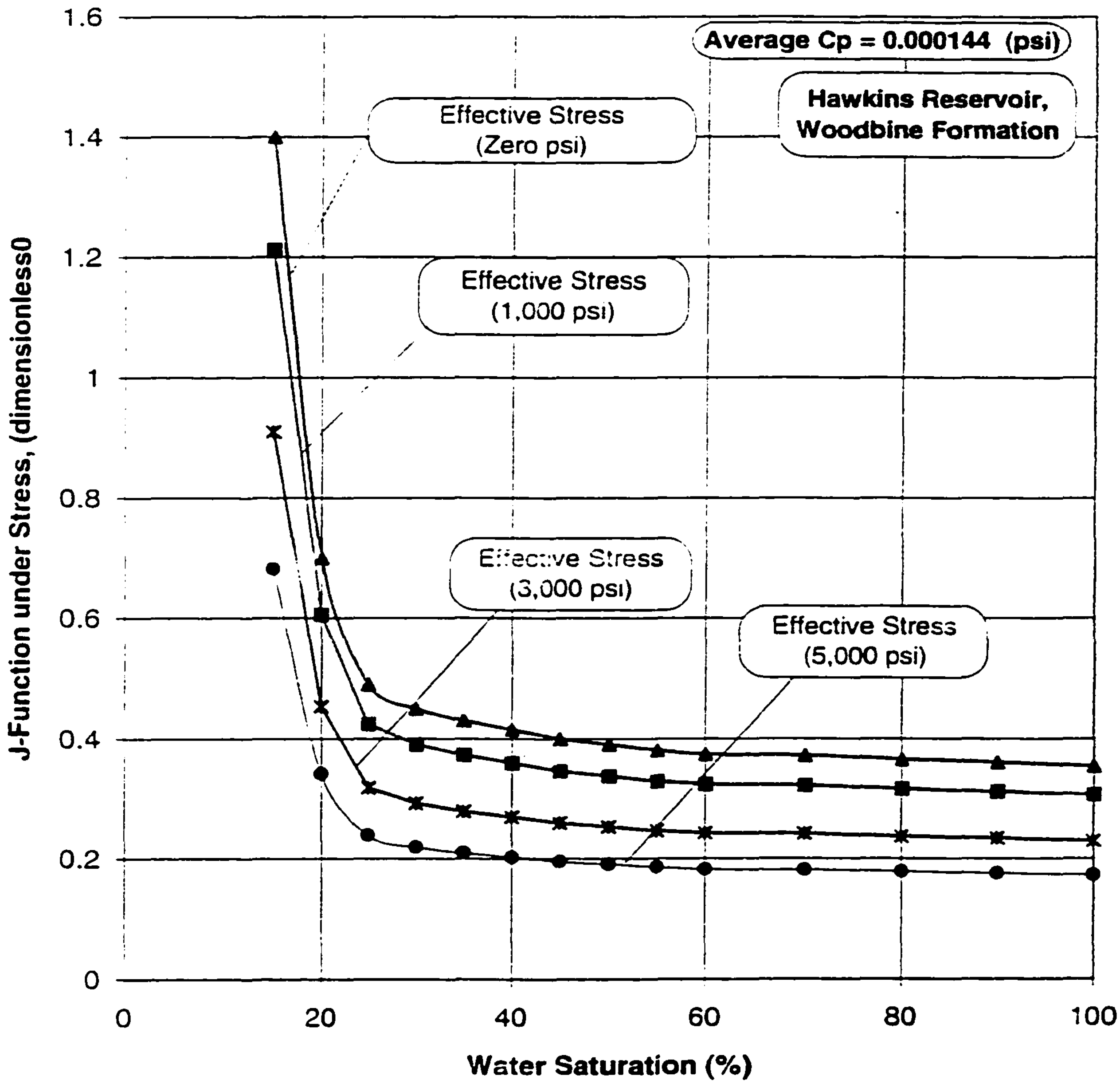

Fig. 6.4-Effect of stress on the J-function of Hawkin's reservoir rock [Actual data from Rose and Bruce, 1949]

change in effective stress leads to a decrease in the value of J-function. In addition, the higher the change in effective stress, the smaller the reduction in J-function under stress. These conclusions are important for development of oil reservoirs especially in cases such as selective plugging, water flooding, and enhanced oil recovery processes wherever reservoir description is important.

6.4. New Approach for Obtaining J-Function In Clean And Shaly Reservoirs Using In-Situ Measurements

Two models have been developed in this section to calculate the J-function using well-logging data which represents a good source for in-situ measurements. The first model is obtained using Tixier's equation (1949) for permeability and Archie's equation for water saturation. This new J-function is validated using actual field data for clean reservoirs. The second model is derived using Tixier's equation for permeability (1949) in combination with Schlumberger shale model (1987) for water saturation calculation. Validation of this new J-function for shaly formations is shown by application of this new J-function to field data.

The major advantages of these newly-developed J-functions for clean and shaly reservoirs are

1. Laboratory measurements of capillary pressure, porosity and permeability have been eliminated,
2. In-situ measurements of resistivity log (more representative to the reservoir rock) have been used, and

3. They are economically feasible and more effective.

Using well-logging data has two major advantages:

1. It is more representative of the reservoir rock types and conditions, and
2. It is economically feasible since it is already available for almost all of the drilled wells.

6. 4. 1. J-Function In Clean Reservoirs

Capillary pressure J-function has been defined by equation (6-2) as follows

$$J(S_w) = \frac{P_c}{\sigma_{ow} Cos\theta_c} * \sqrt{\frac{K}{\varphi}} \qquad (6\text{-}2)$$

Capillary pressure is a function of the elevation above the oil-water contact (free-water level) and the density difference of the wetting (water) and non-wetting (oil) phases. Capillary pressure can be expressed as:

$$P_c = \frac{h(\rho_w - \rho_o)}{2.3} \qquad (6\text{-}5)$$

where

P_c = capillary pressure, (psi)

h = free-water level, (ft), and

ρ_w, ρ_o = densities of water and oil, (gm/cc)

Substituting equation (6-5) into the J-function, equation (6-2), results in the following equation

$$J(S_w) = \frac{h(\rho_w - \rho_o)}{2.3 * \sigma_{ow} Cos\theta_c} * \sqrt{\frac{K}{\varphi}} \qquad (6\text{-}6)$$

Tixier (1949) developed an empirical equation showing that the reservoir quality index $\left(\sqrt{K/\varphi}\right)$ is inversely proportional to the capillary pressure. He also developed an equation to estimate rock permeability from the true formation resistivity gradient, $(\Delta R_t / \Delta h)$. Wyllie and Rose (1950) showed that the relationship used by Tixier would follow Leverett's correlation if the porosity, the interfacial tension, and the contact angle were identical or have a mutually compensation in their effects in the formation under consideration.

Tixier's permeability equation is given as follows

$$K(md) = 105.8 * \left[\frac{1}{R_o(\rho_w - \rho_o)}\left(\frac{\Delta R_t}{\Delta h}\right)\right]^{2.0} \qquad (6\text{-}7)$$

where

K	=	rock permeability, (md)
R_o	=	resistivity of 100 % formation water saturated rock, (ohm-m)
$(\Delta R_t / \Delta h)$	=	true-resistivity gradient, (ohm-m/ft)
ρ_w, ρ_o	=	densities of water and oil, (gm/cc)

Substituting equation (6-7) into equation (6-6) results in

$$J(S_w) = \frac{4.47 * h}{\sigma_{ow} Cos\theta_c R_o \sqrt{\varphi}}\left(\frac{\Delta R_t}{\Delta h}\right) \qquad (6\text{-}8)$$

Equation (6-8)) is a new model for the J-function using in-situ measurements. If porosity logs are not available, equation (6-8) can be modified to replace porosity with resistivity log readings. Archie's equation for calculating water saturation in clean formation is given by the following equation:

$$S_w^n = \frac{aR_w}{\varphi^m R_t} \qquad (6\text{-}9)$$

Morris and Biggs (1967) introduced a correlation between porosity and irreducible water saturation as follows:

$$\varphi * S_{wirr} = Constant = C_{MB} \qquad (6\text{-}10)$$

where

C_{MB} = Morris-Biggs constant (a constant for a particular rock type and/or grain size).

Aguilera (1985) showed that equation (6-10) can be used for water saturation also and not only at irreducible water saturation condition. Therefore equation (6-10) can be rewritten as follow:

$$\varphi * S_w = Constant = C_{MB} \qquad (6\text{-}11)$$

Solving equation (6-11) for water saturation (S_w) and raising the resultant equation to the power (n) yields

$$S_w^n = \left(\frac{C_{MB}}{\varphi}\right)^n \qquad (6\text{-}12)$$

Equating equations (6-9) and (6-12) and then solving for the porosity, one obtains

$$\varphi = \left(\frac{aR_w}{C_{MB}^n R_t}\right)^{(n-m)} \qquad (6\text{-}13)$$

Taking square root of equation (6-13) and inserting the resultant equation into equation (6-8) yields the following new equation for the J-function in clean reservoir as follows:

$$J(S_w) = \frac{4.47 * h * C_{MB}^{n(n-m)/2}}{\sigma_{ow} Cos\theta_c R_o (aR_w)^{(n-m)/2}} \left(\frac{\Delta R_t}{\Delta h}\right) * R_t^{(n-m)/2} \qquad (6\text{-}14)$$

Equation (6-14) represents a new model for obtaining the J-function using in-situ measurements. Only the interfacial tension and the contact angle will be measured using laboratory measurements at reservoir conditions. All of the other parameters involved in this new J-function, equation (6-14), can be easily obtained from well logging-derived data such as the coefficient a, R_t, R_o, R_w, the formation thickness (h), resistivity gradient $(\Delta R_t / \Delta h)$, Morris-Biggs constant ($C_{MB} = (\varphi * S_{wirr})$, water saturation ($S_w$) and porosity exponents (n).

A detailed calculation showing the application of this new model is explained in the next section of this chapter. Table 6. 2 shows the actual field data that will be used for this application. The resultant J-function is graphically presented in Fig. 6. 6.

In such a case where porosity exponent (m) is equal to water saturation (n), then equation (6-14) can be simplified to the following form

$$J(S_w) = \frac{4.47 * h * C_{MB}}{\sigma_{ow} Cos\theta_c R_o (aR_w)} \left(\frac{\Delta R_t}{\Delta h} \right) * R_t \qquad (6\text{-}15)$$

At this point, it is clear that this new expression of the J-function for clean formations, equation (6-14), is a function of free-water level (h), formation resistivity (R_t), and water saturation (S_w) which is implicitly included in Morris-Biggs constant (C_{MB}). Porosity exponent has a minor effect on the estimated values of $J(S_w)$.

6. 4. 2. J-Function In Shaly Reservoirs

Schlumberger (1987) introduced a shale model to calculate water saturation in shaly formations. This shale model was based upon laboratory investigations and field experience. It was found that the model works well for many shaly formations independent of the shale distribution and also covers a practical range of water saturation values. This model is given by:

$$\frac{1}{R_t} = \frac{\varphi^2 S_w^2}{aR_w(1-V_{sh})} + \frac{V_{sh}S_w}{R_{sh}} \qquad (6\text{-}16)$$

where

a = Archie's equation coefficient

R_{sh} = shale resistivity, (ohm-m)

Rw = formation water resistivity, (ohm-m)

R_t = true formation resistivity, (ohm-m)

V_{sh} = shale volume, (fraction)

S_w = water saturation in shaly formation, (ohm-m)

φ = formation porosity, (fraction)

Rearranging equation (6-16) yields

$$S_w^2 + \frac{aR_w(1-V_{sh})}{\varphi^2}S_w - \frac{aR_wR_{sh}(1-V_{sh})}{\varphi^2 V_{sh}R_t} = 0 \qquad (6\text{-}17)$$

Equation (6-17) is a quadratic equation which can be solved easily and its positive root will be given by

$$S_w = \frac{1}{2}\left\{\frac{-aR_w(1-V_{sh})}{\varphi^2} + \sqrt{\left(\frac{aR_w(1-V_{sh})}{\varphi^2}\right)^2 + 4\left(\frac{aR_wR_{sh}(1-V_{sh})}{\varphi^2 V_{sh}R_t}\right)}\right\} \qquad (6\text{-}18)$$

Equation (6-18) can be formulated in the following simple form

$$S_w = \frac{G_{sh}}{2} \qquad (6\text{-}19)$$

where

G_{sh} = a collective shale group given by the following equation

$$G_{sh} = \left\{\sqrt{A_{sh}^2 + 4B_{sh}} - A_{sh}\right\} \qquad (6\text{-}20\text{-}A)$$

where

A_{sh} and B_{sh} are shale sub-groups given as follows

$$A_{sh} = \frac{aR_w(1-V_{sh})}{\varphi^2} \qquad (6\text{-}20\text{-}B)$$

$$B_{sh} = \frac{aR_w R_{sh}(1-V_{sh})}{\varphi^2 V_{sh} R_t} \qquad (6\text{-}20\text{-}C)$$

Solving Morris-Biggs equation (1967), equation (6-11), for water saturation (S_w) yields

$$S_w = \frac{C_{MB}}{\varphi} \qquad (6\text{-}21)$$

Equating equations (6-19) and (6I-21), and taking the square root of the resultant equation, one obtains

$$\sqrt{\varphi} = \sqrt{\frac{2C_{MB}}{G_{sh}}} \qquad (6\text{-}22)$$

Substituting capillary pressure equation, equation (6-5), and Tixier's permeability equation, (6-7), into J-function equation, equation (6-2), results in the following equation

$$J(S_w) = \frac{4.47 * h}{\sigma_{ow} Cos\theta_c R_o \sqrt{\varphi}}\left(\frac{\Delta R_t}{\Delta h}\right) \qquad (6\text{-}23)$$

Then, substituting equation (6-22) into equation (6-23) introduces the formation shaliness into $J(S_w)$ and yields a new model for obtaining J-function in shaly formations as follows:

$$J_{sh}(S_w) = \frac{3.161 * h}{\sigma_{ow} Cos\theta_c R_o} \left(\frac{\Delta R_t}{\Delta h} \right) \sqrt{\frac{G_{sh}}{C_{MB}}} \quad (6\text{-}24)$$

where

$J_{sh}(S_w)$ = J-function in shaly formation, (dimensionless)

S_w = water saturation in shaly formation (using total shale model), (fraction)

Equation (6-24) is a new model for obtaining J-function in shaly formation using in-situ measurements (well-logging data). One of the advantages of this new J-function is its independence on porosity, permeability, and capillary pressure laboratory measurements. Also, it is applicable under different conditions of stress, especially for stress-sensitive formations. In addition, this newly-developed J-function considers the heterogeneity of shale formation.

6. 5. Field Applications

Actual well logs data for Layton formation in Oklahoma, (USA), Fig. 6. 5, and shaly Miocene sand in South Louisiana, Fig. 6. 8, are used to validate the newly-developed J-function models. Layton formation for clean formation and shaly Miocene sand for shaly reservoir.

6. 5. 1. J-Function In Clean Reservoir

The newly-developed J-function, equation (6-14), has been validated using actual field data of Layton formation in Oklahoma, (USA). Fig. 6. 5 shows SP and electrical logs of Layton formation. This log is used for determining true formation resistivity (R_t), free-water level (h), resistivity of 100 % saturated with brine (R_o), and resisitivity gradient $(\Delta R_t / \Delta h)$, Table 6. 2.

Water saturation is estimated using Archie's equation $S_w = \sqrt{R_o / R_t}$ for clean formations and J-function is calculated using equation (6-14), Table 6.2. The resultant values of J-function, J(S_w), is presented versus water saturation in Fig. 6.6. A log-log plot of the newly-developd J-function, J(S_w), versus water saturation (S_w) is shown in Fig. 6.7.

The use of curve fitting technique shows that an exponential equation correlating J(Sw) and water saturation (S_w) can be obtained, and is given by

$$J(S_w) = 17.969 * e^{-0.0496 * S_w} \qquad (6\text{-}25)$$

This equation, (6-24), can be used for obtaining the J-function for that specific formation (Layton, Oklahoma) without need for laboratory measurements of several parameters included in the J-function.

6. 5. 2. J-Function In Shaly Reservoir

Application of the newly-developed J-function in shaly formation is slightly different from that for clean sands. Shaly reservoirs are heterogeneous because of gross changes in sand grain size, variation of shale content, and severe variation of pore-throat/pore-body distribution. For these reasons, calculated values of the J-function is expected to have more scattering degree and to be less coherent than in clean reservoirs.

For the sake of validation of the J-function in shaly reservoirs, Induction-Electrical Survey of Shaly Miocene Sand in South Louisiana (USA) is used, Fig. 6. 8. Actual well-

Table 6. 2 - Data used for validating the newly-developed J-function in clean reservoirs using electric log of Layton, OK, (USA) [actual data from Tixier, 1949]

Cos (θ) [Contact Angel = 72°] (assumed)	= 0.31
Equation Coefficient (a) (assumed)	= 0.62
Porosity Exponent (m) (assumed)	= 2.15
Water Saturation exponent (n) (assumed)	= 2.0
Oil-Water Interfacial Tension (σ_{ow}) (assumed)	= 30 mN/m
Formation Water Resistivity (R_w) (assumed)	= 0.054 ohm-m
Morris-Biggs Constant (C_{MB}) = 0.30* 0.3742	= 0.1123
True Formation Resistivity (R_t)[at h = 2.785 ft]	= 28 ohm-m
True Formation Resistivity (R_t)[at h = 2,833 ft]	= 3.0 ohm-m
Rock Resistivity (100 % Saturated by Formation Water) (R_o)	= 3.5 ohm-m
True Formation Resistivity Gradient $\left(\Delta R_t / \Delta h\right)$ = [(28-3.0)/48]	= 0.52 ohm-m/ft

Depth (ft)	(R_t) ohm-m	(h) (ft)	Sw (%)	J (Sw)
2,795	27.5	50	33	3.5827
2,790	25	45	34.6	3.2476
2,785	23	40	36.1	2.9048
2,800	20	35	38.7	2.5685
2,805	17	30	42	2.2286
2,810	15	25	44.7	1.8747
2,815	12	20	50	1.525
2,820	10	15	54.8	1.1595
2,825	7	10	65.5	0.794
2,830	5	5	77.5	0.4071
2,833	3.5	2	92.6	0.1673
2,835	3	0	100	0

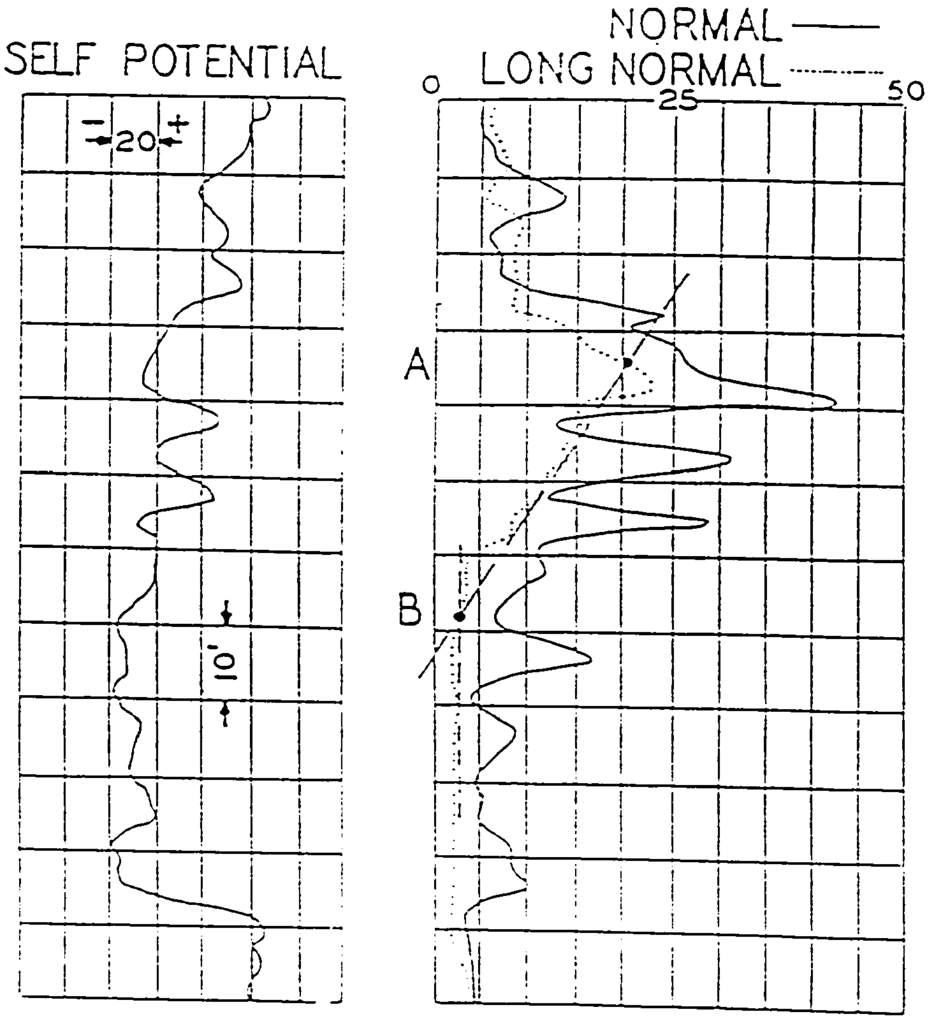

Fig. 6. 5 - Electric-Logs at Layton (Oklahoma, USA), [Tixier, 1949]

logging data are used to obtain the required parameters included in the newly-developed J-function.

A high resistivity zone. zone A (depth from 12.576 ft to 12.602 ft) is selected to obtain formation resistivity (R_t), free-water level (h), shale content (Vsh), Table 6.3. Resistivity gradient $(\Delta R_t / \Delta h)$ is calculated to be [(10-1.2)/(12.602-12.576)] = 0.338 ohm-m/ft]. Corresponding values of porosity is used from Table 2 of Morris-Biggs study (1967). Then. shale groups A_{sh}, B_{sh}. and G_{sh} are calculated using equations (6-20-B). (6-20-C). and (6-20-A) respectively.

Water saturation is calculated using total shale model. Schlumberger (1987). and the newly-developed J-function then estimated using equation (6-24). Values of oil-water contact angle (θ_{ow}). coefficient (a). oil-water interfacial tension (σ_{ow}), and formation water resistivity (R_w) are assumed as shown in Table 6. 3.

A plot of the resultant J-function versus water salutation. both for shaly formation. is presented in Fig. 6.9. A log-log plot of the newly-developd J-function for shaly formations. $J_{sh}(S_w)$. versus water saturation (S_w) is shown in Fig. 6.10

The use of curve fitting technique yields an equation for obtaining the J-function. This equation is given as:

$$J_{sh}(S_w) = -0.0001(S_w)^2 - 0.0049 * (S_w) + 1.8258 \qquad (6\text{-}26)$$

where

$J_{sh}(S_w)$ = J-function in shaly formation, (dimensionless)

S_w = water saturation in shaly formation (using total shale model), (fraction)

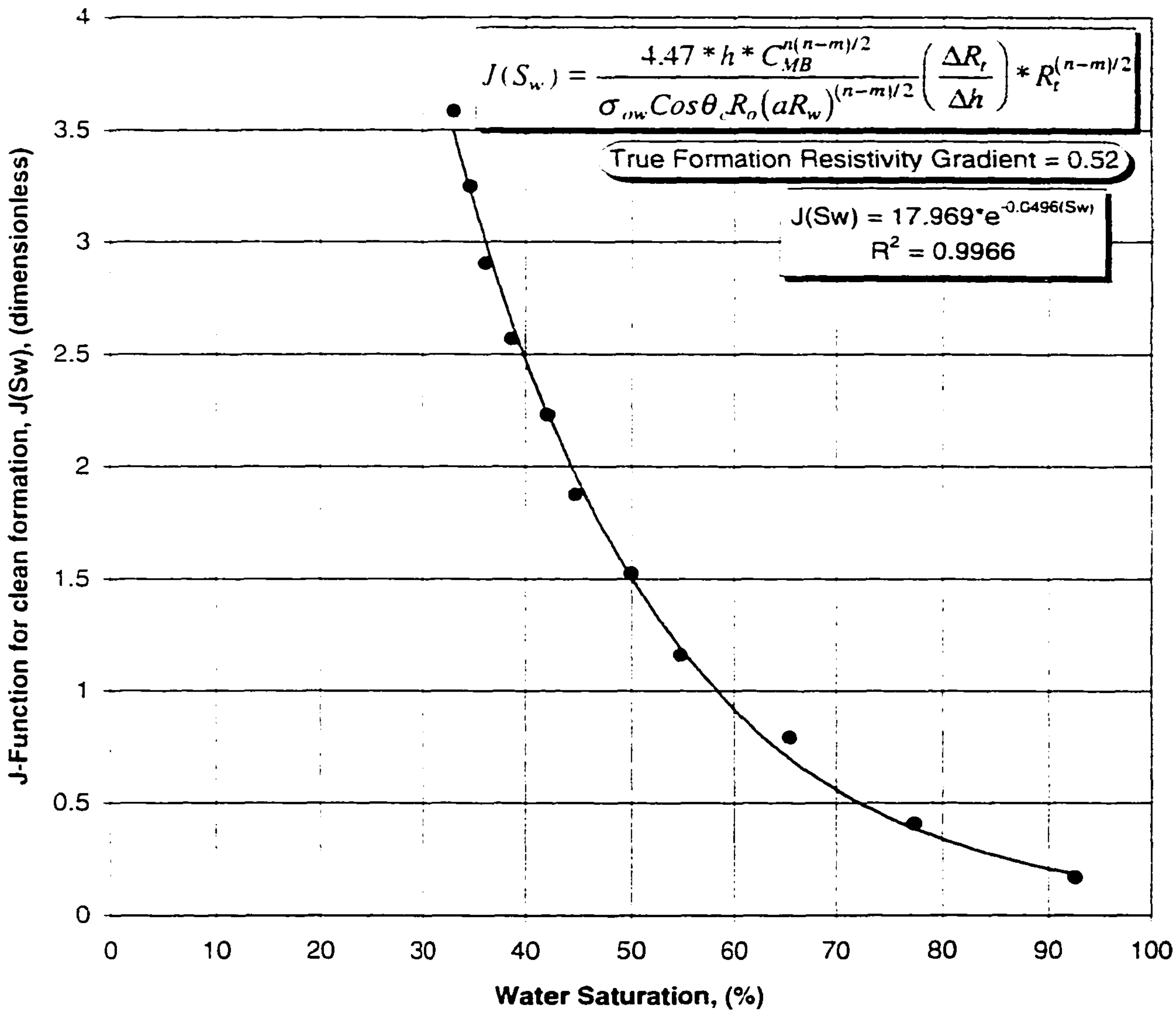

Fig. 6. 6 - J-function curve using newly-developed model [Actual data from Layton formation, Oklahoma, USA, Tixier, 1949]

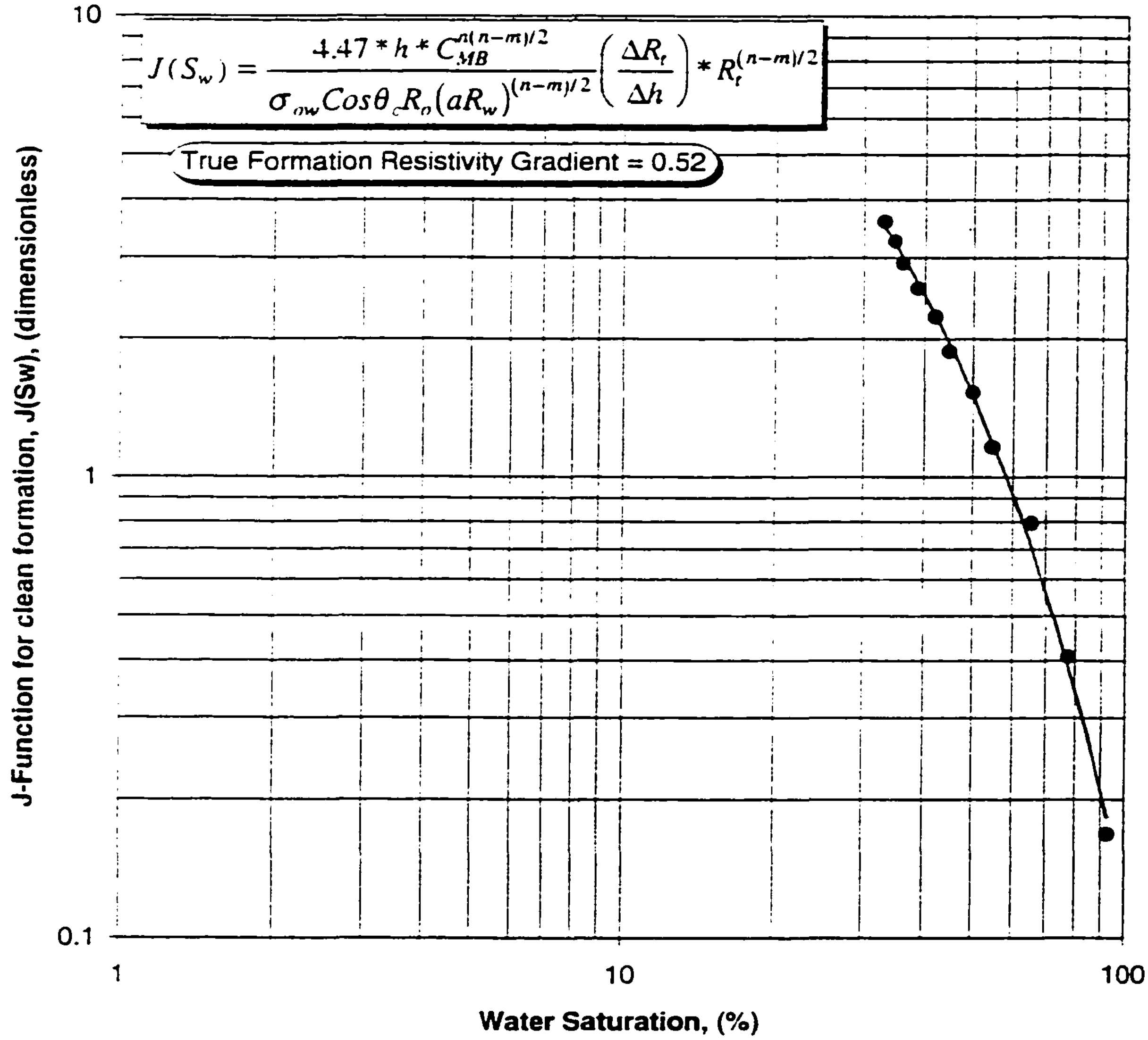

Fig. 6.7-A log-log plot of the newly-developed J-function versus water saturation [Actual data from Layton formation, Oklahoma, USA, Tixier, 1949]

Table 6. 3 - Data used for validating the newly-developed J-function in shaly reservoirs using Induction-Electrical survey of a shaly sand, Louisiana, (USA), [Morris-Biggs, 1967]

Cos (contact angel = 72) = 0.31
Equation Coefficient (a) (assumed) = 0.81
Water Saturation Exponent (n) (assumed) = 2.0
Oil-Water Interfacial Tension (assumed) = 30 mN/ft
Formation Water Resistivity (Rw) = 0.054 ohm-m
True Formation Resistivity (Rt) [at depth = 2,785 ft] = 28 ohm-m
True Formation Resistivity (Rt) [at depth = 2,833 ft] = 3.0 ohm-m
True Formation Resistivity Gradient = [(10-1.2)/26] = 0.338 ohm-m/ft
Rock Resistivity (100 % saturated with formation Water) (Ro) = 1.5 ohm-m

Depth (ft)	(R_t) (ohm-m)	Porosity Density (%)	Neutron (%)	Average Porosity (%)	Shale Content (%)	Ash	Bsh	Gsh	Sw (%)	h (ft)	Jsh(Sw)
12,576	10	18.1	25.1	21.6	27.3	0.68	0.3	0.61	30.4	26	1.5861
12,578	6.5	21.2	21.5	21.35	29.4	0.68	0.43	0.79	39.62	24	1.6715
12,580	6.8	21.2	21.5	21.35	35.3	0.62	0.31	0.65	32.73	22	1.3927
12,582	6	18.1	17.9	18	35.3	0.87	0.49	0.78	39.13	20	1.3842
12,586	2.2	23	28	25.5	47.6	0.35	0.4	0.97	48.33	16	1.2307
12,588	3.4	18.1	17.9	18	41.2	0.79	0.68	1.04	51.83	14	1.1151
12,590	3	13.9	17.9	15.9	41.2	1.02	0.99	1.22	60.78	12	1.0351
12,594	1.8	20	28.7	24.35	35.3	0.48	0.9	1.48	74.03	8	0.7616
12,596	1.6	20	28.7	24.35	35.3	0.48	1.01	1.59	79.63	6	0.5924
12,598	1.5	19.5	26.3	22.9	35.3	0.54	1.22	1.74	86.85	4	0.4124
12,600	1.4	18.3	25.3	21.8	35.3	0.6	1.45	1.88	94.1	2	0.2147
12,602	1.5	17.5	23.2	20.35	35.3	0.68	1.55	1.9	94.88	1	0.1078

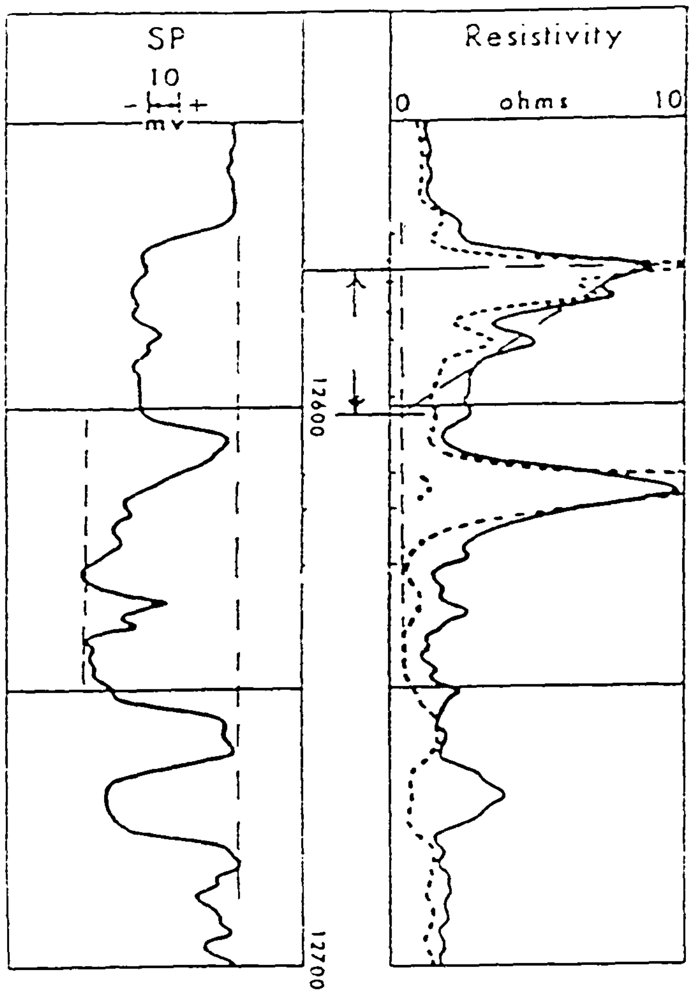

Fig. 6. 8 - Induction-Electrical Survey of shaly Miocene, Louisiana, [Morris-Biggs, 1967].

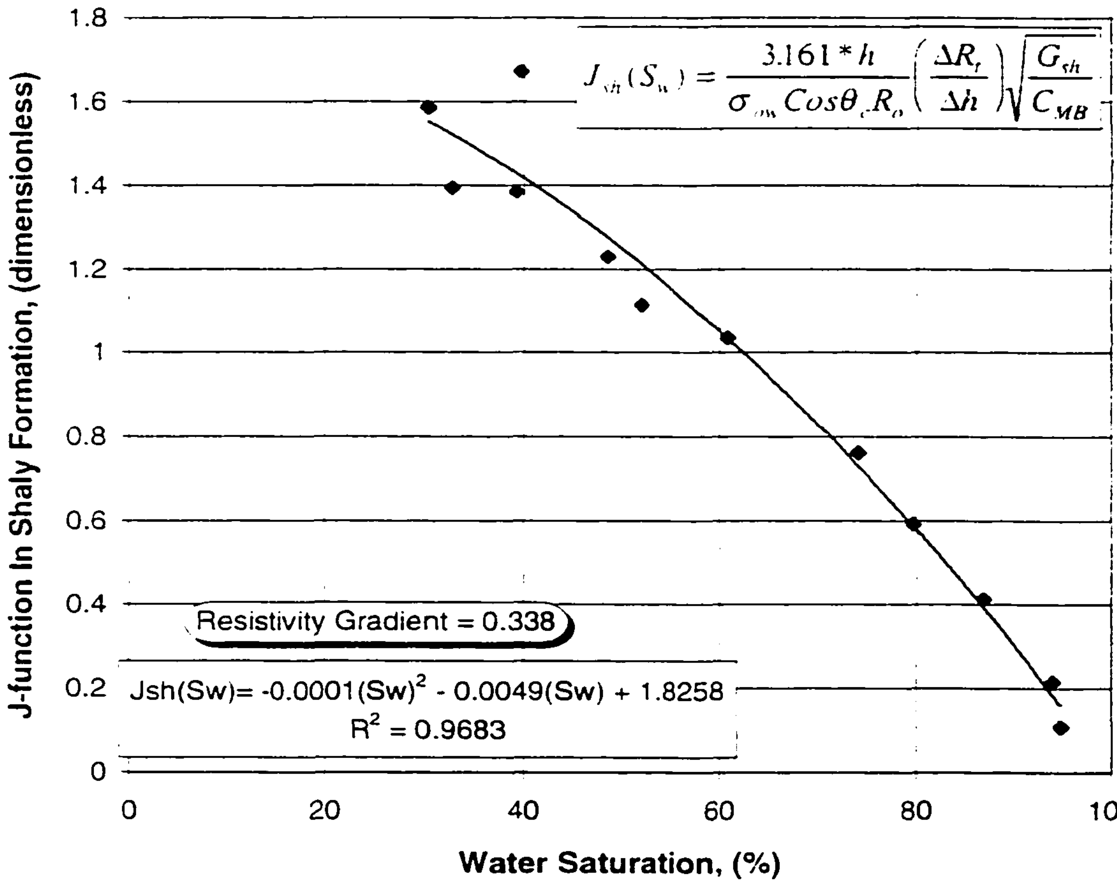

Fig. 6. 9 - J-function curve using newly-developed model for shaly formation, [Shaly Miocene Sand, Louisiana, USA], [Morris-Biggs, 1967]

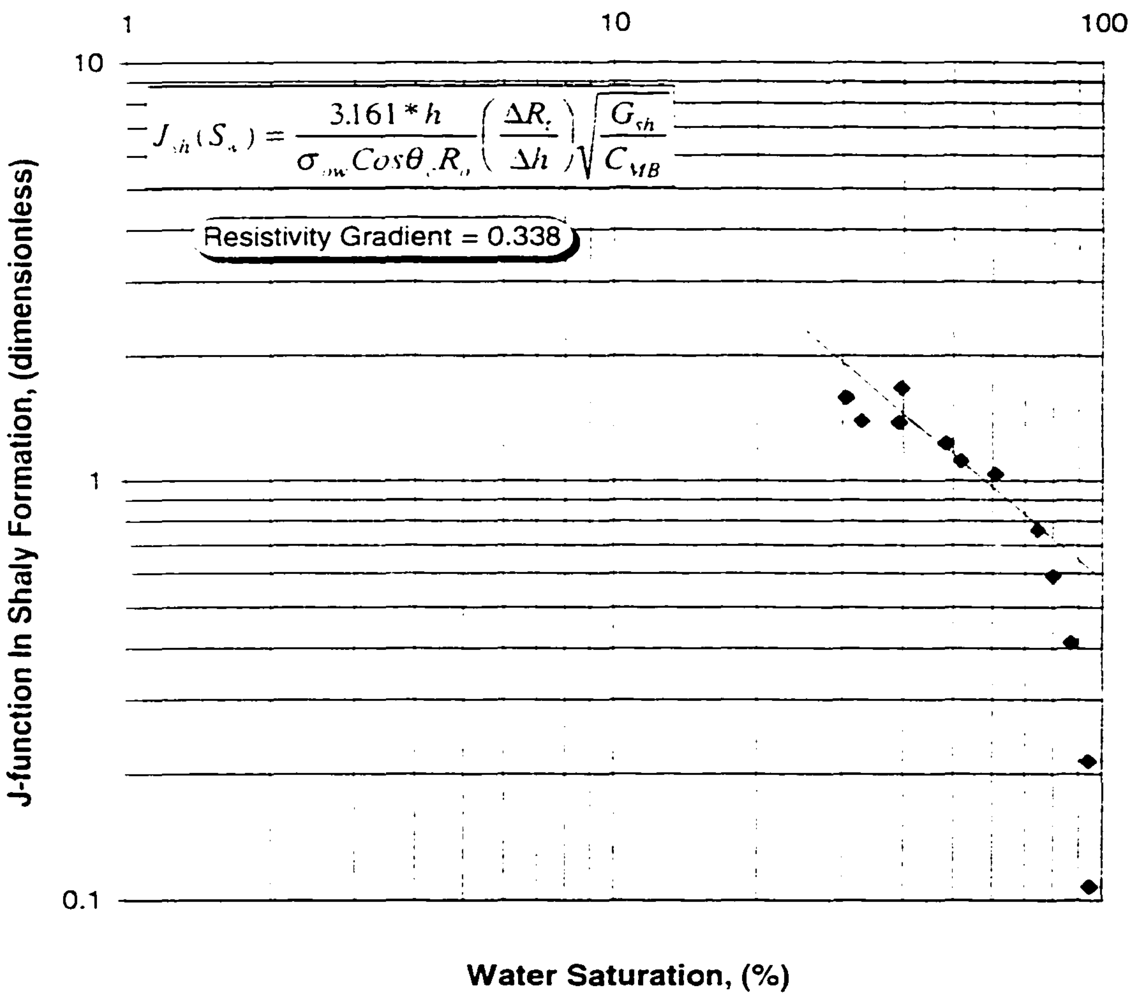

Fig. 6. 10 - A Log-Log Plot Of Jsh(Sw) versus Sw using the newly developed J-Function for Shaly Formation [Shaly Miocene Sand, Louisiana, USA], [Morris-Biggs, 1967]

This curve fits the calculated data points with R-square value of 0.9683. This proves that the degree of data point scattering in shaly formation if higher that that in clean formation, although both of them shows good curve fitting to the calculated data points

This chapter reviews the concept of J-function. A new J-function that depends upon the stress effect is developed, $J_s(S_w)$. The $J_s(S_w)$ can be used to convert the laboratory measurements of porosity and permeability at zero stress conditions to that under reservoir conditions. In addition, this chapter aslo includes a step by step derviation of two new models capable of obtaining the J-function using the well-logging derived data. These new J-functions are dveloped for clean and shaly reservoirs and validated using real field data.

CHAPTER 7

SUMMARY AND CONCLUSIONS

7. 1. Summary and Critical Discussion

This study is devoted to investigating the effect of stress on reservoir characterization and petrophysical properties (flow units) in clean and shaly heterogeneous reservoirs. For the purpose of achieving reservoir characterization and flow unit identification in clean and shaly, stress-insensitive reservoirs, several porosity-permeability relationships are identified and used for developing new flow unit models.

Several new models are developed for reservoir characterization of stress-sensitive reservoirs in clean and shaly heterogeneous formations. New Reservoir Quality Index for clean formation under stress (RQIs) and Reservoir Quality Index for shaly heterogeneous formation under stress (SRQIs) are also developed. These RQIs and SRQIs are used to study the effect of stress on petrophysical properties of reservoirs. In addition, generalized flow unit models are derived to be used with any porosity-permeability relationship (function of porosity and irreducible water saturation). The generalized flow unit model for shaly stress-sensitive formation can also be used to identify flow units in other types of formations including (a) clean stress-insensitive formations, (b) shaly stress-insensitive formations, and (c) clean stress sensitive formations.

The concept of the J-function is covered and the effect of stress on the J-function is investigated. New J-function models are developed to consider stress-sensitive (clean and shaly heterogeneous) reservoirs and also to eliminate the need for laboratory measurements of several parameters involved in the J-function.

Several permeability equations are used, in this study, to develop flow unit models. These equations were derived empirically by several authors (Ahmed et al 1991, and Nelson, 1994). These flow unit models are used effectively to characterize clean and shaly heterogeneous reservoirs using laboratory and/or in-situ measurements.

Appendix B lists the permeability equations used, their assumption(s) and limitation(s). Common features of these permeability equations is that they are empirical and have different coefficient (C_1, C_2, or n). In addition, all of these equations are developed for clean formations using laboratory measurements.

However, in case of new reservoirs or reservoirs that obey other permeability equations, generalized flow unit models are developed.

7. 2 Conclusions

Major contributions of this study are summarized under the following conclusions:

1. Several new flow unit models are developed to enhance reservoir characterization. These models include (a) five models for stress-insensitive clean formations, (b) five models for stress-insensitive shaly formations, (c) four models for stress-sensitive clean formations, (d) five models for stress-sensitive shaly formations, and (e) two J-function models for clean and shaly heterogeneous formations using well-logging data.
2. New permeability-porosity models for clean formations are investigated and used to develop several flow unit models which can be used to identify and characterize reservoirs. With respect to the newly-developed flow unit models for clean formations, the slope of a log-log plot of reservoir quality index (RQI) versus total porosity (φ) is

mainly a function of porosity exponent (m). The higher the porosity exponent, the higher the slope of the proposed straight line defining flow unit on a log-log plot.

3. New Reservoir Quality Indices are developed for stress-insensitive shaly formations (SRQIo) and for stress-sensitive shaly formations (SRQIs). SRQIo is a function of porosity and formation shaliness while SRQIs is a function of porosity, formation shaliness, and effective stress (or pressure drop of the reservoir).

4. The new flow unit models for stress-insensitive shaly formations introduce unique parameters to better describe such shaly reservoirs. These parameters include: (1) slope of a log-log plot of Shaly Reservoir Quality Index "SRQI" versus porosity (φ) which also can be used to define shale type and (2) Shaly Flow Unit Factor (SFUF). The new flow unit models for stress-sensitive shaly formations introduce two unique parameters (1) slope of a log-log plot of Shaly Reservoir Quality Index under stress (SRQIs) versus porosity of shaly formation under stress (φ_{s-sh}) which also can be used to define shale type and (2) shale stress factor (σ).

5. Several models are developed for characterization and identification of flow units residing in stress-sensitive clean and shaly reservoirs. The models for shaly reservoirs are derived using laminated, dispersed, total and cation-exchange capacity models of shale in combination with porosity and permeability equations under stress effect.

6. Flow unit models of stress-sensitive clean and shaly formations show that assumption of constant values of porosity, permeability, and reservoir quality index over the extended life of the reservoir can lead to errors in reservoir characterization.

7. A generalized flow unit model is developed. This model can be used for reservoir characterization and flow unit identification in different types of formations and with any permeability equation (function of porosity and irreducible water saturation).

8. A new J-function is developed for stress-sensitive, clean/shaly heterogeneous reservoirs, $J_S(S_W)$. The increase in effective stress (or oil production) leads to a severe reduction in the J-function under stress, $J_S(S_W)$. Also, a new approach is developed to use well-logging data for estimating the J-function in clean and shaly heterogeneous reservoirs. The newly-developed J-function models in clean and shaly reservoirs are validated using actual well-logging derived data.

7. 3. Recommendations

Although several achievements have been gained in reservoir characterization, there is still no universal method that can be applied to different heterogeneous reservoirs. This study introduced several new flow unit models and some generalized models, which represent a significant step toward the optimization of reservoir characterization. The study deals with different scales of reservoir heterogeneity, shale types, and stress conditions. These issues and problems require some attention. The following recommendations are suggested to further optimize the process of reservoir characterization:

1. Core and well-logging data must be integrated. This integration is expected to provide accurate mathematical expressions describing flow properties (permeability and reservoir quality index) within the reservoir.

2. A generalized model is required for describing fractured formations. This model is expected to consider other conditions such as stress-sensitivity of formations, formation shaliness, and random patterns of fracture distribution in the formation.

3. The flow unit models developed in this study are recommended for use in current reservoir simulators such as STRATA-SIM*. This is expected to enhance reservoir description and flow unit identification, especially in shaly reservoirs and unconsolidated (stress-sensitive) formations.

4. Mathematical models are needed to combine fluid flow equations with flow unit approach. These models are expected to be 3-D that will consider directional permeability, and different fluids types flowing in the reservoir.

5. Future study is recommended to consider the effects of injected fluids such as CO_2 and enhanced oil recovery (EOR) chemicals. These fluids will alter the wettability and relative permeabilities. Changes in wettability and relative permeability are expected to change the flow patterns and distribution of flow units in the reservoir.

* STRATA-SIM is a trade mark of the Reservoir Characterization Institute at The University of Oklahoma, Norman, OK.

Nomenclature

a : Equation coefficient

a_k, a_v, c : Curve Fitting Constants

A_{sh} : Sub-group of shale for J-function in shaly formation

B : Specific concentration conductivity, (mho/m per meq/cc)

B_{sh} : Sub-group of shale for J-function in shaly formation

C : Constant of a particular rock type and/or grain size

C_1 : Coefficient of general permeability equation, (dimensionless)

C_2 : Coefficient of porosity exponent in general permeability equation, (dimensionless)

C_{MB} : Morris-Biggs Constant for the J-function in clean formation $(C_{MB} = \varphi * S_{wirr})$

C_P : Pore Compressibility of the Rock, (1/psi)

F : Formation resistivity factor for clean formation,(dimensionless)

F^* : Formation resistivity factor of CEC shale model, (dimensionless)

FUF : Flow Unit Factor

FUF_{S-G} : Flow Unit Factor of clean stress-sensitive formation using Jorgensen equation, (dimensionless)

FUF_{G-S-Sh}: Flow Unit Factor of shaly stress-sensitive formation using general permeability equation, $\left(1/\sqrt{ohm-m}\right)$

FUF_{S-TM} : Flow Unit Factor of clean stress-sensitive formation using Timur equation, (dimensionless)

FUF_{S-WR} : Flow Unit Factor of clean stress-sensitive formation using Wyllie and Rose equation, (dimensionless)

G_{sh} : Collective group of shale for the J-function in shaly formation

$J(S_w)$: Capillary pressure J-function for clean formation, (dimensionless)

$J_S(S_w)$: Capillary pressure J-function for stress-sensitive formation, (dimensionless)

$J_{sh}(S_w)$: Capillary pressure J-function for clean formation, (dimensionless)

K : Permeability of the formation (md)

K_o : Permeability of the rock at zero stress condition, (md)

K_S : Permeability of the rock under stress condition, (md)

K_{sh} : Permeability of shaly formation, (md)

K_{s-sh} : Permeability of shaly formation under stress effect, (md)

h : Free-water level, (ft)

LSFUF : Low Shaly Flow Unit Factor

m : Cementation factor (porosity exponent) of Archie's equation

n : Water Saturation exponent (n=2) of Archie's equation

P : Pressure, (psi)

P_o : Initail reservoir pressure, (psi)

P_C : Capillary pressure, (psi)

PV : Pore volume, (fraction)

q : The fraction of clean-sand intergranular space occupied by clay (shale)

Qv : Cation Exchange capacity, (meq/cc)

R_o : Rock resistivity (100% saturated with formation water), (ohm-m)

R_{sh} : Resistivity of adjacent shale, (ohm-m)

R_t : True formation resistivity, (ohm-m)

R_{disp} : Resistivity of dispersed shale, (ohm-m)

R_{sh} : Resisitivity of shale, (ohm-m)

R_w : Formation water resistivity, (ohm-m)

RQI : Reservoir Quality Index, (μ m)

S : Stress correction factor for porosity and permeability, (dimensionless)

S_w : Water saturation, (fraction)

S_{wirr} : Irreducible water saturation, (fraction)

SFUF : Shaly Flow Unit Factor

SFUFs : Shaly Flow Unit Factor for formation under stress

SRQI : Shaly Reservoir Quality Index, (μ m)

$SRQI_O$: Shaly Reservoir Quality Index without stress effect, (μ m)

$SRQI_S$: Shaly Reservoir Quality Index of formations under stress, (μ m)

S_{wi-c} : Irreducible water saturation estimated by NMR, (fraction of PV)

S_{im} : The fraction of the "intermatrix porosity "φ_{im}" occupied by the formation-water, dispersed shale matrix mixture, (fraction of PV)

S_{WB} : Water saturation of bound water, (fraction of PV)

SRQI : Shaly Reservoir Quality Index, (μ m)

T_1 : Geometric mean longitudinal relaxation time from NMR, (μ Sec)

UFFI : Un-free fluid index, (μ Sec)

V : Volume, (cc)

V_{sh} : Shale content of the formation, (fraction)

VSFUF : Very shaly Flow Unit Factor

Greek

ρ : Rock density

σ : Effective stress

Δ : Change in rock property

α : Correlating constant

ε : Void to solid ratio of porous rock

φ_e : Effective porosity of the formation, (fraction)

φ_{to} : Total porosity of the rock, (fraction)

φ_S : Effective porosity of the rock under stress condition, (fraction)

φ_{s-sh} : Effective porosity of shaly formation under stress condition, (fraction)

φ_{NMR} : Porosity from NMR, (fraction)

σ_{ow} : Interfacial tension between oil and water, (mN/m)

θ : Contact angle, (degree)

Subscripts

D : Density Log

Disp : Dispersed

e : Effective

f : Fluid

g : Grain

Im : Intermatrix

Irr : Irreducible

G-s-sh : General for permeability of shaly formation under stress

Lam : Laminated

max : Maximum

min : Minimum

MB : Morris-Biggs

N : Neutron Log

NMR : Nuclear Magnetic Resonance

o : Oil

o-sh : Shaly formation without stress effect

P : Pore

r : rock

s : solid

S-G : stress-sensitive formation using Jorgensen equation

S-TM : stress-sensitive formation using Timur equation

s-sh : Shaly formation under stress effect

s-po : Porosity under stress

S-WR : stress-sensitive formation using Wyllie and Rose equation

Wirr : Irreducible water

WB : Bound Water

Superscripts

m : Porosity exponent

n : water saturation exponent

References

Ahmed, U., Crary, S. F., and Coats, G. R.,: "Permeability Estimation: The Various Sources and Their Interrelationships," JPT, May, (1991), p. 578-587.

Aguilera, R.: "A New Approach for Analysis the Nuclear Magnetic Log-Resistivity Log Combination," Journal of Canadian Petroleum Technology, (1990), vol. 29, p. 67-71.

Aguilera, R.,: "Extensions of Pickett Plots for the Analysis of Shaly Formations by Well Logs," The Log analyst, Sept.-Oct., (1990), p. 304-312.

Alpin, L.M.: "The methods for Logging in Cased Wells," USSR Patent 56026 (1939).

Amaefule, J.O., Altunbay, M., Tiab, D., Kersey, D. G., and Keelan, D.K.,: "Enhanced Reservoir Descriptions: Using Core and Log Data to Identify Hydraulic (Flow) Units and Predict Permeability in Uncored Intervals/Wells," SPE 26436, 68th Annual Technical Conference & Exhibition of Soc. Pet. Eng., Houston, TX, USA, Oct. 3-6, (1993), p. 205-220.

Archie, G.E.,: "Electrical Resistivity Log as an Aid in Determining Some Reservoir Characteristics," Trans. AIME (1942), vol. 146, p. 54-61.

Archie, G.E.,: Discussion of T. P., No. 2936: Trans. AIME, (1950), vol. 307, p. 1189.

Archie, G.E.,: "Classification of Carbonate Rocks and Petrophysical Considerations," AAPG Bulletin, (1952), vol. 36, p. 278-98.

Bassiouni, Z.,: Theory, Measurement, and Interpretation of Well Logs: Society of Petroleum Engineers, Richardson, TX, (1994).

Bear, J.: Dynamic of Fluids in Porous Media: New York, Elsevier, (1972).

Borgia, G.C.,: "A New Un-free Index in Sandstones Through NMR Studies," SPE # 28336, SPE 69 th Annual Tech. Conference and Exhibition, New Orleans, 25-28 Sept., (1994), p. 37-44.

Brown, H. W.,: "Capillary Pressure Investigation," Petroleum Trans., AIME, vol. 192, (1951), p. 67-74.

Carmen, R.C., "Fluid Flow Through Granular Beds," Trans. ALChE, (1937), vol. 15, p. 150-166.

Chierici, G. L., Ciucci, G. M., Eva, F. and Long, G.,: "Effect of the Overburden Pressure on Some Petrophysical Parameters of Reservoir Rocks," Proc. 7th World Petrol. Conf., Mexico City, (1967), p. 309-330.

deWitte, L.,: "Relations Between Resistivities and Fluid Contents of Porous Rocks," Oil and Gas Journal, Aug. 24, (1950), p. 120-132.

Dewan, J.T.: Essentials of Modern Open-Hole Log Interpretation,: PennWell Books, Tulsa, OK (1983).

Doberynin, V.,: "Effect of Overburden Pressure on Formation Properties of Sandstones," SPE Journal, Dec. (1960), p. 360-66.

Doyle, J. O' Meara, Jr, D. J., and Witterholt, E. J.,: "The "Gypsy" Field Research Program In Integrated Reservoir Characterization," SPE 24710, Presented at 67th Annual Technical Conference and Exhibition of the Society of Petroleum Engineers, Washington, D. C., Oct. 4-7, (1992), p. 92-104.

Dunlap, H.F.,: "The Relation Between Electrical Resistivity and Brine Saturation in Reservoir Rocks," Pet. Trans. AIME, Oct. (1948), p. 259-271.

Ebanks. W.J.. Jr: Scheihing. M.H.. and Atkinson. C.D..: "Flow Units for Reservoir Characterization." AAPG. (1983). p. 282-289.

Fatt. I..: "The Effect of Overburden Pressure on Relative Permeability," Pet. Trans., AIME. vol. 198. (1953). vol. 41. p. 325-26.

Fertl. W. H. and Hammack, G. W..: "A Comparative Look At Water Saturation Computation In Shaly Pay Sands," SPWLA 12th Annual Logging Symposium. May 2-5. (1971). vol. 197. p. 1-17.

Fertl. W. H..: "Log-Derived Evaluation of Shaly Clastic Reservoirs." JPT. Feb.. (1987), p. 175-194.

Fertl. W.H.. and Chilingarian. G.V..: "Types and Distribution Modes of Clay Mineral from Well-Logging Data," Journal of Petroleum Science and Engineering, vol. 3, (1990). p. 321 -332.

Gorgensen. G. D.,: "Estimating Permeability in Water-Saturated Formations," The Log Analyst. Nov.-Dec.. (1988), p. 401-409.

Green. D.E..: "Subsidence Monitoring in the Gulf Coast," SPE 22884, Presented at 68th Annual Technical Conference and Exhibition, Dallas, TX, Oct. 6-9, (1991), p.665-678.

Fogg, G. E., Lucia, F. G., and Senger, R. K.,: Stochastic Simulation of Interwell Scale Heterogeneity For Improved Prediction of Sweep In a Carbonate Reservoir, Reservoir Characterization-II., Academic Press. Inc.. San Diego, (1991).

Forgotson. Jr. J.,: Role of Reservoir Characterization In Improved Petroleum Recovery, School of Geology and Geophysics. University of Oklahoma. Norman. Oklahoma. Course # GEOL 6970. (1993).

Klkanl. J. and Pedrosa. O.,: "Perturbation Analysis of Stress-Sensitive Reservoirs," SPEFE. Sept. (1991). p. 379-386.

Keller. G. V.,: "Effect of The Wettability On The Electrical Resistivity of Sands," Oil and Gas Journal. Vol. 51. No. 34, (1953). p. 62-71.

Jones. C.S. "Two-Points Determination Of Permeability and PV Vs. Net Confining Stress," SPEFE. March (1988). p. 235-41.

Guyod. H., World Oil. No. 8. (1948). p.120.

Gray. D.H. and Fatt. I.,: " Effect of Stress on Permeability of Sandstone Cores," SPEJ, June. (1963). p. 95- 100.

Hantush, M.S.,: Hydraulics of Wells-Advances in Hydroscience, V. T. Chow (ed.), Academic Press, New York, (1964), p. 281-432.

Hilchic. D. W.,: The Effect of Pressure and Temperature On The Resistivity of Rocks, Ph.D. Thesis, The University Of Oklahoma, (1964).

Holen-Hoeksema, R. C.,: "The Future Role of Geophysics In Reservoir Engineering," Geophysics, The Leading Edge of Exploration, Dec. (1990), p. 89-97.

Honarpour, M. M., Schatzing, R. A., Szpakiewiez, M. J., Jackson, S. R., Sharma, B., Thomusta, L., and Chang, M. M.,: "Integrated Methodology For Constructing A Quantified Hydrodynamic Model For Clastic Petroleum Reservoir," Prepared for

U.S. Department of Energy, Bartlesville Project Office, NIPER-439 (DE 90000211), (1990), p. 156.

Leverett, M. C., "Capillary Behavior in Porous Solids," Trans. AIME, (1940), vol. 142, p. 152-169.

Leverett, M. C., Lewis, W. B., and True, M. E.,"Dimensional-Model Studies of Oil Field Behavoir," Trans. AIME, Oct. (1941), p. 175-193.

Lewis, M. G., Sharma, M. M., and Dunlap, H. F., "Wettability and Stress Effects on Saturation and Cementation Exponents," SPWLA, 29 th Annual Logging Symposium, June 5-8, (1988), paper K, p. 1-24.

Lines, L. et al.: "Integrated Reservoir Characterization: Beyond Tomography," SPE 24710, Presented at the Annual Technical Conference and Exhibition of the Society of Petroleum Engineers, New Orleans, LA, Sept. 25-28, (1994), p. 229-234.

Logan, D., Morriss, C.E., and Williams, R.,: "Nuclear Magnetic Resonance Logging in the Delaware Formation," SPE 30627, SPE Annual Technical Conference and Exhibition, Dallas, TX, USA, 22-25 Oct. (1995), p.76-89.

Longeron, P. G., Argand, M., J., and Feraud, J. P.,: "Effect of Overburden Pressure, Nature and Microscopic Distribution of the Fluids on Electrical Properties of Rock Samples," SPE 15383, L. A., Oct. 5-8 (1986), p.1-13.

Lucia, F. J., "Petrophysical Parameters Estimated From Visual Descriptions of Carbonate Rocks: A Field Classification of Carbonate Pore-Space," JPT, v. 35, No. 3 (1983), p. 629-637.

Mann, R.L. and Fatt, I. Geophysics, (1960), vol. 25, p. 433.

McKee. C.R.. Bumb. A.C.. and Koenig. R.A.. "Stress-Dependent Permeability and Porosity of Coal and Other Geologic Formations." SPE Formation Evaluation. March (1988). p. 81-91

Miyairi. M. and Itoh. T..: " Determination of Shaly Parameters In Shay Sands." SPWLA. 9 th Annual Logging Symposium. June 13-16, (1978). p.1-19.

Morita. N.. Gray. K. E.. Soruji. F.A.. and Jogi, P.N., "Rock Property Change During Reservoir Compaction." SPE 13099. presented at 68 th Annual Technical Conference and Exhibition. Houston. TX. Sept. 16- 19. (1984). p. 1-17.

Morris. R.L.. and Biggs. W.P..: "Using Log-Derived Values of Water Saturation and Porosity," Trans. of SPWLA. 8 th Annual Logging Symposium. June 12-14. (1967). Paper X, p. 1-26.

Morton-Thompson. D. and Woods (Editors): Development Geology Reference Manual. AAPG Methods in Exploration Series. No.10, Tulsa, OK.

Neasham. J.W.: "The Morphology of Dispersed Clay in Sandstone Reservoir and Its Effects on Sandstone Shaliness. Pore Space and Fluid Flow Properties," SPE 6858. Denver. Oct. 9-12. (1977), p. 231-242.

Nelson, P.H.,: "Permeability-Porosity Relationships In Sedimentary Rocks," The Log Analyst, May-June (1994), p. 38-61.

Ohen, H.A; Ajufo, A, and Curby, F.M;: "A Hydraulic (Flow) Unit Based Model for the Determination of Petrophysical Properties from NMR Relaxation Measurements," SPE # 030626, Annual Tech. Conf. & Exhibition- Dallas, 22-25 Oct., (1995), 983-96.

Pickett. G.R..: "A Review of current techniques for determination of water saturation from logs," JPT. (1966). vol. 18. p. 1425-1433.

Pickett. G.R..: " Pattern recognition as a mean of formation evaluation" Paper A. 14 th Annual Logging Symposium Transactions: Society of Professional Well Log Analyst. (1973). Paper A. p. 1-21.

Poupan. A. and Leveaux. J..: "Evaluation of Water Saturation in Shaly Formations," SPWLA Symposium. May 2-5 (1971). abstract only. p. 1.

Rose. W. R. and Bruce. W. A..: "Evaluation of Capillary Character in Petroleum Reservoirs Rock. " Trans. AIME. May (1949). vol. 186. p. 127-133.

Sanyal. S.K.. and Ellithorpe. J.E..: "A Generalized Resistivity-Porosity Crossplot Concept," SPE 7145. California. (1978), p. 123-136..

Shao. H., Brimhall. R. M.. Ahr. W. M., and Wu. C. H.,: "An Application of Idealized Carbonate Depositional Sequences for Reservoir Characterization," SPE 28458. Presented at the Annual Technical Conference and Exhibition of the Society of Petroleum Engineers. New Orleans. LA. Sept. 25-28, (1994), p. 959-971.

Schlumberger: Log Interpretation. Principles/Applications: Schlumberger Educational Services, Houston, Texas, (1987).

Schlumberger, : Log Interpretation. Volume 1- Principles, Schlumberger Limited, New York. (1972).

Sen, P. N., Stratley, C., Kenyon, W.E., and Whittingham, M.S.,: "Surface-to-Volume Ratio, Charge Density, Nuclear Magnetic Relaxation, and Rock Permeability in Clay Bearing Sandstones," Geophysics, (1990) vol. 55, n. 1, p. 61-69.

Serra, O.: Fundamentals of Well-Log Interpretation-2. The Interpretation of Logging Data, p. 457-468.

Simandoux, P.,"Dielectric Measurements in Porous Media and Applications to Shaly Formations," Review de Institute Francais du Petrole, Supplementary Issue, (1963), p. 193-215.

Timur, A.,: "An Investigation of Permeability, Porosity, and Residual Water Saturation Relationships," SPWLA Ninth Annual Logging Symposium, June 23-28, (1968), Paper K, p. 1-17.

Timur, A; Hempkins, W.B.; and Worthington, A.E.,: "Porosity and Pressure Dependence of Formation Resistivity Factor For Sandstone," Trans. Canadian Well logging Society, (1972), 4, Paper D, p. 1-12.

Tixier, M. P., "Evaluation Of Permeability from Electric-Log Resistivity Gradient," Oil and Gas Journal, June, (1949), vol. 48, p. 113-123.

Walsh, J.B., " Effect of Pore Pressure and Confining Pressure on Fracture Permeability," Int. J. Rock Mech. Min. Sci. Geomech. Abstracts, (1981), vol. 18, No. 5, p. 429-35.

Waxman, M.H., and Smits, L. J. M.,: "Electrical Conductivities in Oil-Bearing Shaly Sands," SPEJ, June, (1968), p. 107-122.

Well Logging and Interpretation Techniques,: "Overview of Shaly Content Evaluation (Mixed Lithology)-The Course for Home Study" Dresser Industries Inc., (1982).

Winsaur, H. M. et al "Resistivity of Brine-Saturated Sands in Relation to Pore Geometry," AAPG Bulletin, Feb. (1952), vol. 36, No. 2, p. 253-77.

Winsaur, W.O. and McCardell, W. .M..: "Ionic Double-Layer Conductivity in Reservoir Rock" Trans. AIME, (1953), vol. 198, p. 129-34.

Worthington, P. F..: "The Evolution of Shaly Sands Concepts in Reservoir Evaluation." Log Analyst, Jan-Feb, (1985), vol. 24, No. 1. p. 234-248.

Wyllie, M. R. and Rose, W. D..: "Some Theoretical Considerations Related to the Quantitative Evaluation of the Physical Characteristics of Reservoir Rock from Electrical Log Data," Petroleum Trans., AIME, vol. 189, (1950), p. 105-118.

Appendix A

Water Saturation Equations in Shaly Clastic Reservoir Rock

Poupan et al Model for Laminated Shale

$$\left(\frac{1}{R_t}\right) = \frac{\phi^2 S_w^2}{aR_w(1-V_{lam})} + \frac{V_{lam}}{R_{sh}}$$

deWitte Model for Dispersed Shale

$$\left(\frac{1}{R_t}\right) = \frac{\phi_{im}^2 S_{im}}{a}\left(\frac{q}{R_{dis}} + \frac{S_{im}-q}{R_w}\right)$$

Total Shale Model

$$\left(\frac{1}{R_t}\right) = \frac{V_{sh}}{R_{sh}} + \frac{S_w^n}{F R_w}$$

Waxman & Smits Shale Model "Cation Exchange Capacity(CEC)" Model

$$S_w^2 = \frac{R_w F^*}{R_t\left(1 + \frac{R_w B Q_v}{S_w}\right)}$$

Hossin Model

$$\frac{1}{R_t} = \frac{S_w^2}{FR_w} + \frac{V_{Sh}^2}{R_{sh}}$$

Simandoux Model

$$\frac{1}{R_t} = \frac{S_w^2}{FR_w} + \varepsilon\frac{V_{Sh}^2}{R_{sh}}$$

where

$\varepsilon = 1.0$ for high S_w, and $\varepsilon < 1.0$ for low S_w

Patchett and Rausch Model

$$R_t = \frac{S_w^2}{FR_w} - \frac{V_{sh}^2}{R_s}$$

where

C, = shale resitivity(not equal to R_{sh})

Bardon and Pied

$$\frac{1}{R_t} = \frac{S_w^2}{FR_w} + \frac{V_{sh}}{R_{sh}} S_w$$

Schlumberger Model

$$\frac{1}{R_t} = \frac{S_w^2}{FR_w(1 - V_{sh})} + \frac{V_{sh}}{R_{sh}} S_w$$

Clavier et al

$$\frac{1}{R_t} = \frac{S_w^2}{F_o R_w} + \frac{(C_{bw} - C_w) V_Q * Q_v}{F_o} S_w$$

Juhasz Model

$$\frac{1}{R_t} = \frac{S_w^2}{FR_w} + \left(\frac{1}{F_{sh} R_{sh}} - \frac{1}{R_w} \right) \frac{V_{sh} * \varphi_{sh} * S_w}{\varphi}$$

Doll Model

$$\frac{1}{R_t} = \frac{S_w^2}{FR_w} + 2V_{sh}\sqrt{\frac{1}{FR_w R_{sh}}} + \frac{V_{sh}^2}{R_{sh}}$$

Appendix B

<u>List of Permeability Equations</u>

 # Perm. Equation **Assumption(s) and Limitation(s)**

1. Timur

$$K(md) = (93)^2 * \left(\frac{\varphi^{4.4}}{S_{wirr}^2}\right)$$

- applicable for (a) Gulf Coast field (depth 9,000-12,000 ft)
  (b) Colorado field (depth 6,000-7,000 ft), and (c) California field (depth 9,000 ft - 10,000 ft),
- requires lab. measurements of porosity and permeability,
- consolidated sandstones

2. Sen et al

$$K(md) = 0.794 * \left(\varphi^m T_l\right)^{2.15}$$

- clean consolidated Sandstones
- based on NMR measurements.

3. Wyllie and Rose

$$K(md) = 62500 * \left(\frac{\varphi^{3m}}{S_{wirr}^n}\right)$$

- C_1 = 62,500, and C_2 = 3.
- clean consolidated sandstones
- assumes P_c is inversely proportional to SQRT(K)
- permeability derived from wel-log data
- permeability is based on Tixier's equation

4. Jorgensen

$$K(md) = 84105 * \left[\frac{\varphi^{m+2}}{(1-\varphi)^2}\right]$$

- clean sandstone reservoirs
- assumes that perm. is only a function of porosity and (m)
- requires lab. measurements of porosity and perm.

5. Morris-Biggs

$$K(md) = C_1 * \left(\frac{\varphi^{3m}}{S_{wirr}^n}\right)$$

- clean formations
- $C_1 = (250)^2$ for medium gravity oil
- Permeability derived from wel-log data